Aus dem Institut für Lungenforschung
Geschäftsführender Direktor: Prof. Dr. Bernd Schmeck
des Fachbereichs Medizin der Philipps-Universität Marburg

# RNA species in the host-pathogen dynamics during *Legionella* infection of human macrophages

Inaugural-Dissertation
zur Erlangung des Doktorgrades der Naturwissenschaften

dem Fachbereich Medizin
der Philipps-Universität Marburg
vorgelegt von

**Christina Elena Herkt**
aus Wetzlar

Marburg, 2018

Angenommen vom Fachbereich Medizin der Philipps-Universität Marburg am: 03.08.2018

Gedruckt mit der Genehmigung des Fachbereichs.

Dekan: Prof. Dr. Helmut Schäfer

Referent: Prof. Dr. Bernd Schmeck

1. Korreferent: Prof. Dr. Stefan Bauer

# Table of Contents

## Zusammenfassung

*Legionella pneumophila* (*L.p.*) ist ein gram-negatives, intrazelluläres Pathogen und eine häufige Ursache von schweren ambulant-erworbenen Pneumonien. *L.p.* repliziert im Menschen hauptsächlich in Alveolarmakrophagen. Durch die Sekretion von über 300 Effektorproteinen in das Zytosol der Wirtszelle manipuliert das Bakterium wichtige Wirtszellfunktionen wie den Vesikeltransport und die Genexpression. Somit ändert *L.p.* wichtige Funktionen der Wirtszelle, um seine eigene Replikation zu fördern. Eine globale Analyse der molekularen Veränderungen und biologischen Prozesse, die mit bakteriellen Infektionen von humanen Zellen verbunden sind, kann neue Einblicke in die Wirts-Pathogen-Interaktionen ermöglichen. Daher war ein Ziel dieser Studie, die Expressionsveränderungen verschiedener RNA-Spezies nach Infektion mit *L.p.* in primären Blutmakrophagen (BDMs) oder differenzierten THP-1-Zellen zu untersuchen. Diese Arbeit ist in zwei Teile gegliedert: (1) Eine funktionelle Studie, wie eine miRNA-Manipulation die Replikation von *L.p.* in Makrophagen beeinflussen kann, und (2) eine globale Analyse von Transkriptom-Veränderungen in Wirt und Pathogen während der Infektion. (1) In den letzten Jahrzehnten haben sich miRNAs als wichtige Modulatoren der Immunfunktion etabliert. Daher sollte das miRNA-Profil von *L.p.*-infizierten Makrophagen identifiziert und der funktionelle Einfluss einer miRNA-Manipulation auf die *L.p.*-Replikation untersucht werden. Dafür wurden BDMs von gesunden Spendern mit *L.p.* des Stammes Corby infiziert. Die Sequenzierung der kleinen RNAs führte zur Identifizierung des miRNA-Profils von *L.p.*-infizierten BDMs. Es wurde eine Hochregulation von miR-146a und miR-155, sowie eine Herunterregulation von miR-221 und miR-125b in Makrophagen mittels qPCR validiert. Die miRNA-Regulation nach einer *L.p.*-Infektion scheint auf die transkriptionelle Veränderung von miRNA-Promotoren zurückzuführen zu sein, da die Acetylierungslevel und die pri-miR-Expression mit der miRNA-Expression nach einer *L.p*-Infektion korrelierten. Zur funktionellen Charakterisierung wurden Überexpressions- und *Knockdown*-Experimente der miRNAs miR-125b, miR-221 und miR-579 durchgeführt. Diese zeigten einen Einfluss auf die bakterielle Replikation. Mit der Hilfe eines SILAC-Ansatzes wurde MX1 als herunterreguliertes Protein nach gleichzeitiger Überexpression aller drei miRNAs identifiziert. MX1 ist ein Interferon-induziertes GTP-bindendes Protein, das für die antivirale Abwehr wichtig ist. Wie durch Validierungsexperimente gezeigt wurde, führte der *Knockdown* von MX1 zu einer erhöhten Replikation von *L.p.*, die auch nach Überexpression der miRNAs beobachtet wurde. Da *in silico*-Analysen keine Bindungsstellen für die miRNAs in der 3'UTR von MX1 vorhersagten, wurde eine *Ingenuity-Pathway*-Analyse durchgeführt, um konnektive Moleküle zu identifizieren. DDX58 (RIG I), ein Sensor für zytosolische RNA, wurde als Zielmolekül der miR-221 validiert, während der Tumorsuppressor TP53 mittels Luciferase-Reporter-Assay als Zielmolekül der

miR-125b bestätigt wurde. Eine siRNA-vermittelte Herunterregulation von TP53 als auch DDX58 führte zu einer verstärkten Replikation von *L.p*. in Makrophagen. Daher wurden DDX58 und TP53 als verbindende Moleküle zwischen den drei miRNAs und MX1 validiert. Zusätzlich zeigte der oben erwähnte SILAC-Ansatz eine Herunterregulierung von LGALS8, welches anschließend als Zielmolekül der miR-579 identifiziert wurde. LGALS8 ist ein zytosolisches Lektin, das Kohlenhydrate bindet. Der *Knockdown* von LGALS8 erhöhte die intrazelluläre Replikation in Makrophagen. Zusammenfassend wurden MX1 und LGALS8 als Zielmoleküle der drei miRNAs (miR-125b, miR-221, miR-579) identifiziert, die zur Verminderung der *L.p.*-Replikation in humanen Makrophagen beitragen. (2) Das Transkriptionsprofil von *L.p.*-Infektion in humanen Makrophagen wurde mittels *dual RNA-Seq* untersucht, um die Regulation von kodierenden und nicht-kodierenden RNAs während einer Infektion von Wirt und Pathogen gleichzeitig zu bestimmen. Nach Anpassung und Optimierung bestehender Protokolle wurden die Makrophagen mit einem GFP-exprimierenden *L.p*.-Stamm infiziert. Um infizierte Zellen (gfp+) von den nicht infizierten Zellen (gfp-) zu trennen, wurden durchflusszytometrische Sortierungen durchgeführt. Eine differentielle Genexpressionsanalyse wurde unter Verwendung von DESeq2 durchgeführt, wodurch 4.144 differentiell exprimierte humane Gene und 2.707 differentiell exprimierte bakterielle Gene identifiziert wurden. Die DESeq-Analyse der Wirtszellen zeigte differentiell exprimierte mRNAs (3.504), lncRNAs (495) und miRNAs (145). Davon waren 1.128 differentiell exprimierte Gene ausschließlich in den infizierten Zellen (gfp+ nach 8 und 16 h) signifikant reguliert. Einigen von diesen Genen wurden erfolgreich mittels qPCR validiert (*BCL10*, *SOD1*, *IRS1*, *CYR61*, *ATG5*, *RND3* und *JUN*). Außerdem wurde die Regulation der Gene *ZFAND2A* und *HSPA1* validiert, die in gfp- als auch in gfp+ Zellen eine Hochregulation aufwiesen. Die Analyse der bakteriellen mRNAs zeigte eine inverse Regulation zwischen 8 und 16 h. Dazu gehörten Gene, die am Eisenstoffwechsel, der Stressantwort, der Glykolyse und der Lipidbiosynthese beteiligt sind. Zusammenfassend wurden also differentiell exprimierte Legionellen-Gene in verschiedenen Wachstumsphasen des Infektionszyklus identifiziert. Die Daten des dualen Sequenzierungsansatzes, die in dieser Arbeit generiert wurden, sind die ersten, die ein intrazelluläres, respiratorisches Bakterium untersuchen. Mit Hilfe dieser Daten können die Regulationen aller kodierender und nicht-kodierender RNAs von Pathogen und Wirt in einem großen, umfassenden Netzwerk dargestellt werden.

Zusammengefasst haben die Ergebnisse dieser Arbeit die Kenntnisse des Infektionsprozess von *L.p.* und seine Wirtszellen vertieft. Die Daten werden dazu beitragen das komplexe Zusammenspiel zwischen ihnen besser zu verstehen, indem die *in silico* Konstruktion eines RNA-Interaktions-Netzwerkes ermöglicht wird. Darüber hinaus wird die vorliegende Studie helfen, potenzielle neue Kandidaten für Diagnose und Therapie zu etablieren.

## Summary

*Legionella pneumophila* (*L.p.*) is a gram-negative, intracellular pathogen and a common cause of severe community-acquired pneumonia. In humans, *L.p*. replicates primarily within alveolar macrophages. It manipulates vital host cell functions such as vesicle trafficking and gene expression by the secretion of over 300 effector proteins into the host cell cytosol. Thus, *L.p.* modifies its host cell to promote its own replication. An unbiased and global analysis of the molecular changes and biological processes that are associated with bacterial infections of human cells can provide new insights into host-pathogen interactions. Therefore, one goal of this study was to characterize expression changes of different RNA species in response to infection with *L.p.* in human primary blood-derived macrophages (BDMs) or differentiated THP-1 cells. This work is structured into two parts: (1) a functional study on how miRNA manipulations can alter *L.p.* replication in macrophages and (2) an in depth analysis of transcriptomic events in host and pathogen during infection.

(1) In the last few decades, miRNAs have been established as critical modulators of immune function. Therefore, one aim of this study was to identify the miRNA profile of *L.p.*-infected macrophages and to determine the functional impact of a miRNA manipulation on *L.p.* replication. BDMs of healthy donors were infected with *L.p*. strain Corby. Small RNA sequencing revealed the miRNA profile in BDMs following *L.p.* infection. An upregulation of miR-146a and miR-155, as well as downregulation of miR-221 and miR-125b was validated by qPCR in macrophages. miRNA regulation in response to infection seems to be due to transcriptional regulation of miRNA promoters, since the histone acetylation levels at the promoter and the pri-miR expression correlated with the miRNA expression upon *L.p.*-infection. Overexpression and knock down experiments of miR-125b, miR-221 and miR-579 in combination were performed for functional characterization and showed an influence of all three miRNAs on bacterial replication. A SILAC approach revealed the protein MX1 as downregulated following simultaneous overexpression of all three miRNAs. MX1 is an interferon-induced GTP-binding protein important for antiviral defence. As shown by validation experiments, MX1 knockdown in macrophages led to an increased replication of *L.p.*, as seen following overexpression of the miRNAs. Since *in silico* analysis predicted no binding sites for either miRNA in the 3'UTR of MX1, Ingenuity pathway analysis was performed to find the linking molecules. DDX58 (RIG-I), a sensor for cytosolic RNA, was validated as a target for miR-221, while the tumour suppressor TP53 was shown to be targeted by miR-125b via luciferase reporter assays. An siRNA-mediated knockdown of both, TP53 and DDX58, respectively, led to an enhanced replication of *L.p.* in macrophages. Thus, DDX58 and TP53 were validated as linking molecules between the three miRNAs and MX1. Additionally, the

aforementioned SILAC approach revealed a downregulation of LGALS8 which was later validated as a target of miR-579. LGALS8 is a *cytosolic lectin* which binds carbohydrates and localizes to damaged vesicles. Knockdown of LGALS8 enhanced intracellular replication in macrophages. Thus, MX1 and LGALS8 were identified as targets of the three miRNAs (miR-125b, miR-221, miR-579) and to be responsible for the restriction of *L.p.* replication within human macrophages.

(2) The transcriptional profile of *L.p.* during the course of infection in human macrophages was next to be established. Dual RNA-Sequencing was performed to determine the regulation of coding and non-coding RNA species during the course of infection of both, host and pathogen, simultaneously. After adaptation and optimization of existing protocols, macrophages were infected using a GFP-expressing *L.p.* strain Corby. To separate infected cells (gfp+) from the non-invaded bystander cells (gfp-), flow cytometry sorting was performed. Furthermore, Pam3CSK4 was used to generate TLR2-activated cells. RNA from all different samples, and also RNA from cultivated *Legionella*, was sequenced. Differential gene expression analysis was performed using DESeq2 resulting in 4,144 differentially expressed human genes (across multiple conditions) and 2,707 differentially expressed *Legionella* genes (across two time points). The DESeq analysis of the separated RNA fractions from host cells revealed differentially expressed mRNAs (3,504), lncRNAs (495), and miRNAs (145). 1,128 differentially expressed genes were exclusively significantly regulated in invaded cells (gfp+ at 8 and 16 h). Some of these were validated via qPCR including *BCL10*, *SOD1*, *IRS1*, *CYR61*, *ATG5*, *RND3* and *JUN*. In addition, the simultaneous upregulation of the genes *ZFAND2A* and *HSPA1* in the bystander and in *Legionella*-invaded cells was validated. The analysis of the bacterial mRNAs revealed a switch of gene usage, i.e. inverse regulation at 8 and 16 h post infection. This switch included genes which are involved in iron metabolism, stress response, glycolysis and lipid biosynthesis. Hence, differentially expressed genes within different growth phases of the infection cycle were identified. This dataset is the first of its kind to cover a respiratory pathogen. The dual RNA-Sequencing performed in this study provides data to encapsulate the RNA landscape of coding and non-coding RNAs in pathogen and host.

In summary, the results have deepened our insight into the infection process and the molecular interaction of *L.p.* and its host cells and will help to understand the complex interplay between host and pathogen by allowing for the *in silico* re-construction of an RNA interaction network. Furthermore, the present study will help to establish potential new candidates for diagnosis and therapy.

## List of Abbreviations

| | |
|---|---|
| % | percent |
| °C | Grad Celsius |
| A | Ampère |
| ADP | adenosine diphosphate |
| AECs | airway epithelial cells |
| Ago2 | Argonaute 2 |
| AIM2 | absent in melanoma 2 |
| AM | alveolar macrophage |
| AMP | adenosine monophosphate |
| APS | ammonium persulfate |
| ATCC | American Type Culture Collection |
| ATG5 | Autophagy Related 5 |
| ATP | adenosine triphosphate |
| AUF1 | AU-rich binding factor 1 |
| BAL | bronchoalveolar lavage |
| BCL10 | B-Cell CLL/Lymphoma 10 |
| BCYE | Buffered charcoal yeast extract |
| BDM | blood-derived macrophage |
| BMDM | bone marrow derived macrophage |
| bp | basebairs |
| BSA | bovine serum albumin |
| CD | cluster of differentiation |
| cDNA | complementary DNA |
| CFU | colony forming unit |
| cGAS | cyclic GMP-AMP synthase |
| ChIP | chromatin-immunoprecipitation |
| circRNA | circular RNA |
| cm | centimeter |
| $CO_2$ | carbon dioxide |
| COPD | chronic obstructive pulmonary disease |
| CRD | carbohydrate-recognition domain |
| Ct | threshold cycle |
| CYR61 | Cysteine Rich Angiogenic Inducer 61 |
| Da | Dalton |
| DALYs | disability-adjusted life-years |
| DAMP | danger associated molecular pattern |
| DCs | dendritic cells |
| DDX58 | DExD/H-Box Helicase 58 |
| DMSO | dimethyl sulfoxide |
| DNA | deoxyribonucleic Acid |
| DNase | deoxyribonuclease |
| dNTP | deoxyribonucleoside triphosohate |
| *dot* | defective in organelle trafficking |
| ds | double stranded |
| ECL | enhanced chemoluminescence |

| | |
|---|---|
| ECM | extracellular matrix |
| EDTA | ethylenediaminetetraacetic acid |
| e.g. | *exempli gratia* (for example) |
| ER | endoplasmatic reticulum |
| ERK | extracellular signal–regulated kinase |
| et al. | *et alii* |
| FACS | fluorescence-activated cell sorting |
| FCS | fetal calf serum |
| Fig. | figure |
| g | acceleration of gravity |
| g | gramm |
| GDP | guanosine diphosphate |
| GFP | green fluorescent protein |
| GM-CSF | granulocyte-macrophage colony stimulating factor |
| GMP | guanosine monophosphate |
| GTP | guanosine-5'-triphosphate |
| h | hour |
| $H_2O$ | water |
| $H_2O_2$ | hydrogen peroxide |
| HAT | histone acetyltransferase |
| HCV | hepatitis C virus |
| HDAC | histone deacetylase |
| HEPES | 4-(2-hydroxyethyl)-1-piperazineethanesulfonic acid |
| HIV | Human immunodeficiency virus |
| HOTAIR | HOX transcript antisense RNA |
| HRP | horseradish peroxidase |
| hsp | Heat Shock Protein |
| HSPA1A | Heat Shock Protein Family A (Hsp70) Member 1A |
| IAV | influenza A virus |
| *icm* | intracellular multiplication |
| i.e. | *id est* |
| IFN | interferon |
| Ig | immunoglobulin |
| IL | interleukin |
| iNOS | inducible nitric oxide synthase |
| IPA | Ingenuity pathway analysis |
| IPS-1 | interferon-beta promoter stimulator 1 |
| IRAK1 | Interleukin-1 receptor-associated kinase 1 |
| IRF | interferon regulatory factor |
| IRS1 | Insulin Receptor Substrate 1 |
| ISGs | interferon-stimulated genes |
| JAK | Janus kinase |
| JNK | c-Jun N-terminale kinase |
| JUN | Jun Proto-Oncogene |
| kDa | kilo Dalton |
| L | liter |

| | |
|---|---|
| LB | lysogeny broth |
| LC3 | Microtubule-associated protein 1A/1B-light chain 3 |
| LCV | *Legionella* containing vacuole |
| LDH | L-Lactate dehydrogenase |
| LGALS8 | Lectin, Galactoside-Binding, Soluble, 8 (galectin-8) |
| lincRNA | long intergenic noncoding RNA |
| lncRNA | long non coding RNA |
| *L.p.* | *Legionella pneumophila* |
| LPS | lipopolysaccharide |
| LRR | leucine-rich repeats |
| m | milli |
| M | Molar |
| MACS | magnetic activated cell sorting |
| MAPK | mitogen-activated protein kinase |
| MAVS | Mitochondrial antiviral-signalling protein |
| M-CSF | macrophage colony-stimulating factor |
| MDA5 | Melanoma Differentiation-Associated protein 5 |
| mg | Milligramm |
| MHC | Major Histocompatibility Complex |
| MIF | mature infectious form |
| min | Minutes |
| miR | microRNA |
| miRISC | miRNA induced silencing complex |
| miRNA | microRNA |
| mL | Milliliter |
| mM | Millimolar |
| mmHg | Millimeter Quecksilbersäule |
| MOI | multiplicity of infection |
| mRNA | messenger RNA |
| MUT | mutated |
| MX1 | MX Dynamin Like GTPase 1 |
| MyD88 | myeloid differentiation primary response protein 88 |
| NaCl | sodium chloride |
| $NAD^+$ | nicotinamide adenine dinucleotide (oxidative form) |
| NADH | nicotinamide adenine dinucleotide (reduced dorm) |
| $NADP^+$ | nicotinamide adenine dinucleotide phosphate (oxidative form) |
| NADPH | nicotinamide adenine dinucleotide phosphate (reduced form) |
| NAT | natural antisense transcript |
| ncRNAs | non-coding RNAs |
| NFAT | nuclear factor of activated T-cells |
| NFκB | nuclear factor kappa-light-chain-enhancer of activated B cells |
| NLR | NOD-like receptor |
| NLRC | NOD-like receptor family CARD domain containing |
| nm | Nanometer |
| NO | nitric oxide |
| NOD | nucleotide-binding oligomerization domain |

| | |
|---|---|
| NP40 | Nonidet P-40 |
| NRON | non-coding repressor of NFAT |
| nt | nucleotides |
| $O_2$ | oxygen |
| OD | optical density |
| PAA | polyacrylamide |
| PAMP | pathogen-associated molecular pattern |
| PBMC | peripheral blood mononuclear cell |
| PBS | Phosphate buffered saline |
| PCA | principal component analysis |
| PCR | polymerase chain reaction |
| PE | phycoerythrin |
| PFA | paraformaldehyde |
| pH | *potentia hydrogenii* |
| piRNA | piwi-interacting RNA |
| PMA | Phorbol-12-myristat-13-acetat |
| PRC2 complexes | polycomb repressive complex 2 |
| pre-miRNA | precursor miRNA |
| pri-miRNA | primary miRNA |
| PRR | pathogen recognition receptor |
| RIG-I | retinoic acid-inducible gene |
| RIN | RNA integrity number |
| RIP2 | receptor interacting protein-2 |
| RISC | RNA-induced silencing complex |
| RNA | ribonucleic acid |
| RNAP | RNA polymerase |
| RNase | ribonuclease |
| RNasin | ribonuclease inhibitor |
| RND3 | Rho Family GTPase 3 |
| RP | replicative phase |
| rpm | rounds per minute |
| RPMI | Rosswell Park Memorial Institute |
| rRNA | ribosomal RNA |
| RT | room temperature |
| SAPK | Stress-Activated Protein Kinase 1c |
| scr | scramble |
| SDS | sodium dodecyl sulfate |
| SDS-PAGE | sodium dodecyl sulfate polyacrylamide gel electrophoresis |
| Sec | Seconds |
| SEM | standard error of the mean |
| Seq | Sequencing |
| SILAC | stable isotope labeling with amino acids in cell culture |
| siRNA | small interfering RNA |
| snRNA | small nuclear RNA |
| snoRNA | small nucleolar RNA |
| SOD1 | Superoxide Dismutase 1 |

| | |
|---|---|
| ss | single stranded |
| STAT1 | Signal transducer and activator of transcription 1 |
| STING | stimulator of interferon genes |
| t | time |
| T2SS | type II secretion system |
| T4BSS | type IV B secretion system |
| T4SS | type IV secretion system |
| Taq | *Thermus aquaticus* |
| TEMED | tetramethylethylendiamine |
| TERC | Telomerase RNA component |
| TIR | Toll/IL-1 receptor |
| TLDA | Taqman Low Density Array |
| TLR | Toll-like receptor |
| TNF | tumour-necrosis factor |
| TP | transmissive phase |
| TP53 | Tumor protein p53 |
| TRAF | TNF receptor associated factor |
| tRNA | transfer RNA |
| TTP | tristetraprolin |
| U | unit |
| USA | United States of America |
| UTR | untranslated region |
| UV | ultraviolet |
| V | Volt |
| vs. | versus |
| WB | western blot |
| WHO | world health organisation |
| WT | wildtype |
| ZFAND2A | Zinc Finger AN1-Type Containing 2A |
| α | Anti |
| Δ | Delta, difference |
| λ | wave length |
| µ | micro |
| µg | microgramm |
| µl | microliter |
| µm | micrometer |

# 1 Introduction

## 1.1 Lower respiratory tract infections

Lower respiratory tract infections are among the leading causes of death worldwide. In 2015, they accounted for 3.2 million deaths (WHO 2017). Five conditions primarily contribute to the respiratory disease burden, including lung cancer, chronic obstructive pulmonary disease (COPD), asthma, tuberculosis and acute respiratory infections. The world Health Organization (WHO) estimates that these lung diseases accounted for one-tenth of the disability-adjusted life-years (DALYs) lost worldwide in 2008. Besides their influence worldwide, respiratory infections are, most notably, the leading cause of death in developing countries (Ferkol and Schraufnagel 2014).

### 1.1.1 Pneumonia as respiratory disease

One form of acute respiratory infection that affects primarily the small air sacs of the lung (alveoli) is pneumonia. Pneumonia is one of the leading causes of death in children worldwide and responsible for 16% of all deaths of children under five years old. In 2015, pneumonia killed 920,136 children under the age of five. It is most prevalent in South Asia and sub-Saharan Africa, but other regions are also affected (WHO 2017). Indeed, pneumonia kills far more children than human immunodeficiency virus or malaria (Wardlaw 2006).

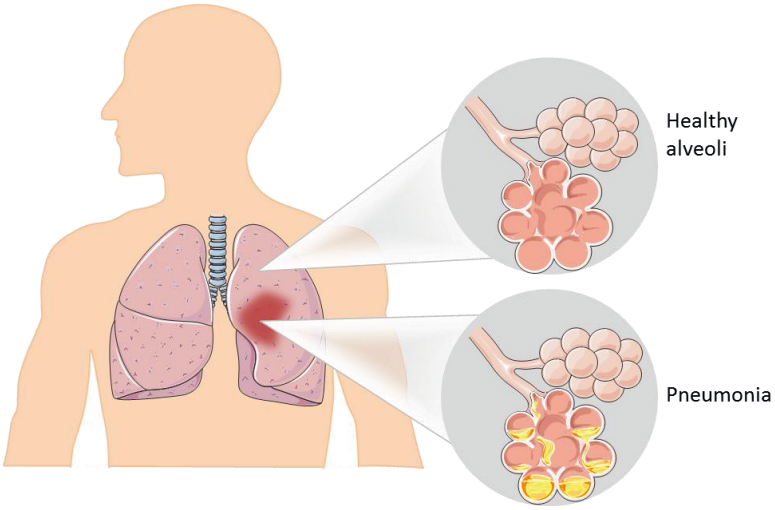


**Figure 1.1: Pneumonia as an acute respiratory infection.** The infection primarily affects the small air sacs (alveoli) of the lung which are then filled with pus and fluid. Therefore, the gas exchange is limited resulting in painful breathing, productive or dry cough, chest pain and fever. In comparison, within healthy alveoli, the oxygen uptake into the blood is functional. Adapted from: https://smart.servier.com.

During pneumonia, the alveoli are filled with pus and fluid, leading to painful breathing and limited oxygen uptake into the blood (WHO 2017). Other symptoms of pneumonia are

productive or dry cough, chest pain and fever (Turkington and Ashby 2007). To confirm diagnosis, chest X-ray and laboratory tests (blood tests, culture of the sputum) are used (Wardlaw 2006). Pneumonia can be life-threatening, but otherwise healthy people can recover within one to three weeks (AmericanLungAssociation 2017). The infection spreads via coughing, sneezing, touching or inhaling contaminated air droplets. It can be prevented by immunization, adequate nutrition, and by addressing environmental factors (WHO 2017). The disease is classified by the location of acquisition as community-acquired, or health care associated pneumonia (NHLBI 2011).

Pneumonia can be caused by different pathogens, including bacteria, viruses, fungi, parasites, or various chemicals (WHO 2017). More than 30 different causes are known. Therefore, understanding the cause of pneumonia is important to find the appropriate therapy. For example, bacterial pneumonia can be treated with antibiotics, but only one third of children with pneumonia receive the appropriate antibiotics (AmericanLungAssociation 2017).

The most common cause of a bacterial pneumonia is *Streptococcus pneumoniae*, affecting over 900,000 Americans every year. However, another important bacterium causing pneumonia is *Legionella pneumophila (L.p.)*. According to estimates, 4% of ambulant pneumonia cases are caused by *Legionella* in Germany (Robert-Koch-Institut 2012). In 2016, the surveillance atlas of infectious disease recorded 7,069 reported cases of Legionnaires' disease in the EU ((ECDC) 2018).

### 1.1.2 Impact of Legionellosis as pneumonic form of infection

Legionellosis describes the pneumonic and the non-pneumonic form of infection with the genus *Legionella* from water or potting mix (WHO 2017).

The non-pneumonic form of legionellosis, also called Pontiac fever, is an acute, self-limiting, influenza-like illness. It lasts usually 2-5 days and has an incubation period varying from a few up to 48 hours. This disease is not life-threatening and associated with symptoms including fever, chills, headache, malaise and muscle pain (myalgia) (WHO 2017).

In contrast, the pneumonic form of legionellosis is also known as Legionnaires' disease. It is characterized as progressive pneumonia with respiratory failure accompanied by multi-organ failure and a death rate of 5 – 30%. The incubation period lasts from 2 to 10 days. Symptoms of this disease are fever, loss of appetite, headache, malaise and lethargy and is often associated with an initial mild cough (WHO 2017).

The exact incidence of Legionnaires' disease is not yet known, according to differences in awareness levels, diagnostic methods, and reporting of the disease in different countries. Generally, it accounts for 2 - 9% of cases of community acquired pneumonia (Stout and Yu

1997). In the USA, the reported incidence of Legionnaires' disease showed an increase of 192% from year 2000 to 2009 (MMWR 2011). Primarily elderly and immuno-compromised people get infected. Furthermore, incidence of the disease seems to be season-dependent, since 62% of all cases occur during summer and early autumn. This fact might be due to better growth and survival conditions for the bacterium including higher humidity (Cunha, Connolly et al. 2015). Moreover, most of the cases were travel-associated and only 4% of cases were attributed to a known outbreak or possible cluster of Legionnaires' disease (Garcia-Vidal, Labori et al. 2013).

For correct treatment of Legionnaires' disease, it first needs to be diagnosed. The Bacteria can be detected by both, culture and non-culture techniques (Cunha, Burillo et al. 2016). One possibility is the urinary antigen detection test. It is the fastest diagnostic technique and recognizes components of the cell wall lipopolysaccharide of *Legionella* serogroup 1 in urine. The test sensitivity is 56 – 99%. Thus, this test does not detect approximately 40% of Legionnaires' disease cases (Helbig, Uldum et al. 2003; Shimada, Noguchi et al. 2009; Jarraud, Descours et al. 2013). The gold standard for detecting Legionnaires' disease is still to sample culture of the lower respiratory tract, since it allows the diagnosis of all *Legionella* spp., outbreak investigation, and further epidemiological studies, or even antimicrobial susceptibility testing (Jarraud, Descours et al. 2013; Pierre, Baron et al. 2017). However, also other techniques are used for detection, including several microscopy methods or nucleic acid amplification-based methods (Murdoch, Podmore et al. 2013; Ratcliff 2013). The advantages of these PCR-based techniques are the detection of other serogroups and species and a higher sensitivity (about 30%) compared to culture-methods, which leads to improved diagnoses (Murdoch, Podmore et al. 2013; Ratcliff 2013). Nevertheless, Legionnaires' disease is underdiagnosed and underreported. In 97% of cases, diagnosis was made by means of urinary antigen testing, and only 5% were confirmed by culture. Since the urinary antigen test can only detect *Legionella* serogroup 1, the test should be used in conjunction with other diagnostic tests as many other species and serogroups are pathogenic (Pierre, Baron et al. 2017). Therefore, better diagnostic tests are needed for detection of all *L.p.* serotypes and species. (Cunha, Burillo et al. 2016).

Given the fact that *Legionella* are intracellular pathogens and invasion is necessary to cause infection, antibiotics should accumulate and be bioactive inside the host cells (Cunha, Burillo et al. 2016). As a first-line of therapy to treat legionellosis, macrolides are used. These are glycosides and inhibit protein biosynthesis of gram-positive and gram-negative bacteria including *Legionella*. In severe cases, Rifampicin is also given (Longo D.L. 2012). Rifampicin blocks the DNA-dependent RNA polymerase, thus specifically preventing bacterial

transcription. The duration of therapy should be at least 14 days and in immune-compromised people, three weeks. Macrolides such as Azithromycin and Clarithromycin are effective and show fast anti-bacterial capacities *in vitro*. Both are often used to treat infections of the respiratory tract and disturb the protein biosynthesis of bacteria. Their application is especially recommended for immuno-compromised people (Longo D.L. 2012).

## 1.2 The genus *Legionella*

The genus *Legionella* consists of 58 different species, three subspecies (Rizzardi, Winiecka-Krusnell et al. 2015) and has more than 80 serogroups. All *Legionella* species were isolated from aqueous environments, such as *Legionella pneumophila* (*L.p.*), *Legionella longbeachae* or *Legionella bozemanii*.

*Legionella* are ubiquitous in aquatic habitats at temperatures between 25°C and 55°C (optimal at 35°C) (WHO 2017). In nature, the pathogen survives as an intracellular parasite of amoeba, ciliated protozoa, or slime moulds (Fields, Benson et al. 2002). *Legionella* infects amoeba including *Hartmannella, Acanthamoeba* and *Naegleria* which can be found in naturally occurring biofilms (Rowbotham 1986; Fields 1996; Fields, Benson et al. 2002; Abdel-Nour, Duncan et al. 2013). *Legionella* also inhabits human-made environments, including water pipes, air-conditioning systems, cooling towers, fountains and spa baths (Fraser, Deubner et al. 1979; Sethi and Brandis 1983; Spitalny, Vogt et al. 1984). In nature, low abundances of *Legionella* are found in aquatic habitats, while it inhabits human-made aquatic environments in higher numbers (Eisenreich and Heuner 2016).

Some species and serogroups are more virulent than others and can cause infections in humans. The majority of human infections are caused by *Legionella pneumophila* serogroup 1 (Fields 1996; Yu, Plouffe et al. 2002). *Legionella pneumophila* is also the most common causative agent of Legionnaires' disease (WHO 2017).

### 1.2.1 *Legionella pneumophila*

*Legionella pneumophila* is a rod-shaped bacterium with strict growth requirements for iron and cysteine. It is a non-encapsulated, aerobic bacillus with a single polar flagellum. The size of the pathogen is approximately 2 µm in length and 0.3 – 0.9 µm in width (Lederberg 2000). As a gram-negative bacterium, it is surrounded by a cell wall consisting of a double set of covering membranes. The inner membrane encloses the bacterial cytoplasm, whereas the outer membrane covers the inner membrane and consists of phospholipids, lipopolysaccharides (LPS) and also carries proteins (Beveridge 1999).

The first recognized occurrence of this pathogen was in 1976 in the Bellevue-Stratford Hotel in Philadelphia. During that time a convention for veterans of the American legion was hosted by the hotel and 182 of 4400 persons became acutely ill, often associated with pneumonia. Overall, the 182 cases resulted in 29 deaths and the hospitalization of 147 people (Fraser, Tsai et al. 1977). One year later, the causative agent could be isolated from lung tissue of a fatality and subsequently identified as a gram-negative bacterium. Therefore, it was termed *Legionella pneumophila*, which reflects both its victims and the newly described Legionnaires' disease (Brenner, Steigerwalt et al. 1979).

The general route of infection in humans is via the inhalation of contaminated aerosols (Arnow, Chou et al. 1982; Cunha, Burillo et al. 2016). Another less common mode is for example direct contact with surgical wounds (Johnson, Yu et al. 1985; Marrie, Haldane et al. 1991). Humans are accidental dead-end hosts for *Legionella* and therefore, the transmission from human to human is generally not observed, but there may be exceptions. One case has been described where a probable person-to-person transmission of *L.p.* serogroup 1 occurred in Portugal in 2014 (Borges, Nunes et al. 2016; Correia, Ferreira et al. 2016). However, aerosol producing systems such as cooling towers, hot tubs, industrial equipment, domestic plumbing systems, thermal spas, water outlets, respiratory devices and nebulisers, or nasogastric tubes in hospitals leading to the spread of the pathogen and are often associated with outbreaks of Legionnaires' disease in humans (Cunha, Burillo et al. 2016; WHO 2017). For example, hospital-acquired Legionnaires' disease has been connected to the presence of *Legionella* in the water supply (Stout, Yu et al. 1982). Studies have shown that *Legionella* spp. was detectable in hot water distribution systems in 12 – 70% of hospitals (Lin, Stout et al. 1998). A further risk for disease acquisition is augmented exposure to the source harbouring *Legionella* which comprises the frequency and duration of exposure (Mandell, Bennett et al. 2010). Furthermore, the likelihood of an infection depends on the virulence of the bacteria, the concentration, the effectiveness of dissemination, and the aerosol type (Cunha, Burillo et al. 2016). After transmission to the human lung, bacteria are infecting alveolar macrophages. *Legionella* replicate within macrophages, leading to inflammation and pneumonia (Newton, Ang et al. 2010; Copenhaver, Casson et al. 2014). In Germany, the last big outbreak occurred in Warstein in summer 2013 with 78 laboratory-confirmed cases, including two fatalities (Maisa, Brockmann et al. 2015). *Legionella pneumophila* serogroup 1 could be identified to be responsible for the epidemic. The sources harbouring the epidemic strain were cooling towers of different companies, the waste water treatment plants of the city and one company as well as water samples of the river and its branches (Petzold, Ehricht et al. 2017). This represented the biggest *Legionella pneumophila* outbreak in Germany to date.

### 1.2.2 The *Legionella* intracellular life cycle

The innate ability of *Legionella* to multiply within different protozoa has equipped the pathogen with the capacity to replicate in human alveolar macrophages. As *L.p.* has the ability to infect amoeba and macrophages, combined with the fact that only one case of human-to-human transmission has been described, has led to the hypothesis that the interaction of *L.p.* with amoeba has equipped the bacteria with the factors allowing replication within human macrophages (Newsome, Baker et al. 1985; Cianciotto and Fields 1992; Franco, Shuman et al. 2009; Al-Quadan, Price et al. 2012). Thus, *Legionella* uses amoeba as 'training grounds' for replication in human macrophages (Molmeret, Horn et al. 2005). Both, free-living amoeba and human macrophages are eukaryotic cells which share conserved molecular pathways targeted by *L.p.* (Molmeret, Horn et al. 2005; Al-Quadan, Price et al. 2012; Richards, Von Dwingelo et al. 2013).

*L.p.* exhibits at least a biphasic life-cycle (Rowbotham 1986; Byrne and Swanson 1998; Garduno, Garduno et al. 2002; Molofsky and Swanson 2004). The appearance of further life stages or forms were also discussed (Robertson, Abdelhady et al. 2014). Briefly, *L.p.* alternates between a transmissive (virulent) and replicative (avirulent) form. In the replicative form, *L.p.* multiplies within the *Legionella* containing vacuole (LCV) inside the host or in media and is non-motile and non-cytotoxic. It stays in this form as long as sufficient nutrients and living space are available. When nutrients become scarce, *L.p.* differentiates into the transmissive form. In protozoa, it changes into a flagellated spore-like mature infectious form (MIF) that is stress-resistant and almost metabolically dormant (Rowbotham 1986; Byrne and Swanson 1998; Heuner, Brand et al. 1999; Garduno, Garduno et al. 2002; Hammer, Tateda et al. 2002; Greub and Raoult 2003; Molofsky and Swanson 2004; Abdelhady and Garduno 2013). Thus, differences in morphology, motility, pathogen metabolism and gene expression controlled by regulatory systems are detectable between the two life stages (Molofsky and Swanson 2004).

The lifecycle of *Legionella* in protozoa was first described by Timothy Rowbotham who could show that *L.p.* is able to infect amoeba (Rowbotham 1983). The infection cycle starts with the adhesion of the bacterium to the host cell. It is followed by cell entry as one of the most important steps, which requires the flagellum, pili and bacterial surface proteins, such as major outer membrane proteins, heat shock proteins, and the mip protein (Cunha, Burillo et al. 2016). The mip gene was the first detected gene associated with macrophage infectivity of *L.p.* (Engleberg, Carter et al. 1989). The method of internalization by eukaryotic cells is still not completely understood. Several competing theories differ on whether it is a host-directed response or driven by the pathogen. In general, internalization of the bacteria depends on the host cell type and bacterial strain. Phagocytes usually take up bacteria by conventional

phagocytosis (Newton, Ang et al. 2010). The less common coiling phagocytosis has been observed for the uptake of *L.p.* in mammalian cells and amoeba (Horwitz 1984; Bozue and Johnson 1996). Another form of internalization such as macropinocytosis was found in bone marrow-derived macrophages (Watarai, Derre et al. 2001). Further mechanisms of uptake include the zipper-like conventional phagocytosis or the opsonin-dependent phagocytosis (Reynolds and Newball 1974; Rechnitzer and Blom 1989). The ability of *L.p.* to infect non-professional phagocytes such as HeLa epithelial cells suggests the hypothesis of an uptake that is cell-dependent (Dreyfus 1987; McCusker, Braaten et al. 1991).

In the second step of the infection process, internalized *L.p.* employs its type IV B secretion systems (T4BSS) to form the LCV in which the bacterium differentiates into the replicative form for efficient replication (Isberg, O'Connor et al. 2009). *Legionella* possess two protein secretion systems: Lsp type II secretion system (T2SS) and Dot/Icm type IV secretion system (T4SS). Both play major roles in the pathogenesis of *Legionella* (Cianciotto 2013; Kubori and Nagai 2016). In T2SS, protein substrates are first translocated across the inner membrane. When T2SS pilus-like apparatus is active, the proteins exit the bacterial cell through a specific outer membrane pore (Nivaskumar and Francetic 2014). It was shown that the T2SS secretes over 25 proteins, including 18 confirmed enzymes and novel proteins, which seem to be unique for *Legionella* (DebRoy, Dao et al. 2006; Tyson, Pearce et al. 2013). Via the Dot/Icm type IV secretion system (T4SS), *L.p.* secretes over 330 effector proteins to promote the formation of the LCV and its own replication. Many bacterial pathogens use dedicated translocation systems to deliver arsenals of effector proteins to their hosts, but *L.p.* maintains the largest arsenal of effectors.

Once inside the host cytosol, these effectors modulate eukaryotic cell biology to acquire nutrients, block microbial degradation, subvert host defences, and enable pathogen transmission to other hosts (Ensminger 2016). Therefore, the T4BSS is crucial for replication of *L.p.* within amoeba and macrophages. The Dot/Icm secretion system is a multiprotein apparatus. It is encoded by the *dot/icm* (*dot*: defective in organelle trafficking; *icm*: intracellular multiplication) genes which are highly conserved among all *Legionella* species (Berger and Isberg 1993; Brand, Sadosky et al. 1994). About 10% of the genome of *L.p.* code for these effector proteins (Al-Quadan, Price et al. 2012) and many of them possess eukaryotic-like domains. Thus, *L.p.* is able to modulate host cell function by interaction with host proteins and organelles (Cazalet, Rusniok et al. 2004; de Felipe, Glover et al. 2008; Nora, Lomma et al. 2009; Hubber and Roy 2010; Rolando and Buchrieser 2012). The mutant strain dotA, which has no functional T4SS, lacks the capacity to replicate within the host and the ability to escape from the phagosome-lysosome fusion, a hallmark feature of *Legionella* infections (Berger, Merriam et al. 1994; Tilney, Harb et al. 2001).

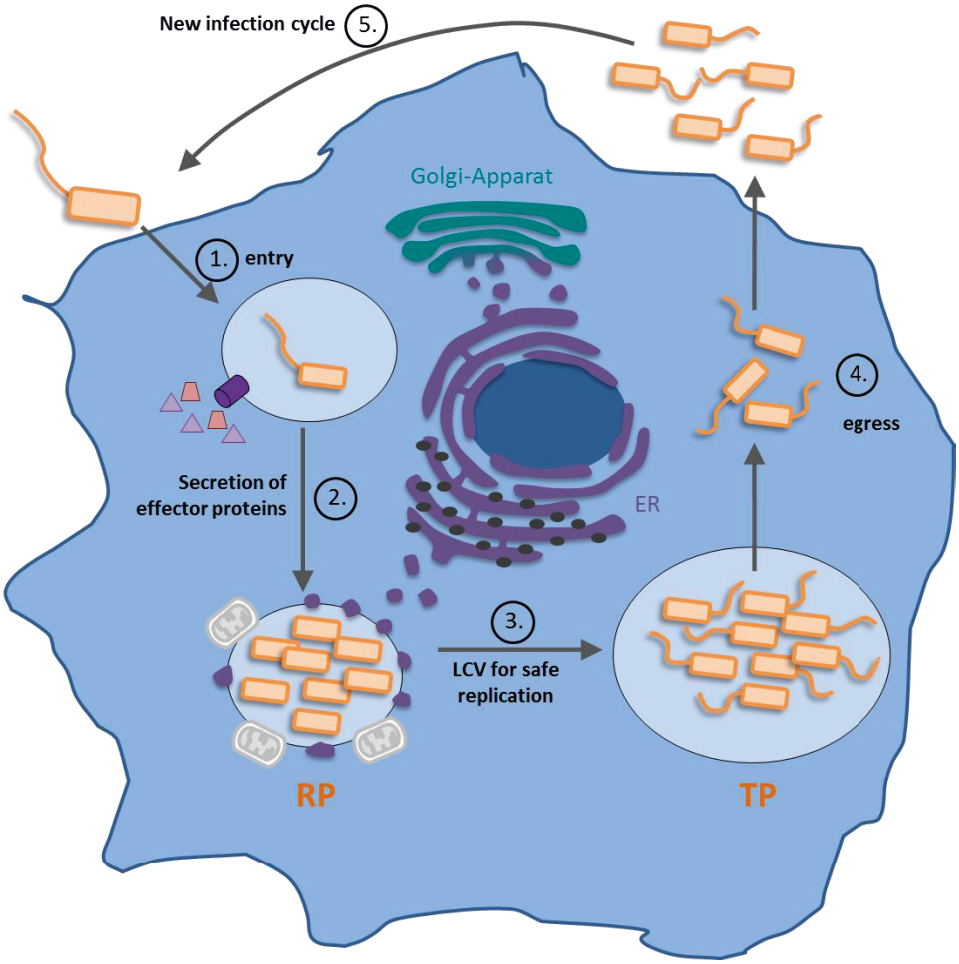


**Figure 1.2: Biphasic life cycle of *Legionella pneumophila*.** 1.) *Legionella pneumophila* (*L.p.*) adheres to the host cell and is taken up within the phagosome. 2.) *L.p.* secretes over 330 effector proteins into the host cell cytosol via the T4BSS to establish the LCV. *L.p.* recruits ER vesicles and mitochondria to the LCV and replicates safely within the LCV (replicative phase). 3.) When nutrients became limited, the bacterium differentiates into the flagellated transmissive form. 4.) *L.p.* is released into the host cell cytosol which results in the egress of the bacteria. 5.) A new infection cycle starts with the initiation of infection of neighbouring host cells. ER, endoplasmic reticulum; LCV, *Legionella* containing vacuole; RP, replicative phase; TP, transmissive phase; T4BSS, type 4 b secretion system. Adapted from: Eisenreich and Heuner, FEBS Letters, 2016.

The LCV is negative for canonical markers of the endocytic pathways such as Rab5 for early endosomes, Rab7 for late endosomes and Lamp-1 for lysosomes (Roy, Berger et al. 1998; Clemens, Lee et al. 2000). Thus, a LCV does not undergo acidification and maintains a pH ~6.1 and prevents fusion with the lysosome (Horwitz 1983b; Horwitz 1983a; Horwitz and Maxfield 1984). The escape from phagosome lysosome fusion is a hallmark of *Legionella* pathogenesis. Since mutant strains lacking this capacity are not able to multiply within human macrophages, it is essential for virulence (Horwitz 1987). Through the injection of effector proteins by the T4SS, the LCV is surrounded by mitochondria, ribosomes and smooth vacuoles derived from the endoplasmatic reticulum (ER). Thus, membrane thickness of LCV changes to resemble that of the ER within the first 15 minutes post infection (Horwitz 1983b; Tilney, Harb et al. 2001).

Furthermore, small GTPases such as Rab1, Sar1 and ADP ribosylation factor 1 (Arf1) are targeted by bacterial effector proteins and are subsequently recruited to the LCV. These are fused to the LCV and critical for ER-to-Golgi trafficking. At four hours post infection, ER-derived structures as well as mitochondria start to disappear from the LCV and ribosomes are recruited to the LCV resulting in a rough ER-like vacuole.

In the third step of the infection procedure, *L.p.* inhibits the bactericidal activity of the phagocyte and converts the phagosome into a safe intracellular niche for its replication (Escoll, Rolando et al. 2013). After replication within the LCV, when nutrients become limited, *L.p.* differentiates into the flagellated transmissive form (Garduno, Garduno et al. 2002). Afterwards, *L.p.* eventually ruptures the LCV membrane by pore formation and membrane lysis (Kirby, Vogel et al. 1998; Alli, Gao et al. 2000). The release into the host cell cytosol is hypothesized to cause disintegration of the plasma membrane and structural and functional disruption of cytoplasmic organelles. This results in host cell osmotic lysis and subsequently in the egress of the bacteria into the extracellular milieu. Then, a new infection cycle can start with the initiation of infection of neighbouring host cells.

## 1.3 Immunity

The immune system faces daily exposure to millions of potential pathogens, such as bacteria or viruses. The transmission of these pathogens can occur through direct contact, ingestion, and inhalation. In order to cope with those pathogens and to protect the host against microbial infections mammals have developed a highly specific immune system consisting of an innate and an adaptive immune system, which cooperate.

A single bacterium can produce almost 20 million progeny in a single day with a doubling time of one hour. Thus, to fight infections, the innate immune system is needed for initial protection and fast immune response (Alberts 2002). The adaptive immune system activates innate effector mechanisms in an antigen-specific manner. This immune response remembers previous contacts with specific pathogens and destroys them upon re-infection (Alberts 2002; Medzhitov 2007). The adaptive immune response comprises the activation and expansion of specific clones of B and T cells. Therefore, the adaptive immune response against a new pathogen can take a week before it is effective. Furthermore, the adaptive immune system requires the stimulation and activation of the innate immune system through antigen presenting cells such as macrophages (Medzhitov 2007). Therefore, the innate immune response is important for both, the fast defence against pathogens and the activation of the adaptive immune system.

### 1.3.1 Innate Immunity

The innate immune system represents the first line of defence and is not specific to particular pathogens (Alberts 2002). It is an older evolutionarily defence strategy comprising conserved regulatory mechanisms and found in multiple organisms such as plants, fungi, insects, and primitive multicellular organisms (Murphy, Travers et al. 2012). The innate immune system consists of a humoral as well as a cellular section that recognizes conserved features of pathogens and is quickly activated to destroy invaders.

The humoral part is mainly represented by the complement system which marks the pathogens for destruction. It consists of about 20 interacting soluble proteins mainly originating in the liver and primarily produced by hepatocytes. The plasma proteins are circulating in the blood and extracellular fluid and are inactive until the invasion of a pathogen. They were originally identified by their ability to "complement" the action of antibodies to clear pathogens (Alberts 2002). In short, the complement system helps to identify bacteria, activates cells and promotes the clearance of opsonized antigens or dead cells.

In contrast, the cellular part of the innate immune system possesses different cell types from the hematopoietic lineage that originates in the bone marrow (Alberts 2002). Those innate leukocytes include natural killer cells, eosinophils, basophils, mast cells and the phagocytic cells such as macrophages, neutrophils, and dendritic cells (Murphy, Travers et al. 2012). The cells from the innate immune system need to differentiate self from non-self. Therefore, the innate immune system relies on the recognition of molecules that are absent in the host, but common to many pathogens. These so called PAMPs stimulate two types of innate immune responses, the inflammatory response by the secretion of cytokines, and phagocytosis by macrophages and neutrophils. Both responses are very quick, act within minutes and occur even if the host has never been previously exposed to this kind of pathogen (Alberts 2002). In summary, the major functions of the innate immune system are the opsonisation of pathogens for phagocytosis through the complement system, the recruitment of immune cells to sites of infection through production of chemotactic factors such as cytokines, and the identification and elimination of pathogens that might cause infection (Alberts 2002; Murphy, Travers et al. 2012).

### 1.3.2 Pathogen recognition

Since innate immune recognition is based on the detection of molecular structures that are unique to microorganisms, innate leukocytes express pattern recognition receptors (PRRs) (Medzhitov 2007; Murphy, Travers et al. 2012). These PRRs have broad pathogen specificity and are able to bind to a large number of pathogen-associated molecular patterns (PAMPs)

which have common structural motifs or patterns. PAMPs are often molecules that are invariant among microorganisms of a given class, are products of pathways that are unique to microorganisms or have essential roles in microbial physiology. Bacterial PAMPs are for example components of the cell wall, such as lipopolysaccharide, peptidoglycan, lipoteichoic acids and cell-wall lipoproteins. The detection of viral components via the innate immune system is different, because all viral components are synthesized within host cells. Therefore, the main targets of immune recognition are viral nucleic acids. The differentiation of self and external nucleic acids is based on structural modifications which are unique to viral RNA and DNA (Medzhitov 2007).

The PRRs include several distinct classes such as Toll-like receptors (TLRs), NOD-like receptors (NLRs) and cytosolic nucleic acid sensors. The best described and investigated class are the TLRs. They are type I transmembrane proteins containing an extracellular domain with leucine-rich repeats (LRRs) and a cytoplasmic tail with a conserved region called the Toll/IL-1 receptor (TIR) domain (Gay, Gangloff et al. 2006). TLRs are evolutionarily conserved receptors and received their name from their similarity to the toll gene, first identified in *Drosophila* in 1985. These receptors were found to be important during the defence against microbial infection (Hansson and Edfeldt 2005). In humans, 11 different TLRs are described, whereas in mice 13 different TLRs are known (Mahla, Reddy et al. 2013). TLRs are transmembrane proteins which are located on the membranes of innate leukocytes including dendritic cells, macrophages and natural killer cells. However, cells of the adaptive immune system (T and B lymphocytes) and non-immune cells (epithelial cells, endothelial cells, fibroblasts) also express several TLRs (Delneste, Beauvillain et al. 2007). During the immune response TLRs activate tissue-resident macrophages to produce pro-inflammatory cytokines such as tumour-necrosis factor (TNF), interleukin-1β (IL-1β) and interleukin-6 (IL-6). Those secreted cytokines trigger the local and systemic inflammatory response leading to the recruitment of leukocytes to the site of infection and the prevention of pathogen spreading. Furthermore, IL-1ß and IL-6 activate hepatocytes to produce acute-phase proteins which activate the complement system and opsonize pathogens for phagocytosis by macrophages and neutrophils. Additionally, TLRs directly trigger an inflammatory response of macrophages by inducing the production of antimicrobial proteins and peptides for pathogen defence. However, all exact functions of TLRs in antimicrobial defence are not examined, yet, but in general, TLRs elicit inflammatory and antimicrobial responses upon activation by their specific ligands (Medzhitov 2007).

### 1.3.3 Macrophages as first line of defence

One major function of the innate immune system is the activation of professional phagocytes to eliminate invading pathogens or particles. Professional phagocytes are distinguished from non-professional phagocytes according to how effective they are at phagocytosis. Professional phagocytic cells express a multitude of receptors on their surfaces for the recognition of signals that are not normally found in healthy tissues, such as TLRs. Those cells are, besides macrophages, monocytes and DCs, along with neutrophils and mast cells (Mantovani, Rabinovitch et al. 1972). Macrophages mainly arise from myeloid precursors located in the bone marrow and are the most efficient phagocytes. The precursors are released into circulation as monocytes. Their role is to replenish the pool of tissue-resident macrophages and DCs in steady state and in response to inflammation. The spleen serves as reservoir for immature monocytes. After migration of the monocytes, they differentiate into macrophages or dendritic cells (Geissmann, Manz et al. 2010). Macrophages are able to migrate outside of the vascular system to sites of pathogen invasion. The binding of bacterial molecules to surface receptors triggers phagocytosis and the destruction of pathogens. Briefly, tissue-resident macrophages are the first line of defence against extrinsic invaders and coordinate leukocyte penetration in innate immunity. Phagocytic macrophages maintain the equilibrium between antigen removal by phagocytosis and degradation of microbes, apoptotic cells, and neoplastic cells (Gordon 2003).

Two hallmarks of macrophages are diversity and plasticity. Two phenotypes exist for macrophage polarization, which can be activated in a variety of different ways: Classically activated M1 and alternatively activated M2 macrophages. Numerous pathways of signal transduction, transcriptional and post-transcriptional networks of regulation are involved in the polarization process of macrophages. Classically activated macrophages (M1) have antimicrobial and tumoricidal activities and release pro-inflammatory cytokines which retard cellular proliferation surrounding the tissue leading to tissue damage. In contrast, alternatively activated macrophages (M2) secrete anti-inflammatory cytokines leading to wound healing and tissue repair. M2 macrophages are linked to immunosuppression, tumorigenesis and elimination of parasites. These macrophages are further sub-categorized into M2a, M2b, M2c and M2d based upon gene expression profile (Arora, Dev et al. 2017). The nomenclature of polarized macrophage populations is still a matter under discussion. Murray and colleagues claim that researchers should describe stimulation scenarios and adopt a nomenclature linked to the activation standards and avoid M2a, M2b and so forth (Murray, Allen et al. 2014). Nevertheless, overshooting imbalance in M1/M2 activation may have detrimental effects which can result in disease or inflammation (Wang, Liang et al. 2014).

Phenotypic differentiation depends on a variety of different stimuli including the tissue microenvironment, microbes, or their products. Macrophages can be stimulated to M1 macrophages by the release of IFN-γ. Furthermore, a combination of IFN-γ with microbial stimuli like lipopolysaccharide (LPS) or other cytokines such as granulocyte-macrophage colony stimulating factor (GM-CSF) and TNF-α lead to the M1 phenotype of macrophages (Martinez and Gordon 2014; Murray, Allen et al. 2014).

A *Legionella* infection of human macrophages results in an M1-like phenotype. The recognition of *L.p.* in human macrophages is described in the following section.

### 1.3.4 Sensing of *Legionella pneumophila* in macrophages

The innate immune system recognizes *L.p.* by different PRRs such as TLRs, NLRs and cytosolic acid sensors (Massis and Zamboni 2011; Cunha and Zamboni 2014; Naujoks, Lippmann et al. 2017).

TLRs are expressed on the membranes of innate leukocytes for the recognition of pathogen structures. TLR2 is activated by lipopeptides and lipoproteins, which are cell wall components of *Legionella*. Furthermore, lipidA signals via TLR2 to induce the expression of CD14. Other co-receptors influencing agonist-TLR2 interaction, are CD36 and integrins (van Bergenhenegouwen, Plantinga et al. 2013). The LPS of *Legionella* is mainly recognized by TLR2 (Akamine, Higa et al. 2005; Shim, Kim et al. 2009). The atypically LPS structure of *Legionella* is unique and supports adherence to the membrane of target cells including alveolar macrophages. Moreover, it differs from the LPS structure of other bacteria such as *Salmonella typhimurium* (Zahringer, Knirel et al. 1995). A recent study suggests that *Legionella* might be able to partly evade TLR2-mediated recognition in humans via its type 2 secretion system (T2SS) (Mallama, McCoy-Simandle et al. 2017). Nevertheless, this receptor is critical to the outcome of *L.p*. infections in mice as previously demonstrated. Mice deficient in the *tlr2* gene showed impaired cytokine production and an increased susceptibility to bacterial replication in the lungs (Hawn, Smith et al. 2006). Aside from this, TLR5 senses flagellin of *Legionella* and plays an important role in *Legionella* infection in humans (Hawn, Berrington et al. 2007). Since a stop codon polymorphism in the gene of TLR5 has been shown to be linked with susceptibility to Legionnaires' disease (Hawn, Verbon et al. 2003). Endosomal TLR9 is activated by bacterial DNA in the phagosome (Newton, Perkins et al. 2007). Mice lacking TLR9 produced less cytokines after *Legionella* infection. Therefore, these mice were more permissive of *Legionella* replication in the lungs (Newton, Perkins et al. 2007). Generally, all mentioned TLRs lead to activation of the adapter molecule myeloid differentiation primary response protein 88 (MyD88) which mediates the downstream NFκB-dependent production of pro-inflammatory

mediators, such as TNF-α and various other cytokines (Archer and Roy 2006; Archer, Alexopoulou et al. 2009).

In addition to the TLR-mediated recognition of *Legionella*, NOD1 and NOD2 are activated by *Legionella* cell wall peptidoglycan leading to activation of NFκB, mediated by receptor interacting protein-2 (RIP2). Knockout studies with mice deficient in both NLRs NOD1 and NOD2 or deficient in RIP2 revealed impaired neutrophil recruitment and reduced bacterial clearance during lung infection (Frutuoso, Hori et al. 2010). Moreover, the NLRs NAIP5 and NLRC4 form a multiprotein complex called the inflammasome (NAIP5/NLRC4 inflammasome), which recognizes intracellular flagellin delivered by the T4SS of *Legionella* (Ren, Zamboni et al. 2006; Lightfield, Persson et al. 2008; Lightfield, Persson et al. 2011; Pereira, Morgantetti et al. 2011; Kortmann, Brubaker et al. 2015). This inflammasome-complex contributes to caspase-1 activation to regulate production of IL-1β and IL-18, and to restrict *L.p.* growth in human macrophages and mice. The restriction of *Legionella* growth also relies on gasdermin D-dependent cell death called pyroptosis due to pore formation and on the induction of the fusion of LCV and lysosome (Molofsky, Byrne et al. 2006; Ren, Zamboni et al. 2006; Shi, Zhao et al. 2015). This observation is confirmed by a study showing that the non-flagellated *Legionella* species *L. longbeachae* fails to trigger pyroptosis and is not restricted by the NAIP5/NLRC4 inflammasome (Pereira, Marques et al. 2011).

Another crucial pathway for sensing *Legionella* is the detection of bacterial nucleic acids in the cytosol. *Legionella*-DNA is recognized by the DNA sensor cyclic GMP-AMP synthase (cGAS), which directly binds DNA. The binding mediates the production of the second messenger cyclic 2'3'-GMP-AMP (2'3'-cGAMP), which in turn activates STING-dependent signalling (Sun, Wu et al. 2013; Watson, Bell et al. 2015). In contrast, intracellular *Legionella*-RNA is detected by the cytosolic RNA sensors RIG-I (retinoic acid-inducible gene I) which is encoded in humans by the DDX58 gene. RIG-I is part of the RIG-I-like receptor family, which also includes MDA5 (Melanoma Differentiation-Associated protein 5). Both, RIG-I and MDA5, are involved in the activation of MAVS (Mitochondrial antiviral-signalling protein), also known as IPS-1 (Hou, Sun et al. 2011). Thus, STING-dependent signalling and activation of MAVS leads to the activation of the transcription factor interferon regulatory factor 3 (IRF3). IRF3 is phosphorylated by the serine/threonine-protein kinase TBK1 triggering the secretion of type I interferons (IFNs) including IFN-α and IFN-β (Opitz, Vinzing et al. 2006; Stetson and Medzhitov 2006; Lippmann, Muller et al. 2011). Type I IFNs in turn strongly activate macrophage-intrinsic defence mechanisms and, together with IFNγ, induce antibacterial clearance *in vivo* (Lippmann, Muller et al. 2011; Naujoks, Tabeling et al. 2016).

Furthermore, cytosolic DNA is also sensed by the AIM2 inflammasome composed by the cytosolic helicase AIM2. It directly binds the *Legionella*-DNA and uses the adaptor protein ASC to trigger the activation of caspase-1 leading to pyroptosis and production of IL-1α and IL-1β (Burckstummer, Baumann et al. 2009; Fernandes-Alnemri, Yu et al. 2009; Hornung, Ablasser et al. 2009).

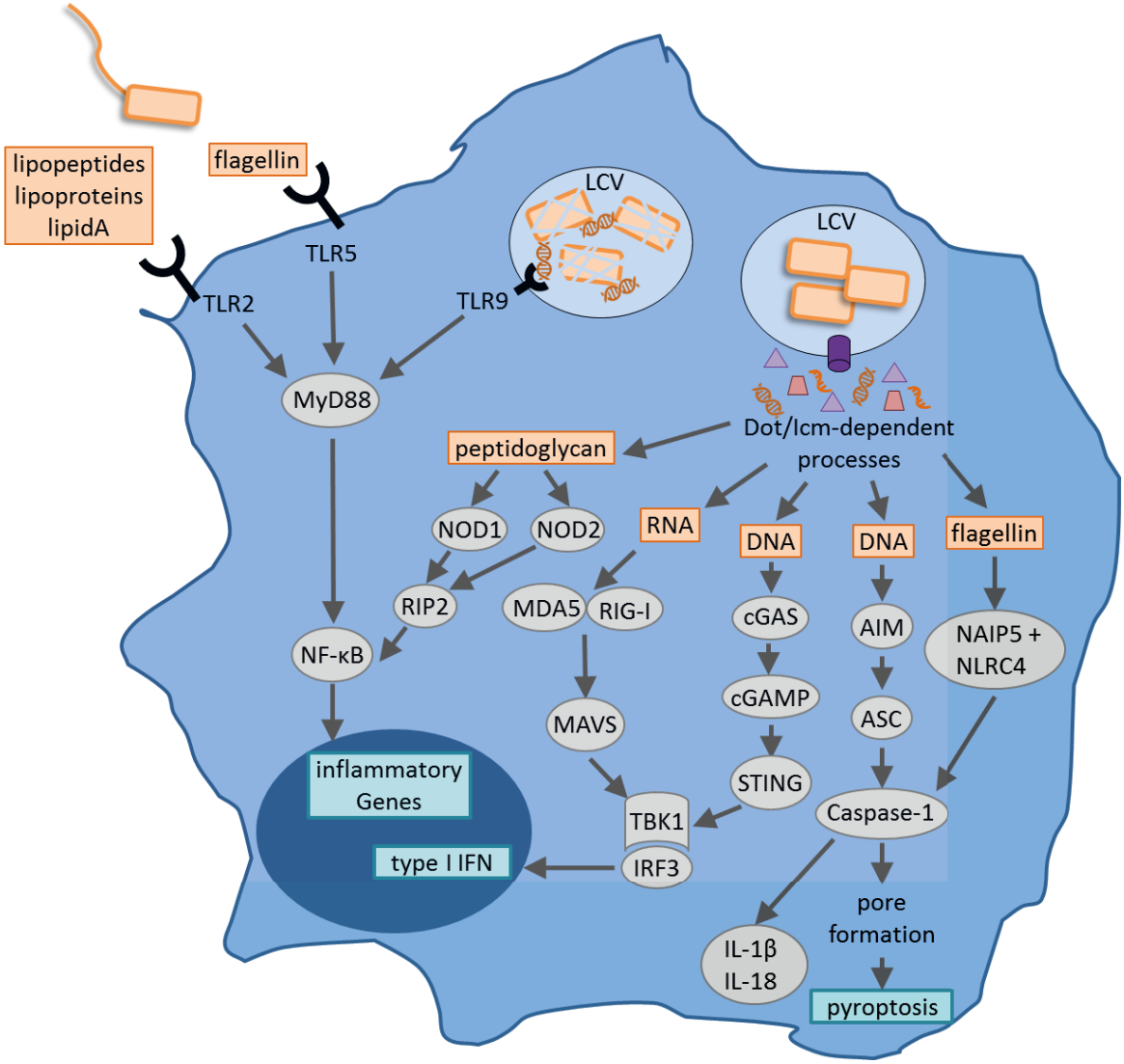


**Figure 1.3: Overview of the innate immune sensing of *Legionella* in macrophages.** *L.p.* is recognized by TLR2 and TLR5 on the cell surface and by TRL9 in the phagosome. All TLRs displayed activate NFκB via MyD88 to induce production of pro-inflammatory mediators. Additionally, NOD1/NOD2, RIG-I and MDA5, cGAS, AIM inflammasome and NAIP5/NLRC4 sense bacterial peptidoglycan, RNA, DNA and flagellin, which are localized in the host cell cytosol through the T4SS. NAIP5/NLRC4 and AIM form an inflammasome leading to the activation of Caspase-1 and thus to the production of IL-1β and IL-18 and pyroptosis. NOD1 and NOD2 signal via RIP2 to stimulate the expression of NFκB-dependent pro-inflammatory genes. The DNA sensor cGAS induces the expression of type I IFNs including IFN-α and INF-β via STING, TBK1 and IRF3 signalling. Moreover, the RNA-sensor RIG-I and MDA5 as well as their adapter molecule MDA5 might contribute to the production of type I IFNs via TBK1 and IRF3. Adapted from: Massis and Zamboni, frontiers in Microbiology, 2011)

## 1.4 Non-coding RNAs of eukaryotes

Non-coding RNAs (ncRNAs) are RNA molecules that are not translated into proteins. Although 98.5% of the human genome is comprised of non-protein coding DNA sequences, most of the genome is transcribed into RNA (Birney, Stamatoyannopoulos et al. 2007; Lander 2011). The exact number of non-coding RNAs is unknown, but according to bioinformatics and transcriptomics analyses the predicted number is more than several thousands (Birney, Stamatoyannopoulos et al. 2007; Washietl, Pedersen et al. 2007; Morris 2012).

The majority of studies so far have focused on the function of proteins, but comparably less is known about the function of ncRNAs (Carninci, Kasukawa et al. 2005; Kapranov, Cheng et al. 2007). Although many ncRNAs were considered to be non-functional (junk RNA), studies have shown that ncRNAs play important roles in the regulation of gene expression
(Palazzo and Lee 2015). Different classes of non-coding RNAs contribute to many cellular processes such as gene expression regulation, cell differentiation, RNA maturation, protein synthesis and development (Chen, Satpathy et al. 2017). ncRNAs can be separated into two groups: (1) classical housekeeping RNAs which are constitutively expressed and play critical roles in protein biosynthesis including ribosomal RNAs (rRNAs), transfer RNAs (tRNAs), small nuclear RNAs (snRNAs) and small nucleolar RNAs (snoRNAs); and (2) regulatory RNAs that comprise small regulatory RNAs such as microRNAs (miRNAs), silencer RNAs (siRNAs), piwi-interacting RNAs (piRNAs) and long non-coding RNA (lncRNAs) (Wu, Su et al. 2016). In the following sections, the major functions of long non-coding RNAs and miRNAs will be highlighted.

### 1.4.1 Long non-coding RNAs

LncRNAs are transcripts with a length greater than 200 nucleotides which do not encode a protein (Iyer, Niknafs et al. 2015). In mammals, lncRNAs are mainly transcribed by RNA polymerase (RNAP) II or III and are capped, polyadenylated and spliced in the same manner as that of mRNAs (Struhl 2007; Bierhoff, Schmitz et al. 2010; Rinn and Chang 2012). No defining biochemical features can be exclusively ascribed to lncRNAs (Mercer and Mattick 2013). lncRNAs were first described as a transcript class during the large-scale sequencing of full-length cDNA libraries in mice (Okazaki, Furuno et al. 2002). It could be shown that humans also express lncRNAs. Genome wide transcriptome studies in humans have led to the discovery and annotation of nearly 50,000 lncRNA genes (Iyer, Niknafs et al. 2015). Most annotated lncRNAs are expressed at lower levels than mRNAs and are cell type specific (Atianand, Caffrey et al. 2017). Thus, RNA sequencing data of multiple developmental stages and tissue types are necessary to achieve comprehensive annotations (Cabili, Trapnell et al. 2011; Derrien, Johnson

et al. 2012). According to literature, lncRNAs can be classified based on their genomic location with respect to nearby proteins or based on their function.

According to their genomic location, lncRNAs can be separated into long intergenic noncoding RNAs (lincRNAs), intronic lncRNAs, natural antisense transcripts (NATs), sense lncRNAs, and bidirectional lncRNAs. With the exception of lincRNAs, the other classes often show some degree of overlap with nearby protein-coding genes (Wu, Su et al. 2016; Atianand, Caffrey et al. 2017). LincRNAs are located in the intergenic region between two protein-coding genes, while intronic lncRNAs are transcribed within the introns of protein-coding genes. Therefore, they contain no sequence complementarity to the mature, spliced mRNA of the protein-coding gene. In contrast, NATs are transcribed from the complementary strand of a protein-coding gene and contain one or more regions of sequence complementary to the mRNA of the protein-coding gene (Atianand, Caffrey et al. 2017). Such antisense lncRNAs are particularly common, and up to 72% of genomic loci in mice show evidence of generation of antisense lncRNAs (Werner, Carlile et al. 2009). Moreover, bidirectional lncRNAs are located within 1 kb of promoters of protein-coding genes and they are transcribed from the opposite direction.

According to their function, lncRNAs can be classified into cis- and trans-acting lncRNAs. A cis-acting lncRNA targets the neighboring locus and its effect is restricted to the chromosome from which it is transcribed. In contrast, trans-acting lncRNAs affect genes on other chromosomes. It is still a matter of debate how lncRNAs act preferentially. A prevalence of cis-regulatory lncRNAs would explain the relatively low expression levels of many lncRNAs and their generally limited sequence conservation (Ulitsky and Bartel 2013). Furthermore, only about 3% of human lncRNAs have expression profiles strongly correlated with those of their neighboring genes. Strong negative correlations are exceedingly rare, which argues against widespread cis regulation by lncRNAs (Derrien, Johnson et al. 2012).

Generally, LncRNAs were initially thought to be non-functional and even transcriptional noise, but recently it became clear that many lncRNAs are important for several cellular processes. LncRNAs can carry out scaffolding functions by the formation of RNA-protein complexes or subcellular structures. An example of a lncRNA with scaffolding functions is the lncRNA TERC (Telomerase RNA component). TERC serves as a template for telomere replication by telomerase and acts as a molecular scaffold for the polymerase enzyme around the RNA (Lingner, Hughes et al. 1997). Furthermore, lncRNAs can influence protein activity and modulate their localization. The lncRNA NRON (non-coding repressor of NFAT) was found to repress the nuclear factor of activated T-cells (NFAT). NFAT is a $Ca^{2+}$-regulated transcription factor that controls gene expression in many cell types. NRON binds NFAT, thereby limiting the nuclear-cytoplasmic trafficking of NFAT which results in the repression of NFAT target gene

expression (Sharma, Findlay et al. 2011). In addition, lncRNAs can regulate the expression of genes through a variety of mechanisms including epigenetic modifications, transcription and post-transcriptional processing (Mercer, Dinger et al. 2009; Kornienko, Guenzl et al. 2013). It was shown that lncRNAs are involved in epigenetic regulation by recruiting chromatin-remodeling complexes to specific locations in the genome. Thus, HOTAIR (HOX transcript antisense RNA) guides the PRC2 complexes (polycomb repressive complex 2) to the HOXD cluster, thereby repressing transcription in trans (Rinn, Kertesz et al. 2007). Moreover, the well-known lncRNA XIST coats the X chromosome in cis and also recruits the PRC2 complex. This induces the formation of heterochromatin, which ultimately leads to X-chromosome inactivation (Brockdorff 2011; Pontier and Gribnau 2011). LncRNAs also play a role in transcriptional regulation. In eukaryotes, RNAP II transcribes protein-coding genes into mRNA in collaboration with general transcription factors. Therefore, some lncRNAs regulate the transcription by directly affecting the loading and activity of RNAP II or general transcription factors (Espinoza, Allen et al. 2004). Another way for lncRNAs to regulate mRNA transcription is to modulate the activity of a particular transcription factor by acting as a co-factor or inhibitor. The lncRNA Evf2 acts as a co-activator of the transcription factor DLX2, resulting in an induced gene expression of DLX5 and DLX6 (Feng, Bi et al. 2006). Additionally, lncRNAs can regulate the post-transcriptional processing of mRNAs, including mRNA editing, splicing, transport, translation and degradation (Wu, Su et al. 2016). As an example, NAT Zeb2 can bind the Zeb2 mRNA through complementary base-pairing and thereby prevent the splicing processing of the intron. This results in the upregulation of the Zeb2-protein without an alteration on transcriptional level (Beltran, Puig et al. 2008).

In general, lncRNAs play an important role in many different cell types, since they coordinate many processes in cell and tissue development (Hu, Alvarez-Dominguez et al. 2012). LncRNAs regulate the development of cardiomyocytes, stem cells, epithelial cells, erythrocytes and adipocytes and are also involved in the development and differentiation of several different immune cell lineages (Guttman, Donaghey et al. 2011; Hu, Yuan et al. 2011; Grote, Wittler et al. 2013; Kretz, Siprashvili et al. 2013; Sun, Goff et al. 2013; Alvarez-Dominguez, Hu et al. 2014).

In contrast to miRNAs or proteins, the function of lncRNAs can only partly be inferred from sequence or structure and they use a variety of mechanisms to regulate processes. Thus, the biological function of any lncRNA needs to be determined on a case-by-case basis.

### 1.4.2 microRNAs

miRNAs are endogenous, non-coding, single-stranded RNA molecules with a length of 20 - 24 nucleotides that negatively regulate gene regulation at a post-transcriptional level (Bartel 2004). Initially, miRNAs have been discovered in the nematode *Caenorhabditis elegans* (*C. elegans*) in 1993. It was observed that the small regulatory RNA lin-4 was important for the developmental transition in early larval stage progression of *C. elegans* by targeting lin-14 mRNA. Therefore, lin-4 was the first identified miRNA with a length of 22 nucleotides (Lee, Feinbaum et al. 1993). Although the identification of unknown miRNAs in different species is still ongoing work, already known miRNAs have shown striking sequence conservation across species and phyla. This observation hints towards similarities in function among them (Das, Garnica et al. 2016). miRNAs are expressed in a tissue-specific or developmental-stage-specific manner, thereby contributing to cell-type-specific protein-expression profiles (Krol, Loedige et al. 2010). Intriguingly, miRNAs can be found in bodily fluids including serum, plasma, urine, saliva and milk (Weber, Baxter et al. 2010). In humans, over 2,500 matured miRNAs (based on miRBase.org, released August 2010, Last Update: November 2010) have been identified so far and about 60% of all protein-coding genes are predicted to be regulated by them (Friedman, Farh et al. 2009). Bioinformatics predictions of miRNA targets have provided an important tool to explore the functions of miRNAs. However, the overall success rate of such predictions remains to be determined by experimental validation (He and Hannon 2004).

#### 1.4.2.1 Biogenesis and function

miRNA genes can be transcribed either from independent miRNA genes or are embedded within introns, and occasionally exons of other genes (Carthew and Sontheimer 2009). Two pathways of the miRNA biogenesis are possible: the canonical and the non-canonical pathway.
In the canonical pathway, miRNA genes are transcribed into long primary miRNA transcripts (pri-miRNAs) by RNA polymerase II and occasionally by RNA polymerase III (Cai, Hagedorn et al. 2004; Lee, Kim et al. 2004; Borchert, Lanier et al. 2006). The sequence of pri-miRNAs can be several kilobases in size and they can contain stem loops of several mature miRNAs, which give rise to one miRNA cluster. The dsRNA binding protein DGCR8 (DiGeorge critical region 8) recognizes the hairpin structure of the pri-miRNA and brings it in close proximity to the RNAse III enzyme Drosha (Krol, Loedige et al. 2010). Both form the nuclear microprocessor complex leading to the cleavage of the pri-miR into hairpin shaped structures called pre-miRNA with a length of approximately 70 nucleotides (Lee, Ahn et al. 2003). In the non-canonical pathway, miRNA precursors are located in mRNA introns and are spliced out and therefore bypass the microprocessor complex (Schamberger, Sarkadi et al. 2012). In both pathways, the

pre-miRNA is exported from the nucleus into the cytoplasm by exportin-5 in a Ran-GTP dependent manner (Yi, Qin et al. 2003; Lund, Guttinger et al. 2004). The pre-miRNA is only bound by exportin-5 if the 3' overhang that derives from Drosha cleavage is present. Thus, the export is selective for correctly processed RNAs (Zeng and Cullen 2004). In the cytoplasm, the pre-miRNA is recognized and its terminal loop is cut off by the RNAse Dicer in complex with the double-stranded RNA binding protein TRBP (transactivation-responsive (TAR) RNA-binding protein). Therefore, a ~20 bp-mature miRNA/miRNA duplex is produced that dissociates from Dicer and TRBP (Hutvagner, McLachlan et al. 2001). The miRNA/miRNA duplex is processed and unwound by the activity of several helicases, assisted by Argonaute 2 (Ago2) (Winter, Jung et al. 2009). Thereby, the guide strand stays associated with Ago2 in the miRNA induced silencing complex (miRISC), while the remaining strand (passenger strand) is degraded. In most cases, there is a preference for which strand is incorporated into miRISC due to factors such as thermodynamic stability. Typically, the strand with the lower thermodynamic stability at its 5' base pair is incorporated into miRISC (Schwarz, Hutvagner et al. 2003). The miRISC guides the miRNA to its target mRNA. Thereby, binding of miRNA and mRNA in the RISC can lead to translational repression, mRNA deadenylation and mRNA degradation. Thus, miRNA binding is a mechanism for post-transcriptional regulation of gene expression (Winter, Jung et al. 2009).
In detail, miRNAs bind to complementary sequences in the 3' untranslated region (3'UTR) of mRNA transcripts. However, they do not require perfect complementarity for binding. Only the nucleotides 2-7 of the miRNA, also known as seed region, have to perfectly match a sequence of the 3'UTR for binding (Lewis, Shih et al. 2003). miRNA-mediated gene regulation relies on two mechanisms. Multiplicity describes the phenomenon that one miRNA can bind hundreds of different target mRNA. If one mRNA is targeted by several miRNAs that act together, it is called as synergy (Krek, Grun et al. 2005). In general, miRNAs reduce protein levels of their mRNA targets, but this might not always be the case. Since miRNA-binding also occurs in the 5' untranslated region (5'UTR) of target mRNAs, exons or DNA elements, translation and transcription can be enhanced, respectively (Lytle, Yario et al. 2007; Vasudevan, Tong et al. 2007; Place, Li et al. 2008; Fang and Rajewsky 2011; Lin, Liu et al. 2011).

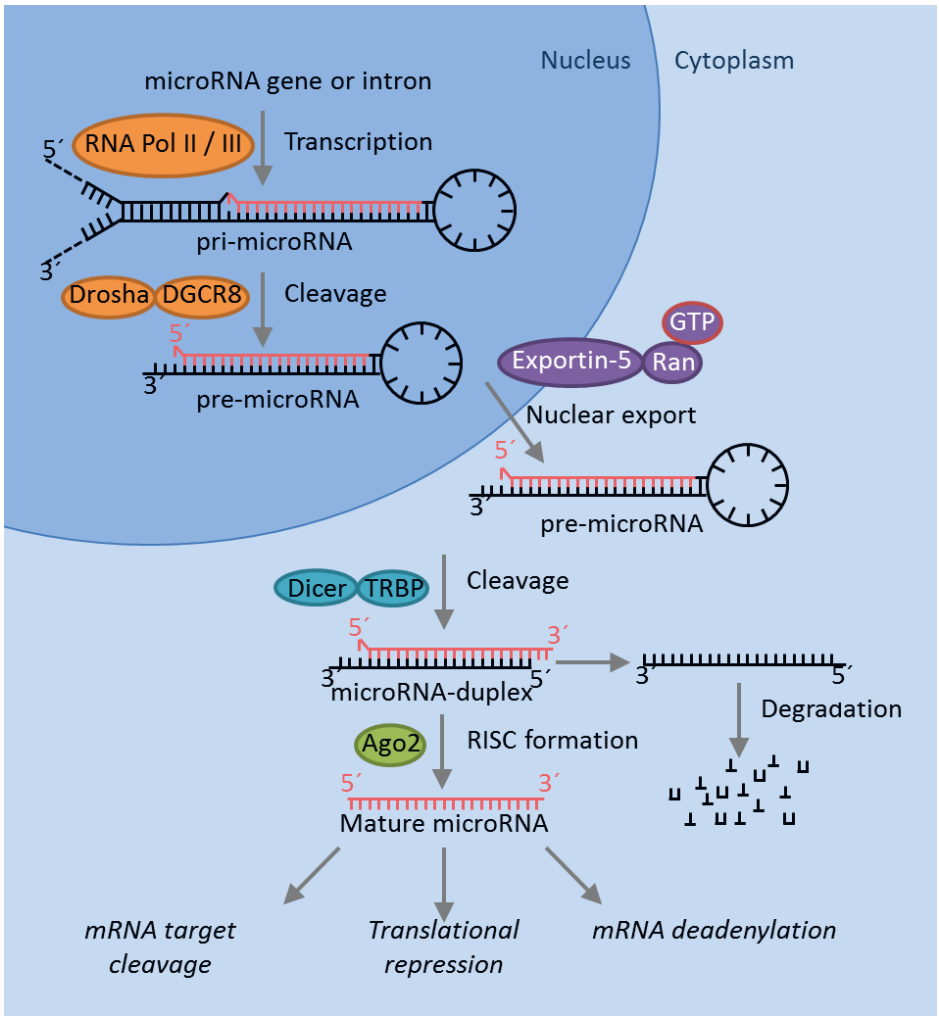


**Figure 1.4: Simplified schematic of the canonical pathway of miRNA processing.** RNA polymerase II/III (RNA Pol II/III) generates the primary miRNA transcript (pri-miRNA). The pri-miRNA is cleaved by the microprocessor complex Drosha-DGCR8 in the nucleus. The resulting hairpin, pre-miRNA, is exported into the cytoplasm by exportin-5 in a Ran-GTP dependent manner. Dicer cleaves the terminal loop of the pre-miRNA with the aid of the dsRNA binding protein TRBP resulting in the miRNA-duplex. The guide strand of the miRNA-duplex is incorporated into the Ago2 containing miRISC complex whereas the passenger strand is degraded. miRNA-guided binding of miRISC to specific target mRNAs through base-pair complementarity within the miRNA seed region mediates translational repression, mRNA target cleavage or mRNA deadenylation. Adapted from: Winter et al, Nature Cell, 2009)

### 1.4.2.2 microRNAs in the innate immune system

miRNAs can have many different targets because only the seed region needs to be complementary to mediate its function. Therefore, miRNAs can have a variety of different functions. miRNAs are important regulators of cell differentiation and function and mediate a variety of processes including controlling innate and adaptive immunity. miRNA regulation has been studied in a wide range of leukocytes and in the immune response of non-leukocytes. Indeed, the activation of innate immune cells including macrophages, dendritic cells and natural killer cells is partly controlled by miRNAs (Montagner, Orlandi et al. 2013; Smyth, Boardman et al. 2015; Essandoh, Li et al. 2016). More precisely, miRNAs are for example

involved in the polarization process of macrophages. A number of studies have been performed to determine the miRNA expression profiles in M1 and M2 polarized human and murine macrophages. These studies revealed that miR-9, miR-127, miR-155, and miR-125b promote M1 polarization, while miR-124, miR-223, miR-34a, let-7c, miR-132, miR-146a, and miR-125a-5p induce M2 polarization by targeting various transcription factors and adaptor proteins (Zhang, Zhang et al. 2013; Cobos Jimenez, Bradley et al. 2014). M1 and M2 phenotypes play distinctive roles in cell growth and progression of inflammation-related diseases. Thus, miRNAs which are relevant for the polarization process of macrophages may have therapeutic potential in the treatment of inflammation-related diseases such as sepsis, obesity, cancer, and multiple sclerosis (Essandoh, Li et al. 2016). Moreover, miRNAs contribute to a balanced immune response between elimination of pathogens and immune dysregulation as seen in sepsis or chronic inflammation. The best illustrated example is provided by their regulation of TLR signalling. TLR-signalling leads to the induction of miRNAs which in turn target elements of TLR signalling pathways such as signalling proteins, regulatory molecules, transcription factors or cytokines. Therefore, the role of miRNAs as fine tuners is fulfilled by their function in complex feedforward and feedback loops (Drury, O'Connor et al. 2017). Besides that, the most studied miRNAs, miR-146a and miR-155, are important regulators of inflammation. In response to pathogens, both miRNAs are upregulated, but show opposing effects. miR-155 is induced by TLR2, TLR3, TLR4 and TLR9 signalling in many cell types and generally functions as a pro-inflammatory miRNA. miR-155 targets factors which negatively regulate inflammation (Wang, Hou et al. 2010; Thounaojam, Kundu et al. 2014). To prevent exaggerated inflammation, the miR-155 expression is controlled by IL-10 which inhibits its transcription (McCoy, Sheedy et al. 2010). By contrast, miR-146a negatively regulates TLR signalling through a negative feedback loop by targeting IRAK1 and TRAF6. miR-146a was originally identified in a screen which aimed at identifying miRNAs induced by LPS stimulation and is expressed widely throughout the hematopoietic system (Taganov, Boldin et al. 2006). In general, its expression appears to be low in precursors and resting cells and increases with maturation and activation (Boldin, Taganov et al. 2011; Rusca, Deho et al. 2012). Knockout studies in mice have clearly displayed the importance of miR-146a in the regulation of the immune response. Mice deficient in miR-146a are hyperresponsiveness to LPS, they develop an immune-proliferative disorder characterized by splenomegaly, lymphadenopathy, premature death and a very significant induction of myeloproliferation (Rusca, Deho et al. 2012). In summary, miR-155 enhances inflammation, whereas miR-146 inhibits inflammation (Taganov, Boldin et al. 2006; O'Connell, Chaudhuri et al. 2009).

In addition to the role of miR-155 in inducing immune responses, a study has shown that miR-155 also regulates mRNA targets involved in pro-inflammatory transcriptional processes as seen for miR-146a. Therefore, it is suggested that miR-155 acts as a broad limiter of pro-inflammatory gene expression once the miR-146-dependent barrier to LPS triggered inflammation has been breached (Schulte, Westermann et al. 2013). Thus, miR-155 post-transcriptionally inhibits negative regulators of inflammation, such as SHIP-1, SOCS-1 or PIK3CA (Gottwein, Mukherjee et al. 2007; Lu, Thai et al. 2009; O'Connell, Chaudhuri et al. 2009; Thounaojam, Kundu et al. 2014), pro-inflammatory signalling components, such as TAB2, IKKε or FOS (Gottwein, Mukherjee et al. 2007; Lu, Weidmer et al. 2008; Ceppi, Pereira et al. 2009), and mediators of programmed cell death (Koch, Mollenkopf et al. 2012).

Furthermore, an involvement of miRNAs in endotoxin tolerance (LPS tolerance) has been demonstrated (Quinn, Wang et al. 2012). Endotoxin tolerance is a controlled immune response to prevent tissue damage, overwhelming sepsis and mortality, and refers to a phenomenon that cells show a reduced responsiveness towards repeated endotoxin stimulation (Greisman, Young et al. 1969). Thus, miRNAs play a role in switching from a strong, early pro-inflammatory response to the resolution of the inflammatory process (O'Neill, Sheedy et al. 2011). Studies by el Gazzar and McCall have demonstrated that not only miR-146a and miR-155 are regulating the TLR4 signalling pathway. Moreover, miR-221, miR-579 and miR-125b are increased significantly in LPS-tolerized cells compared to naive cells. The study revealed that miR-221 accelerates TNF-α degradation, whereas miR-125b and miR-579 block its translation. The effect of these miRNAs on the TNF-α 3'UTR is mediated via recruitment of specific RNA-binding proteins, which act as mRNA destabilizers and translational inhibitors, respectively. In conclusion, the miRNAs are upregulated to inhibit TNF-α mRNA to prevent an exaggerated immune response to a second stimulus (El Gazzar and McCall 2010). Other miRNAs are also involved in endotoxin tolerance by controlling TLR4 signalling. For instance, let-7e was shown to negatively target TLR4 and reduced levels of miR-98 are increasing IL-10 secretion. Both, downregulation of miR-98 and increased levels of let-7e, contribute to LPS hyporesponsiveness (Androulidaki, Iliopoulos et al. 2009; Liu, Chen et al. 2011).

The expression of miRNAs is highly regulated. miRNA-mediated control of mRNAs levels is very fast, but not as rapid as the effects of proteosomal degradation. However, it allows a strong initial immune response that is gradually dampened down. Therefore, their function as immunomodulators is well placed. (O'Neill, Sheedy et al. 2011).

#### 1.4.2.3 microRNAs in infectious diseases

miRNAs play crucial roles in the regulation of many cellular processes such as proliferation, metabolic pathways, immune response and development (Bartel 2004; Kloosterman and Plasterk 2006; Taganov, Boldin et al. 2007; Deiuliis 2016). Expression of miRNAs at normal levels maintains homeostasis in eukaryotes (Das, Garnica et al. 2016). Therefore, expression changes of miRNAs may have drastic effects. It can result in serious diseases in humans including cancer, kidney failure, cardiac disease, diabetes and liver cirrhosis (Kloosterman and Plasterk 2006; Rome 2013; Finch, Marquardt et al. 2014; Trionfini, Benigni et al. 2015; Santovito, Egea et al. 2016). Besides that, miRNAs are also important during several infectious diseases. The miRNA expression profile is altered when pathogens infect host cells which was firstly monitored in viral infection (Cullen 2011). Moreover, bacterial pathogens also alter host miRNAs which has already been studied and well described in infections with different kind of bacteria, such as *Helicobacter pylori*, *Listeria monocytogenes*, *Salmonella enteria serovar Thyphimurium* and *Mycobacterium tuberculosis* (Eulalio, Schulte et al. 2012; Harapan, Fitra et al. 2013; Staedel and Darfeuille 2013; Maudet, Mano et al. 2014a). However, the miRNA expression profile is not only altered in response to an infection as part of the host response to limit bacterial replication. Since miRNAs play an important role in the regulation of the innate and adaptive immune response, it is not surprising that pathogens have evolved to exploit host miRNAs to modulate the immune response (Drury, O'Connor et al. 2017). It has already been deciphered that host cellular miRNAs are manipulated by pathogens, such as viruses and many intracellular bacteria, to promote their own survival (Das, Garnica et al. 2016; Drury, O'Connor et al. 2017). For instance, HIV-1 induces upregulation of miR-34a which targets phosphatase 1 nuclear-targeting subunit (PNUTS) to promote its replication (Swaminathan, Murray et al. 2013). Furthermore, Epstein-Barr virus latent membrane protein 1 induces miR-146a expression to negatively regulate the interferon response and promote its survival (Cameron, Yin et al. 2008). In hepatocytes, the genome of hepatitis C virus (HCV) is stabilized by the binding of host miR-122. This binding protects HCV from degradation by innate antiviral endonucleases (Jopling, Yi et al. 2005). This shows that a pathogen can also be dependent on endogenous expression of host miRNAs that promote their survival or replication which results in tissue tropism. As mentioned before, intracellular bacteria also appear to manipulate host cell miRNA expression to downregulate inflammatory cytokines, factors and pathways that promote autophagy and cell apoptosis (Drury, O'Connor et al. 2017). For instance, miR-26a is downregulated in macrophages by *Mycobacterim tuberculosis* (*M. tuberculosis*). Therefore, the target of miR-26a, Krüpple-like factor 4 (KLF4), is repressed which usually promotes macrophage polarization towards an anti-inflammatory M2 phenotype. In M2 macrophages,

bactericidal mechanisms are repressed, which leads to an increased replication of *M. tuberculosis* (Sahu, Kumar et al. 2017). Additionally, miR-146a expression was shown to be induced after *Mycobacterium bovis* infection. miR-146a suppresses the inducible nitric oxide (NO) synthase (iNOS) expression and NO generation by targeting TRAF6, thus promoting mycobacterial survival in macrophages (Li, Wang et al. 2016). Moreover, *in vitro* studies indicate that *Salmonella* modulates host miRNAs in epithelial cells as well as macrophages. A downregulation of let-7a was detected in RAW264.7, HeLa cells and macrophages, and miR-21, miR-146 and miR-155 were upregulated in RAW264.7 in response to a *Salmonella* infection (Schulte, Eulalio et al. 2011). All of these miRNAs were associated with pro- and anti-inflammatory responses, but not with invasion or replication of *Salmonella*. In 2014, a study described how Salmonella exploit host miRNAs. Maudet and colleagues identified a *Salmonella*-mediated downregulation of the miR-15 family in HeLa cells using a library of miRNA mimics. Cyclin D1 protein is targeted by the family and associated with cell cycle progression. Therefore, cells remain in G1/S phase that favors the intracellular replication of *Salmonella* (Maudet, Mano et al. 2014b). Additionally, the miRNAs miR-30c and miR-30e are also involved in intracellular replication of *Salmonella* (Verma, Mohapatra et al. 2015).

Given that miRNAs mediate the host response to infection, miRNA dysregulation could contribute to susceptibility to disease and immunopathology. Therefore, understanding how dysregulation of miRNAs can contribute to disease progression may provide new therapeutic targets or prognostic indicators. Disease-related miRNAs have already been detected in bodily fluids and were used as biomarkers or as targets for therapeutics (Guay and Regazzi 2013; Mulrane, Klinger et al. 2014; Pal, Jaiswar et al. 2015; Hayes and Chayama 2016).

## 1.5 Objective of the study

In the last few decades, non-coding RNAs have been found to be important regulators of gene expression at the post-transcriptional level by binding to target transcripts or by mediating gene regulation. The goal of this study was to understand the influence of an infection with *L.p.* on non-coding RNAs in human macrophages to understand the closely connected host-pathogen processes from the angle of putative trans-species regulatory RNA networks. The novelty herein is the specific focus on transcriptome events in host and pathogen simultaneously. This work is structured into two parts: (1) a functional study on how *Legionella*-infections influence the miRNA response of the host and (2) an in depth analysis of transcriptomic events in host and pathogen during infection.

(1) Many physiological cellular processes, including immune responses to infections, are regulated at the post-transcriptional level by miRNAs. As an intracellular bacterium, *L.p.* can survive and replicate in phagocytic cells and modulate the defence of the host cell in a very sophisticated way. Therefore, the hypothesis arose that *L.p.* could alter the miRNA expression of the host to its own benefit. Since a global analysis of host miRNA expression changes upon *Legionella* infection of human macrophages had never been established before, high throughput sequencing of small RNAs was used to determine the miRNA profile of *L.p.*-infected human macrophages. This study aims to assess the influence of miRNA expression changes on the course of infection with *L.p.* in human macrophages and their functional consequences. Furthermore, the present work also inspects the mechanism behind a miRNA dysregulation in response to infection.

(2) The transcriptional profile of *L.p.* during the course of infection in human macrophages is yet to be investigated. Additionally, the altered gene expression of *Legionella* infected macrophages has only been performed in a mixed population of infected and non-infected cells. Therefore, the second part of the study aims to uncover the most important transcriptional events in both, host cell and bacterium, during the course of infection. To elucidate the transcriptional profile of the host and pathogen simultaneously, we used a dual RNA-Seq approach. This method allows the definition of the RNA landscape including coding and non-coding RNAs of pathogen and host, in great depth and with high accuracy. One important step of this work was the establishment of the method and the first analysis and validation experiments.

# 2 Materials and Methods

## 2.1 Materials

### 2.1.1 Instruments and equipment

**Table 2.1: List of instruments and equipment**

| Instruments | Type | Company |
|---|---|---|
| analytical column | Acclaim PepMap RSLC, packed with 2.6 µm C18 particles of 150 Å pore size | Thermo Fisher Scientific Waltham, MA, USA |
| Automated cell counter | TC10™ | BioRad Laboratories Hercules, USA |
| Bioanalyzer | 2100 Bioanalyzer Instrument | Agilent Technologies Santa Clara, USA |
| Bioluminescence and Chemoluminescence Imager | ChemoCam Imager 3.2 | INTAS Science lmaging Göttingen,Germany |
| Camera | AxioCam MRm | Zeiss Oberkochen, Germany |
| Cell Counting Chamber | Neubauer Counting Chamber | Paul Marienfeld GmbH & Co. KG Lauda-Königshofen, Germany |
| Cell culture bench | SAFE 2020 | Thermo Fisher scientific Schwerte, Germany |
| Centrifuge | HERAEUS Multifuge X3R | Thermo Fisher scientific Schwerte, Germany |
| Centrifuge | Gentrifuge 5424R | Eppendorf Hamburg, Germany |
| Centrifuge | Sprout® Mini-Gentrifuge | Heathrow Scientific ® LLC lllinois, USA |
| Centrifuge | Heraeus Fresco L7 | Thermo Fisher scientific Schwerte, Germany |
| co2 Incubator | HERAcell 240i | Thermo Fisher scientific Schwerte, Germany |
| Dispenser | Multipette® plus | Eppendorf Hamburg, Germany |
| Dispenser | Multipette® Xstream | Eppendorf Hamburg, Germany |
| FACS | Guava easyCyte ™ | Merck Millipore TM Billerica, USA |
| FACS-Sorter | FACS Aria III Cell Sorter | Miltenyi Biotec GmbH Bergisch Gladbach, Germany |
| Fluorometer | Qubit® 2.0 Fluorometer | Thermo Fisher scientific Schwerte, Germany |
| Gel comb | 10 Well, 14 Well | Peqlab Erlangen, Germany |
| Gel documentation apparatus | Gel-x Imager | INTAS Science lmaging Göttingen,Germany |
| Gel electrophoresis apparatus | PerfectBiue Gel System | Peqlab Erlangen, Germany |
| Gel preparation equipment | Multiple Gel Casting | Peqlab Erlangen, Germany |
| Gel preparation equipment | Gel Trays | Peqlab Erlangen, Germany |
| Hybridization Oven / UV | HL-2000 HybriLinker | UVP |

| | | |
|---|---|---|
| Crosslinker | | Cambridge, UK |
| Illuminator | HXP 120 C | Zeiss<br>Oberkochen, Germany |
| Incubated/refrigerated stackable Shaker | MaxQ 600 | Thermo Fisher scientific<br>Schwerte, Germany |
| Labaratory roller mixer | SRT6D | Stuart ®<br>Marseille, France |
| Labaratory shaker | See-Saw rocker SSL4 | Stuart ®<br>Marseille, France |
| Liquid nitrogen storage tanks | Cryo Plus 2 | Thermo Fisher scientific<br>Schwerte, Germany |
| low flow liquid chromatography system | UltiMate™ 3000 RSLCnano System | Dionex/Thermo Fisher Scientific<br>Idstein, Germany |
| Macs multi stand magnet | quadroMacs | Miltenyi Biotec GmbH<br>Bergisch Gladbach, Germany |
| Magnetic & Heating Stirrer | RCT Standard | IKA<br>Staufen, Germany |
| Magnetic stand for 1.5 mL tubes | PureProteome™ Magnetic Stand | Merck Millipore TM<br>Billerica, USA |
| MAP magnetic bead-based multi-analyte panels | MAGPIX® System | Merck Millipore TM<br>Billerica, USA |
| Mass spectrometer | Q Exactive mass spectrometer | Thermo Fisher Scientific<br>Waltham, MA, USA |
| Microscope | AXIO Vert a1 | Zeiss<br>Oberkochen, Germany |
| Microscope | PrimoVert | Zeiss<br>Oberkochen, Germany |
| Microwave | Inverter | SHARP<br>Hamburg, Germany |
| PCR Cycler | PeqSTAR 2x Gradient | Peqlab<br>Erlangen, Germany |
| Photometer | Ultraspec 10 CeII densitometer | Amersham Biosciences<br>Freiburg, Germany |
| Pipetboy | Accu-jet pro | BRAND GMBH&CO KG<br>Wertheim, Germany |
| Pipette (0.1 - 10001JI) | | Gilson<br>Middelton, USA |
| Plate reader | Tecan Infinite M200 PRO | Thermo Fisher scientific<br>Schwerte, Germany |
| Power supplies | PeqpowerE300 200/300V | Peqlab<br>Erlangen, Germany |
| Precision Scales | | Denver Instruments<br>Göttingen, Germany |
| Real Time PCR System | ViiA7 TM | Life Technologies ™<br>Darmstadt, Germany |
| Real Time PCR System | QuantStudio3 | Thermo Fisher scientific<br>Schwerte, Germany |
| Spectrophotometer | NanoDrop 2000c | Thermo Fisher scientific Schwerte, Germany |
| Steam sterilizer | Varioklav® | HP Medizintechnick GmbH<br>Oberschleißheim, Germany |
| Surgical preparation set | | Fine Science Tools<br>Heidelberg, Germany |
| Thermomixer (1.5 mL; 2 mL) | Thermomixer Comfort | Eppendorf<br>Hamburg, Germany |

| | | |
|---|---|---|
| trap column | Acclaim™ PepMap™ 100 C18-LC-column | Thermo Fisher Scientific<br>Waltham, MA, USA |
| TriVersa NanoMate source | | Advion, Ltd.<br>Harlow, UK |
| Ultrasonic homogenizer | SONOPULS HD 2070 | BANDELIN electronic GmbH & Co. KG<br>Berlin, Germany |
| Vacuum pump | AC 04 | VACUUBRAND GMBH + CO KG<br>Wertheim, Germany |
| Vortex | VortexGenie2 | Scientific Industries<br>New York, USA |
| Vortex | IKA®MS3 | Agilent Technologies<br>Santa Clara, USA |
| Vortex | Vortex V-1 plus | Peqlab<br>Erlangen, Germany |
| Water bath | | GFL®<br>Burgwedel, Germany |

### 2.1.2 Consumables and plasticware

**Table 2.2: List of consumable and plasticware**

| Subject | Name | Company |
|---|---|---|
| µ slide for microscopy | µ-Slide (chambered coverslip) with 8 wells | ibidi<br>Planegg / Martinsried |
| 1 mL Norm-Jet syringe | | Henke-Sass Wolf GmBH<br>Tuttlingen, Germany |
| 100 mL containers, polypropylene | | SARSTEDT AG & Co.<br>Nümbrecht, Germany |
| 15 - 50 mL tube | Falcon | SARSTEDT AG & Co.<br>Nümbrecht, Germany |
| 6-well plate, 12-well plate, 24-well plate, 96-well plate | CELLSTAR® Cell culture plate | Greiner Bio-One GmbH<br>Frickenhausen, Germany |
| 96-well plate (white) for luciferase-Assay | Cell Grade Brand plates | BRAND GMBH + CO KG<br>Wertheim, Germany |
| 96-well plate for ELISA | | Thermo Fisher scientific<br>Schwerte, Germany |
| 96-well plate for LDH | Mikrotestplatte | SARSTEDT AG & Co.<br>Nümbrecht, Germany |
| Canula | | BD Biosciences<br>Heidelberg, Germany |
| Cap tube for cultivation of bacteria | 14 mL PP tube | Greiner Bio-One GmbH<br>Frickenhausen, Germany |
| Cell culture dish | | Greiner Bio-One GmbH<br>Frickenhausen, Germany |
| Cell culture flask (T25; T75) | TC Flask | SARSTEDT AG & Co.<br>Nümbrecht, Germany |
| Cell scraper (25 - 50 cm) | | SARSTEDT AG & Co.<br>Nümbrecht, Germany |
| Cotton buds | Cotton buds, Rotilabo | Carl Roth GmbH & Co. KG<br>Karlsruhe, Germany |
| Coverslips (11 - 18 mm) | | Thermo Fisher scientific<br>Schwerte, Germany |
| Cryo-tubes | | SARSTEDT AG & Co.<br>Nümbrecht, Germany |
| Cuvette (polystyrene) | | SARSTEDT AG & Co.<br>Nümbrecht, Germany |
| Disposal Bags | | Carl Roth GmbH & Co. KG<br>Karlsruhe, Germany |
| Dissecting set | | Fine Science Tools GmbH<br>Heidelberg, Germany |

| | | |
|---|---|---|
| DNA Chip | | Agilent Technologies<br>Santa Clara, USA |
| Filter | Cell Strainer 40 - 100 µm Nylon | BD Biosciences<br>Heidelberg, Germany |
| High sensitivity Chip | | Agilent Technologies<br>Santa Clara, USA |
| Inoculation spreader | | SARSTEDT AG & Co.<br>Nümbrecht, Germany |
| Inoculation tube | Loop Soft 10 µL | VWR International GmbH<br>Darmstadt, Germany |
| Lab gloves | Examination gloves, latex free | Sempercare®<br>Vienna, Austria |
| Lintfree tissues | Delicate task wipes | Kimberly-Ciark Professional®<br>Roswell, USA |
| Magnetic columns | MACS LS Columns | Miltenyi Biotec GmbH<br>Bergisch Gladbach, Germany |
| Microscope slides (76 x 26 mm) | | Thermo Fisher scientific<br>Schwerte, Germany |
| Nitrocellulose Blotting membrane | Amersham Protran, 0.2 µm | GE Healthcare Life Science Hyclone laboratories<br>Logan, USA |
| NuPAGE4-12% acrylamide Bis-Tris Midi Gel | | Novex Life Technologies<br>Darmstadt, Germany |
| Optical adhesive film | microAmp® | Life Technologies™<br>Darmstadt, Germany |
| Parafilm | PARAFILM® M | VWR International GmbH<br>Darmstadt, Germany |
| Pasteur pipette | | Glaswarenfabrik Karl Hecht GmbH &Co KG - "Assistent"<br>Sondheim, Germany |
| PVDF membrane | Immobilon-PSQ transfer Membran, 0.2 µm | Merck Millipore TM<br>Billerica, USA |
| qPCR 96- weil plates (0.1 mL) | | Life Technologies™<br>Darmstadt, Germany |
| RNA Nano Chip | | Agilent Technologies<br>Santa Clara, USA |
| Serological pipette (5 mL - 25 mL) | | SARSTEDT AG & Co.<br>Nümbrecht, Germany |
| Steril filtration filters (0.2 µm) | Filtrepur S | SARSTEDT AG & Co.<br>Nümbrecht, Germany |
| Surgical diposable scalpel | | B. Braun Melsungen AG<br>Melsungen, Germany |
| Tips (0.5 mL – 25 mL) | Combitips advanced® | Eppendorf<br>Hamburg, Germany |
| Tips (10 µL - 1000 µL) | Safe Seal-Tips ®professional | Biozym Scientific GmbH<br>Hessisch Oldendorf, Germany |
| Tips (10 µL - 1000 µL) | | Gilson<br>Middelton, USA |
| Tips (10 µL - 1000 µL) | Diamond ® | Gilson<br>Middelton, USA |
| Tips (10 µL - 1000 µL) | TOWERPACK™ | Gilson<br>Middelton, USA |
| Tips (5 mL - 50 mL) | Tips for PIPETMAN® | Gilson<br>Middelton, USA |
| Tubes | | Eppendorf<br>Hamburg, Germany |
| Tubes (0.5 - 2.0 mL) | Safelock Tubes | Eppendorf<br>Hamburg, Germany |
| Tubes (1.8 mL) | CryoPure Tubes | SARSTEDT AG & Co.<br>Nümbrecht, Germany |
| Tubes (2 mL) | Phaselock Gel | 5Prime GmbH<br>Hilden, Germany |

| | | |
|---|---|---|
| Ultra- low attachment Cluster plate (6-well, 10 cm-dish) | Costar® | Corning Inc. Amsterdam, Netherlands |
| ZipTip® Pipette Tips | | Merck Millipore TM Billerica, USA |

### 2.1.3 Chemicals

**Table 2.3: List of chemicals**

| Chemical | Name | Company |
|---|---|---|
| 2-Mercaptoethanol | | Carl Roth GmbH & Co. KG Karlsruhe, Germany |
| 4.6-Diamin-2-Phenylindol (DAPI) | | ATT Bioquest Sunnyvale, USA |
| AB-Serum | | Sigma-Aldrich St. Louis, USA |
| ACES | | Carl Roth GmbH & Co. KG Karlsruhe, Germany |
| Acetic acid | | Carl Roth GmbH & Co. KG Karlsruhe, Germany |
| Acetonitrile | | Sigma-Aldrich St. Louis, USA |
| Acid phenol chloroform | | Ambion by life technologies Carlsbad, USA |
| Acrylamide | Acrylamide (Rotiphoresis Gel 30, 37.5:1) | Carl Roth GmbH & Co. KG Karlsruhe, Germany |
| Agar Agar (Kobe I) | | Carl Roth GmbH & Co. KG Karlsruhe, Germany |
| Agarose | Biozym LE Agarose | Biozym Scientific GmbH Hessisch Oldendorf, Germany |
| Ammonium bicarbonate | | Carl Roth GmbH & Co. KG Karlsruhe, Germany |
| Ammonium Persulfate (APS) | | Carl Roth GmbH & Co. KG Karlsruhe, Germany |
| Ammonium sulfate (NH4)2SO4 | | Sigma-Aldrich St. Louis, USA |
| Ampicilin Sodium Salt | | Sigma-Aldrich St. Louis, USA |
| Aqua-PCI | Roti® Aqua-Phenol/Chloroform/Isoamyl alcohol | Carl Roth GmbH & Co. KG Karlsruhe, Germany |
| Bradford Assay | | BioRad Laboratories Hercules, USA |
| BSA | Albumin Fraktion V | Carl Roth GmbH & Co. KG Karlsruhe, Germany |
| Calcium chloride | | Carl Roth GmbH & Co. KG Karlsruhe, Germany |
| Charcoal activated | | Carl Roth GmbH & Co. KG Karlsruhe, Germany |
| Chloramphenicol | | Carl Roth GmbH & Co. KG Karlsruhe, Germany |
| Chloroform | Trichloromethane | Carl Roth GmbH & Co. KG Karlsruhe, Germany |
| Complete Mini Protease Inhibitor Cocktail | | Roche Mannheim, Germany |
| Coomassie Brilliant Blue | | Merck Millipore TM Billerica, USA |
| CutSmart® Buffer | | New England Biolabs Ipswich, USA |
| DL-Dithiothreitol | | Fermentas, Thermo Fisher Scientific |

| | | |
|---|---|---|
| | | Carlsbad, USA |
| DMSO | Dimethyl sulfoxide | Carl Roth GmbH & Co. KG<br>Karlsruhe, Germany |
| ECL Reagent | ECL Prime Western Blotting Detection Reagent | GE Healthcare Life Science<br>Hyclone laboratories<br>Logan, USA |
| EDTA | | Carl Roth GmbH & Co. KG<br>Karlsruhe, Germany |
| Ethanol | Ethanol absolute | Sigma-Aldrich<br>St. Louis, USA |
| Ethidium bromide | | Invitrogen Thermo Fisher scientific<br>Carlsbad, USA |
| Ethylene Diamine Tetra-Acetic Acid (EDTA) | | Carl Roth GmbH & Co. KG<br>Karlsruhe, Germany |
| Fetal Calf Serum (FCS) | FBS Superior | Biochrom GmbH<br>Berlin, Germany |
| Ficoll | | Carl Roth GmbH & Co. KG<br>Karlsruhe, Germany |
| GelRed nucleic acid stain | GelRed™ | Biotium<br>Scarborough, Canada |
| Gentamicin | | gibco™ life technologies<br>Thermo Fisher Scientific<br>Carlsbad, USA |
| Glutamaxx | | gibco™ life technologies<br>Thermo Fisher Scientific<br>Carlsbad, USA |
| Glycerol | | Carl Roth GmbH & Co. KG<br>Karlsruhe, Germany |
| GlycoBlue | GlycoBlue™ | Invitrogen Thermo Fisher scientific<br>Carlsbad, USA |
| HEPES | 4-(2-hydroxyethyl)-1-piperazineethanesulfonic acid | Carl Roth GmbH & Co. KG<br>Karlsruhe, Germany |
| HPLC-grade water | | J. T. Baker,<br>Center Valley, PA, USA |
| Human Serum off-the-clot, Type AB | | Lonza GmbH<br>Basel, Switzerland |
| Iodoacetamide | | Sigma-Aldrich<br>St. Louis, USA |
| Iron (III) nitrate nonahydrate | | Carl Roth GmbH & Co. KG<br>Karlsruhe, Germany |
| Isopropanol | | Carl Roth GmbH & Co. KG<br>Karlsruhe, Germany |
| Kanamycin sulphate | | Carl Roth GmbH & Co. KG<br>Karlsruhe, Germany |
| Labeled Arginine | 13C arginine | Sigma-Aldrich<br>St. Louis, USA |
| Labeled lysine | 13C lysine | Sigma-Aldrich<br>St. Louis, USA |
| LB Agar | LB Agar (Lennox) | Carl Roth GmbH & Co. KG<br>Karlsruhe, Germany |
| LB Broth | LB Broth (Lennox) | Carl Roth GmbH & Co. KG<br>Karlsruhe, Germany |
| L-Cysteine | | Carl Roth GmbH & Co. KG<br>Karlsruhe, Germany |
| Lipofectamine 2000 | | Invitrogen Thermo Fisher scientific<br>Carlsbad, USA |
| Liquid Nitrogen | | Linde<br>Düsseldorf, Germany |

| | | |
|---|---|---|
| Loading Dye | 6x Mass Ruler | Thermo Fisher scientific<br>Schwerte,Germany |
| Methanol | | Carl Roth GmbH & Co. KG<br>Karlsruhe, Germany |
| Mowiol 4-88 | | Carl Roth GmbH & Co. KG<br>Karlsruhe, Germany |
| Nonidet P40 | Nonidet P40 BioChemica (Substitute) | AppliChem<br>Darmstadt, Germany |
| NuPAGE™ LDS Sample Buffer (4X) | Sample Buffer | Novex Life Technologies<br>Darmstadt, Germany |
| NuPAGE™ Sample Reducing Agent (10X) | Reducing agent | Novex Life Technologies<br>Darmstadt, Germany |
| NuPAGE™ Transfer Buffer (20X) | Transfer Buffer | Novex Life Technologies<br>Darmstadt, Germany |
| Paraformaldehyde | | Carl Roth GmbH & Co. KG<br>Karlsruhe, Germany |
| PBS (1x) | Phosphate Buffered Saline (1x) | Healthcare Life Science<br>Logan, USA |
| Pen/Strep | Penicillin/Streptomycin | Biochrom GmbH<br>Berlin, Germany |
| phosphoric acid | | Carl Roth GmbH & Co. KG<br>Karlsruhe, Germany |
| Potassium chloride | | Carl Roth GmbH & Co. KG<br>Karlsruhe, Germany |
| Powdered milk | | Carl Roth GmbH & Co. KG<br>Karlsruhe, Germany |
| Saponin | | Carl Roth GmbH & Co. KG<br>Karlsruhe, Germany |
| siPORT™ NeoFX™ | | Invitrogen<br>Thermo Fisher scientific<br>Carlsbad, USA |
| SOB Broth | | Carl Roth GmbH & Co. KG<br>Karlsruhe, Germany |
| Sodium Acetate | | Carl Roth GmbH & Co. KG<br>Karlsruhe, Germany |
| Sodium Azide | | Carl Roth GmbH & Co. KG<br>Karlsruhe, Germany |
| Sodium Chloride | | Carl Roth GmbH & Co. KG<br>Karlsruhe, Germany |
| Sodium Dodecyl Sulfate Pellets | SDS Pellets | Carl Roth GmbH & Co. KG<br>Karlsruhe, Germany |
| T4 DNA Ligase Buffer | | New England Biolabs<br>Ipswich, USA |
| Tetraethymethylenediamine (TEMED) | | Carl Roth GmbH & Co. KG<br>Karlsruhe, Germany |
| Thiourea | | Sigma-Aldrich<br>St. Louis, USA |
| Tri (hydroxymethyl) aminomethane (TRIS) | | Carl Roth GmbH & Co. KG<br>Karlsruhe, Germany |
| TRIS hydrochloride | | Carl Roth GmbH & Co. KG<br>Karlsruhe, Germany |
| Triton X100 | | Carl Roth GmbH & Co. KG<br>Karlsruhe, Germany |
| Trizol | TRI Reagent® | Sigma-Aldrich<br>St. Louis, USA |
| TWEEN 20 | | Carl Roth GmbH & Co. KG<br>Karlsruhe, Germany |
| Ultra Pure water | | Biochrom GmbH<br>Berlin, Germany |
| Urea | Urea, Bioscience Grade | Carl Roth GmbH & Co. KG<br>Karlsruhe, Germany |

| | | |
|---|---|---|
| Yeast extract | | Carl Roth GmbH & Co. KG<br>Karlsruhe, Germany |

### 2.1.4 Enzymes

**Table 2.4: List of enzymes**

| Enzyme | Company |
|---|---|
| NotI | New England Biolabs<br>Ipswich, USA |
| RNasin® Ribonuclease Inhibitor | Promega<br>Mannheim, Germany |
| T4 DNA Ligase | New England Biolabs<br>Ipswich, USA |
| T4 RNA Ligase, truncated | Epicentre<br>Madison, USA |
| Trypsin Gold, Mass Spectrometry Grade | Promega<br>Madison, USA |
| Trypsin-EDTA 0.05% (1x) | gibco™ life technologies<br>Thermo Fisher Scientific Carlsbad, USA |
| XhoI | New England Biolabs<br>Ipswich, USA |

### 2.1.5 Stimulants and cytokines

**Table 2.5: List of stimulants and cytokines**

| Name | | Company |
|---|---|---|
| Flagellin | Fla-ST (100µg) | Invitrogen Thermo Fisher scientific<br>Carlsbad, USA |
| GM-CSF (human) | granulocyte macrophage colony-stimulating factor | PeproTech<br>Hamburg, Germany |
| IL-1β (human) | Interleukin 1 beta | Sigma-Aldrich<br>St. Louis, USA |
| LPS | Lipopolysaccharide | Sigma-Aldrich<br>St. Louis, USA |
| Pam3CSK4 | | Invitrogen Thermo Fisher scientific<br>Carlsbad, USA |
| Phorbol-12-myristat-13-acetat (PMA) | | Sigma-Aldrich<br>St. Louis, USA |

### 2.1.6 Kits

**Table 2.6: List of Kits**

| Kits | Name | Company |
|---|---|---|
| Accuracy & fluorescence detection Kit | Guava easy Check Kit | Millipore<br>Darmstadt, Germany |
| Cloning Kit | StrataClone Blunt PCR Cloning Kit | Agilent Technologies<br>Santa Clara, USA |
| Cytotoxicity Detection Kit | Cytotoxicity Detection Kit (LDH) | Roche<br>Mannheim, Germany |
| DNA Polymerase Kit | Taqman Polymerase | Thermo Fisher Scientific<br>Schwerte, Germany |
| DNA, RNA and protein purification | Nucleo Spin® Gel and PCR clean up | Macherey-Nagel GmbH & Co. KG<br>Düren, Germany |
| DNase digestion | Promega™ RQ1 RNase-Free | Promega<br>Mannheim, Germany |

| | | |
|---|---|---|
| | DNase | |
| ELISA Kit for human Interleukin 8 | DuoSet®ELISA Kit for human Interleukin 8 | R&D Systems Inc.<br>Minneapolis, USA |
| Luciferase Assay Kit | DualGlo® Luciferase Assay System Kit Promega | Promega<br>Mannheim, Germany |
| MicroRNA Reverse Transcription Kit | TaqMan® MicroRNA Reverse Transcription Kit | Thermo Fisher Scientific<br>Schwerte, Germany |
| miRNA library preparation Kit | TruSeq Small RNA Library Preparation Kits - Set A | Illumina Inc.<br>San Diego, USA |
| Multiplex Assay Kit | Milliplex High sensitivity human cytokine Kit | Merck Millipore TM<br>Billerica, USA |
| Phusion DNA Polymerase | Phusion® High-Fidelity DNA Polymerase | New England Biolabs<br>Ipswich, USA |
| Plasmid Midi Kit | Nucleobond® Xtra Midi Plus EF | Macherey-Nagel GmbH & Co. KG<br>Düren, Germany |
| Plasmid Mini Kit | Nucleo Spin® Plasmid Quick Pure | Macherey-Nagel GmbH & Co. KG<br>Düren, Germany |
| Protein Detection Kit | Pierce BCA Protein Assay Kit | Thermo Fisher Scientific<br>Schwerte, Germany |
| qPCR Master Mix | Fast SYBR® Green Master Mix | Thermo Fisher Scientific<br>Schwerte, Germany |
| qPCR Master Mix | TaqMan® Fast Advanced Master Mix | Thermo Fisher Scientific<br>Schwerte, Germany |
| Reverse Transcription Kit | High Capacity cDNA Reverse Transcription Kit | Thermo Fisher Scientific<br>Schwerte, Germany |
| RNA isolation | mirvana™ miRNA Isolation Kit | Ambion by life technologies<br>Carlsbad, USA |

### 2.1.7 Antibodies

**Table 2.7: List of primary antibodies**

| Specificity | Source | class | Conjugate | Company | Ordering number | Application |
|---|---|---|---|---|---|---|
| Actin | goat | IgG | - | Santa Cruz Biotechnology, Inc. Santa Cruz, USA | sc-1616 | Western Blot |
| CD14 | - | - | Magnetic microbeads | Miltenyi Biotec GmbH Bergisch Gladbach, Germany | 130-050-201 | MACS |
| IgG | rabbit | IgG | - | Santa Cruz Biotechnology, Inc. Santa Cruz, USA | sc-66931 | Immunofluorescence, cytometric analysis |
| MX1 | rabbit | IgG | - | Abcam plc Cambridge, United Kingdom | ab95926 | Immunofluorescence, cytometric analysis, Western Blot |
| TP53 | mouse | IgG2a | - | Abcam plc Cambridge, United Kingdom | ab1101 | Western Blot |
| Tubulin | mouse | IgG2a | - | Santa Cruz Biotechnology, Inc. Santa Cruz, USA | sc-5286 | Western Blot |

**Table 2.8: List of secondary antibodies**

| Specificity | Source | class | Conjugate | Company | Ordering number | Application |
|---|---|---|---|---|---|---|
| Anti-mouse | goat | IgG | Alexa Fluor 555 | Invitrogen Thermo Fisher scientific Carlsbad, USA | A21422 | Immunofluorescence |
| Anti-mouse | goat | IgG | Alexa Fluor 488 | Invitrogen Thermo Fisher scientific Carlsbad, USA | A11001 | Immunofluorescence |
| Anti-rabbit | goat | IgG | Alexa Fluor 555 | Invitrogen Thermo Fisher scientific Carlsbad, USA | A21428 | Immunofluorescence |
| Anti-goat | donkey | IgG | HRP | Santa Cruz Biotechnology, Inc. Santa Cruz, USA | sc-2020 | Western Blot |
| Anti-mouse | goat | IgG | HRP | Santa Cruz Biotechnology, Inc. Santa Cruz, USA | sc-2005 | Western Blot |
| Anti-rabbit | mouse | IgG | HRP | Cell Signaling Technology Leiden, Netherlands | 5127S | Western Blot |

## 2.1.8 Oligonucleotides

**Table 2.9: Custom oligonucleotides for mRNA target detection**

| gene | List name | Custom oligonucleotides for mRNA target detection | application |
|---|---|---|---|
| hATG5 | OBS-1406 | Fwd: CAACTTGTTTCACGCTATATCAGG | qPCR |
| | OBS-1407 | Rev: CACTTTGTCAGTTACCAACGTCA | qPCR |
| hBCL10 | OBS-530 | Fwd: GTGAAGAAGGACGCCTTAGAAA | qPCR |
| | OBS-531 | Rev: TCAACAAGGGTGTCCAGACCT | qPCR |
| hCXCL8 | OBS-0017 | Fwd: ACTGAGAGTGATTGAGAGTGGAC | qPCR |
| | OBS-0018 | Rev: AACCCTCTGCACCCAGTTTTC | qPCR |
| hCYR61 | OBS-1402 | Fwd: GGCTCCCTGTTTTTGGAATGG | qPCR |
| | OBS-1403 | Rev: TTTGAGCACTGGGACCATGA | qPCR |
| hDDX58 | OBS-1542 | Fwd: ATCCCAGTGTATGAACAGCAG | qPCR |
| | OBS-1543 | Rev: GCCTGTAACTCTATACCCATGTC | qPCR |
| hHSPA1A | OBS-1394 | Fwd: TAACCCCATCATCAGCGGAC | qPCR |
| | OBS-1395 | Rev: AACAGCAATCTTGGAAAGGCCC | qPCR |
| hIL1β | OBS-0134 | Fwd: AGC TCG CCA GTG AAA TGA TGG | qPCR |
| | OBS-0135 | Rev: CAG GTC CTG GAA GGA GCA CTT C | qPCR |
| hIRS1 | OBS-1282 | Fwd: CAGCTCACCTTCTGTCAGG | qPCR |
| | OBS-1283 | Rev: AGGTCCATCTTCATGTACTCC | qPCR |
| hJUN | OBS-1414 | Fwd: GAGCTGGAGCGCCTGATAAT | qPCR |
| | OBS-1415 | Rev: CCCTCCTGCTCATCTGTCAC | qPCR |
| hLGALS8 | OBS-1382 | Fwd: TTGAGATCGTGATTATGGTGCT | qPCR |
| | OBS-1383 | Rev: ATCCTGTGGCCATAGAGCAG | qPCR |
| hMX1 | OBS-731 | Fwd: AAGAGCTCCGTGTTGGAGG | qPCR |
| | OBS-732 | Rev: TGGTAACTGACCTTGCCTCTC | qPCR |

| | | | |
|---|---|---|---|
| hMX1 | OBS-1366 | Fwd: GGGCTTTGGAATTCTGTGGC | qPCR |
| | OBS-1367 | Rev: CCTTGGAATGGTGGCTGGAT | qPCR |
| hRND3 | OBS-1430 | Fwd: GAAACAAAGCAGTCGGCTCG | qPCR |
| | OBS-1431 | Rev: ATTTTCTCTCTGAAACGCGGC | qPCR |
| hRPS18 | OBS-0107 | Fwd: GCGGCGGAAAATAGCCTTTG | qPCR |
| | OBS-0108 | Rev: GATCACACGTTCCACCTCATC | qPCR |
| hSOD1 | OBS-1432 | Fwd: CACTGGTGGTCCATGAAAAAGC | qPCR |
| | OBS-1433 | Rev: ACACCACAAGCCAAACGACT | qPCR |
| hSOD2 | OBS-275 | Fwd: ATGTTGAGCCGGGCAGTGTG | qPCR |
| | OBS-276 | Rev: GCGCGTTGATGTGAGGTTCC | qPCR |
| hTP53 | OBS-1500 | Fwd: GGGCTTCTTGCATTCTGG | qPCR |
| | OBS-1501 | Rev: CCTCCGTCATGTGCTGTG | qPCR |
| hZFAND2A | OBS-1400 | Fwd: CTACGGAGGAGGACACCTGA | qPCR |
| | OBS-1401 | Rev: TTAAGTGTCACCTGGCTCTCG | qPCR |
| LINC00278 | OBS-873 | Fwd: AGCCAGGAGTGAAGACGACAG | qPCR |
| | OBS-874 | Rev: AGGTCCTGTAGCACACTGTTCC | qPCR |
| LINC00346 | OBS-875 | Fwd: TCATGGAGTGAGTGCGGAAGAC | qPCR |
| | OBS-876 | Rev: TGGATCTGATGACACTGCAGC | qPCR |

**Table 2.10: Cloning primers for insert amplification and restriction site integration. Restriction sites for NotI and XhoI are underlined**

| name | List name | Custom oligonucleotides for 3'UTR amplification | application |
|---|---|---|---|
| DDX58_fwd3'UTR _3XhoI | OBS-1791 | GTTTCTCGAGtatcaggtcctcaatcttcagc | cloning 3´UTR |
| DDX58_rev_short_NotI | OBS-1793 | GTTTGCGGCCGCgctgaccactgtagagtggatac | cloning 3´UTR |
| TP53_fwd_short_XhoI | OBS-1789 | GTTTCTCGAGgatgatctggatccaccaagac | cloning 3´UTR |
| TP53_rev_NotI | OBS-1790 | GTTTGCGGCCGCcctcagacacacaggtggc | cloning 3´UTR |

**Table 2.11: Commercial Taqman Probes for miRNA detection**

| Probe | mature miRNA sequence (5´- 3´) | Assay-ID | Company |
|---|---|---|---|
| hsa-miR-125a-3p | ACAGGUGAGGUUCUUGGGAGCC | 02199 | Thermo Fisher Scientific Schwerte, Germany |
| hsa-miR-125b-5p | UCCCUGAGACCCUAACUUGUGA | 00449 | Thermo Fisher Scientific Schwerte, Germany |
| hsa-miR-130b-5p | ACUCUUUCCCUGUUGCACUAC | 02114 | Thermo Fisher Scientific Schwerte, Germany |
| hsa-miR-146a-5p | UGAGAACUGAAUUCCAUGGGUU | 00468 | Thermo Fisher Scientific Schwerte, Germany |
| hsa-miR-155-5p | UUAAUGCUAAUCGUGAUAGGGGU | 002623 | Thermo Fisher Scientific Schwerte, Germany |
| hsa-miR-221-3p | AGCUACAUUGUCUGCUGGGUUUC | 000524 | Thermo Fisher Scientific Schwerte, Germany |
| hsa-miR-222-3p | AGCUACAUCUGGCUACUGGGU | 002276 | Thermo Fisher Scientific Schwerte, Germany |
| hsa-miR-26a-2-3p | CCUAUUCUUGAUUACUUGUUUC | 002115 | Thermo Fisher Scientific Schwerte, Germany |
| hsa-miR-27a-5p | AGGGCUUAGCUGCUUGUGAGCA | 002445 | Thermo Fisher Scientific Schwerte, Germany |

| | | | |
|---|---|---|---|
| hsa-miR-29b-1-5p | GCUGGUUUCAUAUGGUGGUUUAGA | 002165 | Thermo Fisher Scientific Schwerte, Germany |
| hsa-miR-579-3p | UUCAUUUGGUAUAAACCGCGAUU | 002398 | Thermo Fisher Scientific Schwerte, Germany |
| RNU48 | GAUGACCCCAGGUAACUCUGAGUGUGU CGCUGAUGCCAUCACCGCAGCGCUCUGACC | 001006 | Thermo Fisher Scientific Schwerte, Germany |

**Table 2.12: Commercial oligonucleotides for detection of primary miRNAs (pri-miRNAs)**

| name | Assay-ID | Company |
|---|---|---|
| hsa-miR-125b | Hs03303224_pri | Thermo Fisher Scientific Schwerte, Germany |
| hsa-miR-146a | Hs03303259_pri | Thermo Fisher Scientific Schwerte, Germany |
| hsa-miR-155 | Hs03303349_pri | Thermo Fisher Scientific Schwerte, Germany |
| hsa-mir-16-2 | Hs03303046_pri | Thermo Fisher Scientific Schwerte, Germany |
| hsa-miR-221 | Hs03303007_pri | Thermo Fisher Scientific Schwerte, Germany |
| hsa-miR-579 | Hs03304404_pri | Thermo Fisher Scientific Schwerte, Germany |

## 2.1.9 siRNA pools

**Table 2.13. List of siRNA pools**

| name | ordering number | Ensembl identifiers | company |
|---|---|---|---|
| Silencer™ Select Negative Control No. 1 siRNA | 4390843 | ´- | Thermo Fisher Scientific Schwerte, Germany |
| SMARTpool: ON-TARGETplus DDX58 siRNA | L-012511-00-0005 | ENSG00000107201 | GE Healthcare Europe GmbH Freiburg, Germany |
| SMARTpool: ON-TARGETplus LGALS8 siRNA | L-010607-00-0005 | ENSG00000116977 | GE Healthcare Europe GmbH Freiburg, Germany |
| SMARTpool: ON-TARGETplus MX1 siRNA | L-011735-00-0005 | ENSG00000157601 | GE Healthcare Europe GmbH Freiburg, Germany |
| SMARTpool: ON-TARGETplus RPL13A siRNA | L-013601-00-0005 | ENSG00000142541 | GE Healthcare Europe GmbH Freiburg, Germany |
| SMARTpool: ON-TARGETplus TP53 siRNA | L-003329-00-0005 | ENSG00000141510 | GE Healthcare Europe GmbH Freiburg, Germany |

## 2.1.10 Synthetic miRNAs

**Table 2.14: List of miRNA mimics**

| name | Assay-ID | company |
|---|---|---|
| mirVana® miRNA mimic miR-125b-5p | MC10148 | Thermo Fisher Scientific Schwerte, Germany |
| mirVana® miRNA mimic miR-221-3p | MC10337 | Thermo Fisher Scientific Schwerte, Germany |
| mirVana® miRNA mimic miR-579 | MC12340 | Thermo Fisher Scientific Schwerte, Germany |
| mirVana™ miRNA Mimic, Negative Control #1 | 4464058 | Thermo Fisher Scientific Schwerte, Germany |

**Table 2.15: List of miRNA inhibitors**

| name | Assay-ID | company |
|---|---|---|
| mirVana® miRNA inhibitor miR-125b-5p | MH10148 | Thermo Fisher Scientific Schwerte, Germany |
| mirVana® miRNA inhibitor miR-221-3p | MH10337 | Thermo Fisher Scientific Schwerte, Germany |

| | | |
|---|---|---|
| mirVana® miRNA inhibitor miR-579-3p | MH12340 | Thermo Fisher Scientific Schwerte, Germany |
| mirVana™ miRNA Inhibitor, Negative Control #1 | 4464076 | Thermo Fisher Scientific Schwerte, Germany |

### 2.1.11 Plasmids

**Table 2.16: List of plasmids**

| Vector | company |
|---|---|
| pSC-A-amp/kan | Agilent Technologies<br>Santa Clara, USA |
| psiCHECK2 Vector | Promega<br>Mannheim, Germany |
| pUCIDT | Integrated DNA Technologies, Inc.<br>Skokie, USA |

### 2.1.12 Media and buffers

**Table 2.17: List of media and buffers**

| Medium | Name | Company |
|---|---|---|
| DMEM | Dulbecco's Modified Eagle Medium | gibco™ life technologies<br>Thermo Fisher Scientific Carlsbad, USA |
| OptiMEM | Opti-MEM® (1x) Reduced Serum Medium | gibco™ life technologies<br>Thermo Fisher Scientific Carlsbad, USA |
| PBS | Phosphate Buffered Saline (1x) | GE Healthcare Life Science Hyclone laboratories<br>Logan, USA |
| RPMI | RPMI Medium 1640 (1x) | gibco™ life technologies Thermo Fisher Scientific Carlsbad, USA |
| RPMI + supplements | RPMI Medium 1640 (1x)<br>[+] 4.5 g/L D-Glucose<br>[+] 2.383 g/L HEPES Buffer<br>[+] L-Glutamine<br>[+] 1.5 g/L Sodium Bicarbonate<br>[+] 110 mg/L Sodium Pyruvate | gibco™ life technologies Thermo Fisher Scientific Carlsbad, USA |
| SILAC DMEM | Dulbecco's Modified Eagle Medium | Thermo Fisher scientific<br>Schwerte, Germany |

### 2.1.13 Cell lines

**Table 2.18: List of cell lines**

| Cultivated cells | origin | cultivation |
|---|---|---|
| Blood-derived macrophages | Isolated from Buffy-coats | 1% Glutamaxx |
| HEK293 | ATCC | 10% FCS<br>In DMEM |
| THP-1 cells | ATCC | 10% FCS<br>in RPMI 1640 + supplements |

### 2.1.14 Bacteria

**Table 2.19: List of bacterial strains**

| Bacterial strain | source |
|---|---|
| *Legionella pneumophila* (Corby) gfp (#69) | provided by the Robert Koch Institut (Berlin, Germany) |

| | |
|---|---|
| *Legionella pneumophila* (Corby) wt (#20) | provided by the Robert Koch Institut (Berlin, Germany) |
| Supercompetent *E. Coli* DH5a | New England Biolabs (Ipswich, USA) |

### 2.1.15 Prepared buffers and solutions

**Table 2.20: List of prepared buffers and solutions**

| name | composition |
|---|---|
| BCYE agar | 10 g ACES<br>10 g Yeast extract<br>2.5 g Charcoal (activated)<br>15 g Agar<br>ad 1 L in $H_2O$ to pH 6.9<br>after autoclavation:<br>0.4 g L-cysteine<br>0.25 g ferric nitrate |
| Buffer A | 2% (v/v) acetonitrile<br>0.1% (v/v) acetic acid<br>in HPLC-grade $H_2O$ |
| ELISA coating buffer | 7.13 g Natriumhydrogencarbonat<br>1.59 g Natriumcarbonat<br>ad 1 L $H_2O$<br>to pH 9.5 with 10 N NaOH |
| ELISA dilution buffer | 10% v/v FCS<br>in 1x PBS |
| ELISA wash buffer | 0.05% v/v Tween<br>in 1x PBS |
| FACS blocking buffer | 10% v/v FCS<br>0.5% v/v Tween<br>in PBS |
| FACS Fixation buffer | 4% v/v PFA<br>in PBS |
| FACS Permeabilisation buffer | 0.5% v/v Tween<br>in PBS |
| FACS Wash Buffer | 5% v/v FCS<br>in PBS |
| Laemmli Buffer | 13.15 % v/v Stacking Buffer<br>21.05 % v/v 10 % SDS<br>10.5 % v/v Glycerol<br>5.75 % v/v 1 % Bromphenol Blue |
| LB Agar | 3.5 % w/v LB Agar<br>in $H_2O$ |
| LB Medium | 2 % w/v LB Broth<br>in $H_2O$. |
| Lysis Buffer | 0.6 M Tris-HCl pH 6,8<br>25X Proteaseinhibitor Cocktail<br>20% v/v NP40<br>Ad 1 mL in Phosphoprotein Wash Buffer |
| MACS Buffer | 0.5% v/v FCS<br>0.2 mM EDTA<br>in PBS |
| Phosphoprotein Wash Buffer | 2.5 mM $Na_3VO_4$<br>125 mM NaF<br>18.75 mM $Na_4P_2O_7$<br>in PBS |
| RIPA Buffer | 10 mM Tris, pH 7.5<br>150 mM NaCl<br>1% v/v NP-40<br>1% v/v Desoxycholat<br>1 mM EDTA |
| SOB medium | 30.7 g SOB |

| | |
|---|---|
| | ad 1 mL in $H_2O$ |
| TAE buffer (50X) | 242 g Tris-Base<br>57.1 mL Ethanoic acid<br>100 mL EDTA (0.5 M)<br>ad 1 L in $H_2O$ |
| TBS buffer (10x) | 10 mM Tris<br>0.9% (w/v)<br>90 g NaCl<br>ad 1 L $H_2O$<br>to pH 7.4 with 37% (v/v) HCl |
| TBST-T | 100 mL 10X TBS buffer<br>0.1% (v/v) Tween-20<br>ad 1 L in $H_2O$ |
| UT-Buffer | 8 M Urea<br>2 M Thiourea<br>in $H_2O$ |
| Western Blot Blocking Solution | 10% (w/v) milk<br>5% (w/v) BSA<br>in 1X TBS-T |
| Western Blot Resolving Gel 10 % | 4.94 mL ddH2O<br>7.56 mL Tris-HCl pH 8.8<br>6.68 mL Acrylamide/Bisacrylamide<br>500 µL 10% (v/v) Glycerol<br>200 µL 10% (w/v) SDS<br>100 µL 10% (w/v) APS<br>20 µL TEMED |
| Western Blot Running Buffer for SDS-PAGE (10X) | 250 mM Tris<br>1.92 M Glycin<br>in $H_2O$ |
| Western Blot Running Buffer for SDS-PAGE (1X) | 100 mL Western Blot Running Buffer for SDS-PAGE<br>0.1% SDS<br>ad 1 L $H_2O$ |
| Western Blot Stacking Gel 5 % | 5.68 mL ddH2O<br>2.5 mL Tris-HCl pH 6,8<br>1.66 mL Acrylamid/Bisacrylamid<br>100 µL 10% (w/v) SDS<br>50 µL 10% (w/v) APS<br>10 µL TEMED |
| Western Blot Wet Blot Buffer (10X) pH 8.3 | 250 mM Tris<br>1.92 M Glycin<br>ad 1 L $H_2O$<br>to pH 7.4 with 37% (v/v) HCl |
| Western Blot Wet blot running buffer (1X) | 200 mL 10X Wet-Blot Puffer<br>20% (v/v) Methanol<br>0.1% (w/v) SDS<br>ad 2 L $H_2O$ |

### 2.1.16 Computational resources

**Table 2.21: List of computational resources**

| Software | Version |
|---|---|
| Adobe Photoshop CS | 5.1 |
| Agilent 2100 Expert Software | B.02.08.SI648 (SR1) |
| Clonemanager | 9 |
| FlowJo v. 7.6.5 | 2.0 |
| GENtle | |
| GraphPad Prism | 6 |

| | |
|---|---|
| ImageJ | 2 |
| LabImage 1D | |
| Microsoft Office 2010 | |
| NEB Cutter | |
| Quant Studio design and analysis | |
| ViiA7 RUO | 1.2 |
| Windows | 7 Professional |

### 2.1.17 List of websites

**Table 2.22: List of used websites**

| Homepages | Link |
|---|---|
| Ensembl | http://www.ensembl.org/index.htmL |
| NCBI | https://www.ncbi.nlm.nih.gov/ |
| Reverse complement tool | http://www.bioinformatics.org/sms/rev_comp.htmL |
| Seqlab | http://www.seqlab.de/ |

## 2.2 Methods

### 2.2.1 Cell culture

#### 2.2.1.1 Preparation and cultivation of primary human monocytes

Monocytes were isolated from donor buffy coats provided by the Centre for Transfusion Medicine and Haemotherapy in Giessen, Germany. All donors gave informed written consent for use of their blood samples for scientific purposes. The blood sample was carefully stacked onto a cushion of Ficoll solution. The two layers were centrifuged for 25 minutes at 800 x g with minimal acceleration and deceleration. The centrifugation yielded a distinct leukocyte layer. Leukocytes were aspirated, resuspended in ambient temperature PBS and washed twice. The pellet was taken up in MACS Buffer. An appropriate amount of cells was incubated with anti-CD14 magnetic microbeads for 20 minutes at 4°C. Labeled cells were magnetically retained in a MACS LS column and eluted after depletion of unlabeled leukocytes. Over 90% of the prepared cells were CD14-positive as tested by FACS analysis. After counting, 8 - 12 x $10^6$ cells were seeded in ultra-low attachment 10cm-plates. Cells were left to adhere for two hours in RPMI medium without supplements. Afterwards, adhesion of cells was validated by microscopy, and 1% (v/v) of human AB serum was added. Monocytes were cultivated for 6 days at 37°C and 5% $CO_2$ without media replacement. Maturation to macrophages was

confirmed by microscopy. For subsequent experiments, macrophages were replated (section 2.2.1.2) for transfections (section 2.2.1.7.1) or infections with *Legionella pneumophila* (section 2.2.1.5.2).

#### 2.2.1.2 Replate of primary human monocytes

After 6 days of cultivation, cells were detached and seeded in cell culture plates to obtain the accurate cell number for experimentation. Therefore, cells were incubated with warm PBS for 10 minutes and detached from the low attachment plate by careful rinsing. Macrophages were centrifuged for 10 minutes at RT with 250 x g and the cell pellet was dissolved in RPMI medium without supplements to obtain the desired cell concentration. Finally, cells were seeded for infection with *L.p.* or used for transfection experiments with siRNA.

#### 2.2.1.3 THP-1 cell culture and PMA

THP-1 cells are immortalized isolates of a one year old infant male with leukemia and used as a model for human monocytes (Tsuchiya, Yamabe et al. 1980). The cell line was purchased from the American Type Culture Collection (ATCC). The human monocytic suspension cell line was cultured in RPMI medium + 10% (v/v) fetal calf serum (FCS) in T75 tissue culture flasks at a density of 2 – 10 x $10^6$ cells/mL. Cells were split regularly to maintain the appropriate density. Cells were discarded upon exceeding the 16th passage, and the culture was re-launched from a frozen stock aliquot. THP-1 cells were passaged and frozen as suggested by ATCC (ATCC®TIB-202TM). To obtain adherent macrophage-like cells, THP-1 monocytes were stimulated with 20 nM Phorbol-12-myristat-13-acetat (PMA) for 24 h. Upon differentiation to macrophages, morphology changes and PMA induced a growth arrest via upregulation of cyclin-dependent kinase inhibitor 1 (p21) (Traore, Trush et al. 2005). Subsequently, media was renewed and differentiated THP-1 cells were used for further experiments.

#### 2.2.1.4 HEK-293T cell culture

Human embryonic kidney cells 293T (HEK-293T) display an adherent epithelial morphology. The cell line was cultured in DMEM + 10% (v/v) FCS in T75 tissue culture flasks at 37°C and 5% $CO_2$ and split regularly to maintain 70 - 90% confluency. Cells were discarded upon exceeding the 22nd passage, and the culture was re-launched from a frozen stock aliquot. Cells were detached by swilling with media and then diluted for further cultivation. The HEK-293T cells were only used for the luciferase-based reporter assay (section 2.2.4.9).

#### 2.2.1.5 Determination of macrophage bactericidal capacity

##### 2.2.1.5.1 Preparing infection cultures for *Legionella pneumophila*

Infection experiments were performed with the Corby strain of *Legionella pneumophila* (*L.p.*). The wildtype strain (#20) or the GFP-expressing strain (#69) of *L.p.* (Table 2.19) was used. Bacteria from frozen glycerol stock were streaked on a BCYE agar plate and incubated for 2 days at 37°C with 5% $CO_2$. This culture was stored at 4°C and used for up to one week. For infection, bacteria were taken from this stored culture with a sterile cotton swab and streaked on a new BCYE agar plate. This plate was incubated for 3 days at 37°C with 5% $CO_2$ and was used on day 3 to prepare the infection solution. The selection of the kanamycin-resistent gfp-expressing strain (#69) was achieved by the cultivation on BCYE agar plates containing 20 µg/mL kanamycin.

##### 2.2.1.5.2 Infection of macrophages with *Legionella pneumophila*

Only differentiated macrophages were infected with *Legionella pneumophila*. Bacteria were scraped from the prepared infection culture and resuspended in PBS to an $OD_{600}$ of 1 which equals 2 x $10^9$ bacteria or colony forming units (CFUs) per mL. Serial dilutions were performed in PBS (infection solution). The ratio of bacteria to cells is defined as the multiplicity of infection (MOI). In order to achieve the desired multiplicity of infection (MOI), the required volume of infection solution was diluted in medium (RPMI + 10% (v/v) FCS) and carefully added to the macrophages. The MOI and infection time was set as indicated in the respective experiments.

For determination of the precise MOI, 50 µL of the dilutions from the infection solution were streaked on BCYE agar plates and incubated for 3 days at 37°C. After incubation, colony forming units (CFUs) were counted and the precise MOI was calculated (CFU/mL= counted colonies x dilution factor).

##### 2.2.1.5.3 Colony forming unit (CFU) assay

In order to assess replication of *L.p.* in human macrophages, CFU assays were performed. The assays were always performed in transfected and differentiated BDMs or THP-1 cells, as described in section 2.2.1.7. To obtain reliable results for one independent experiment, technical triplicates of each treatment and time points were performed. 24, 48 and 72 h post infection with *L.p.*, macrophages were lysed by addition of saponin (1% final concentration) and incubated for 10 minutes at 37°C. Cell lysis was confirmed by microscopy. Lysates were transferred into a new tube and serially diluted in a range from 1:10 to 1:1,000,000 in PBS.

Dilutions were streaked on BCYE agar plates and incubated for three days at 37°C and 5% $CO_2$. Individual colonies were counted and total bacterial load was calculated.

#### 2.2.1.5.4 Determination of infection efficiency by flow cytometry

In order to identify infection efficiencies of THP-1 cells with *Legionella pneumophila*, flow cytometry was used. PMA-differentiated THP-1 cells were infected with a GFP-expressing strain at MOI 10 according to section 2.2.1.5.2.

After the indicated infection time, cells were washed once with PBS and incubated for 4 minutes at 37°C with Trypsin/EDTA for detaching. Subsequently, cells were centrifuged for 8 minutes at room temperature at 300 x g. The pellet was resuspended in PBS with 5% (v/v) FCS and measured on the Guava® easyCyte flow cytometer (Merck Millipore). The data were analysed using FlowJo v. 7.6.5..

### 2.2.1.6 Stimulation of human macrophages

For the dual RNA-Seq approach (section 2.2.3), a synthetic control for TLR2-activating *Legionella* LPS was needed. Therefore, THP-1 cells were stimulated with the TLR2 agonist Pam3CSK4 (Pam3) for 8 and 16 h, respectively. Pam3 stimulation and infection with *L.p.* was performed simultaneously. The bacterial lipoprotein analog Pam3 was added at a final concentration of 100 ng/mL.

### 2.2.1.7 Transfection of human macrophages

#### 2.2.1.7.1 Transfection of BDMs with siRNAs

Blood-derived macrophages were transfected with an siRNA-pool against specific targets (Dharmacon). Transfection was achieved by cultivating cells in medium containing Lipofectamine 2000 and Optimem in a 1:50 ratio plus the respective siRNA-pool at a final concentration depending on the specific siRNA (table 2.23). $4 \times 10^5$ cells were transfected in a volume of 1 mL (100 µL mixed transfection solution + 900 µL cell suspension). Cells were centrifuged for 2 h at 37°C for 2,000 rpm to achieve maximal transfection efficiency. After centrifugation, 1% (v/v) human AB-Serum was added to the cells. After 24 h of incubation, medium was renewed and cells were used for further experiments (e.g. infections with *L.p.* section 2.2.1.5.2). Knockdown of mRNA mediated by siRNA was validated by qPCR (section 2.2.2.5.1) or Western Blot (section 2.2.5.2).

#### 2.2.1.7.2 Transfection of THP-1 cells with siRNAs

Monocytic THP-1 cells (not differentiated) were transfected with an siRNA-pool against specific mRNAs (Dharmacon). Transfection was achieved by cultivating the cells in medium containing Lipofectamine 2000 and Optimem in a 1.5:100 ratio plus the respective siRNA-pool in a final concentration depending on the specific siRNA (table 2.23). $5 \times 10^5$ cells were transfected in a volume of 1 mL (100 µL mixed transfection solution + 900 µL cell suspension). After 24 h, THP-1 cells were stimulated with 20 nM PMA, as previously described (section 2.2.1.3) and incubated for an additional 24 h. Thereafter, medium was renewed and cells were used for further experiments. Knockdown of mRNA mediated by the siRNA-pool was validated via qPCR (section 2.2.2.5.1) or Western Blot (section 2.2.5.2).

**Table 2.23: Transfected amount of siRNA**

| siRNA targets | amount of siRNA |
|---|---|
| DDX58 | 20 nM |
| LGALS8 | 30 nM |
| MX1 | 50 nM |
| TP53 | 30 nM |

#### 2.2.1.7.3 Transfection of macrophages with synthetic miRNAs

Undifferentiated, monocytic THP-1 cells were transfected with double-stranded miRNA precursors. Transfection was achieved by cultivating the cells in medium containing siPort NeoFX and Optimem in 3:100 ratio plus the respective miRNA precursors in a final concentration of 30 nM. $1 \times 10^5$ cells were transfected in a volume of 1 mL (100 µL mixed transfection solution + 900 µL cell suspension). After 24 h, THP-1 cells were stimulated with 20 nM PMA, as previously described (section 2.2.1.3) and incubated for an additional 24 h. Thereafter, medium was renewed and cells were used for further experiments. Overexpression of the given miRNA was verified by qPCR (section 2.2.2.5.3).

### 2.2.2 Investigation of the global macrophage RNA profile upon infection

#### 2.2.2.1 RNA Isolation

In order to estimate changes on the transcriptional level upon infection, RNA expression was analyzed. To this end, cell culture medium was removed. 500 µL TRIZOL® Reagent was added to the cells followed by an incubation for 5 min. The suspension was then transferred to an tube and 100 µL chloroform was added. The mixture was vigorously shaken for 1 minute. After

3 minutes of incubation, samples were centrifuged at 16,000 x g for 15 minutes at 4°C to separate into an aqueous and an organic layer. The aqueous phase, containing the RNA, was transferred into a new tube. RNA precipitation was achieved by the addition of 250 µL isopropanol to the aqueous phase. Additionally, 1 µL of GlycoBlue™ was added to conjugate and visualize precipitated RNA. Precipitation was performed either overnight at -20°C or for 30 minutes at RT followed by a centrifugation step at 16,000 x g for 15 minutes at 4 °C. The supernatant was carefully removed and RNA pellets were washed twice with 500 µL of 75% (v/v) ethanol at 4°C for 5 minutes with 12,000 x g. The remaining pellet was air-dried and resuspended in 15 µL sterile nuclease free water. Potential RNA secondary structures were dissolved by incubating at 58°C for 5 minutes. RNA was stored at -20°C or kept on ice to prevent degradation. The concentration was determined by the Spectrophotometer Nanodrop (Thermo Fisher scientific) or Qubit Fluorometer (Thermo Fisher scientific) if higher sensitivity was required.

#### 2.2.2.2 DNase digestion of RNA

In order to remove potential DNA contamination from the RNA preparation, DNase digestion was performed with DNase I from Roche according to manufacturer´s instructions. The following reaction mix was applied for 1 µg RNA.

**Table 2.24: Mastermix for DNase digestion of RNA**

| component | Final concentration |
|---|---|
| Total RNA | 1 µg |
| 10X incubation buffer | 2 µL |
| DNase I recombinant, RNase-free | 1 Unit |
| Ultrapure water | Ad 20 µL |

The reaction mix was incubated at 37°C for 15 - 20 minutes. Thereafter, the volume was filled up to 200 µL and an equal volume aqua- Phenol, Chloroform und Isoamylalkohol (aqua-PCI) was added for RNA precipitation. The mixture was vigorously shaken and centrifuged at 16,000 x g for 15 minutes at 4°C. The upper phase was transferred and precipitation with isopropanol was performed as described (section 2.2.2.1).

#### 2.2.2.3 Determination of RNA integrity by gel electrophoresis

In order to test the quality of all RNA samples before sequencing, RNA integrity was verified on a Bioanalyzer 2100 (Agilent) according to the manufacturer´s protocol. The ratio of intact 18s

and 28s rRNA was used to calculate an RNA integrity number (RIN). The ration should be 2.1:1, deviations from that indicate RNA degradation. A RIN of 10 reflects perfect RNA quality, while a RIN of 5 means partial degradation. Based on this guideline, RINs > 8 were considered to indicate sufficient RNA quality and useful for further analysis.

#### 2.2.2.4 miRNA analysis by Illumina small RNA sequencing

The miRNome of *L.p.*-infected BDMs was determined by Illumina TruSeq small RNA sequencing. BDMs of three different donors were infected with *L.p.* at an MOI of 0.25 for 24 and 48 h or left untreated as control. RNA was isolated using TRIZOL® (section 2.2.2.1) and the quality was examined on a Bioanalyzer 2100 (Agilent). Samples with sufficient RNA quality were used for Illumina library preparation according to the manufacturer´s instructions.

Briefly, 3' and 5' adapters were ligated to 1 µg total RNA with T4 RNA ligase (Epicentre). Following the reverse transcription of the RNA into cDNA, PCR amplification was performed. To distinguish the prepared samples, different index primers were added. Afterwards, samples with unique indices were pooled into two libraries and cDNA was loaded on a PAA-gel. The fraction with a size of 145 – 160 bp was cut from the gel to enrich for small RNAs. This fraction contained the cDNA transcribed from mature miRNAs generated from 22 nt RNA fragments. Following elution of the cDNA, the final libraries were concentrated by ethanol precipitation. Finally, prepared libraries were validated by a Bioanalyzer run and sent for sequencing.

Sequencing was performed in the lab of Wei Chen in the Max Delbrück Center for Molecular Medicine (MDC) in Berlin. Sequencing was performed in a multiplexed run of 1x51 cycle +7 (index) on an Illumina HiSeq2000 (Illumina).

Bioinformatics analysis of the high-throughput data was carried out by Prof. Dr. Annalisa Marsico (Freie Universität Berlin, Germany).

#### 2.2.2.5 Quantitative real-time PCR analysis

The quantitative real-time PCR (qPCR) is a laboratory method to monitor transcriptional expression changes. It is based on reverse transcription followed by a polymerase chain reaction (PCR). It is used to quantify the amplification of a targeted DNA molecule during the PCR in real-time (Weis, Tan et al. 1992). In this study, qPCR was used to determine expression changes of mRNAs, miRNAs and primary miRNAs (pri-miRNAs).

#### 2.2.2.5.1 mRNA – reverse transcription and quantification

Total RNA was transcribed into cDNA via the High Capacity reverse transcription kit (Thermo Fisher Scientific). According to the manufacturer's protocol, 200 – 2,000 ng RNA were used for the transcription via random hexamer primers. The reaction was set to a final volume of 20 µL with ultrapure water.

**Table 2.25: Mastermix for the reverse transcription of mRNAs**

| Component | Volume for 20 µL reaction |
|---|---|
| 10X RT buffer | 2 µL |
| 10X Random Primers | 0.8 µL |
| 100 mM dNTPs | 2 µL |
| 50 U/µL multiscribe reverse transcriptase | 1 µL |
| RNA (250 – 2000 ng) | X µL |
| Ultrapure water | Ad 20 µL |

The following thermal cycling program was applied:

**Table 2.26: mRNA reverse transcription thermo protocol**

| Cycle step | Temperature | Time |
|---|---|---|
| annealing | 25°C | 10 minutes |
| elongation | 37°C | 2 hours |
| deactivation | 85°C | 5 minutes |
| hold | 8°C | ∞ |

The obtained cDNA was diluted to a final concentration of 5 ng/µL and subsequently quantified on a ViiA7 Real-Time PCR System (Thermo Fisher Scientific) using the SYBR Green detection method. This dye intercalates into double stranded DNA thereby allows detection of the amplified product. The following mastermix with specific primers (table 2.9) was used to detect expression changes of target genes.

**Table 2.27: Mastermix for mRNA quantification by quantitative real time PCR**

| Component | Volume for 20 µL reaction |
|---|---|
| 2X FAST SYBRR Green Master Mix | 10 µL |
| 10 µM Primer forward | 0.4 µL |
| 10 µM Primer reverse | 0.4 µL |
| cDNA (7.5 ng final) | 1.5 µL |
| Ultrapure water | Ad 20 µL |

The following program was used for cDNA amplification:

**Table 2.28: High capacity reverse transcription thermo protocol**

| | Cycle step | Temperature | Time |
|---|---|---|---|
| | denaturation | 95°C | 20 seconds |
| 40 cycles | primer binding/elongation | 60°C | 20 seconds |
| | denaturation | 95°C | 15 seconds |
| | cycling end | 60°C | 1 minute |
| | melting curve | 60 - 95°C | 0.05 °C/s gradually |
| | | 95°C | 15 s |

The cycle threshold (Ct) was determined by the ViiA7 software (Thermo Fisher Scientific). The Ct value indicates the number of cycles at which the fluorescent signal is higher than the background. The higher the cDNA amount in the sample, the sooner the threshold cycle is reached, and the lower the Ct value. Ct values of the target genes were normalized to the constant Ct value of an endogenous reference gene yielding the ΔCT and used to determine differences in expression between samples. The ribosomal 18S-RNA (RPS18) represented the endogenous reference gene for mRNAs. Expression analysis was performed with the $2^{(-\Delta CT)}$ method suggested by Livak et al. (Livak and Schmittgen 2001):

**ΔCt** = Ct target gene - Ct reference gene

**ΔΔCt** = ΔCt (treated/infected sample) - ΔCt (control/uninfected sample)

**- (ΔΔCt)** = log2-fold change

$\mathbf{2^{(-\Delta\Delta Ct)}}$ = linear x-fold change

The log2-fold change was used to display the qPCR results.

#### 2.2.2.5.2 miRNA – reverse transcription and quantification

In order to detect miRNA expression changes, 350 – 1,000 ng of total RNA were transcribed into cDNA using the Taqman microRNA reverse transcription kit (Thermo Fisher Scientific). A multiplex reaction with specific RT-primer and the RT-primer for the endogenous control was applied to reverse transcribe several miRNAs in one reaction. Reverse transcription was performed according to manufacturer's protocol.

**Table 2.29: Mastermix for the reverse transcription of miRNAs**

| Component | Volume for 15 µL reaction |
|---|---|
| 10X RT buffer | 1.5 µL |
| RT primerpool (0.05X each) | 6 µL |
| 100 mM dNTPs | 0.3 µL |

| | |
|---|---|
| 50 U/µL multiscribe reverse transcriptase | 3 µL |
| RNA (350 – 1000 ng) | X µL |
| Ultrapure water | Ad 15 µL |

The following thermal cycling program was applied:

**Table 2.30: miRNA reverse transcription thermo protocol**

| Cycle step | Temperature | Time |
|---|---|---|
| annealing | 16°C | 30 minutes |
| elongation | 42°C | 30 minutes |
| deactivation | 85°C | 5 minutes |
| hold | 8°C | ∞ |

The obtained cDNA was usually diluted at a final concentration of 6.66 ng/µL with one exception. For detection of the miR-125b, cDNA was applied undiluted for quantification on the ViiA7 Real-Time PCR System. The detection of the amplified product was performed by sequence-specific TaqMan probes. The resulting reactionmix with the addition of specific Taqman probes was used to detect expression changes. Reaction volume was set to 20 µL with ultrapure water.

**Table 2.31: Mastermix for miRNA quantification by quantitative real time PCR**

| Component | Volume for 20 µL reaction |
|---|---|
| 2X TaqMan® Fast Advanced Master Mix | 10 µL |
| TaqMan primer | 1 µL |
| cDNA (10 ng final) | 1.5 µL |
| Ultrapure water | Ad 20 µL |

The same program for cDNA amplification was used as for the reverse transcribed mRNA (table 2.28). The signal of each specific miRNA was normalized to the small nuclear noncoding RNA RNU48. Since it is constantly expressed in normal tissues and cell lines, it was used as an endogenous control (Gordanpour, Nam et al. 2012; Manikandan, Deva Magendhra Rao et al. 2015; Crossland, Norden et al. 2016). The log2-fold change was calculated as previously described.

#### 2.2.2.5.3 pir-miRNA – reverse transcription and quantification

For the detection of primary miRNAs (pri-miRNA), the TaqMan® Pri-miRNA Assay Kit was used. Reverse transcription was performed as previously described for mRNA transcription (section 2.2.2.5.2). Since the primers of the TaqMan® Pri-miRNA Assay will detect genomic DNA, a

DNase digestion of the isolated RNA was performed before reverse transcription (described in section 2.2.2.2).

For the quantification of cDNA the same reaction mix and thermoprofile as used for the detection of mRNA expression was applied (table 2.28).

### 2.2.3 Dual RNA-seq

Dual RNA-seq refers to the application of the high-throughput RNA sequencing technique to a dual system composed of host cells, here infected with *Legionella,* allowing the host and the pathogen transcriptome to be analysed in parallel at different time points during the course of infection. This technique was performed in accordance with the procedure established for *Salmonella* infection of human epithelial cells (Westermann, Forstner et al. 2016). The technique has been adapted and applied for the first time to *Legionella* infection of human macrophages. In the following, the steps of the procedure are described in detail.

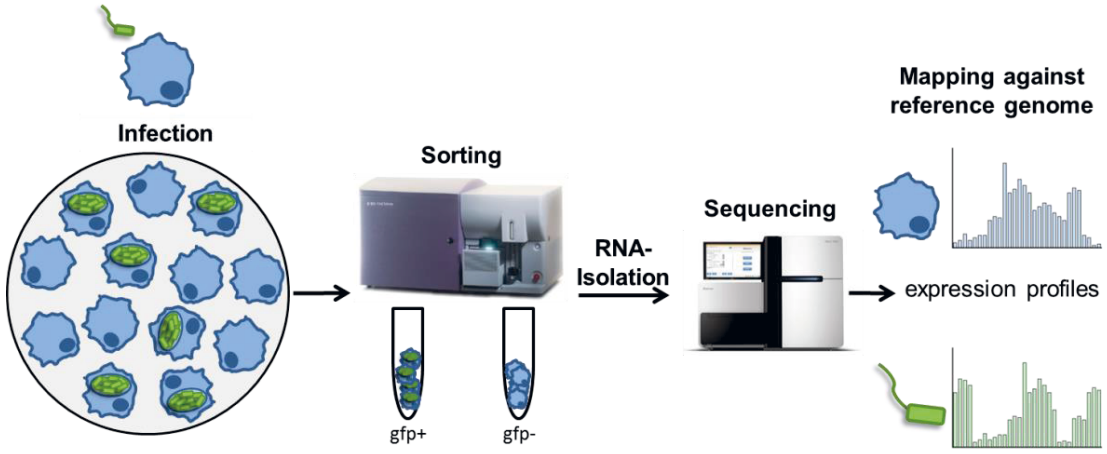


**Figure 2.1: Simplified Scheme of the dual RNA-Seq approach.** Macrophages (host cells) are infected with a GFP-expressing strain of *Legionella pneumophila* (pathogen) *in vitro*. After a certain infection time, *Legionella*-invaded cells (gfp+) are separated from non-infected bystander cells (gfp-) via FACS-sorting. Afterwards, RNA is isolated and processed for sequencing. The separation of host and pathogen is taking place *in silico* via the mapping of the reads against the two different reference genomes. Finally, the expression profiles of both, host and pathogen are determined.

#### 2.2.3.1 Stimulation and *Legionella*-infection of THP-1 cells

THP-1 cells were differentiated in with 20 nM PMA for 24 h (section 2.2.1.3). After medium change, cells were infected with a GFP-expressing strain of *Legionella pneumophila* at an MOI of 10 or stimulated with 100 ng/mL Pam3CSK4 for 8 and 16 h. After the addition of bacteria, cells were centrifuged for 10 minutes at 500 x g to synchronize the infection process. At the same time, control bacteria from the infection solution (*L.p.* T0) were centrifuged for 5

minutes at 4°C with 3,500 x g. Three tubes with 2 x $10^9$ bacteria each were incubated in 1 mL RNAprotect™ solution for 30 minutes. After incubation, 400 µL PBS was added and centrifuged for 5 minutes at 4°C with 6,000 x g followed by two PBS washing steps. Afterwards, bacterial pellets were frozen in liquid nitrogen and stored at -80°C.

At 2 h post infection, THP-1 cells were washed twice with PBS and medium containing 25 µg/mL Gentamycin was added to selectively inactivate extracellular *Legionella*, thus synchronizing the infection and preventing reinfection.

#### 2.2.3.2 Fluorescence activated cell sorting (FACS) of *Legionella* infected macrophages

At 8 and 16 h post infection or stimulation, THP-1 cells were washed once with PBS and subsequently detached using Trypsin/EDTA for 4 minutes at 37°C. Cells were centrifuged for 10 minutes at 300 x g. Cell pellets were resuspended in PBS and cell concentration was determined. Cells were kept on ice and infected macrophages (GFP-positive fraction) were separated from the non-invaded bystander cells (GFP-negative fraction) by cytometric sorting on a BD Aria III (BD Bioscience) machine. Sorting was performed in the Flow Cytometry Core Facility, Marburg, with the assistance of Dr. Hartmann Raifer. Uninfected THP-1 cells (ctr) were also sorted to obtain an appropriate control. At least 4 x $10^5$ cells were sorted into 4 mL RNAprotect™ solution to maintain RNA integrity. After Sorting, cells in RNAprotect™ solution were centrifuged for 10 minutes at 4,500 x g and 4°C. Cell pellets were washed twice. Finally, pellets were frozen in liquid nitrogen and stored at -80°C until RNA was isolated.

In order to assess the sort purity, a post sort analysis was performed where a sub-population of the sorted cells was re-analysed. Secondly, 9 x $10^5$ sorted cells (gfp- and gfp+) were lysed with 1% (v/v) saponin, diluted in PBS and streaked on a BCYE agar plate. Bacterial colonies were counted and CFU/mL was calculated.

#### 2.2.3.3 RNA Isolation (miRVana)

Total RNA was isolated using the mirVana™ miRNA Isolation Kit. According to manufacturer's protocol, thawed pellets were completely lysed in lysis/binding buffer. After organic extraction and washing steps, total RNA was eluted in 100 µL ultrapure water. RNA quality was verified using Bioanalyzer 2100 (Agilent) (section 2.2.2.3).

#### 2.2.3.4 Sequencing

Total RNA was sent for commercial sequencing to Vertis Biotechnologie AG (Freising, Germany). RNA was depleted for bacterial ribosomal RNA (rRNA), eukaryotic cytoplasmic rRNA and mitochondrial rRNA using Ribo-Zero Gold rRNA Removal Kit (Epidemiology) (Illumina). No polyA enrichment was performed to preserve all different RNA species for sequencing, including circular RNAs. Random-primed libraries without cutoff above 50 bp were prepared from biological triplicates and sequenced on an Illumina Illumina NextSeq 500 system with a 75 bp read length. Sequencing the miRNA fraction required additional steps. First, the small RNA fraction (<200 bp) was purified from the total RNA and concentrated using RNeasy MinElute Cleanup kit (Qiagen). Secondly, the miRNAs were isolated by nuclear acid fractionation (Caliper LabChip XT) by help of an internal size marker. Afterwards, the samples were processed and sequenced as previously described.

#### 2.2.3.5 Bioinformatics analysis

The bioinformatics analysis was performed by Prof. Annalisa Marsico (Freie Universität Berlin, Germany) and Dr. Brian Caffrey (MPI MolGen Berlin, Germany) (section 2.2.7.1).

### 2.2.4 Functional microRNA evaluation by luciferase-based reporter constructs

For studying miRNA-mRNA interaction, luciferase assays were performed. Firstly, the vector plasmids were constructed by cloning the 3'UTR fragment into the psiCHECK-2 plasmid. Secondly, HEK 293T cells were transfected with cloned vector constructs and the miRNA mimics followed by the bioluminescence detection.

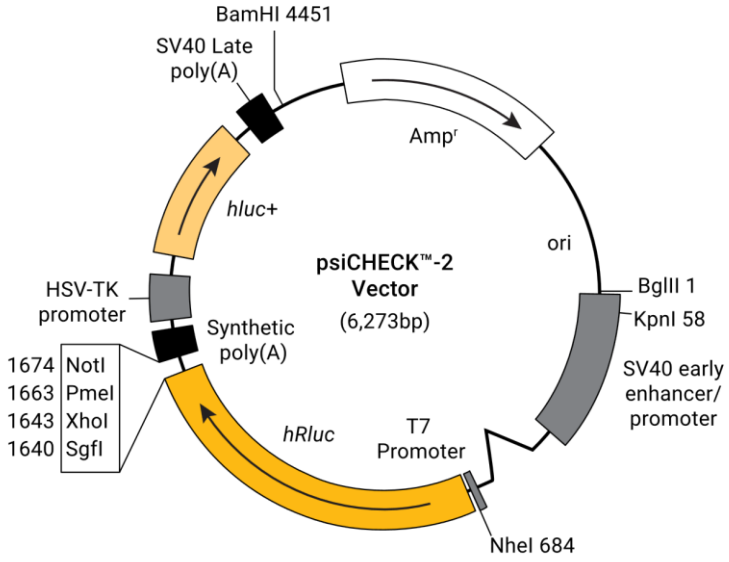


**Figure 2.2: The psiCHECK2 vector.** The plasmid carries a sequence which encodes for firefly luciferase (hluc+) and for *Renilla reniformis* luciferase (hRluc). Located within the hRluc sequence is a multiple cloning site which was used for the insertion of the respective mRNA 3'UTR sequence (wildtype or mutated). For selection purposes, the vector carries an ampicillin resistance gene (Amp$^r$). The vector was designed by Promega.

### 2.2.4.1 Construction of the vector constructs

#### 2.2.4.1.1 PCR for fragment amplification

Polymerase chain reaction (PCR) is a laboratory technique that is used for the amplification of a DNA segment. This method generates thousands to millions of copies of a particular DNA sequence by the use of specific primers (Bartlett and Stirling 2003). In this study, PCR was used to generate and amplify the 3'UTR fragments of DDX58 and TP53. The fragments were amplified from an uninfected cDNA sample of THP-1 cells with the use of specific primers (table 2.10). The forward primer possessed a restriction site for XhoI (CTCGAG), while the reverse primer carried a restriction site for NotI (GCGGCCGC). To verify the absence of NotI and XhoI restriction sites in the 3'UTR fragment, the amplified sequence was screened by Clone Manager (Scientific & Educational Software). PCR was performed with the Phusion® High-Fidelity DNA Polymerase PCR Kit (NEB). PCR was performed according to manufacturer's protocol.

**Table 2.32: Mastermix for fragment amplification via PCR with phusion polymerase**

| Component | Volume for a 50 µL Reaction |
|---|---|
| 5X Phusion HF Buffer | 10 µL |
| 10 mM dNTPs | 1 µL |
| 10 µM Primer forward | 1 µL |

| | |
|---|---|
| 10 µM Primer reverse | 1 µL |
| Phusion DNA Polymerase | 0.5 µL |
| $MgCl_2$ | 1 µL |
| PCR Enhancer | 5 µL |
| Template DNA (500 ng) | x µL |
| Nuclease-free water | Ad 50 µL |

The elongation time and the annealing temperature were adjusted according to fragment size and primer sequence, respectively. A gradient PCR with the indicated cycler program (table 2.33) was performed on a temperature PCR Cycler PeqSTAR 2x Gradient (Peqlab) to determine the optimal annealing temperature.

The following PCR program was applied:

**Table 2.33: Thermo protocol for the phusion polymerase PCR**

| | Cycle step | Temperature | Time |
|---|---|---|---|
| | initial denaturation | 98°C | 1 minute |
| 25 cycles | denaturation | 98°C | 5 seconds |
| | primer binding | X°C | 15 seconds |
| | elongation | 72°C | 60 seconds/1kb |
| | final extension | 72°C | 10 minutes |
| | hold | 4°C | ∞ |

Only the wildtype versions of the 3'UTR of DDX58 and TP53 were amplified with the aforementioned primers. The DNA sequence of the mutated version of TP53 3'UTR was ordered as DNA fragment and directly cloned into the pSC-A-amp/kan PCR Cloning Vector. The plasmid pUCIDT, carrying the mutated sequence of DDX58 3'UTR and the wildtype and mutated version of LGALS8 3'UTR, was also purchased. Thus, the ordered plasmid was directly transformed into competent *E.coli* (Top 10) for amplification (section 2.2.4.6) and subsequently cloned into the psiCHECK-2 vector.

#### 2.2.4.1.2 Stratagene cloning

The StrataClone PCR Cloning Kit is used for the quick cloning of PCR products. It has a high cloning efficiency and the blue-white screening allows for the quick detection of the colonies harboring the vector with the fragment of interest. In order to obtain higher amounts of the 3'UTR fragment, the amplified fragment was firstly cloned into the pSC-A-amp/kan PCR Cloning Vector by the use of the StrataClone PCR Cloning Kit (Agilent). Therefore, the PCR

components were removed by column purification (NucleoSpin Extract II Kit). The method was performed according to the manufacturer´s protocol. Briefly, the fragment was ligated into the StrataClone Vector that contains two DNA arms, each charged with topoisomerase I on one end and a loxP containing recognition sequence on the other end. Taq-amplified PCR products contain 3' adenosine overhangs. Thus, the fragment was efficiently ligated to vector arms through A-U base-pairing followed by topoisomerase I-mediated strand ligation. Subsequently, the ligated linear molecule was cloned into a competent *Escherishia coli* (*E. coli*) engineered to transiently express Cre recombinase. A circular vector is generated by the Cre-mediated recombination between the vector loxP sites. Transformed cells were grown on media containing ampicillin. Since the resulting vector possesses a lacZ´ α-complementation cassette, transformed colonies were selected by blue-white screening. The white colonies harbored the vector with the inserted fragment.

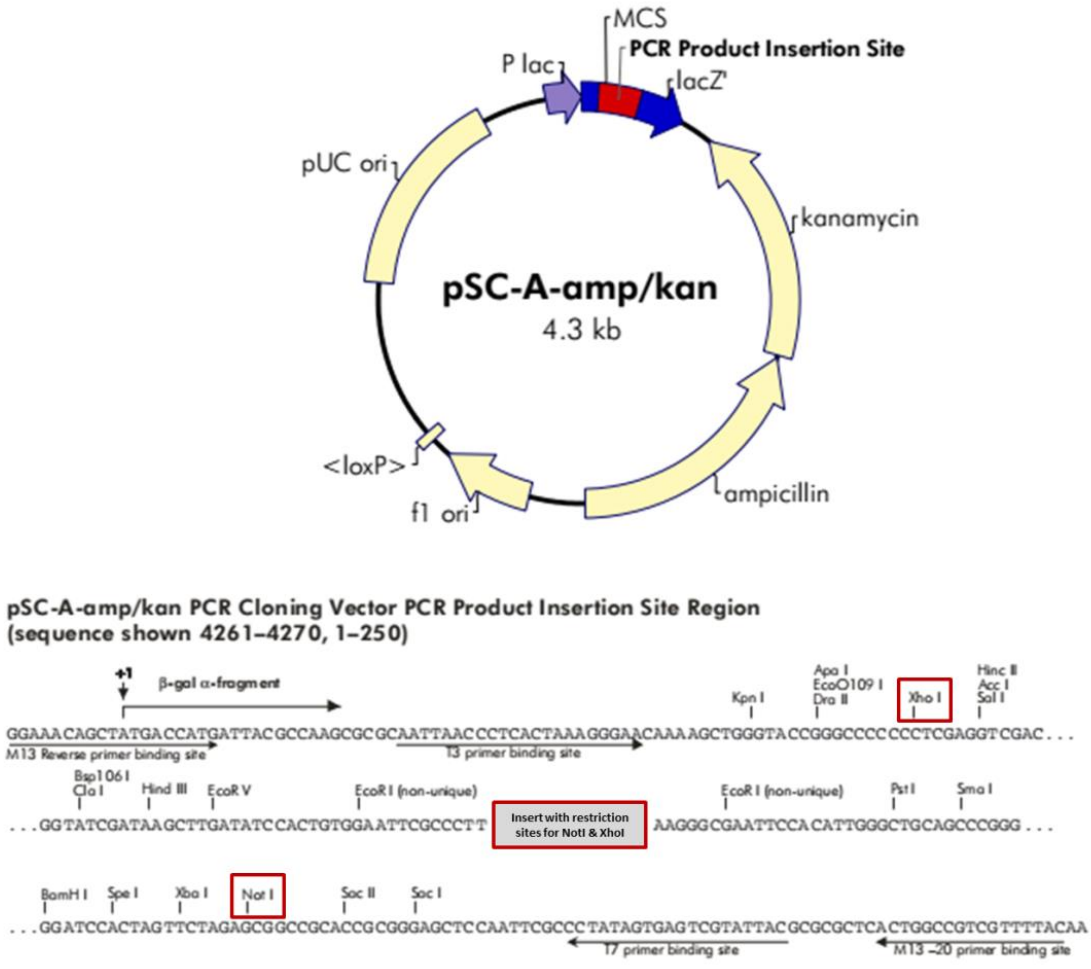


**Figure 2.3: Map for the StrataClone PCR Cloning Vector pSC-A-amp/kan.** Within the rlacZ' sequence is a multiple cloning site located which was used for the insertion of the amplified PCR product. The lacZ´ α-complementation cassette can be used for blue-white screening. For selection purposes, the vector carries an ampicillin and a kanamycin resistance gene. The insert is located within the multiple cloning sequences (MCS) of the vector and different primer binding sites and enzyme restriction sites are indicated in the sequence below. The vector was designed by Agilent.

#### 2.2.4.1.3 Colony PCR

In order to more quickly screen for colonies with correct integration of the insert of interest, colony PCR was performed. Therefore, single colonies were picked and resuspended in the PCR reaction mix containing the DNA-polymerase of *Thermus aquaticus* (Taq polymerase) (Chien, Edgar et al. 1976; Saiki, Gelfand et al. 1988). Amplification was achieved by addition of specific primers that flanking the insert (adjusted to the used vector construct).

**Table 2.34: Mastermix for colony-PCR with Taq polymerase**

| Component | Volume for a 25 µL Reaction |
|---|---|
| 10X Taq Buffer | 2.5 µL |
| 10 mM dNTPs | 0.5 µL |
| 10 µM Primer forward | 0.5 µL |
| 10 µM Primer reverse | 0.5 µL |
| $MgCl_2$ | 1 µL |
| Taq polymerase | 0.2 µL |
| Nuclease-free water | 19.8 µL |
| Picked colony | |

**Table 2.35: Primer pairs used for screening of correct integration of the insert of interest**

| Vector construct | Primer fwd | sequence | Primer rev | sequence |
|---|---|---|---|---|
| pSC-A-amp/kan | OBS-1294 | TATCCACTGTGGAATTCGCC | OBS-1295 | AGCCCAATGTGGAATTCGC |
| pUCIDT | OBS-0113 | GTAAAACGACGGCCAGTG | OBS-0076 | GGAAACAGCTATGACCATGA |
| psiCHECK-2 | OBS-0522 | CAAGAGCTTCGTGGAGCG | OBS-0523 | CGCGAGGTCCGAAGACTC |

Depending on the fragment size and primer sequences, elongation time and annealing temperature were adjusted, respectively.

**Table 2.36: Thermo protocol for the colony PCR with Taq polymerase**

| | Cycle step | Temperature | Time |
|---|---|---|---|
| | initial denaturation | 95°C | 5 minutes |
| 35 cycles | denaturation | 95°C | 30 seconds |
| | primer binding | X°C | 30 seconds |
| | elongation | 72°C | 60 seconds/1kb |
| | final extension | 72°C | 5 minutes |
| | hold | 4°C | ∞ |

#### 2.2.4.2 Agarose gel electrophoresis

For separation of DNA fragments with different lengths, an agarose gel electrophoresis was performed. The DNA fragments are separated by applying an electric field. Since DNA is negatively charged, the DNA moves to the positively charged pole through the agarose matrix. Based on the sieve effect, smaller fragments migrate faster than longer fragments. Therefore, the separation of the DNA fragments depends on the fragment length (Bjornsti and Megonigal 1999). For all experiments, 1.5% or 2% agarose gels with 1X TAE-Buffer and 1X GelRed (Biotium Inc) were used. For determination of fragment size, one lane was loaded with a DNA ladder. Depending on the expected fragment size, the DNA standard Gene Ruler 1 kb or the FastRuler™ Low Range DNA ladder (Thermo Fisher Scientific) was used. The electrophoresis was run in 1X TAE-Buffer at 120 V. DNA was visualized by a Gel documentation apparatus with UV-light (INTAS).
For gel extraction, the agarose gel was run at 80 V and stopped as soon as the DNA fragment of interest was sufficiently separated from the other bands. The UV exposure time was kept at a minimum to avoid damaging of the DNA fragments.

#### 2.2.4.3 Gel extraction

DNA fragments of interest were cut from the agarose gel with a scalpel. DNA extraction was performed with the NucleoSpin Gel and PCR Cleanup Kit (Machery-Nagel) according to the manufacturer's protocol. The concentration of the purified DNA was determined by the Spectrophotometer Nanodrop (Thermo Fisher scientific).

#### 2.2.4.4 Restriction digest

After PCR amplification, PCR components were removed by column purification with NucleoSpin Gel and PCR Cleanup Kit (Machery-Nagel). In order to clone amplified DNA fragments into the psiCHECK-2 vector, the amplified DNA fragments and the empty psiCHECK-2 vector were digested with NotI (NEB) and XhoI (NEB). The reaction was set up as recommended by the manufacturer instructions (https://nebcloner.neb.com/#!/redigest).

**Table 2.37: Mastermix for double digest of DNA**

| Component | Volume for a 25 µL Reaction |
|---|---|
| DNA (1 µg) | X µL |
| 10 X NEBuffer 3.1 | 5 µL |
| XhoI | 1 µL |

| | |
|---|---|
| NotI | 1 µL |
| Nuclease-free water | Ad 50 µL |

Digestion was performed for 15 minutes at 37°C. Restriction enzymes were deactivated at 65°C for 20 minutes. Digested fragments were isolated using gel electrophoresis followed by gel extraction and column purification (section 2.2.4.3).

#### 2.2.4.5 Ligation

The purified and digested DNA fragments were ligated into linearized psiCHECK-2 plasmid. Therefore, 100 ng of digested plasmid and 20 ng of accordingly digested insert were incubated at room temperature for 10 minutes with 1 µL T4 ligase (NEB) at a final volume of 20 µL. Subsequently, the enzyme was heat inactivated at 65°C for 10 minutes. Afterwards, the ligated vector was transformed into competent *E. coli* (Top10) (section 2.2.4.6).

#### 2.2.4.6 Transformation of vector constructs in *E. coli*

The generated or custom-made vector constructs were transformed into a chemically competent *E. coli* strain (Top10) for amplification. The required amount of competent cells was thawed on ice for 10 minutes. Afterwards, 5 µL of ligation reaction or 1 µL of empty plasmid was added to 50 µL competent cells. The solution was incubated on ice for 30 minutes. Subsequently, cells were incubated at 42°C for 45 seconds. Immediately after the heat shock step, cells were placed on ice for 2 minutes. The 5-fold volume of SOC medium was added. Cells were incubated for 30 minutes at 37°C and shaken vigorously (250 rpm). The suspension with the transformed bacteria were plated on pre-warmed LB agar plates containing appropriate antibiotics. Plates were incubated over night at 37°C.

#### 2.2.4.7 Plasmid extraction

Single colonies were picked and inoculated in liquid LB-media containing the appropriate antibiotics. Cultures were grown overnight at 37°C. Isolation of the plasmid was performed with the plasmid mini kit (Nucleo Spin® Plasmid Quick Pure, Macherey Nagel), or with the plasmid midi kit (Nucleobond® Xtra Midi Plus EF from Macherey Nagel) followed by the manufacturer´s instruction. Extracted plasmids were stored at -20°C.

#### 2.2.4.8 Sequencing of generated vector constructs

Cloned and mutated vector constructs were sent for sequencing to validate accuracy of the sequence. The Sanger Sequencing was executed by sequencing service of LMU Munich or by the company Microsynth Seqlab (Göttingen). Sample preparation was performed according to company instructions. The obtained sequences were tested for their accuracy by Clone Manager (Scientific & Educational Software).

#### 2.2.4.9 Transfection of HEK-293T

HEK-293T cells were reverse transfected with Lipofectamine2000 (Thermo Fisher Scientific) and Optimem in a 1:50 ratio. Cells were simultaneously transfected at a final concentration of 2.5 pmol miRNA mimic and 200 ng generated vector construct (psiCHECK-2 with specific 3'UTR) per 100 µL. As control, a scramble mimic was transfected. The empty vector (psiCHECK-2) was transfected in combination with the miRNA mimics to exclude non-specific signals achieved by miRNA overexpression. In this study, mimics for miR-125b, miR-221 and miR-579 were used. If all three miRNAs (miRNA-pool) were added, transfection was performed at a final concentration of 2.5 pmol (each mimic 0.833 pmol). The prepared transfection mix was incubated for 10 minutes at room temperature and then added to the cells. Subsequently, cells were cultured for 72 h at 37°C with 5% $CO_2$. Then, bioluminescence detection was performed.

#### 2.2.4.10 Quantification of microRNA efficiency by bioluminescence

Reporter gene constructs are used to study and quantify expression changes of a target gene which is fused to the reporter gene. The psiCHECK-2 vector contains two reporter genes. The Renilla luciferase is used as primary reporter gene. The sequence of interest (3'UTR of DDX58, TP53 and LGALS8) is cloned into the region located downstream of the Renilla translational stop codon. The co-transfection of a miRNA mimic results in cleavage and subsequent degradation of the transcript, if the miRNA binds to the sequence of interest (Fig. 2.4). Therefore, a decrease in Renilla activity indicates that the miRNA binds to the cloned sequence of interest. The second reporter gene is the Firefly luciferase and allows for the normalization of Renilla luciferase expression and a distinction between specific and global effects. Therefore, a decrease of both luminescences indicates a global impact on the cell population mediated by cell death or inhibition of cell growth. Thus, this reporter assay leads to reproducible results and enables the monitoring of the influence of a miRNA on the 3'UTR by measuring the bioluminescence.

The Dual-Glo® Luciferase Assay System Kit (Promega) was used to measure the interaction between miRNA and 3'UTR. The constructed vectors with 3´UTR of DDX58, TP53 and LGALS8 (wildtype and mutated versions) were used. All steps were performed according to manufacturer´s instructions. Firefly luminescence was determined 10-15 minutes after substrate addition with the Tecan Infinite M200 PRO plate reader (Thermo Fisher Scientific) with 1 s integration time. The ratio of Renilla- and Firefly-luminescence was calculated and further normalized to the empty vector lacking the specific 3´UTR.

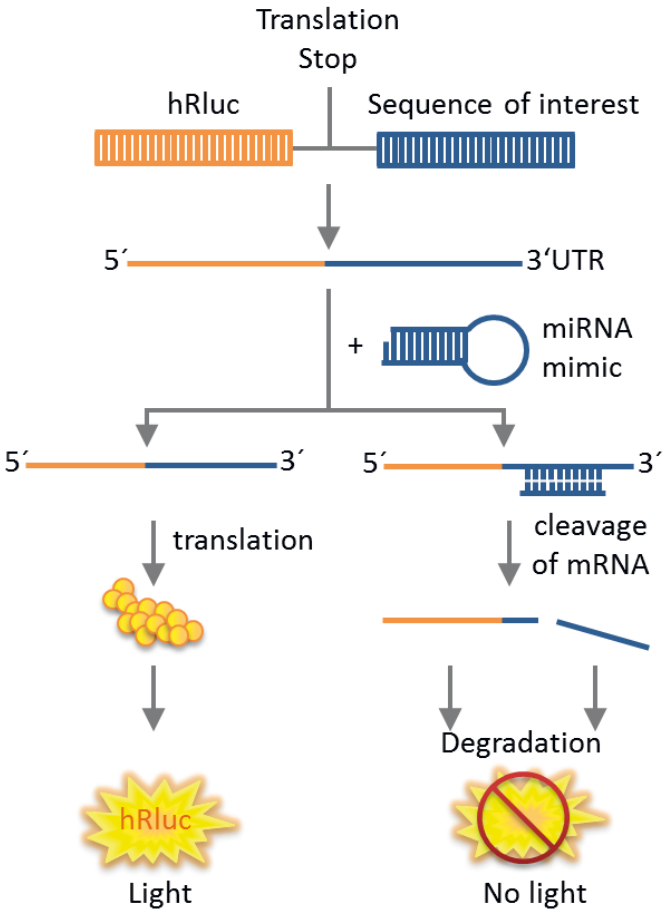


**Figure 2.4: Simplified scheme of the mechanism of action of the quantification of miRNA efficiency by bioluminescence.** Within the Renilla reniformis luciferase (hRluc) sequence is a multiple cloning site located which was used for the insertion of the respective mRNA 3'UTR sequence (sequence of interest). This vector is transfected into HEK-293T cells and a fusion of the Renilla luciferase gene and the gene of interest is transcribed. The miRNA mimic is co-transfected simultaneously. If a specific miRNA binds to 3'UTR of the target mRNA and initiates the RNAi process, the Renilla luciferase fused with target gene will be cleaved and subsequently degraded, leading to a decreased Renilla luciferase signal. Adapted from: Promega, Technical Bulletin for siCHECK™ Vectors, Version 6/09.

### 2.2.5 Biochemical methods

#### 2.2.5.1 Lactate dehydrogenase release (LDH) measurement

In order to determine cytotoxicity in cultured cells, LDH release in harvested supernatants was measured by Cytotoxicity Detection kit of Roche. The procedure was performed as instructed by the manufacturer. Supernatants of THP-1 cells and BDMs were diluted 1:10. Measurements were performed in technical duplicates with the Tecan Infinite M200 PRO plate reader (Thermo Fisher Scientific).

#### 2.2.5.2 Semi quantitative protein analysis by Western Blot

After indicated incubation time, cells were washed with PBS and lysed in RIPA buffer (without SDS). Lysed cells were centrifuged at maximum speed for 20 minutes at 4°C to remove cell debris. Protein concentration was determined by bicinchoninic acid assay (BCA assay). Measurements were carried out with the Pierce™ BCA Protein Assay Kit. All steps were performed according to manufacturer´s instructions. Optical density was measured in the Tecan Infinite M200 PRO plate reader (Thermo Fisher Scientific) at a wavelength of 595 nm, and protein concentration was calculated.

Samples were taken up in Laemmli-buffer at 1:5 ratio and denatured for 5 minutes at 95°C. For protein separation, 10% SDS gels were used, and 20 to 30 µg of protein were loaded per lane and a marker lane was included as reference. For focusing the proteins in the stacking gel, 80 V was applied. Thereafter, voltage was increased to 120 V for transmigration of the proteins into the resolving gel.

Proteins were transferred to a nitrocellulose membrane with the use of a tank blot for 1 h at 100 V.

Afterwards, the membrane was blocked over night at 4°C in a mixture of 10% milkpowder solution with 3% Bovine serum albumin (BSA). Primary antibody (α-MX1-antibody) was added at a 1:1,000 dilution and incubated for 2 hours at room temperature on a tumbling shaker. Unbound protein was removed by several washing steps in TBS-T. HRP-conjugated secondary antibody was given for additional 2 hours at room temperature on a tumbling shaker. After removal of excess antibody by washing, protein signal was detected on the Bioluminescence and Chemoluminescence Imager (INTAS).

When required, quantification of signal was performed by densitometric analysis, using the LabImage 1D software (Kapelan Bio-Imaging GmbH).

#### 2.2.5.3 Determination of secreted Cytokines

##### 2.2.5.3.1 Enzyme Linked Immunosorbent assay (ELISA)

The enzyme-linked immunosorbent assay (ELISA) is an analytic biochemistry assay that uses antibodies to identify the presence of substances (e.g. secreted cytokines) in a liquid samples (Engvall and Perlmann 1971). In this study ELISAs were performed to determine secreted CXCL8 in supernatants of control or *L.p.*-infected samples. Measurement was carried out with the DuoSet® ELISA Kit for human Interleukin-8 (CXCL-8) (BD Biosciences). The applied test uses HRP-conjugated antibodies and color changes to identify protein abundances. Analyses were performed according to manufacturer´s instructions. Supernatants were diluted depending on secretion levels. The measurement readings were performed in technical duplicates with the Tecan Infinite M200 PRO plate reader (Thermo Fisher Scientific).

##### 2.2.5.3.2 MILLIPLEX® Multiplex Assays Using Luminex®

This technology allows measuring multiple cytokines in a single reaction with high sensitivity. The method is a magnetic bead-based assay that determines concentration of up to 50 analytes in one sample. Therefore, this assay was used to determine the concentration of IL-1β, IL-6, GM-CSF, TNF-α and IL-10 in cell-free supernatants of *L.p.*-infected and uninfected macrophages. For THP-1 cells cytokine secretion was measured in samples infected with *L.p.* at an MOI of 0.25 and 0.5 at 24 and 48 h post infection. Since the well number on one plate was limited, the determination of secreted cytokines of BDMs was only performed at 48 h post infection. Samples were diluted accordingly. The MILLIPLEX MAP Human High Sensitivity T Cell Panel Premixed 13-plex - Immunology Multiplex Assay (Millipore) was used and performed according to the manufacturer's instructions. Range of detection for each molecule was [pg/mL]: 21-406 (IL-1β), 23-384 (IL-6), 21-373 (GM-CSF), 23-391 (TNF-α), 24-422 (IL-10). The Infinite® M200 Pro microplate reader (Tecan) and MAGPIX System (Luminex) was used for measurements.

#### 2.2.5.4 Cytometric analysis of intracellular protein by indirect immunofluorescence staining

THP-1 cells were transfected either with synthetic miRNA mimics or with an siRNA-pool against DDX58. As control a scramble mimic or siRNA was transfected. Subsequently, cells were differentiated and infected with *L.p.* at MOI 0.5 for 24 and 48 h or left untreated as control. After the infection time, THP-1 cells were detached with Trypsin/EDTA for 5 minutes at 37°C

and washed once with PBS. Cells were fixed with 4% PFA for 10 minutes in the dark and washed 3 times with PBS (centrifugation: 5 minutes, 2,000 x g). Then, THP-1 cells were permeabilized with 0.5% Tween in PBS for 15 minutes, followed by the blocking of non-specific binding sites for 30 minutes at room temperature in PBS with 0.5% (v/v) Tween and 10% FCS. Cells were centrifuged for 5 minutes at 5,000 x g and room temperature. The obtained cell pellet was solved in 100 µL PBS with 0.5% (v/v) Tween and 10% (v/v) FCS and Human BD Fc Block (BD Bioscience) was added for 10 minutes (2.5 µg for 1 x $10^6$ cells) to block non-specifc binding of antibodies to Fc receptors. Primary antibody (α-MX1 antibody) was additionally added at a 1:500 dilution for 1 hour without any washing step in between. Since an indirect staining was performed, α-IgG antibody as control was necessary to assess the specific fluorescence signal for MX1. This antibody was given at a 1:1,000 dilution to obtain the corresponding antibody amount. For removal of excess antibody cells were washed 3 times with PBS (5% (v/v) FCS) (centrifugation: 5 minutes, 5,000 x g). Afterwards, all cell pellets were incubated with secondary antibody (anti-rabbit Alexa 555) at a 1:2,000 dilution in PBS with 0.5% (v/v) Tween and 10% (v/v) FCS for 30 minutes at room temperature in the dark. After three washing steps with PBS (5% (v/v) FCS), pellets were resuspended in PBS containing 5% (v/v) FCS and analyzed on the Guava® easyCyte flow cytometer (Merck Millipore). The data were analyzed using FlowJo v. 7.6.5..

### 2.2.6 Stable isotope labelling by amino acids in cell culture (SILAC)

#### 2.2.6.1 Labelling of THP-1 cells and production of the heavy standard

In order to allow relative quantification of protein abundance changes in response to miRNA and/or infection, a heavily labelled SILAC standard was prepared. Therefore, THP-1 cells were cultivated in SILAC-DMEM with 2% (v/v) FCS lacking arginine and lysine. The medium was additionally supplemented with heavy isotope labelled $^{13}$C arginine and lysine (Sigma Aldrich) and THP-1 cells were cultured over five passages. Then, 2.4 x $10^8$ THP-1 cells were stimulated with 20 nM PMA and transferred into twenty 10 cm cell culture plates as previously described (section 2.2.1.3). In order to ensure high coverage of proteins in the subsequent internalization experiment, parts of the heavily labelled THP-1 cells were additionally infected with *L.p.* at an MOI of 0.5 for 24 h as described above (section 2.2.1.5.2). Before spiking the heavily labelled standard as quantification reference in all subsequent biological samples, non-infected and infected heavily labelled cells were tested for complete incorporation of heavy $^{13}$C arginine and lysine. To do so, supernatant was removed and cells were washed with PBS and removed from the culture plate by scratching in buffer consisting of 8 mol/L urea and 2 mol/L thiourea in

HPLC-grade water (UT-buffer). Cells were immediately frozen in liquid nitrogen and stored at -80°C until preparation for mass spectrometry. Afterwards, heavily labeled standard was sent to the lab of Prof. Dr. Uwe Völker for further analysis.

In the following, the methods are described in detail performed by Dr. Kristin Surmann and Sascha Blankenburg. Mass spectrometry measurements were done by Manuela Gesell Salazar.

#### 2.2.6.2 Sample preparation for nanoHLPC–MS/MS

Cells were disrupted applying five freezing (liquid nitrogen) and thawing (30°C, 500 rpm, 7 minutes) steps supported with sonication on ice (3x3 s, 50% power, SonoPuls, Bandelin electronic). Supernatant from subsequent centrifugation (room temperature, 20,000 x g, 1 hour) was collected in fresh vials and frozen at -80°C. Prior to tryptic digestion the abundances of protein in the samples was determined using a Bradford assay in technical triplicates.

The heavily labelled THP-1 cells (infected and non-infected THP-1 cells separately) were digested first in gel-free manner for determination of the $^{13}C$ arginine and lysine incorporation rate by mass spectrometry. Therefore, 4 µg of each sample were taken up in 20 mmol/L aqueous ammonium bicarbonate buffer to dilute the urea concentration to less than 1 mmol/L. Proteins were reduced with 2.5 mmol/l dithiothreitol at 60°C for 1 hour, alkylated with 10 mmol/L iodoacetamide at 37°C for 30 minutes in the dark, and digested overnight at 37°C using trypsin (Promega) in a protease to protein (m/m) ratio of 1:25. Digestion was stopped with a final concentration of 1% (v/v) acetic acid. By centrifugation (room temperature, 16,000 x g, 10 minutes) insoluble components were removed. The peptide-containing supernatant was desalted and purified using $C_{18}$ ZipTip columns. Purified peptide solution were dried by lyophilization and reconstituted in 20 µL buffer A [2% (v/v) acetonitrile and 0.1% (v/v) acetic acid in HPLC-grade water (J. T. Baker)]. Samples were stored short-term at -20°C before by nanoHLPC–MS/MS. Since the measurements and data analysis revealed heavy isotope labeling of more than 97% for all peptides and proteins, it was accepted as fully labeled. Finally, protein extracts of infected and non-infected heavily labeled THP-1 cells were mixed in equal protein amounts as global SILAC standard. The protein concentration of this mixed global SILAC standard was determined and aliquots were stored at -80°C to allow addition of the same standard to all future biological samples.

Each 5 µg protein from the miRNA and *L.p.* infection experiment were mixed with 5 µg of the mixed global SILAC standard.

These combined samples (10 µg protein) were separated using one-dimensional gel (1D gel) electrophoresis with NuPAGE4-12% acrylamide Bis-Tris Midi Gels (Novex Life Technologies) according to the molecular weight in order to decrease the complexity of the samples. Samples were supplemented with 1 µL reducing agent and 2.5 µL sample buffer (Novex Life Technologies). The proteins were denatured at 70°C for 10 minutes. Gels were run at 200 mA for 5 minutes and afterwards at 160 mA until additional marker was visible at the bottom of the gel. Gels were stained with Coomassie Brilliant Blue to control separation. To do so, gels were fixed for 1 hour in 40% (v/v) ethanol and 20% (v/v) acetic acid in distilled water and washed twice for 15 minutes in distilled water. Gels were incubated overnight with colloidal Coomassie Silver Blue solution [consisting of 10% (m/v) (NH4)2SO4; 10% (v/v) phosphoric acid; 0.12% (m/v) Coomassie G250 and 20% (v/v) methanol]. The gels were destained twice for 15 minutes in methanol and washed twice for 15 minutes in distilled water. At this stage, images were acquired. Afterwards, each sample lane on the 1D gel was cut into 10 equal sized slices. Prior to tryptic digestion of the enclosed proteins, gel slices were incubated twice with 200 µL 20 mmol/L aqueous ammonium bicarbonate (37°C, 150 rpm, 15 minutes) with removal of the supernatant between the repetitions of this step. The now fully discolored gel slices were then dehydrated with 100 µL acetonitrile (37°C, 150 rpm, 15 minutes). This step was also repeated one more time. Next, 20 µL of 5 ng/µL trypsin (Promega) in 20 nmol/L aqueous ammonium bicarbonate solution was added to the dehydrated gel together with 20 µL 20 nmol/L aqueous ammonium bicarbonate. After incubation at 37°C for 1 hour, the complete rehydration of the gel was controlled. If necessary 20 nmol/L aqueous ammonium bicarbonate was removed or added and tryptic digestion occured at 37°C for further 14 hours. Peptides were extracted from the gels first by incubation with 50 µL aqueous 0.1% (v/v) acetic acid for 30 minutes in an ultrasonic bath and then the supernatants of each two adjacent fractions were combined to reduce the final number of fractions per sample from ten to five. Extraction was repeated with 50 µL 0.05% (v/v) acetic acid in 50% (v/v) acetonitrile for 30 minutes in an ultrasonic bath and the supernatants of the same two adjacent fractions were combined with the once from the acetic acid extraction step. Samples were dried by lyophilization, reconstituted in 40 µL 1% (v/v) acetic acid prior to purification using $C_{18}$ ZipTip columns (Merck-Millipore). After one more lyophylization step, peptides were dissolved in 20 µL buffer A before nanoHLPC-MS/MS.

#### 2.2.6.3 Data acquisition by nanoHLPC–MS/MS

Peptides were analyzed on a Q Exactive mass spectrometer (Thermo Fisher Scientific) after separation on a Dionex UltiMate 3000 nanoLC system (Dionex/Thermo Fisher Scientific) and

ionization with a TriVersa NanoMate source (Advion, Ltd.). Peptide separation was performed with a trap column (2 cm x 75 µm inner diameter, packed with 3 µm $C_{18}$ particles, Acclaim PepMap 100, Thermo Fisher Scientific) and a 25 cm x 75 µm analytical column packed with 2.6 µm C18 particles of 150 Å pore size (Acclaim PepMap RSLC). Peptides were separated by a linear gradient using a binary buffer system of buffer A and buffer B [0.1% (v/v) acetic acid in acetonitrile (Thermo Scientific)] at a flow rate of 300 nl/min from 5% to 25% in 60 minutes (0 min-2% B, 2 min-5% B, 10 min-5% B, 70 min-25% B, 75 min-40% B, 77 min-90% B, 82 min-90% B, 85 min-2% B, 95 min-2% B). For mass analysis the Q Exactive was operated in DDA mode applying a full scan resolution of 70,000 in the range from 300 to 1,650 m/z. The ten most abundant isotope patterns (centroid data) with charge ≥2 from the survey scan were selected for MS/MS analysis and fragmented by higher energy collisional dissociation (HCD).

#### 2.2.6.4 Data analysis

MS data were searched using MaxQuant (Cox and Mann 2008) against a database derived from Uniprot limited to human entries. Oxidation at methionine and $^{13}C$ labeling (+6.02 Da) at arginine and lysine were set as dynamic modification, no missed cleavage of trypsin was performed. The false discovery rate of peptide identifications was set to < 1%. Only peptides which were detected with more than one peptide or with one peptide, if it contributed to at least 10% of the protein sequence coverage were allowed for further analysis. Furthermore, proteins had to be detected in at least three of the four biological replicates per condition for calculation of protein ratios between the conditions or had to be absent in at least three of the four replicates per condition for determination of so-called ON/OFF proteins depending on conditions. In the latter case, ratios were set manually to 1000 (ON) or 0.001 (OFF) to enable proceeding with data visualization. From the MaxQuant analysis, program specifically normalized SILAC ratios (light to heavy) of the peak areas in the experimental samples against the global SILAC standard were retrieved on protein level. These data were compared between infection and control depending on the presence of miRNA and the point in time of harvest. P- and q-values were calculated using the Genedata Analyst v8.0 software (Genedata AG, Basel, Switzerland). Proteins were defined as regulated if the absolute fold change exceeded 1.2 respectively 1.5 and the q-value amounted < 0.05. Venn diagrams were created using JVenn (http://jvenn.toulouse.inra.fr/app/index.html) to visualize general differences on the proteome profiles of the THP-1 cells depending on the treatment.

### 2.2.7 Statistical analyses of conventional experimental data

Statistic evaluation was carried out with GraphPad Prism (Version 7). For data with multiple variables, a two-way ANOVA (Analysis of variance) was performed followed by either Sidak´s comparison test or Tukey´s. For comparison of two data columns, the paired t-test was employed on log2 transformed data. For all tests, a Gaussian distribution was assumed, and the confidence interval was set to 95%. Therefore, p-values ≤ 0.05 were considered significant. All performed statistical tests are specified in each figure legend.

#### 2.2.7.1 Statistical analysis of high-throughput data

The data gained from Illumina RNA sequencing required extensive correlation studies and statistical correction for large sample sizes. Advanced analyses were carried out by Prof. Dr. Annalisa Marsico (Freie Universität Berlin, Germany) and Dr. Brian Caffrey (MPI MolGen Berlin, Germany).

To analyse the dual RNA-Seq data, a workflow as Unix Shell script was implemented.

Read Quality assessment was performed upon next generation sequencing and is the validation of sequence quality. Sequence quality was performed using the FastQC software. Illumina reads in FASTQ format were trimmed with an average Phred quality score cut-off of 20 over every four base pair window by the program Trimmomatic. 3’ adapters were also trimmed using Trimmomatic. Reads shorter than 20 nt after adaptor trimming were discarded before mapping.

RNA-Seq reads were aligned to the human genome assembly of hg19 by using the program STAR. Star conducts ultrafast mapping of RNA reads to a reference by use of uncompressed suffix arrays. This methodology allows for the creation of a joint genomic index for pathogen and host combined. A combined index allows for this simultaneous mapping but also for the removal of reads which map to both genomes. Star was used with default options with the allowance for split reads. Reads mapping to both genomes were not considered under the scope of this thesis.

Differential expression analysis was performed using the DESeq2 R/bioconducter package. DESeq2 identifies genes which have significantly increased/decreased in expression by use of a negative binomial distribution fit as a generalised linear model. Finally, the p-values were adjusted using the procedure introduced by Benjamini and Hochberg.

#### 2.2.7.2 Principal component analysis

In order to visually represent the global sample variation within the RNA sequencing and proteomics experiments, a principal component analysis (PCA) was performed.

PCA was done by Dr. Wilhelm Bertrams according to his doctoral thesis (Bertrams 2014). The DESeq2 normalized reads with an adjusted p-value ≤ 0.01 were used for the PCA of the dual RNA-Seq approach including 5,433 genes. For the proteomics experiments, only calculated ratios of heavy and light protein quantifications were used for creating the PCA (588 quantified proteins included).

# 3 Results

In general, this study aims at creating a comprehensive knowledge of the crosstalk of *Legionella pneumophila* (*L.p.*) infection and non-coding RNAs in human macrophages. It is structured in two parts.

The first describes the changes of miRNA expression in *L.p.*-infected host cells on a global level and their functional consequences on inflammation and bacterial replication.

The second focuses on the identification of the gene expression profile during the course of *Legionella* infection of both, the host and the pathogen, simultaneously.

## 3.1 *L. pneumophila*-induced changes of miRNA expression and their importance for bacterial replication

miRNAs are important regulators of gene expression in development, the innate and adaptive immune response as well as TLR-signalling. Therefore, the question arose whether miRNAs could have a role during the course of infection of human macrophages with *Legionella pneumophila* (Sonkoly, Stahle et al. 2008; Lu and Liston 2009; Xiao and Rajewsky 2009; Nahid, Satoh et al. 2011b).

In humans, *Legionella pneumophila* infects alveolar macrophages (Chandler, Hicklin et al. 1977). Therefore, primary human monocytes were deemed more appropriate as a model for these cells, as opposed to an immortalised cell line. Primary monocytes were isolated from buffy coats of healthy donors by positive magnetic selection for CD14. CD14 is a surface marker and mainly expressed by monocytes (Ziegler-Heitbrock, Ancuta et al. 2010). After differentiation over 6 days with human AB-Serum, the human blood-derived macrophages (BDMs) were infected with *L.p.*.

### 3.1.1 Establishment of macrophage infection with *Legionella pneumophila* (*L.p.*)

The most important initial investigation for characterizing the miRNA-mediated regulatory network in *Legionella* infection was the optimization of infection dose and time points. To this end, human BDMs were infected with increasing multiplicities of infection (MOIs) for 24 and 48 h. A key requirement for the identification of differentially expressed miRNAs in *L.p.*-infected macrophages was low cytotoxicity with a substantial inflammatory response to rule out apoptosis-related miRNA regulation. Therefore, CXCL8 secretion (Fig. 3.1 A) and cytotoxicity (Fig. 3.1 B) were examined. An MOI of 0.25 showed a significant increase in CXCL8

secretion and cytotoxicity below 30% as determined by LDH. An MOI of 0.25 and 0.5 were used for further analysis in this study. To investigate another macrophage-like cell model, THP-1 cells were used and compared to the primary BDMs. This monocytic cell line was differentiated into macrophages by the addition of 20 nM of PMA as previously described (section 2.2.1.3). After 24 h of differentiation, cells were infected with *L.p.* at an MOI of 0.25 and 0.5 and both macrophage cell types were infected for 24 and 48 h. In order to compare the inflammatory response an ELISA was performed to determine CXCL8 secretion (Fig. 3.1 C, D).

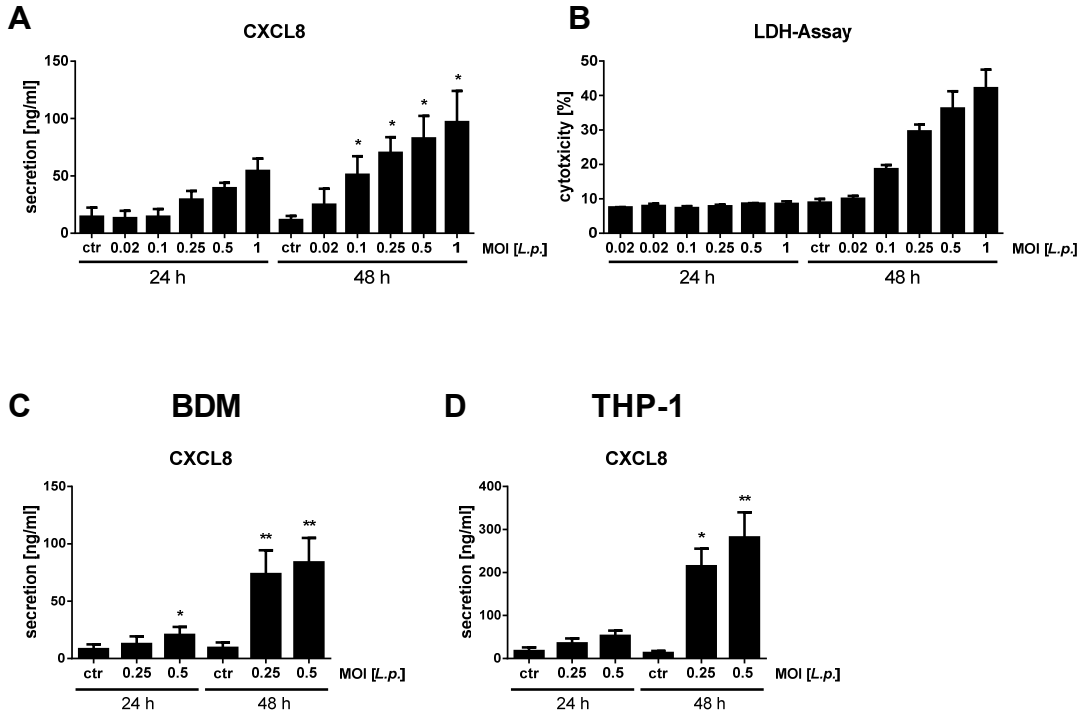


**Figure 3.1: Establishment of the infection of macrophages with *Legionella pneumophila* (*L.p.*).** Blood-derived macrophages (BDMs) from different donors were infected with increasing MOIs of *L.p.*: 0.02; 0.1; 0.25; 0.5; 1 or left untreated as control (ctr). The supernatants were taken 24 or 48 h post infection. CXCL8 secretion was determined by ELISA (A) and cytotoxicity was examined by LDH-Assay (B). MOI of 0.25 and 0.5 were taken for comparison of CXCL8 secretion in BDMs (C) and THP-1 cells (D). THP-1 cells were stimulated with PMA at a final concentration of 20 nM and 24 h later were infected with *L.p.* for 24 and 48 h. Data are shown as mean + SEM of two to four independent biological replicates. Paired t-tests were performed: *p ≤ 0.05, **p ≤ 0.01 compared to corresponding control.

In summary, THP-1 cells secreted more CXCL8 than primary BDMs after 24 and 48 h post infection. Nevertheless, infection with *L.p* led to a comparable inflammatory response in both cell types.

### 3.1.2 Pro-inflammatory cytokine release of macrophages upon infection with *L.p.*

As a further comparison of the inflammatory response of THP-1 cells and BDMs, the secretion levels of additional cytokines were tested. Macrophages were infected with *L.p.* at an MOI of 0.25 and 0.5 for 24 and 48 h. Afterwards, secretion of IL-1ß (Fig. 3.2A, B), IL-6 (Fig. 3.2C, D), GM-CSF (Fig. 3.2E, F), TNF-α (Fig. 3.2G, H) and IL-10 (Fig. 3.2I, J) were measured using the Multiple Luminex assay (section 2.2.5.3.2). Cytokine secretion analyses demonstrated a significant induction of IL-1ß, IL-6, GM-CSF, TNF-α and IL-10 release at 48 h post infection in both cell types. THP-1 cells secreted more IL-1ß and GM-CSF upon infection with *L.p.*, while BDMs responded to the *Legionella* infection with higher secretion of IL-6, TNF-α and IL-10 at 48 h post infection.

In conclusion, the secretion pattern of the BDMs was similar to the pattern observed in THP-1 cells. Thereby, both cell types had shown a pro-inflammatory response following *L.p.* infection at a MOI of 0.25 and 0.5

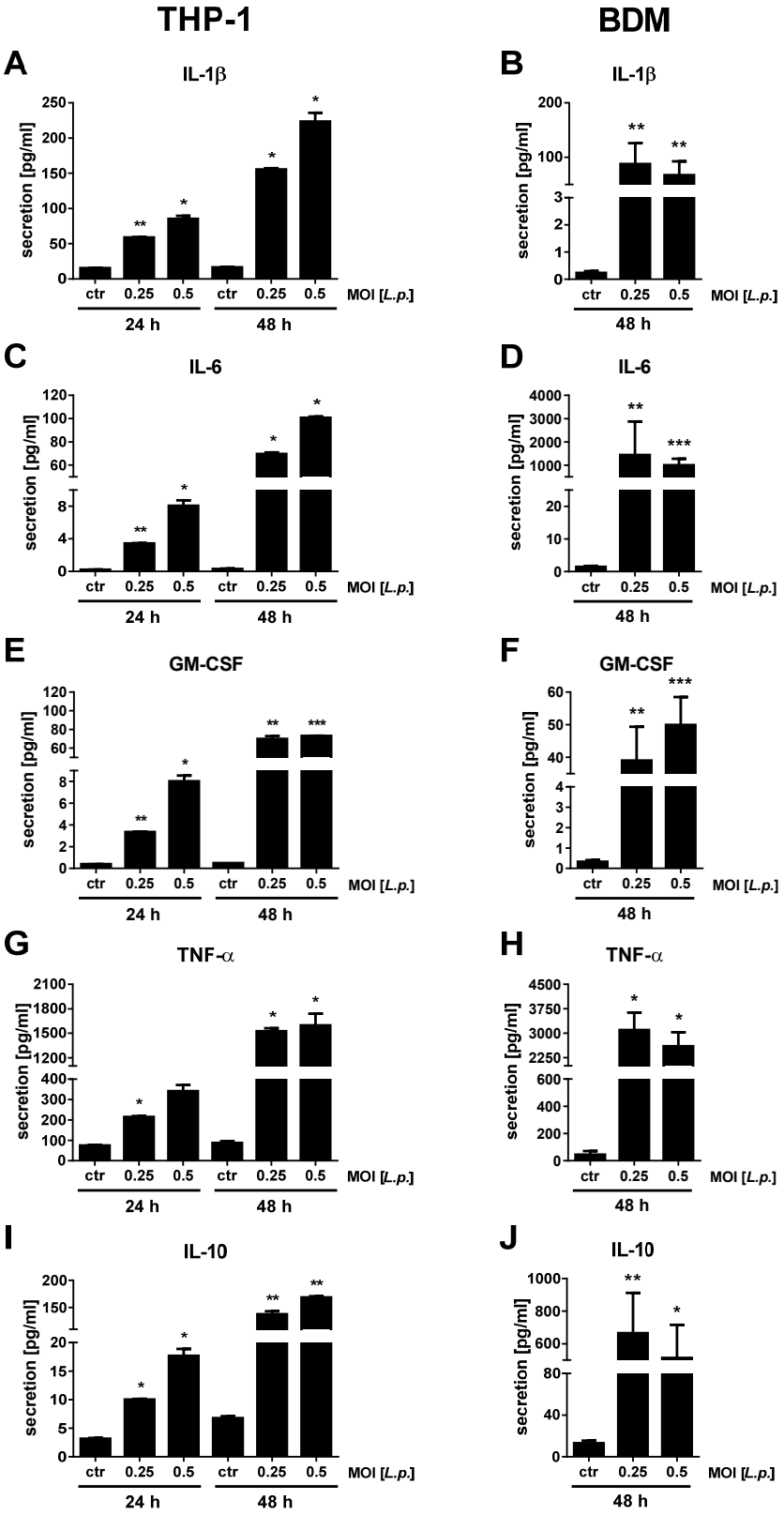


**Figure 3.2: Pro-inflammatory cytokine release of macrophages upon infection with *L.p.*.** BDMs or PMA-differentiated THP-1 cells were infected with *L.p.* at an MOI of 0.25 or 0.5 for 24 or 48 h, respectively. Secretion of IL-1β (A, B), IL-6 (C, D), GM-CSF (E, F), TNF-α (G, H) and IL-10 (I, J) was measured using Multiplex Luminex Assay. Data are shown as mean + SEM of three independent biological replicates. Paired t-tests were performed: *$p \leq 0.05$, **$p \leq 0.01$, ***$p \leq 0.001$ compared to corresponding control.

### 3.1.3 Differentially expressed miRNAs in macrophages after *L.p.* infection.

In order to characterize the miRNA-mediated regulatory network upon *Legionella* infection, human BDMs of three different donors were infected with *L.p.* at an MOI of 0.25 for 24 and 48 h. Libraries for deep sequencing analysis were enriched for RNA species between 20 and 30 nt to enrich human miRNAs in the sequencing libraries. A computational pipeline for the analysis of small RNA sequencing data was developed and applied by Prof. Annalisa Marsico (Freie Universität Berlin, Germany).

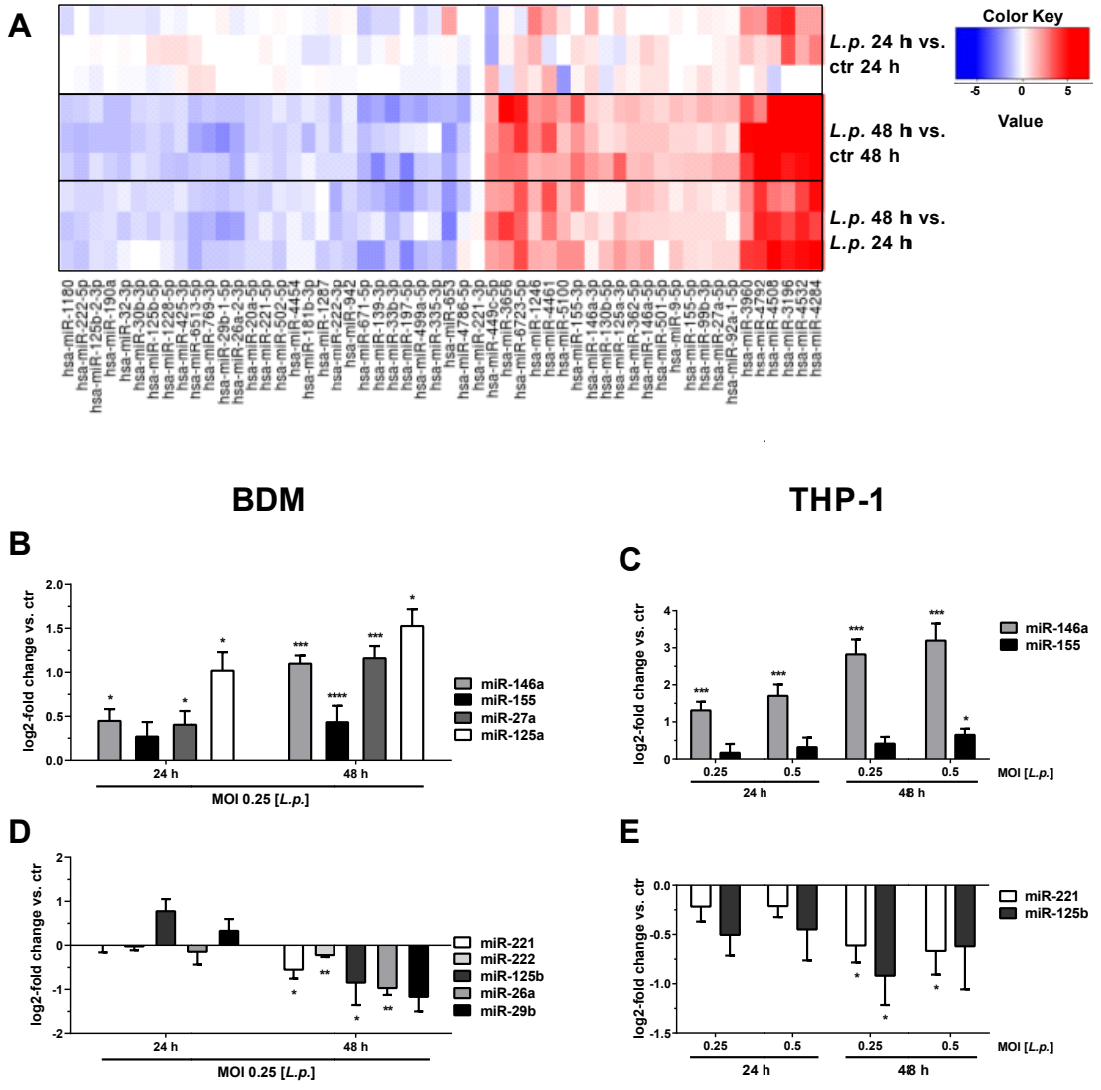


**Figure 3.3: Differentially expressed miRNAs in macrophages after *L.p.* infection.** BDMs from three different donors were infected with *L.p.* at an MOI of 0.25 or left untreated as control (ctr). Samples were taken 24 and 48 h post infection. RNA was isolated and used for library preparation and enriched for small RNAs using the TruSeq™ Small RNA kit. Sequencing was performed in a multiplexed run of 1x51 cycle +7 (index). Results are shown in a heatmap (A). Expression of distinct up (B, C) and downregulated (D, E) miRNAs in BDMs and THP-1 cells after *L.p.* infection was validated by qPCR using TaqMan assays and displayed as log2-fold change. Data are shown as mean + SEM of five to nine independent biological replicates for dysregulated miRNAs. Paired t-tests were performed: *$p \leq 0.05$, **$p \leq 0.01$, ***$p \leq 0.001$, ****$p \leq 0.0001$ compared to the corresponding control.

This pipeline integrates existing tools for quality control, mapping of sequencing reads, identification of putative novel miRNAs as well as several statistical packages for differential expression analysis of miRNAs and validation. The results are depicted in a heatmap which shows 54 statistically significantly dysregulated miRNAs following *L.p.* infection with an MOI of 0.25 at 24 and 48 h, respectively (Fig. 3.3A). The 24 upregulated miRNAs are displayed in red, while the 30 downregulated miRNAs are shown in blue. miR-146a and miR-155 were upregulated following *Legionella* infection and are known to play a crucial role in the inflammatory response following bacterial infection (O'Connell, Taganov et al. 2007; O'Connell, Rao et al. 2010; Nahid, Satoh et al. 2011a). Other miRNAs were also upregulated upon infection with *L.p.* and have not yet been characterized in the context with infection, e.g. miR-3196 or miR-4284. miR-221 and miR-125b showed a downregulation, as well as miR-1228 and miR-1180 which are not described to be associated with bacterial infections yet. Furthermore, a time-dependent regulation of several miRNAs upon infection was observed.

Differentially expressed miRNAs which were relevant to the biological context and well described in the literature were further validated via qPCR experiments in BDMs. The miRNAs miR-146a, miR-155, miR-27a and miR-125a showed a significant upregulation in BDMs 48 h post infection with *L.p.* (Fig. 3.3B), while the miR-221, miR-222, miR-125b, miR-26a and miR-29b were significantly downregulated (Fig. 3.3D). Validation experiments confirmed the results of the sequencing which was indicated by the increasingly significant regulation of the miRNAs over infection time.

To demonstrate that not only the cytokine release is comparable between BDMs and THP-1 cells, the regulation of selected miRNAs was verified and validated in both cell types. The expression of miR-146a, miR-155, miR-221 and miR-125b were analyzed in THP-1 cells infected with *L.p.* at an MOI of 0.25 and 0.5 (Fig. 3.3C, E). miR-146a was induced to a higher extent upon *L.p.* infection in THP-1 cells than in BDMs, while miR-155 was only significantly upregulated in BDMs infected with an MOI of 0.25. In THP-1 cells a higher infection rate was required to achieve a significant regulation of miR-155. The downregulation of miR-125b and miR-221 was comparable between THP-1 cells and BDMs and both showed a significant downregulation at 48 h post infection.

In general, THP-1 cells responded in a similar pattern of miRNA regulation as BDMs. Therefore, THP-1 cells were considered appropriate for subsequent experiments as a cell model to study *Legionella* regulated miRNAs in macrophages.

### 3.1.4 Infection-related chromatin changes on miRNA-promoters

To understand the role of dysregulated miRNAs in infection-activated regulatory networks it is important to understand how they are regulated following an infection with *L.p.*. The promoter regions of four selected miRNAs (miR-155, miR-146a, miR-221, miR-125b) were investigated using the chromatin-immunoprecipitation (ChIP) sequencing data from DuBois et al. (Du Bois, Marsico et al. 2016), where BDMs were infected for 1 h with *L.p.* at an MOI of 10 and ChIP was performed using a pan-ac-H4-antibody. Infected and control samples were normalized to input DNA samples. Acetylation of the Histone H4 is a chromatin mark associated with active transcription. The analysis of the promoter region of the upregulated miR-155 and miR-146a revealed an increase in pan-H4 acetylation in the infected sample vs. uninfected control. For the downregulated miR-221 and miR-125b a decrease in pan-H4 acetylation was detected (Fig. 3.4A).

This observation led to the assumption that rather transcriptional regulation than increased miRNA processing causes the significant regulation in miRNA expression in response to *L.p.* infection.

To test this hypothesis, the pri-miRNA expression levels of the four selected miRNAs (miR-146a, miR-155, miR-125b and miR-221) were analysed by the use of specific qPCR detection assays. Pri-mir-16 served as an endogenous normalization control, which is constitutively transcribed under a large variety of conditions (Schwarzenbach, da Silva et al. 2015; Lange, Stracke et al. 2017). The qPCR analysis showed indeed an upregulation of the primary transcript of pri-mir-155 following infection with *L.p.* for both time points (Fig. 3.4B) and a significantly increased expression of the pri-mir-146a at 48 h post infection with an MOI of 0.25 (Fig. 3.4C). Additionally, *L.p.* infection of macrophages resulted in a downregulation of pri-miR-221 and -125b (Fig. 3.4D, E). To confirm this finding the expression of Dicer and Drosha was monitored. No significant expression changes were detected in *L.p.*-infected macrophages (Fig. 3.4F, G).

In summary, the selected miRNAs were regulated in macrophages on the transcriptional level post infection with *Legionella*.

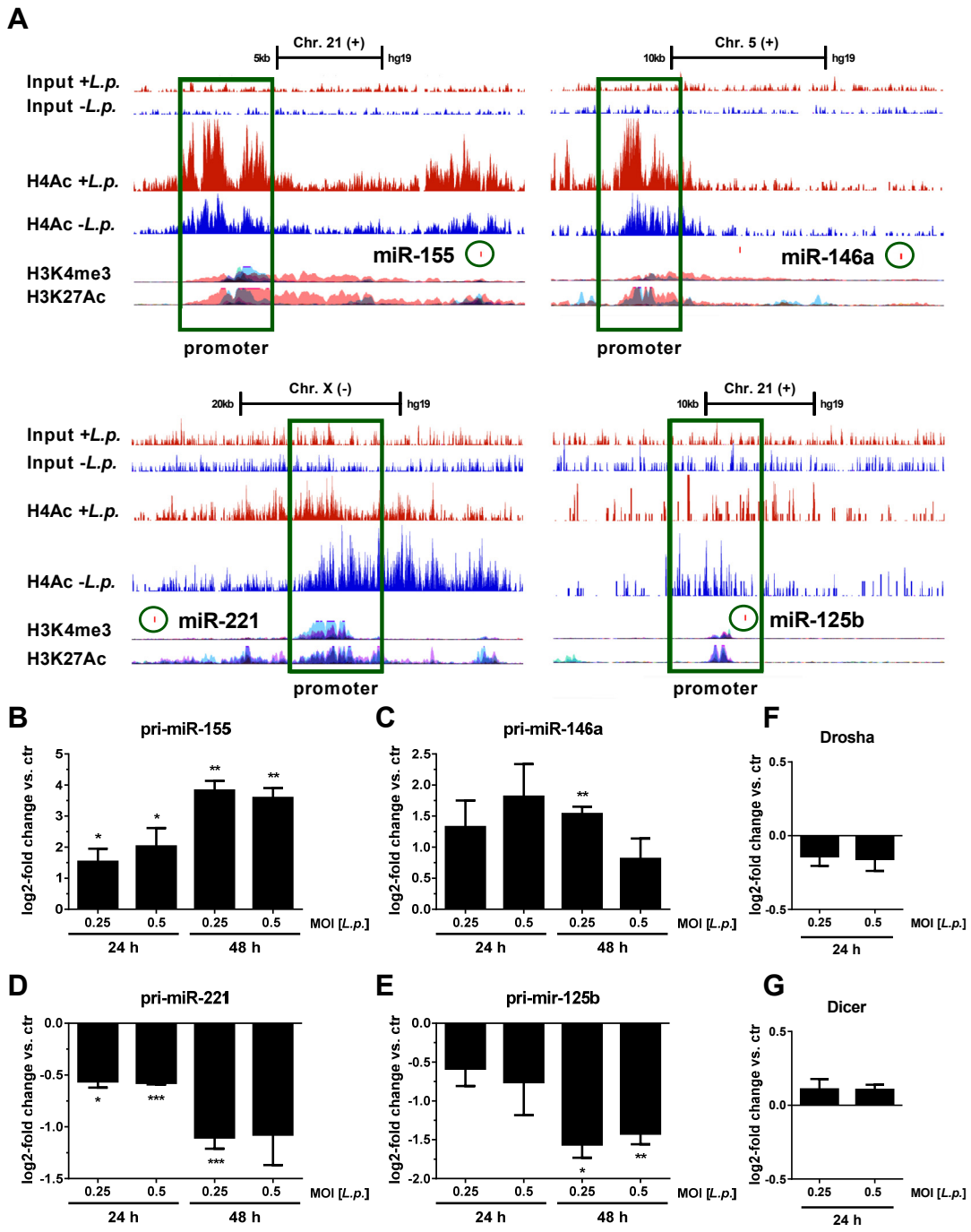


**Figure 3.4: Infection-related chromatin changes on miRNA-promoters.** The alterations of the acetylation pattern at the miRNA-promoter regions of miR-155, miR-146a, miR-221 and miR-125b following *L.p.* infection in BDMs was investigated. BDMs were infected with *L.p.* for 1 h and chromatin-immunoprecipitation was performed using a pan-ac-H4-antibody (Data published in Du Bois et al. 2016). After sequencing, the enrichment of H4-acetylation at the miR-promoters was analysed (A). As control for active sites in the promotor region, IP data for H3K4me3 and H3K27Ac provided by the Encode UCSC browser are shown. Boxes indicate promoter regions, while circles show the mature transcript of the miRNA. The expression of the pri-mirs (B, C, D, E) or Dicer and Drosha (F, G) in BDMs after *L.p.* infection was examined by qPCR and displayed as log2-fold changes. BDMs from different donors were infected with *L.p.* at an MOI of 0.25 and 0.5 for 24 and 48 h. Data are shown as mean + SEM of three to four independent biological replicates. Paired t-tests were performed: *$p \leq 0.05$, **$p \leq 0.01$, ***$p \leq 0.001$ compared to the corresponding control.

### 3.1.5 The influence of miRNAs on bacterial replication in macrophages

Given the known and important effects miRNAs can have upon cells under infection or inflammation, we endeavoured to find a function for those miRNAs which were found to be differentially expressed following *L.p.* infection in macrophages.

Upregulation of miR-125b and miR-221, together with miR-579, have been shown to be important in endotoxin tolerance in macrophages leading to prevention of translation of TNF-α mRNA and therefore to a diminished immune response (El Gazzar and McCall 2010; Quinn, Wang et al. 2012). To assess if dysregulation of miR-125b, miR-221, and miR-579 have an influence on the intracellular *L.p.* replication in macrophages, functional assays were performed. THP-1 cells were transfected with the three miRNA precursors or miRNA inhibitors at a final concentration of 30 nM by lipofection. Following transfection, intracellular replication of *L.p.* was monitored for up to 72 h. The transfection efficiency of the introduced miRNAs was verified with qPCR experiments (Fig. 3.5A, B and C). The overexpression of the individual precursors as well as the transfection of all three miRNAs (10 nM of each precursor) was successful und did not influence the following infection with *L.p.* as tested by qPCR. The high abundance of miR-125b and miR-579 after transfection is due to low expression levels of the miRNAs in untransfected cells. Additionally, the moderate increase of the miR-221 following transfection can be explained by the high native expression level of this miRNA in macrophages. While knockdown of miR-125b, miR-221, and miR-579 resulted in reduced intracellular replication compared to scrambled control (scr), an overexpression of all three miRNAs (miRNA pool) simultaneously resulted in a strong increase of intracellular replication in comparison to scramble control (Fig. 3.5D). A single transfection of each miRNA did not change replication of *L.p.* compared to scramble transfected cells. Therefore, it is assumed that all three miRNAs are necessary to mediate the observed replication effect in macrophages.

In short, the results indicate that manipulation of miRNA expression levels can influence the replication process of *L.p.* in macrophages.

Since miRNA targets can be suppressed on the protein level without being affected on mRNA level, SILAC was performed to unravel the molecular mechanisms responsible for this phenotype. THP-1 cells were transfected with scrambled sequences or the miRNA pool and additionally infected with *L.p.* at an MOI of 0.5 for 24 and 48 h to induce the expression of infection-related proteins or left untreated as control. Subsequently, the proteome of these samples was analyzed using SILAC control cells labelled with heavy isotopes.

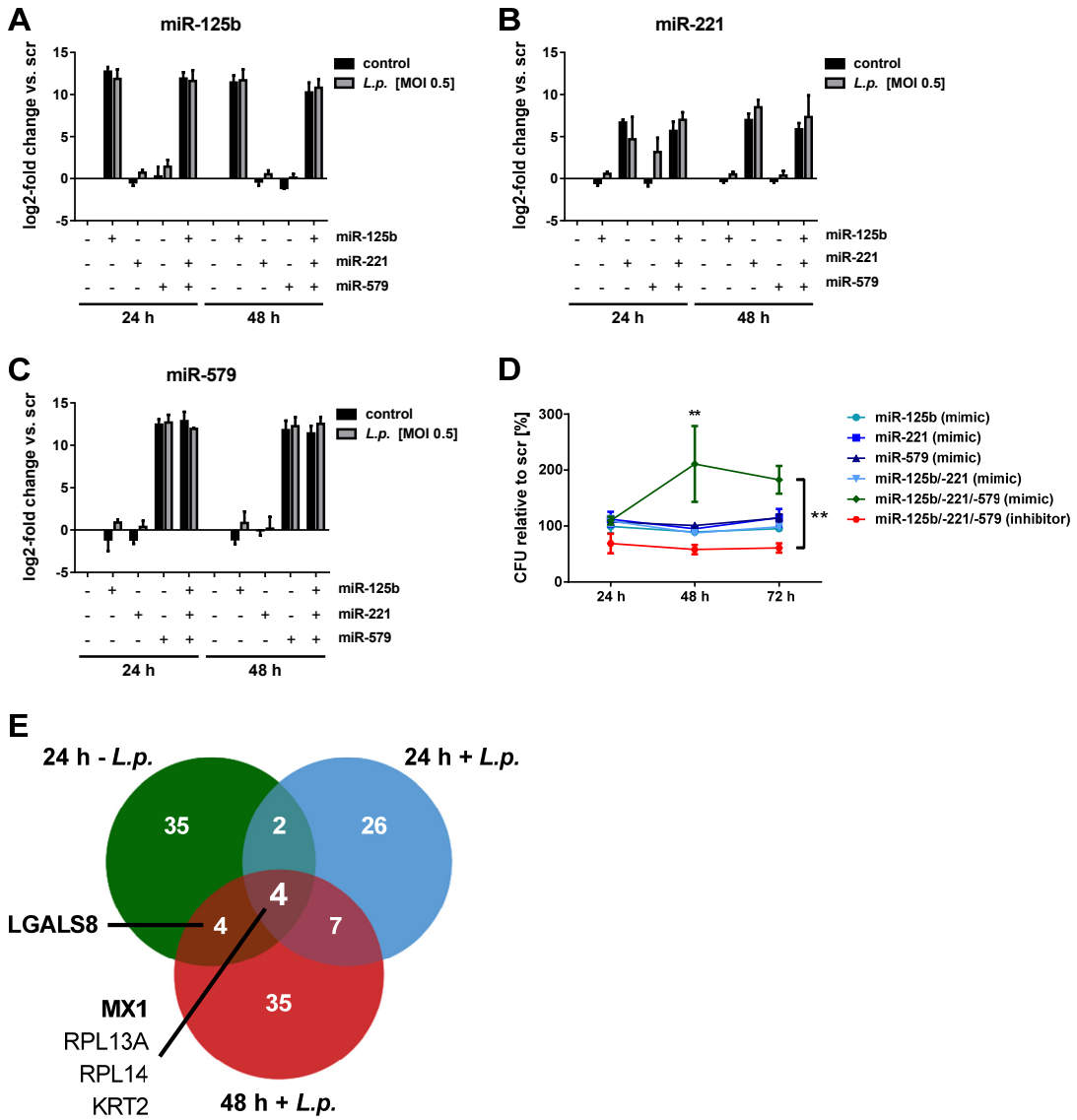


**Figure 3.5: Influence of miRNAs on bacterial replication in macrophages.** THP-1 cells were transfected with miR-125b/-221/-579 mimics or inhibitors at a total concentration of 30 nM. As control, a scrambled LNA (scr) was transfected. 24 h post transfection, THP-1 cells were stimulated with 20 nM PMA for 24 h. Differentiated macrophages were infected with *L.p.* at an MOI of 0.5 or left untreated as control. Overexpression of the transfected miRNAs was validated with qPCR using TaqMan assays and displayed as log2-fold change (A, B, C). Bacterial replication was determined by CFU assay (D). Cells were lysed after 24, 48 and 72 h post infection. Data are depicted as percent relative to CFU count of scramble-transfected (scr) cells at every time point. Data are shown as mean + SEM of three to four independent biological replicates. To test significance, a 2-way ANOVA with Tukey correction was performed: *$p \leq 0.05$, ** $p \leq 0.01$ compared to corresponding control. To identify downregulated targets of the miRNA-pool (miR-125b, miR-221, miR-579), stable isotope labeling by amino acids in cell culture (SILAC) was performed. The proteome of THP-1 cells transfected either with scr or mimics of all three miRNAs versus SILAC control cells labelled with heavy isotopes was analysed by mass spectrometry. Additionally, transfected cells were infected for 24 or 48 h with *L.p.* at an MOI of 0.5 or left untreated as control. Only downregulated proteins following simultaneous overexpression of all three miRNAs compared to scramble transfection are shown in the Venn-diagram (E).

Overall, 1,670 proteins were detected and quantified. In general, differences between infected and uninfected samples were observed (data shown in supplement 1A) which were also time

dependent. To identify the target which led to the replication effect we focused on the comparison of scramble transfected cells to their corresponding overexpression sample to quantify miRNA-induced changes in protein expression. The Venn-diagram (Fig. 3.5E) shows proteins which were downregulated in cells transfected with the miRNA-pool compared to scramble transfected cells after infection of 24 and 48 h (24 h + *L.p.* and 48 h + *L.p.*) or uninfected cells (24 h - *L.p.*). In total, 113 proteins were downregulated following simultaneous overexpression of all three miRNAs. Especially, MX dynamin like GTPase 1 (MX1) and three other proteins (RPL13A, RPL14, KRT2) were downregulated in all triple overexpression samples (irrespective of infection). MX1 is associated with the smooth ER and is regulated by type 1 and type 2 interferons. Since MX1 is known to have broad antiviral activities, it is of further interest for this study (Sadler and Williams 2008; Haller and Kochs 2011). Another protein that was downregulated by microRNA overexpression was LGALS8 (Galectin 8), which showed a decreased protein expression in cells infected with *L.p.* for 48 h and in uninfected cells.

In conclusion, MX1 and LGALS8 were downregulated following overexpression of the miRNA-pool in THP-1 cells.

### 3.1.6 MX1 downregulation following the overexpression of the miRNA-pool

To validate the regulation of MX1 protein upon miRNA-overexpression and *Legionella* infection, the mRNA levels of MX1 were analysed by qPCR experiments. No reduction of MX1 on mRNA level in THP-1 cells was observed and an upregulation was only detected at 48 h post infection with *Legionella* (Fig. 3.6A). To determine the MX1 expression on protein level, intracellular MX1 protein was investigated via indirect immunofluorescence staining and subsequent cytometric analysis. A shift of the population away from the IgG peak (isotype control) in the yellow fluorescence indicates cells positive for MX1. A reduced number of MX1-positive cells following transfection of the miRNA pool were determined (Fig. 3.6B). The numbers of MX1-positve cells of all different samples were calculated relative to the uninfected cells, transfected with scramble at 24 h (Fig. 3.6C). Irrespective of the infection, an overexpression of the miRNA-pool yielded a significant reduction of MX1-positive cells relative to scramble transfected cells (Fig. 3.6C).

In summary, the downregulation of MX1 protein following transfection of all three miRNAs as suggested by the SILAC analyses was validated.

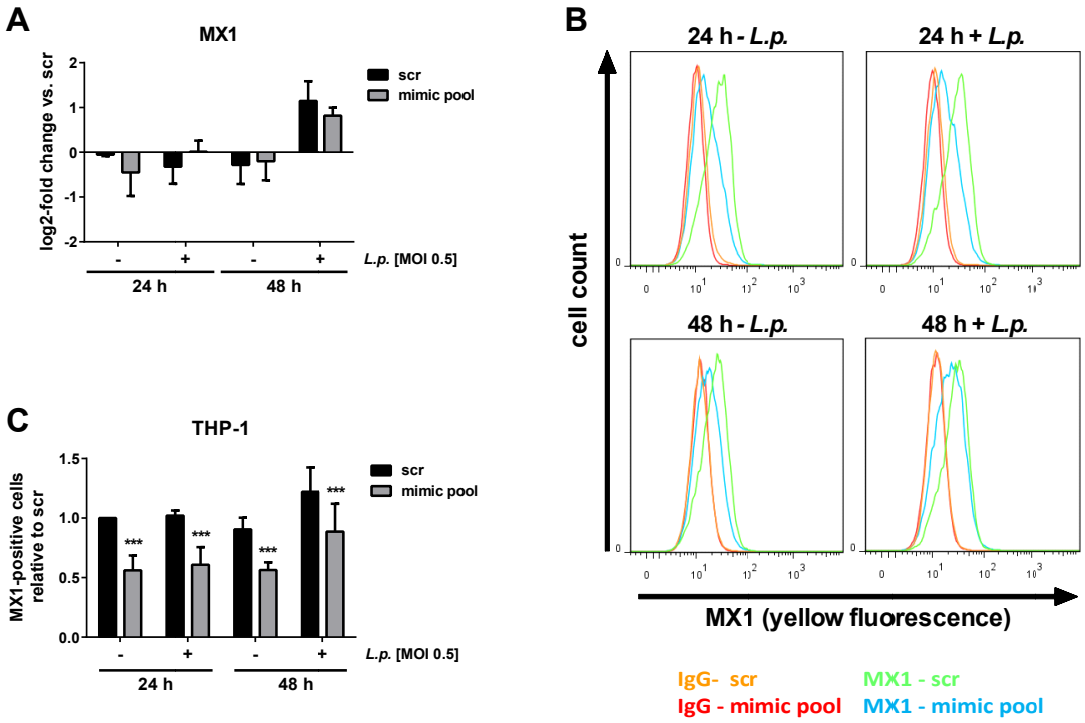


**Figure 3.6: MX1 downregulation following overexpression of the miRNA-pool.** THP-1 cells were transfected with miRNA-125b, miR-221 and miR-579 mimics (miRNA-pool) at a final concentration of 30 nM. For control, a scrambled LNA (scr) was transfected. 24 h post transfection, THP-1 cells were stimulated with 20 nM PMA for 24 h. Differentiated macrophages were infected with *L.p.* at an MOI of 0.5 for 24 and 48 h or left untreated as control. Expression of MX1 was examined by qPCR and displayed as log2-fold change (A). For analysis of the intracellular protein expression of MX1, an indirect fluorescence staining followed by cytrometric analysis was performed. Transfected cells were fixed with 4% PFA and stained with an anti-MX1 antibody or an unspecific IgG antibody as control. Finally, cells were stained by a secondary antibody labelled with Alexa Fluor 555. The percentages of MX1-positive cells were determined with FlowJo 7.6.5.. One representative histogram is shown in (B). The relative number of MX1-positive cells was calculated and the mean of three independent biological replicates + SEM is shown (C). To test significance, a 2-way ANOVA with Sidak correction was performed: *$p \leq 0.05$, **$p \leq 0.01$, ***$p \leq 0.001$ compared to the corresponding control.

### 3.1.7 Downregulation of MX1 enhances *L.p.* replication in macrophages

In order to evaluate a potential functional effect of MX1 mediated by the miRNA-pool, siRNA knockdown experiments were performed. Either THP-1 cells or BDMs were transfected with an siRNA-pool targeting MX1 (siMX1) or with a scrambled siRNA as control. Subsequently, cells were infected with *L.p.* at an MOI of 0.5. The knockdown of MX1 protein in THP-1 cells and BDMs was confirmed via western blot (Fig. 3.7A, B). A densitometric analysis was performed to calculate the knockdown efficiency. In THP-1 cells, a downregulation of MX1 protein of up to 64% was achieved in four biological replicates, regardless of whether cells were infected or not (Fig. 3.7C).

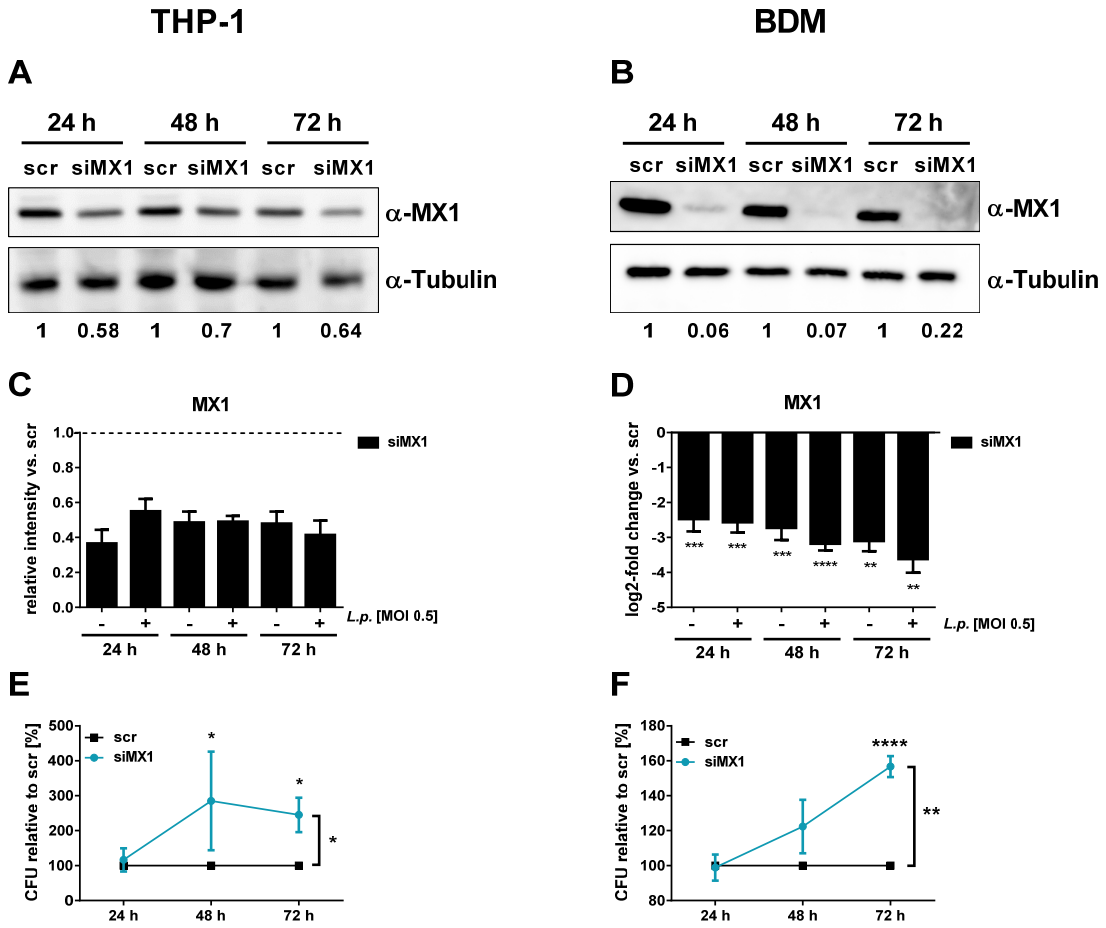


**Figure 3.7: Downregulation of MX1 enhances *L.p.* replication in macrophages.** THP-1 cells or BDMs were transfected with a small interfering RNA targeting MX1 (siMX1) or with a scrambled siRNA as control (scr). 24 h post transfection, THP-1 cells were stimulated with PMA (20 nM) for 24 h. Differentiated THP-1 cells or BDMs were infected with *L.p.* at an MOI of 0.5 for 24, 48 and 72 h. Knockdown of MX1 protein in THP-1 cells (A) and BDMs (B) was verified and quantified by Western Blot. Quantification of the relative protein intensity of four independent western blots was quantified for THP-1 cells (C). MX1 expression in BDMs was analysed by qPCR and displayed as log2-fold change (D). Colony forming units (CFU) were determined 24, 48 and 72 h post infection following MX1-knockdown in THP-1 cells (E) or BDMs (F). Mean values + SEM of three to seven independent biological experiments are depicted and one representative replicate is shown for western blot. To test significance, a 2-way ANOVA with Sidak correction was performed for (E) and (F): *p ≤ 0.05; **p ≤ 0.01, ***p ≤ 0.001 compared to the corresponding control. Paired t-test were performed for the qPCR results: *p ≤ 0.05; **p ≤ 0.01, ***p ≤ 0.001 compared to the corresponding control.

Moreover, the knockdown remained constant over time. Additionally, downregulation of MX1 protein mediated by siRNAs was more efficient in BDMs than in THP-1 cells (Fig. 3.7B). Densitometric analysis validated a knockdown of up to 94% for 24 h in BDMs for the represented experiment. On mRNA level, the downregulation of MX1 in BDMs was significant and stable over time irrespective of an infection with *Legionella* (Fig. 3.7D).

Following successful knockdown of MX1 in THP-1 cells and BDMs, CFU-assays were performed to monitor the influence of MX1 on the *L.p.* replication in macrophages. Knockdown of MX1 resulted in an increased replication of *L.p.* in THP-1 cells, similar to the effect observed upon

miRNA overexpression (Fig. 3.7E). Aside from this, the downregulation of MX1 in primary BDMs also yielded an increase in replication of *Legionella* but to a weaker extent (Fig. 3.7F).
In summary, the miRNA pool regulates the protein expression of MX1, which affects the replication of *Legionella* within human macrophages.

### 3.1.8 MX1 is not directly targeted by the miRNA-pool

As the miRNA-mediated downregulation of MX1 on protein level was validated by FACS-staining, the 3'UTR of MX1 was investigated for binding sites of the miRNA-pool (miR-125b, miR-221 and miR-579). The *in silico* analysis of the 3'UTR by several prediction programs (e.g. TargetScan7.1, microRNA.org) predicted no binding sites for either miRNA in the 3'UTR of MX1. Manual investigation of the 3'UTR for seed regions of these miRNAs in the 3'UTR was equally unsuccessful. Therefore, an Ingenuity pathway analysis (IPA) was performed to find the link between the miRNA-pool and the downregulated MX1-protein. Predicted and published targets of each miRNA were visualized (Fig. 3.8). In the target screening, Filters were set to only include experimentally observed or high-confidence predicted microRNA/mRNA interaction partners. The newly found microRNA targets were interconnected using all available data sources in IPA with restriction to experimentally validated or high-confidence predicted interactions in humans. In the network all targets of the miRNAs influencing MX1, are displayed.
miRNAs downregulate their target mRNAs either by the repression of the translational process via inhibition of the translation machinery or alternatively through the degradation of the mRNA (Winter, Jung et al. 2009). Since overexpression of the miRNA-pool resulted in a downregulation of MX1 protein, only candidates positively regulating MX1 (marked in blue) were of interest for further analyses. Targets contributing to a negative regulation of MX1 were unlikely to be the link between MX1 and the miRNAs (indicated in red).This filter strategy revealed four out of 13 possible candidates. Interferon gamma (IFNG) and Interferon Alpha 2 (IFNA2) showed very low level expression in THP-1 cells and were not detectable via qPCR (data not shown). Therefore, only two likely candidates remained for further analyses: DExD/H-Box Helicase 58 (DDX58), also known as RIG-I, and Tumor protein p53 (TP53). DDX58 encodes for the RIG-I-like receptor dsRNA helicase enzyme. It functions as a pattern recognition receptor that is a sensor for uncapped double or single stranded RNA (Yoneyama, Kikuchi et al. 2004; Pichlmair, Schulz et al. 2006). The gene TP53, also known as p53 (cellular tumour antigen p53), encodes for a protein that is crucial in multicellular organisms and functions as a tumour suppressor (Bourdon, Fernandes et al. 2005; Surget, Khoury et al. 2013).

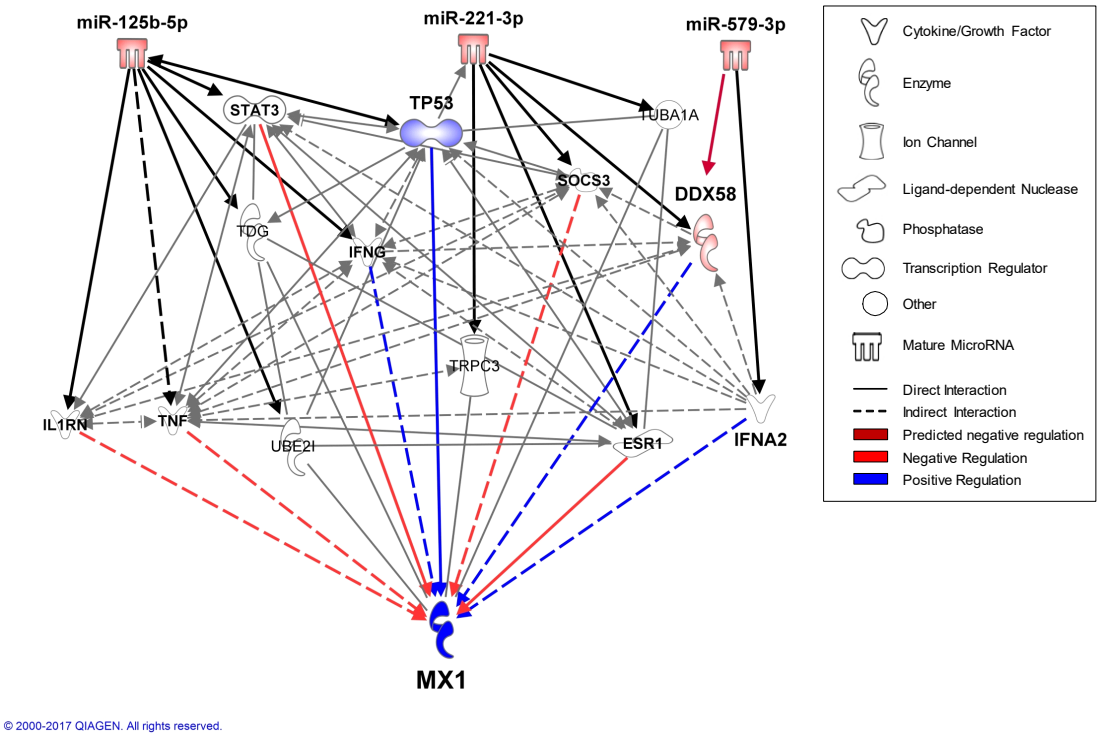




**Figure 3.8: MX1 is not directly targeted by the miRNA-pool.** Igenuity Pathway Analysis (IPA) was performed to investigate the connection between the miRNA-pool (miR-125b, miR-221 and miR-579) and the MX1-protein. In the target screening, Filters were set to only include experimentally observed or high-confidence predicted microRNA/mRNA interaction partners. Output was limited to 13 total candidates. The newly found microRNA targets were interconnected using all available data sources in IPA with restriction to experimentally validated or high-confidence predicted interactions. Direct or indirect relationships between molecules are indicated by solid or dashed lines, respectively. Blue coloured lines depict positive regulations, while red coloured lines indicate negative regulations. Molecule classes (cytokine, enzyme, ion channel, ligand-dependent nuclease, phosphatase, transcription factor, other or mature microRNAs) are indicated by distinct symbols shown in the legend.

### 3.1.9 miRNA-221 and miRNA-579 bind to the 3'UTR of DDX58

IPA revealed that DDX58 is a predicted target of miR-221. However, the 3'UTR of DDX58 also possesses a binding site for miR-579. The in silico analysis of the 3'UTR revealed one binding site for miR-579 at position 157-163 and two binding sites for the miR-221 located at position 685-691 and at 779-786 (Fig 3.9A).

Both miRNAs were tested via qPCR and luciferase-based reporter assays to evaluate their influence on DDX58. Transfection of the individual miR-221 and the miRNA-pool resulted in decreased mRNA expression of DDX58 (Fig. 3.9B). In comparison, overexpression of miR-579 did not result in a reduced DDX58 expression (Fig 3.9B).

To further analyze the miRNA binding of miR-221 and miR-579 to the DDX58 3'UTR, the 3'UTR fragment of DDX58 (length of 813 nt) was cloned into the psiCHECK2 vector. This vector construct (DDX58 wt) and the miRNA mimics were transfected into HEK293T cells. After 72 h,

the luminescence was determined as an indicator of an interaction between miRNA and mRNA. A decrease of luminescence reflects a decrease of the enzyme which indicates a functional binding of the miRNA to the 3'UTR. Relative luciferase activity was calculated and data were normalized to cells transfected with the empty vector and the corresponding miRNA-mimic (Fig. 3.9C). The relative luciferase activity for each transfected miRNA-mimic (miR-125b, miR-221, miR-579 or miR-pool) was compared to cells co-transfected with a non-specific miRNA scramble sequence (scr) to unveil the specific interaction. The co-transfection of miR-221, miR-579 and the miRNA-pool (10 nM of each mimic) resulted in a significantly reduced relative luciferase activity compared to scramble transfected cells.

In order to validate the specific binding of the miRNAs to the 3'UTR of DDX58, the seed regions of all three miRNA binding sites (one binding site for miR-579, two binding sites for miR-221) in the 3'UTR of the vector construct were mutated (DDX58 mut). Transfection of the mutated version of the DDX58 3'UTR vector returned a significant increase of the relative luminescence compared to the wildtype 3'UTR. Therefore, the decreased luminescence was associated with the loss of binding of miR-221 to the 3'UTR of DDX58. The transfection of the miRNA-pool together with the mutated version also provoked a significant decrease in relative luminescence, but less significantly than the wildtype version of the 3'UTR. The co-transfection of the miR-579 precursor with either the wildtype 3'UTR or the mutated version led to a significant reduction of relative luciferase activity compared to scr. Thus, no difference between wildtype and mutated construct was detectable.

In summary, luciferase reporter assays revealed the binding of miR-221 to the DDX58 3'UTR. The indicated positions in the 3'UTR of DDX58 were targeted by miR-221. The reduction of the relative luminescence activity mediated by miR-221 binding was reverted by the mutation of the seed region. miR-579 also bound to the 3'UTR of DDX58, but mutation of the seed region could not abrogate the reduction of the relative luminescence activity.

To analyze the direct interaction between DDX58 and MX1, DDX58 knockdown with subsequent analysis of the protein expression of MX1 was performed. As previously described, intracellular MX1 was stained using immunofluorescence and monitored via cytometric analysis, following downregulation of DDX58. Knockdown of DDX58 resulted in a decreased number of MX1-positive cells compared to scramble transfected cells. The relative number of MX1-positive cells was reduced to 75%.

Overall, the luciferase assay corroborates the observations made on the regulation of native transcript expression and the influence of DDX58 on MX1 protein expression was confirmed.

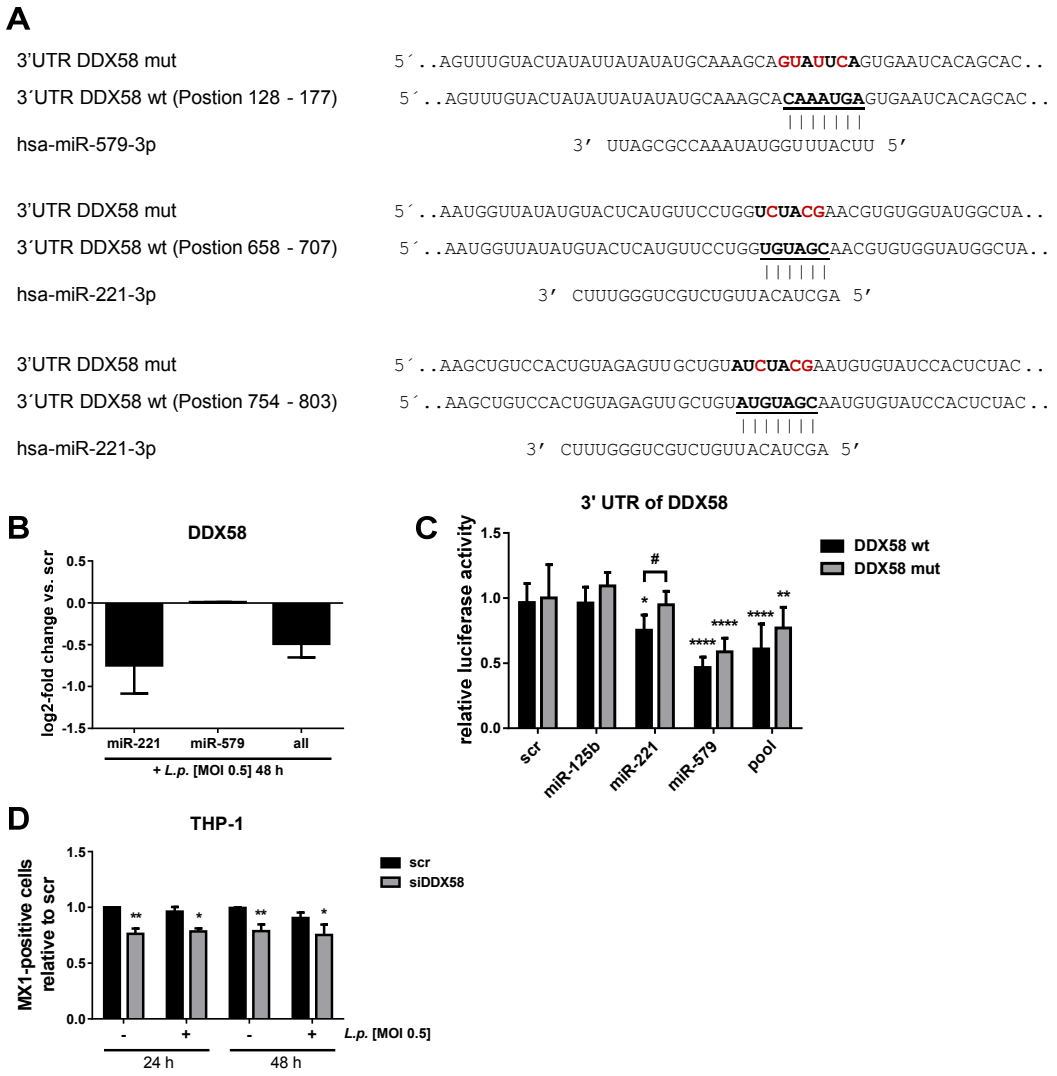


**Figure 3.9: miRNA-221 and miRNA579 bind to the 3'UTR of DDX58**. There are two potential miRNA binding sites for miRNA-221 and one for the miRNA-579 in the 3' UTR of DDX58 (A). Vertical bars represent canonical base pairing (C-G; A-U), while horizontal lines indicate the seed regions of the miRNAs. The mutated bases are depicted in red. THP-1 cells were transfected either with miRNA-221 mimic, miR-579 mimic or the miRNA mimic pool (miR-125b, miR-221 and miR-579) at a final concentration of 30 nM. As a control, a scrambled LNA (scr) was transfected. 24 h post transfection, THP-1 cells were stimulated with 20 nM PMA for 24 h. Differentiated macrophages were infected with *L.p.* at an MOI of 0.5 for 48 h or left untreated as control. DDX58 expression was determined with qPCR and displayed as log2-fold change (B). Luciferase reporter assay analyses were performed with co-transfection of a vector construct and the different miRNA mimics in HEK293T cells (C). The vector construct harboured either the wildtype (DDX58 wt) or the mutated (DDX58 mut) version of the 3'UTR of DDX58. Ratios of renilla and firefly luciferase luminescence were normalized to the empty vector. For analysis of the intracellular MX1, an indirect fluorescence staining followed by cytrometric analysis was performed. Transfected cells were fixed with 4% PFA and stained with an anti-MX1 antibody or an unspecific IgG antibody as control. Finally, cells were stained by a secondary antibody labelled with Alexa Fluor 555. The percentages of MX1-positive cells were determined with FlowJo 7.6.5. The relative number of MX1-positive cells was calculated. Data are shown as mean + SEM of three, six or four independent biological replicates. A two-way ANOVA with Sidak correction was performed: *$p \leq 0.05$, **$p \leq 0.01$, ***$p \leq 0.001$ compared to scramble, $^{\#}$ compared to wildtype.

### 3.1.10 DDX58 knockdown increases *L.p.* replication

In order to elaborate if DDX58 is associated with the observed functional effect of MX1 on *L.p.* replication, CFU-assays following DDX58 knockdown were performed. The knockdown was performed with an siRNA-pool targeting DDX58 (siDDX58) or with a scrambled siRNA as control in THP-1 cells (Fig. 3.10A) and BDMs (Fig. 3.10B). Transfected cells were subsequently infected with *L.p.* at MOI 0.5 to assess replication at 24, 48 and 72 h post infection. Successful knockdown was verified via qPCR.

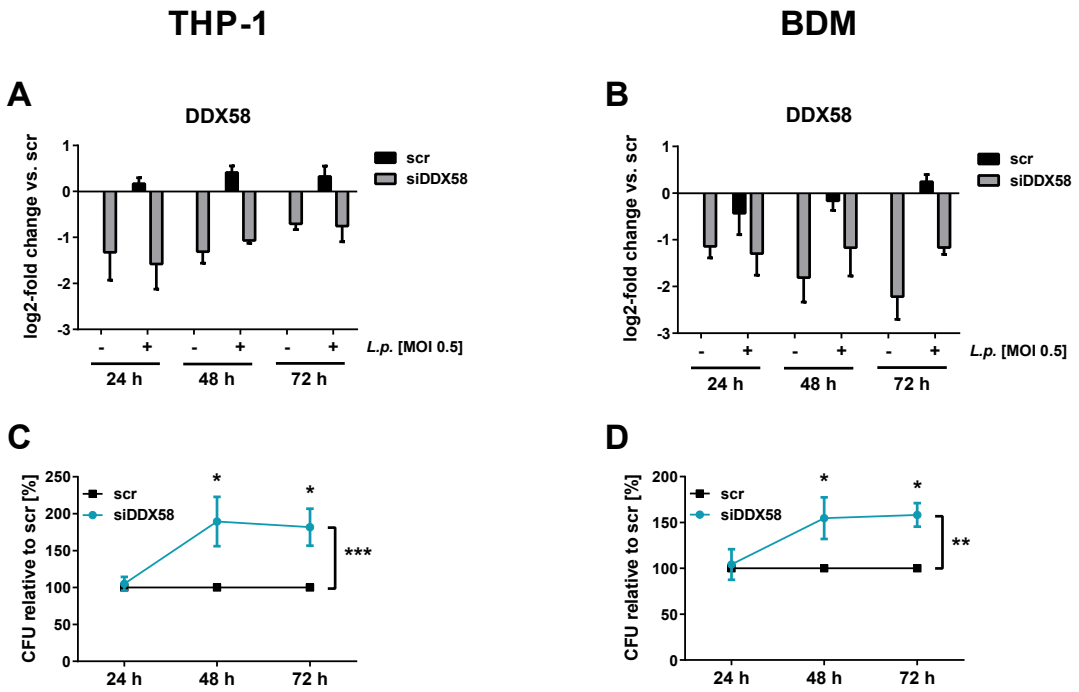


**Figure 3.10: DDX58 knockdown increases *L.p.* replication.** THP-1 cells or BDMs were transfected with a small interfering RNA targeting DDX58 (siDDX58) or with a scrambled siRNA as control (scr). 24 h post transfection, THP-1 cells were stimulated with PMA (20 nM) for 24 h. Differentiated THP-1 cells or BDMs were infected using *L.p.* at an MOI of 0.5 or left untreated as control. Downregulation of DDX58 expression with siRNA in THP-1 cells (A) and BDMs (B) was verified by qPCR and are displayed as log2-fold changes. Colony forming units (CFU) of *Legionella* were determined 24, 48 and 72 h post infection following a knockdown of DDX58 in THP-1 cells (C) or in BDMs (D). Mean values + SEM of three or four independent biological experiments are depicted. For the CFU-Assays a 2-way ANOVA with Sidak correction was performed: *p ≤ 0.05; **p ≤ 0.01, ***p ≤ 0.001 compared to the corresponding control.

The expression of DDX58 mRNA was reduced in both cell types following transfection of the siRNA-pool for DDX58. DDX58 downregulation was not affected by *L.p.* infection. Proceeding time led to a reduction of the knockdown efficiency in THP-1 cells. The longer the infection time the lower the knockdown efficiency. DDX58 knockdown in BDMs was not influenced by transfection time and was even slightly higher with proceeding time. The downregulation of DDX58 was slightly more efficient in BDMs (varying between 76% - 49% knockdown efficiency) than in THP-1 cells (63% - 38%). In THP-1 cells, transfection of the siRNA-pool targeting DDX58 resulted in a doubling (190%) of *Legionella* compared to scramble transfected cells (Fig. 3.10C).

The knockdown of DDX58 in BDMs resulted in an increased count of *L.p.* up to 150% (Fig. 3.10D).

In conclusion, it was shown that DDX58 knockdown affects *Legionella* replication in human macrophages.

### 3.1.11 TP53 is targeted by miR-125b

TP53 is the second candidate to link the miRNA overexpression to MX1 and has already been validated as a target of miRNA-125b by several studies (Le, Teh et al. 2009; Qin, Zhao et al. 2014; Ahuja, Goyal et al. 2016). Bioinformatics analysis identified one binding site for miR-125b at position 733 to 739 in the 3'UTR of TP53 (in isoform NM_001126112.2) (Fig. 3.11A).

In order to analyze the influence of the miR-125b on TP53 mRNA expression, miR-125b was overexpressed in THP-1 cells. The transfection of the individual miR-125b precursor and the miRNA-pool showed a reduction of TP53 expression (Fig. 3.11B).

To analyze of the influence of miR-125b on TP53 3'UTR, the 3'UTR fragment (length of 254 nt) was cloned into the psiCKECK2 vector for luciferase assays. Relative luciferase activity was calculated and the data were normalized as previously described. The co-transfection of miR-125b and the miRNA-pool with the wildtype version of the 3'UTR fragment of TP53 (TP53 wt) resulted in a significant decrease of relative luciferase activity compared to scramble transfected cells (Fig. 3.11C). To identify specific binding of the miRNA to the indicated site, the seed region in the vector construct was mutated (TP53 mut) as shown in figure 3.11A. The transfection of the mutated version of TP53 yielded a significant increase of the relative luminescence compared to the wildtype 3'UTR. Furthermore, lower levels of transfected miRNA mimic also reduced the luciferase activity compared to scramble transfected cells.

In summary, it was shown that miR-125b reduced the TP53 3'UTR dependent luciferase activity and this effect was reversed by the mutation of the miRNA seed region. Therefore, a direct binding of the miR-125b to the 3'UTR of TP53 was shown.

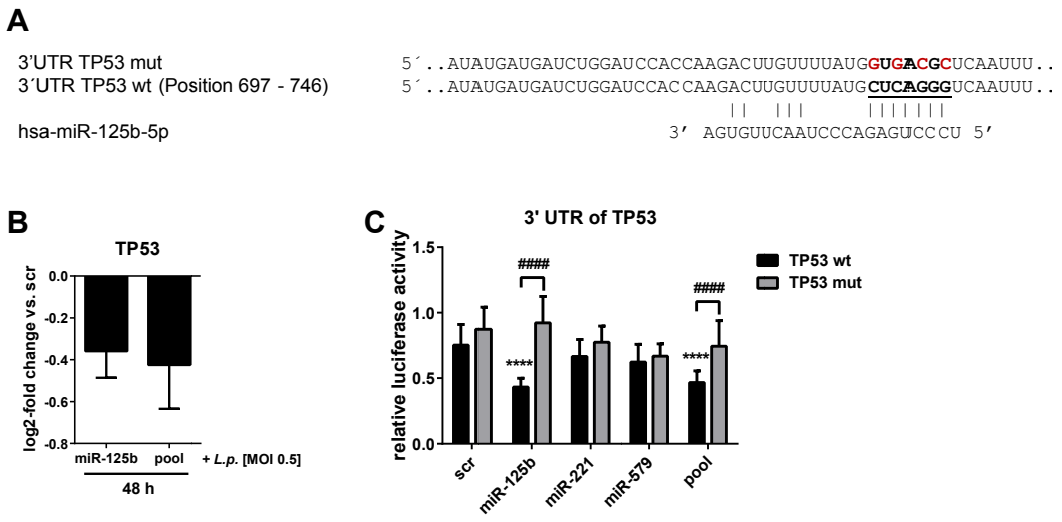


**Figure 3.11: TP53 is targeted by miR-125b.** There is one miRNA binding site for miRNA-125b in the 3'UTR of TP53 (A). Vertical bars represent canonical base pairing (C-G; A-U), while horizontal lines indicate the seed regions of the miRNAs. The mutated bases are depicted in red. THP-1 cells were transfected either with miRNA-125b mimic or the miRNA mimic pool (miR-125b, miR-221 and miR-579) at a final concentration of 30 nM. For control, a scrambled LNA (scr) was transfected. 24 h post transfection, THP-1 cells were stimulated with 20 nM PMA for 24 h. Differentiated macrophages were infected with *L.p.* at an MOI of 0.5 for 48 h or left untreated as control. TP53 expression was examined with qPCR and displayed as log2-fold change (B). Data are shown as mean + SEM of three independent biological experiments. Luciferase reporter assay analyses were performed with co-transfection of vector constructs and the different miRNA mimics in HEK293 cells. The vector construct was harbouring either the wildtype (TP53 wt) or the mutated (TP53 mut) version of the 3'UTR of TP53. Ratios of renilla and firefly luciferase luminescence were normalized to the empty vector. Data are shown as mean + SEM of seven independent biological replicates. 2-way ANOVA with Sidak correction was performed: ****p ≤ 0.0001 compared to the corresponding control, or $^{\#\#\#\#}$p ≤ 0.0001 compared to wildtype.

### 3.1.12 TP53 knockdown enhances *L.p.* replication

In order to strengthen the suggested function of TP53 in the IPA-network, CFU-assays following knockdown of TP53 were performed. Since sufficient knockdown of TP53 mRNA could not be achieved in THP-1 cells, BDMs were transfected with an siRNA-pool targeting TP53. The knockdown of TP53 was highly efficient in BDMs (up to 85%) (Fig. 3.12A). Furthermore, the replication of *L.p.* in macrophages was significantly increased to 157% at 72 h post infection if TP53 was downregulated by transfection of the siRNA-pool (Fig. 3.12B).

Overall, the influence of TP53 on *L.p.* replication, mediated by miR-125b, was confirmed.

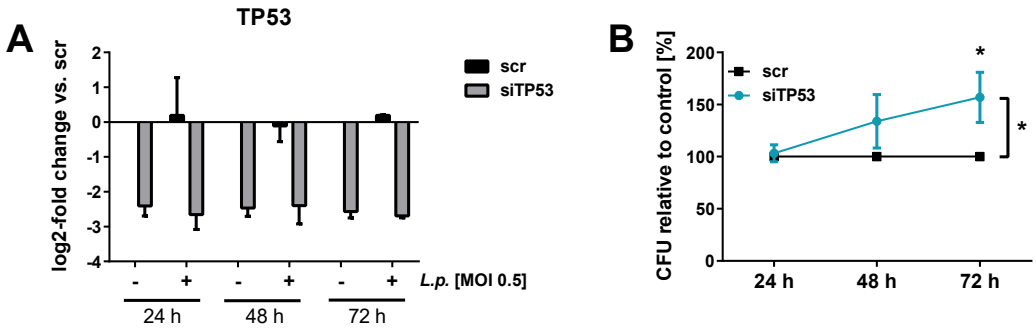


**Figure 3.12: TP53 knockdown enhances *L.p.* replication.** BDMs were transfected with small interfering RNA targeting TP53 (siTP53) or with a scrambled siRNA as control (scr). 24 h post transfection, macrophages were infected using *L.p.* at an MOI of 0.5 for 24, 48 and 72 h. Downregulation of TP53 expression was verified by qPCR and displayed as log2-fold change (A). Mean values + SEM of three to seven independent biological experiments are displayed. Colony forming units (CFU) were determined (B). Mean values + SEM of four independent biological experiments are depicted. 2-way ANOVA with Sidak correction was performed: *p ≤ 0.05; compared to the corresponding control.

### 3.1.13 LGALS8 is targeted by miRNA-579

As previously shown, all three miRNAs are necessary to mediate the replication effect of *L.p.* in macrophages. Of note, binding of miR-579 to the 3'UTR of DDX58 was not reversed by the mutation of the seed region, making direct targeting unlikely. Therefore, another target of miR-579 should be important for the observed replication effect. Since LGALS8 protein was downregulated in cells transfected with the miRNA-pool compared to scramble transfected cells (Fig. 3.5E) and has two binding sites in its 3'UTR for miR-579 (Fig. 3.13A), LGALS8 was further investigated. Firstly, the influence of miR-579 on LGALS8 mRNA was investigated (Fig. 3.13B). The individual overexpression of miR-579 yielded a significantly reduced expression of LGALS8, while transfection of the miRNA-pool showed no influence.

Secondly, the influence of miR-579 binding to the 3'UTR of LGALS8 was investigated using luciferase assay (Fig. 3.13C). The 3'UTR fragment (length of 1634 nt) with two binding sites at position 2406 to 2414 and 3616 to 3622 was cloned into the psiCKECK-2 vector and transfected in HEK293-T cells together with the different miRNA mimics. Relative luciferase activity was calculated and the data were normalized as previously described. The co-transfection of miR-579 and the miRNA-pool with the wildtype version of the 3'UTR fragment of LGALS8 (LGALS8 wt) revealed a significant decrease of relative luciferase activity compared to scramble transfected cells (Fig. 3.13C). The transfection of miR-125b and miR-221 also led to a significantly reduced luciferase signal, but less efficiently when compared to the miR-579 transfection. In order to identify specific binding of the miRNA to the indicated sites, the seed regions of both binding sites in the vector construct were mutated (LGALS8 mut) as shown in

figure 3.13A. The transfection of the mutated version with miR-579 yielded a significant increase of the relative luminescence compared to the wildtype 3'UTR. A significant decrease was detected if miR-125b or miR-221 was co-transfected with the mutated version compared to wildtype construct.

In summary, it has been shown that miR-579 reduced the LGALS8 3'UTR dependent luciferase activity and this effect was reversed by the mutation of the miRNA seed region. Therefore, a direct binding of the miR-579 to the 3'UTR of LGALS8 was shown.

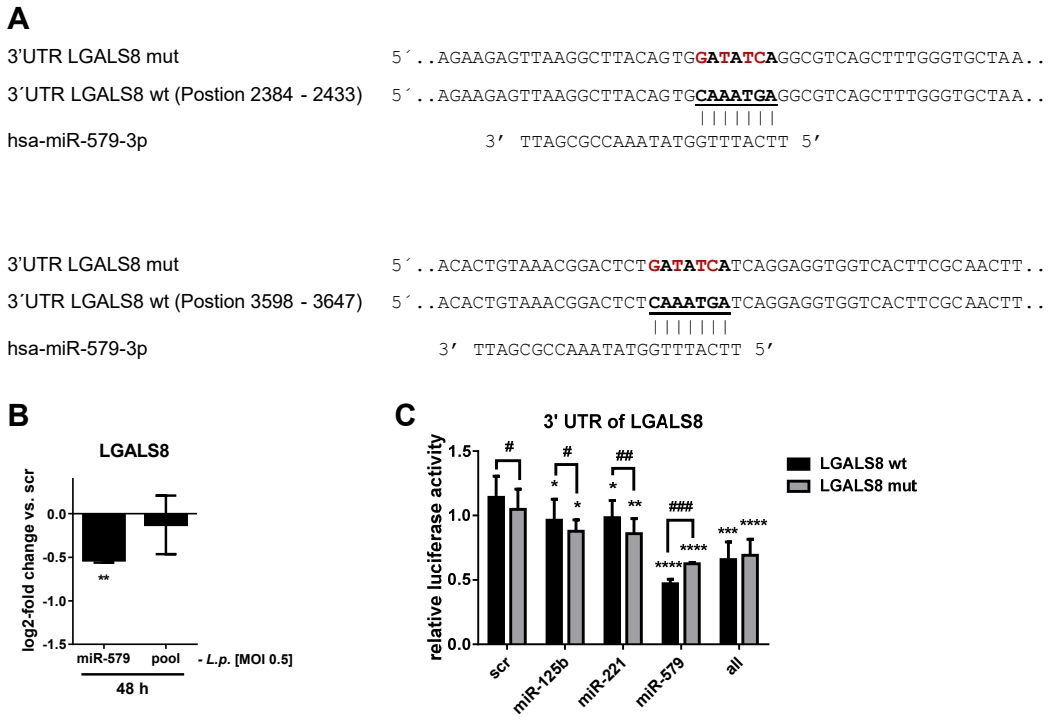


**Figure 3.13: LGALS8 is targeted by miRNA-579**. There are two miRNA binding sites for miRNA-579 in the 3'UTR of LGALS8 (A). Vertical bars represent canonical base pairing (C-G; A-U), while horizontal lines indicate the seed regions of the miRNAs. The mutated bases are depicted in red. THP-1 cells were transfected either with miRNA-579 mimic or the miRNA mimic pool (miR-125b, miR-221 and miR-579) at a final concentration of 30 nM. For control, a scrambled LNA (scr) was transfected. 24 h post transfection, THP-1 cells were stimulated with 20 nM PMA for 24 h. Differentiated macrophages were infected with *L.p.* at an MOI of 0.5 for 48 h or left untreated as control. LGALS8 expression was examined with qPCR and displayed as log2-fold change (B). Data are shown as mean + SEM of three independent biological experiments. Luciferase reporter assay analyses were performed with co-transfection of vector constructs and the different miRNA mimics in HEK293 cells. The vector construct was harbouring either the wildtype (LGALS8 wt) or the mutated (LAGLS8 mut) version of the 3'UTR of LGALS8. Ratios of renilla and firefly luciferase luminescence were normalized to the empty vector. Data are shown as mean + SEM of four independent biological replicates. 2-way ANOVA with Sidak correction was performed: *p ≤ 0.05, **p ≤ 0.01, ***p ≤ 0.001, ****p ≤ 0.0001 compared to the corresponding control, or $^{\#}p \leq 0.05$, $^{\#\#}p \leq 0.01$, $^{\#\#\#}p \leq 0.001$ compared to wildtype.

### 3.1.14 LGALS8 knockdown increases *L.p.* replication

In order to elaborate on the impact of LGALS8 on the infection process, a knockdown of LGALS8 with subsequent CFU-assay was performed. The knockdown was performed with an siRNA-pool targeting LGALS8 (siLGALS8) or with a scrambled siRNA as control in THP-1 cells (Fig. 3.14A) and BDMs (Fig. 3.14B). Transfected cells were subsequently infected with *L.p.* at an MOI 0.5 for 24, 48 and 72 h. Successful knockdown was verified via qPCR. The knockdown in both cell types was successfully achieved and constant over time (Fig. 3.14C, D). SiRNA-mediated downregulation of LGALS8 was more efficient in BDMs (up to 90%) than in THP-1 cells (up to 61%) and not affected by *L.p.* infection.

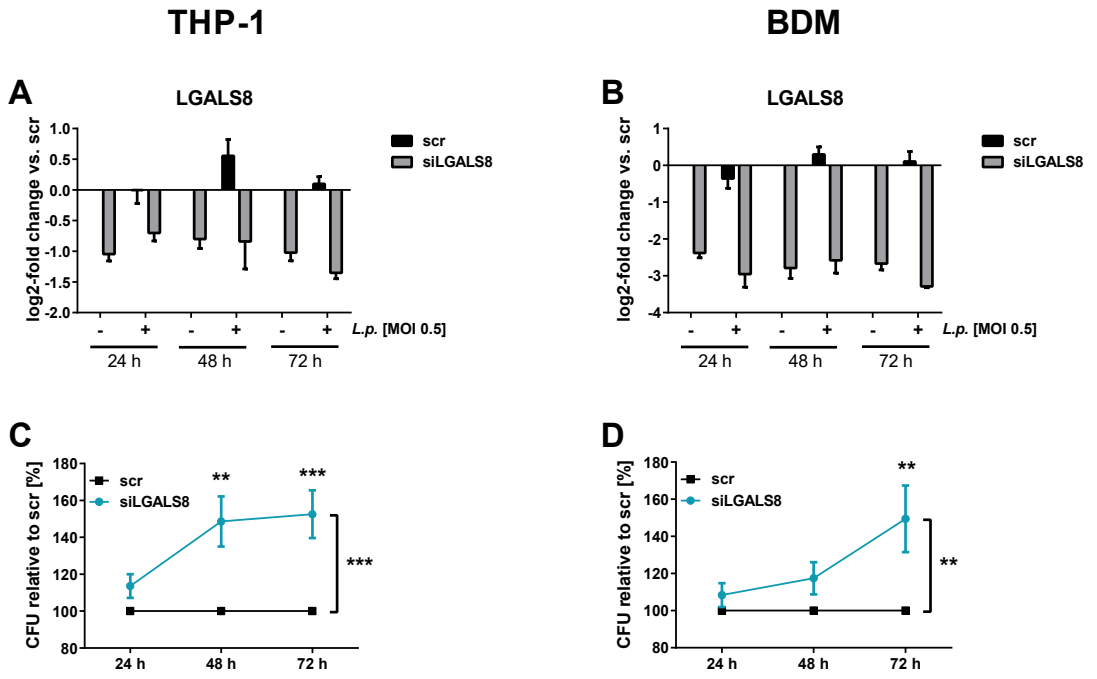


**Figure 3.14: LGALS8 knockdown increases *L.p.* replication.** THP-1 cells or BDMs were transfected with a small interfering RNA targeting LGALS8 (siLGALS8) or with a scrambled siRNA as control (scr). 24 h post transfection, THP-1 cells were stimulated with PMA (20 nM) for 24 h. Differentiated THP-1 cells or BDMs were infected using *L.p.* at an MOI of 0.5 or left untreated as control. Downregulation of LGALS8 expression with siRNA in THP-1 cells (A) and BDMs (B) was verified by qPCR and displayed as log2-fold changes. Mean values + SEM of three to five independent biological experiments are displayed. Colony forming units (CFU) of *Legionella* were determined 24, 48 and 72 h post infection following a knockdown of LGALS8 in THP-1 cells (C) or in BDMs (D). Mean values + SEM of four or five independent biological experiments are depicted. For the CFU-Assays a 2-way ANOVA with Sidak correction was performed: *p ≤ 0.05; **p ≤ 0.01, ***p ≤ 0.001 compared to the corresponding control.

For monitoring the replication of *L.p.*, infected macrophages were lysed at 24, 48 and 72 h post infection. In THP-1 cells, *Legionella* replication was significantly increased in cells transfected with siLGALS8 (up to 152%) compared to scramble transfected cells. The same effect was confirmed in BDMs, where the greatest difference in *L.p.* replication between scramble and siLGALS8 transfected cells was observed at 72 h post infection with an increase of 150%. In

summary, it was shown that LGALS8 knockdown affects *Legionella* replication in human macrophages.

## 3.2 Identification of the gene expression profile during the course of *Legionella* infection by Dual RNA-Seq

The second part of this thesis was set out to uncover the most important transcriptional events in both human host cells and bacteria during infection with the lung pathogen *L. pneumophila*. The dual RNA-Seq method grants the opportunity to define the RNA landscape, including coding and non-coding RNAs of pathogen and host, in great depth and with high accuracy. The procedure has already been established for *Salmonella* infection of human epithelial cells (Westermann, Gorski et al. 2012; Westermann, Forstner et al. 2016). Therefore, one aim of this study was the establishment and adaptation of this method for *L. pneumophila* infection. Furthermore, the first analysis of the sequencing results was performed to identify infection specific markers.

### 3.2.1 Establishment of macrophage infection with *Legionella pneumophila* (*L.p.*) for dual RNA-Seq

In order to study the transcriptional profile of both, host and pathogen via dual RNA-Seq, a macrophage model needed to be selected. In humans, *Legionella pneumophila* infects alveolar macrophages in the lung. However, only relatively small numbers of alveolar macrophages can be isolated from bronchoalveolar lavage (BAL) fluids of healthy donors. Moreover, the dual RNA-Seq approach includes several steps such as infection and sorting, where higher amounts of cells are required to gain enough RNA material for sequencing depths of both organisms. Therefore, THP-1 cells were used as model for human alveolar macrophages.

One of the most important steps for identifying transcriptional profiles of host and pathogen simultaneously via dual RNA-Seq was the optimization of infection dose and time points. In order to synchronize the infection and to prevent reinfection, Gentamycin was given at 2 h post infection to selectively inactivate extracellular bacteria. Therefore, all host cells as well as bacteria should be synchronised in the same cell cycle and replication phase.

In order to characterize the process of infection over time, two time points were determined for sequencing. The time points needed to characterize different growth phases of *L.p.* and

sufficient inflammatory response in the host cells. Firstly, the latest infection time point and the infection dose was defined. Therefore, PMA-differentiated THP-1 cells were infected with increasing MOIs of *L.p.* (MOI of 5, 10 and 15) for 16 and 24 h. A key requirement for optimal identification of the infection conditions was low cytotoxicity with a substantial inflammatory response to minimize apoptosis-related transcriptional regulation. Thus, cytotoxicity (Fig. 3.15A) and CXCL8 secretion (Fig. 3.15B) was examined. Compared to the other MOIs, MOI 15 showed a significant increase (up to 45%) of cytotoxicity at 24 h post infection as determined by LDH-Assay. Furthermore, all chosen MOIs triggered an inflammatory response to infection at both time points as displayed by the significantly increased secretion of CXCL8. An MOI 10 at 16 h post infection showed a substantial inflammatory response and low cytotoxicity. Therefore, an MOI of 10 and the infection duration of 16 h were chosen for further experiments. In order to estimate the earlier, second infection time point, a time course experiment was performed (Fig. 3.15C). PMA-differentiated THP-1 cells were infected with *L.p.* at an MOI of 10 and increasing infection time periods from 2 – 16 h post infection. A peak of CXCL8 expression was recorded at 8 h post infection. Thus, time points for sequencing were set to an MOI of 10 for 8 and 16 h.

By way of synthetic control for TLR2-activating *Legionella* LPS, THP-1 cells were stimulated with the TLR2 agonist Pam3CSK4 (Pam3). In order to determine the concentration for stimulation, PMA-differentiated THP-1 cells were treated with 10, 50, 100, 200 and 300 ng/mL of Pam3 for 8 and 16 h and CXCL8 expression was examined (Fig. 3.15D). A significant increase of CXCL8 expression was detected with 10 ng/mL of Pam3 at 8 h and with 100, 200 and 300 ng/mL of Pam3 at 8 and 16 h post stimulation. Therefore, 100 ng/mL of Pam3 was used for subsequent experiments.

To separate infected, invaded macrophages from non-invaded bystander cells, cytometric sorting was applied. Therefore, it was necessary to use a GFP-expressing strain of *Legionella* to enable sorting. To guarantee that the wildtype strain and the GFP-expressing strain trigger a comparable inflammatory response in macrophages, PMA-differentiated THP-1 cells were infected with the two strains of *L.p.* at an MOI of 10 for 8 and 16 h. CXLC8 (Fig. 3.15E) and miR-146a expression (Fig. 3.15F) was investigated via qPCR. miR-146a is a well-studied miRNA and known to be induced during inflammation (O'Connell, Rao et al. 2012). As positive control for the inflammatory response, cells were stimulated with 1 µg/mL recombinant IL-1β for 8 and 16 h. CXCL8 expression was significantly increased in all three conditions at 8 and 16 h. The expression of miR-146a was only significantly induced in infected THP-1 cells. The comparison between the two strains revealed only a significant difference in CXCL8 expression

at both time points, but not for miR-146a expression. However, both strains showed a comparable inflammatory response to the *L.p.* infection.

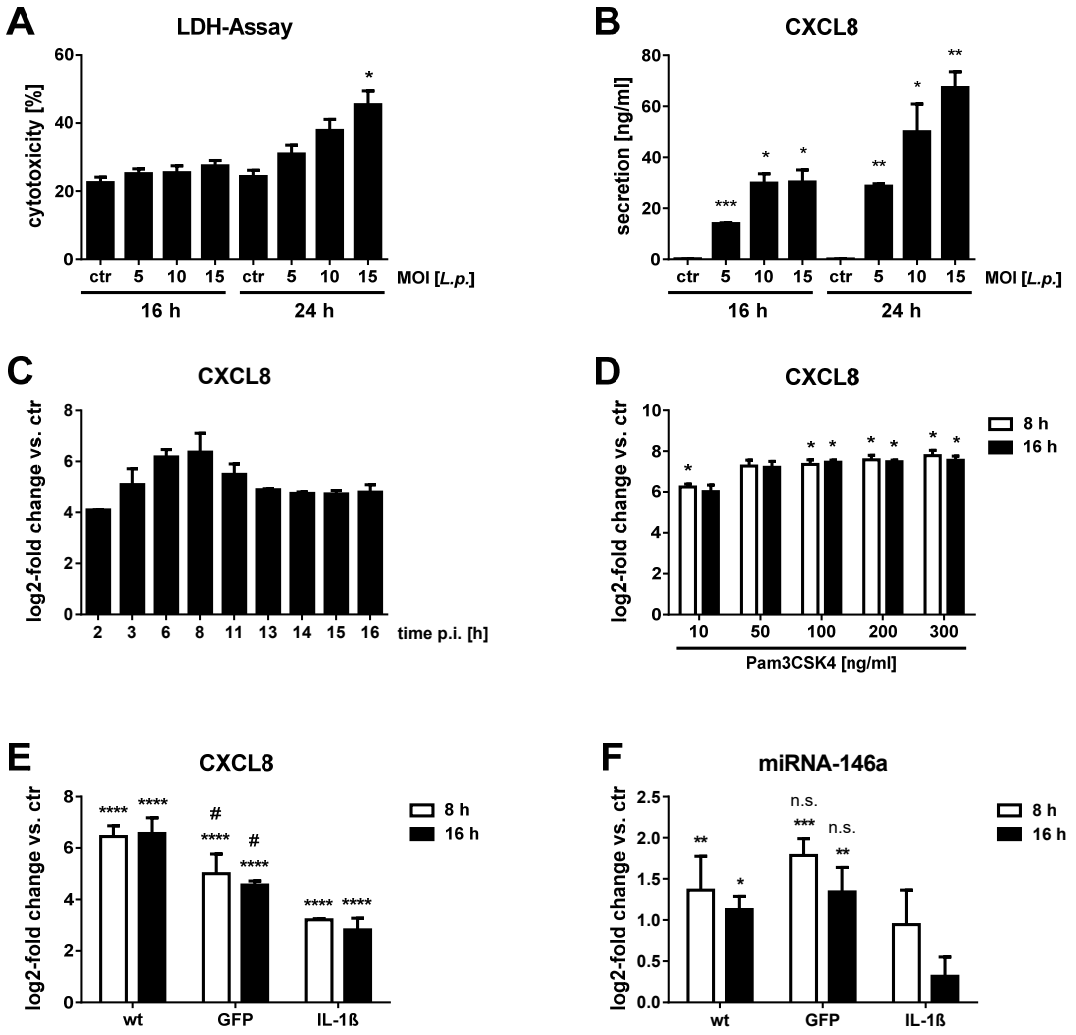


**Figure 3.15: Establishment of macrophage infection with *Legionella pneumophila* (*L.p.*) for dual RNA-Seq.** PMA-differentiated THP-1 cells were infected with increasing MOIs of GFP-*L.p.*: 5; 10; 15 or left untreated as control (ctr). At 2 h post infection, cells were washed three times with PBS and 25 µg/mL gentamycin was added to the culture medium. Sampling was performed at 16 and 24 h post infection. Cytotoxicity was examined by LDH-Assay (A) and CXCL8 secretion was determined by ELISA (B). Furthermore, CXCL8 expression was investigated via qPCR in a time-course with 2, 3, 6, 8, 11, 13, 14, 15, 16 h post *L.p.* infection at an MOI of 10 (C) or following stimulation with different concentrations of Pam3CSK4 (10, 50, 100, 200 and 300 ng/mL) for 8 and 16 h (D). Expression of CXCL8 (E) and miRNA-146a (F) was analysed following infection with *L.p.* wildtype strain (wt), with a GFP-expressing strain (GFP) or stimulation with 1 µg/mL IL-1β at 8 and 16 h. qPCR data are displayed as log2-fold change. Data are shown as mean + SEM of two to four independent biological replicates. Paired t-tests were performed: *p ≤ 0.05, **p ≤ 0.01, ***p ≤ 0.001, ****p ≤ 0.0001 compared to corresponding control, or $^{\#}$p ≤ 0.05 compared to wildtype strain.

In summary the infection set up for the dual RNA-Seq procedure were determined as follows: Differentiated THP-1 cells were infected with a GFP-expressing strain of *L.p.* Corby for 8 and

16 h at an MOI of 10 or left untreated as control. As positive control, cells were stimulated with 100 ng/mL Pam3CSK4.

### 3.2.2 FACS-sort settings for sequencing

After thorough investigation of the infection duration and dose, the infection procedure for the dual RNA-Seq was established (see section 3.2.1). THP-1 cells were differentiated by the addition of PMA (20 nM) for 24 h. After media change, THP-1 cells were infected at an MOI of 10 with GFP-*L.p.* for 2 h, or left untreated as control (ctr). Afterwards cells were washed three times with PBS to remove residual bacteria which were not internalized. Medium containing 25 µg/mL gentamycin was added to the cells to prevent reinfection during further cultivation. At 8 and 16 h post infection, cells were detached with trypsin for sorting and further analysis (Fig. 3.16A). THP-1 cells invaded by *L.p.* (GFP-positive fraction) were separated from the non-invaded bystander cells (GFP-negative fraction) by flow cytometric sorting. GFP-positive (gfp+) and GFP-negative (gfp-) cells were detected via plotting Phycoerythrin (PE) versus Alexa Fluor 488 (green fluorescence at 488 nm) and subsequently sorted. For sorting, only cells with high GFP-intensity were considered as GFP-positive to guarantee the purity of this fraction. The cells of three independent biological replicates were sorted and the sorting strategy as shown in Figure 3.16B was applied for all three experiments. To obtain an appropriate control, uninfected cells (ctr) were also sorted. At 8 h post infection, approximately 16% cells were identified as GFP-positive. At 16 h post infection, the number of GFP-positive events was 17.7%, while the GFP intensity was higher at 16 h post infection compared to 8 h.

In order to verify the applied sorting strategy, a sub-sample of each cell fraction was sorted into PBS and subsequently lysed with 1% saponin for 10 min. Different dilutions of the lysed cells were plated on BCYE-agar plates to quantify residual bacteria. Colonies were counted and CFU/mL was calculated (Fig. 3.16C). The analysis of the CFU/mL in the different fraction revealed a very low amount of bacteria in the GFP-negative fraction whereas the GFP-positive fraction showed an enrichment of bacteria within the cells. Overall, 460 CFU/mL were detected in the GFP-negative fraction and over 80,000 CFU/mL were detected in the GFP-positive samples. Furthermore, a 10-fold increase of CFU/mL was identified when comparing 8 h to 16 h post infection ($8.07 \times 10^4$ CFU/mL at 8 h and $8.61 \times 10^5$ CFU/mL at 16 h post infection). The remaining assorted cell fractions were sorted into RNAprotect™ solution to maintain RNA integrity and the RNA of all different samples was isolated and sequenced.

In summary, the infection set up as well as the applied sorting strategy for the dual RNA-Seq procedure was established and showed an adequate purity to continue with sequencing.

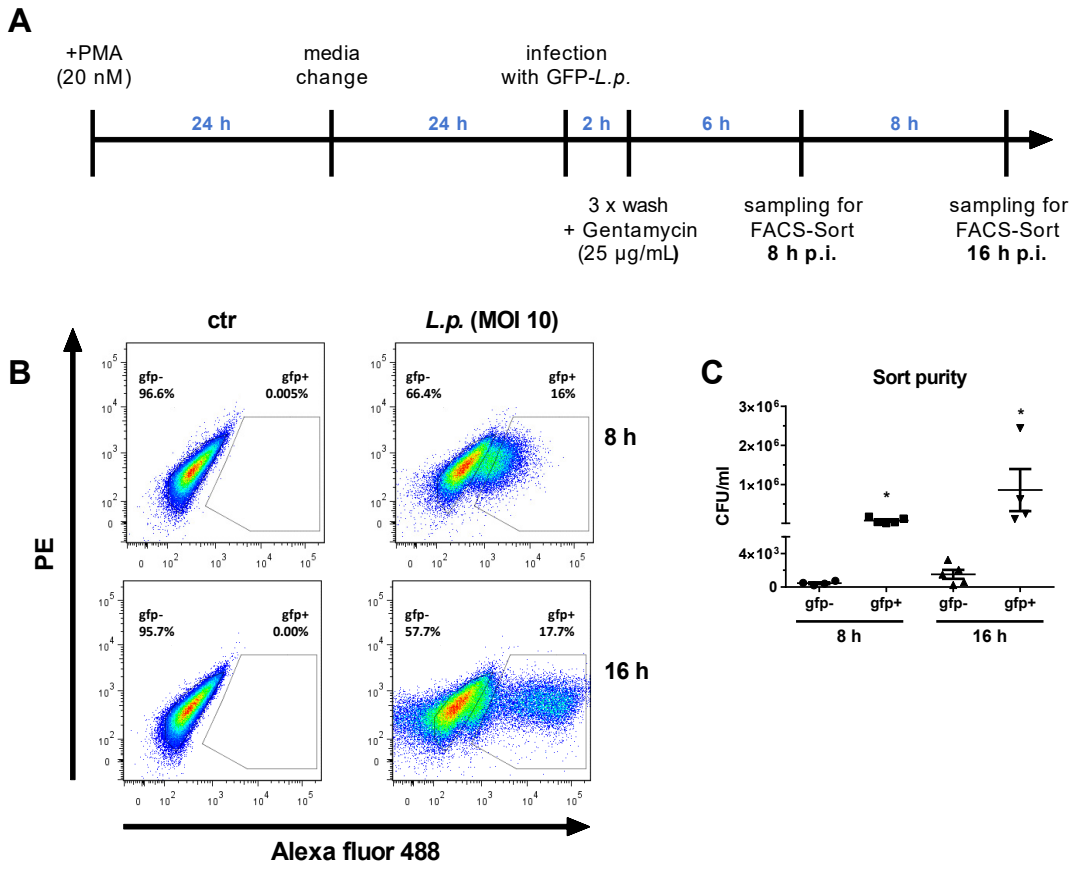


**Figure 3.16: FACS-sort settings for sequencing.** Schematic view of the infection protocol for the dual RNA-Seq approach is displayed (A). THP-1 cells were differentiated by the addition of PMA (20 nM) for 24 h. After media change THP-1 cells were infected at an MOI of 10 with the GFP-*L.p.* for 2 h, or left untreated as control (ctr). Afterwards cells were washed three times with PBS and gentamycin (25 µg/mL) was added to the media for further cultivation. For sorting and further analysis cells were detached at 8 or 16 h post infection. THP-1 cells invaded by *L.p.* were identified via flow cytometry. GFP-positive (gfp+) and GFP-negative (gfp-) cells were detected via plotting PE versus Alexa Fluor 488 and subsequently sorted. One representative plot of the sorting strategy is shown (B). After sorting, bystander (gfp-) and the *L.p.*- invaded (gfp+) THP-1 cells were lysed with 1% saponin for 10 min. Different dilutions of the lysed cells were plated on BCYE-agar plates. Colonies were counted after three days of incubation at 37°C and CFU/mL were calculated. Data are shown as mean + SEM of four to five independent biological replicates.

### 3.2.3 Bioinformatics analysis of the dual-RNA-Sequencing data

In order to characterize the transcriptional profile of both, the host and the bacteria simultaneously, the dual RNA-Seq procedure was applied as described before. The experiment was performed with three replicates and the RNA of the following samples was prepared: Bacteria from inoculum solution (*L.p.* T0), mock treated cells (ctr) for each time point, bystander cells (gfp-) and the *L.p.* invaded cells (gfp+) for each time point. The RNA was isolated and depleted for rRNA. Random-primed libraries were prepared and sequenced commercially by Vertis Biotechnologie AG (Freising, Germany) without cut-off above 50 bp on

an Illumina NextSeq 500 system using 75 bp read length. A computational pipeline for the analysis of the dual-RNA sequencing data was developed and applied by Dr. Brian Caffrey (Max Planck Institute for Molecular Genetics in Berlin, Germany). In short, for each RNA-Seq library, Illumina reads in FASTQ format were trimmed with an average Phred quality score cut-off of 20 over every four base pair window by the program Trimmomatic. 3' adapters were also trimmed using Trimmomatic. Reads shorter than 20 nt after adapter trimming were discarded before mapping. The reads were aligned to the *Legionella* Corby genome (NCBI accession number: 400673 and to the human genome (hg19-GRCh37) simultaneously using the read aligner STAR with default options and allowing for split reads. Reads that mapped to both genomes (mostly tRNAs) were discarded before further analysis.

In total, an average of over 11 million reads could be mapped at 8 and 16 h post *Legionella* infection, respectively (Fig. 3.17A). In the T0 sample, where bacteria from inoculum solution were sequenced, over 4.5 million reads in total were mapped. Of these reads, 2% and 4.5% corresponded to reads mapping to the *Legionella* genome (displayed in green) at 8 and 16 h post infection, respectively (Fig. 3.17B). Roughly 99.8% of the reads of the sequenced sample T0 mapped to the *Legionella* genome. A negligible number of reads were mapped to the *Legionella* genome in the non-infected (ctr, Pam3) and bystander cells (gfp-) at either time point, while the rest of the reads mapped to the human genome (depicted in blue). The mapping to the *Legionella* genome of a control sample (ctr) with a maximum of 0.07% mapping was higher than that of a gfp- sample with 0.05%.

In short, the percentage of bacterial reads increased over time, and nearly all reads were mapped to the human genome in the non-infected cells at both time points. More importantly, an extremely low number of *Legionella* reads were found in the bystander cells (gfp-) reflecting an inbuilt control of the cell sorting process.

A

| Source organism | Sample ID | # human reads (Mean) | # Legionella reads (Mean) | Total reads (Mean) |
|---|---|---|---|---|
| **Legionella** | L.p. T0 | 10,542 | 4,583,946 | 4,594,488 |
| **Human** | ctr | 10,851,482 | 2,681 | 10,854,162 |
| **Human** | PAM3CSK4 | 8,443,769 | 1,609 | 8,445,378 |
| **Human** | gfp- | 13,605,314 | 2,901 | 13,608,214 |
| **Human & Legionella** | gfp+ | 11,584,581 | 328,912 | 11,913,492 |

B

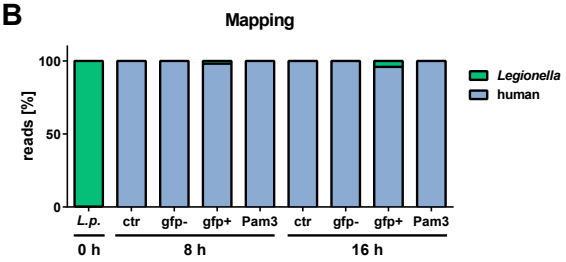


**Figure 3.17: Bioinformatics analysis of the dual RNA-Sequencing data.** PMA-differentiated THP-1 cells were infected with GFP-*L.p.* (MOI 10), stimulated with 100 ng/mL Pam3CSK4 (Pam3) or left untreated (ctr). At 2 h post infection, cells were washed three times with PBS and 25 µg/mL gentamycin was added to the culture medium. Sampling was performed at 8 and 16 h post treatment. After RNA isolation, rRNA was depleted. Libraries were prepared for sequencing of three independent experiments of the following samples: Bacteria from inoculum solution (*L.p.* T0), mock treated cells (ctr) for each time point, bystander cells (gfp-) and the *L.p.* invaded cells (gfp+) for each time point. Random-primed libraries were prepared and sequenced without cut-off above 50 bp on an Illumina NextSeq 500 system using 75 bp read length. Mean total read numbers after trimming and mean reads aligned to either the human or the *Legionella* genome are shown for the indicated samples (A). Percentage of mapped reads either to the human (blue) or the *Legionella* (green) genome for each sample and each time point is displayed (B).

### 3.2.4 Bioinformatics analysis of the host's differentially expressed genes

Given the previous results, the obtained read coverage of mapped reads was sufficient to detect reliable expression levels of both bacterial and human mRNAs, as well as bacterial and human non-coding RNAs. Further expression analysis was focused on the human or the pathogen side.

First, the transcriptional profile of the human macrophages was investigated and the distribution of the RNA species was analysed. In total, 73.8% of all transcripts to the human genome were protein coding, 6.2% processed pseudogenes, 5.7% antisense transcripts, 4.75% lncRNAs and 0.55% miRNAs (Fig. 3.18A). Furthermore, differential gene expression analysis was performed using DESeq2, resulting in a total of 4,144 differentially expressed human genes (across multiple conditions). In general, more upregulated than downregulated genes were identified (Fig. 3.18B). Less significantly regulated genes were detected in the gfp- samples than in the gfp+ or Pam3 samples across both time points. In order to examine the quality and to visually represent the global sample variation of the sequenced samples, a

principal component analysis (PCA) was performed (Fig. 3.18C). PCA was performed by Dr. Wilhelm Bertrams (Institute for Lung Research in Marburg, Germany) and normalized reads of genes (5,433) with an adjusted p-value ≤ 0.01 from the differentially expression analyses were used for the PCA. The PCA uncovered little variances across the biological replicates. The samples tend to cluster well according to the treatment (ctr, gfp-, gfp+ or Pam3) irrespective of the infection time point.

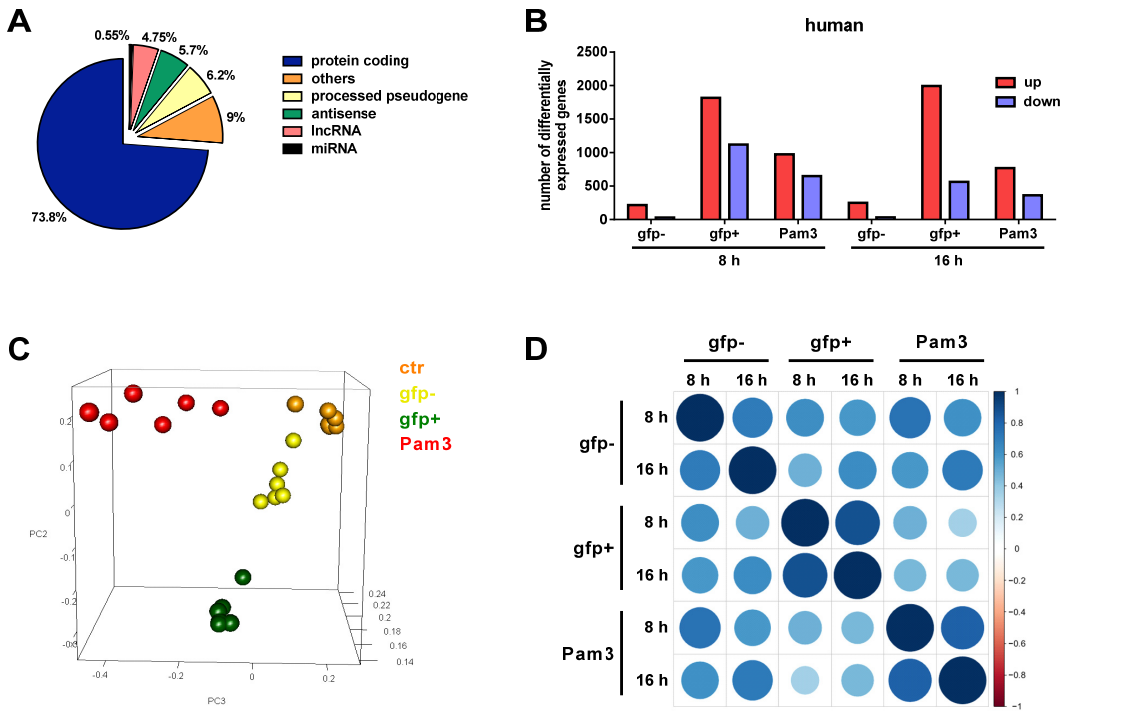


**Figure 3.18: Bioinformatics analysis of the hosts differentially expressed genes.** PMA-differentiated THP-1 cells were infected with GFP-*L.p.* (MOI 10), stimulated with 100 ng/mL Pam3CSK4 (Pam3) or left untreated (ctr). At 2 h post infection, cells were washed three times with PBS and 25 µg/mL gentamycin was added to the culture medium. Sampling was performed at 8 and 16 h post treatment. RNA was isolated and rRNA depletion was performed. Samples were prepared for sequencing of three independent experiments of the following samples: mock treated cells (ctr) for each time point, bystander cells (gfp-), *L.p.* invaded cells (gfp+) and Pam3CSK4 stimulated cells for each time point. Random-primed libraries were prepared and sequenced without cut-off above 50 bp on an Illumina NextSeq 500 system using 75 bp read length. After read trimming and alignment, significantly differentially expressed genes were identified using DESeq2. Cut-offs were set p ≤ 0.05, p adjusted ≤ 0.05 and log2-fold change > 1.5. Percentage distribution of the RNA species of all significant differentially expressed genes of the human samples is displayed (A). The numbers of the human differentially expressed genes are indicated for the different samples (gfp-, gfp+ or Pam3). The sum of all differentially up- (red) and downregulated (blue) genes is shown (B). Principal component analysis (PCA) of all significant differentially expressed genes was performed (C). A correlation analysis for the human samples based on the similarity of the differentially expressed genes is displayed (D). High correlation is indicated by dark and big circles, while low correlation is shown by bright small circles.

In order to visualize the correlation between the different conditions and time points, a correlation analyses was performed by Dr. Brian Caffrey. In this plot, correlation coefficients,

indicating the similarity of the differentially expressed genes, are colored and sized according to the degree of association between variables (Fig. 3.18D). High correlation is indicated by dark and big circles, while low correlation is shown by bright small circles. The gfp+ cells at 8 h post treatment are highly correlated to the gfp+ cells at 16 h and less correlated to Pam3 stimulated cells at 8 h and 16 h post treatment, respectively. Furthermore, the correlation plot indicates a high similarity between gfp- and Pam3 at 8 h as well as at 16 h post treatment.
In summary, the general analysis of the sequencing data of the host side revealed very reliable results based on the distribution of the different RNA species, the clustering and correlation analysis between the different conditions.

### 3.2.5 Differentially expressed mRNAs in macrophages during *L.p.* infection

As mentioned above, the sequencing data were normalized to the non-infected control samples and differential expression analysis was performed using DESeq2. The analysis revealed 3,504 differentially expressed mRNAs during the course of *L.p.* infection. Data are displayed in a heatmap, which shows upregulated mRNAs in red and downregulated mRNAs in blue (Fig. 3.19A). Above the heatmap a dendrogram is depicted. A dendrogram is a tree diagram that is used to visualize the arrangement of the clusters produced by hierarchical clustering (Everitt 1998). In this plot, the dendrogram shows a clustering for each condition between the 8 and 16 h time point. Additionally, gfp- cells cluster closely to the Pam3 stimulated cells than to the gfp+ cells. Therefore, the gfp+ cells show a distinct position besides gfp- and Pam3.
Furthermore, the heatmap of differentially expressed mRNAs shows gene clusters which indicate differential gene regulation at different times and conditions. It allows for the recognition of clusters indicating genes which are upregulated or downregulated in all conditions (gfp+, gfp-, Pam3) or mainly upregulated in Pam3 samples. To validate the transcription of genes showing an upregulation in all three conditions, a qPCR analysis was performed. The expression of the inflammatory cytokine IL-1β (Fig. 3.19B) and the member of the superoxide dismutase SOD2 (Fig. 3.19C) was significantly increased in gfp-, gfp+ and Pam3 cells compared to the ctr samples. Additionally, the expression of IL-1β and SOD2 was significantly increased in gfp+ compared to gfp- cells. Therefore, an increase in all fractions (gfp-, fgp+ and Pam3) was observed. Furthermore, clusters specific for the gfp+ sample were detected in the heatmap. One cluster displays genes only highly upregulated or downregulated in gfp+. Another cluster shows genes upregulated in gfp+ with a downregulation in gfp- and Pam3, which displays an interesting section of genes.

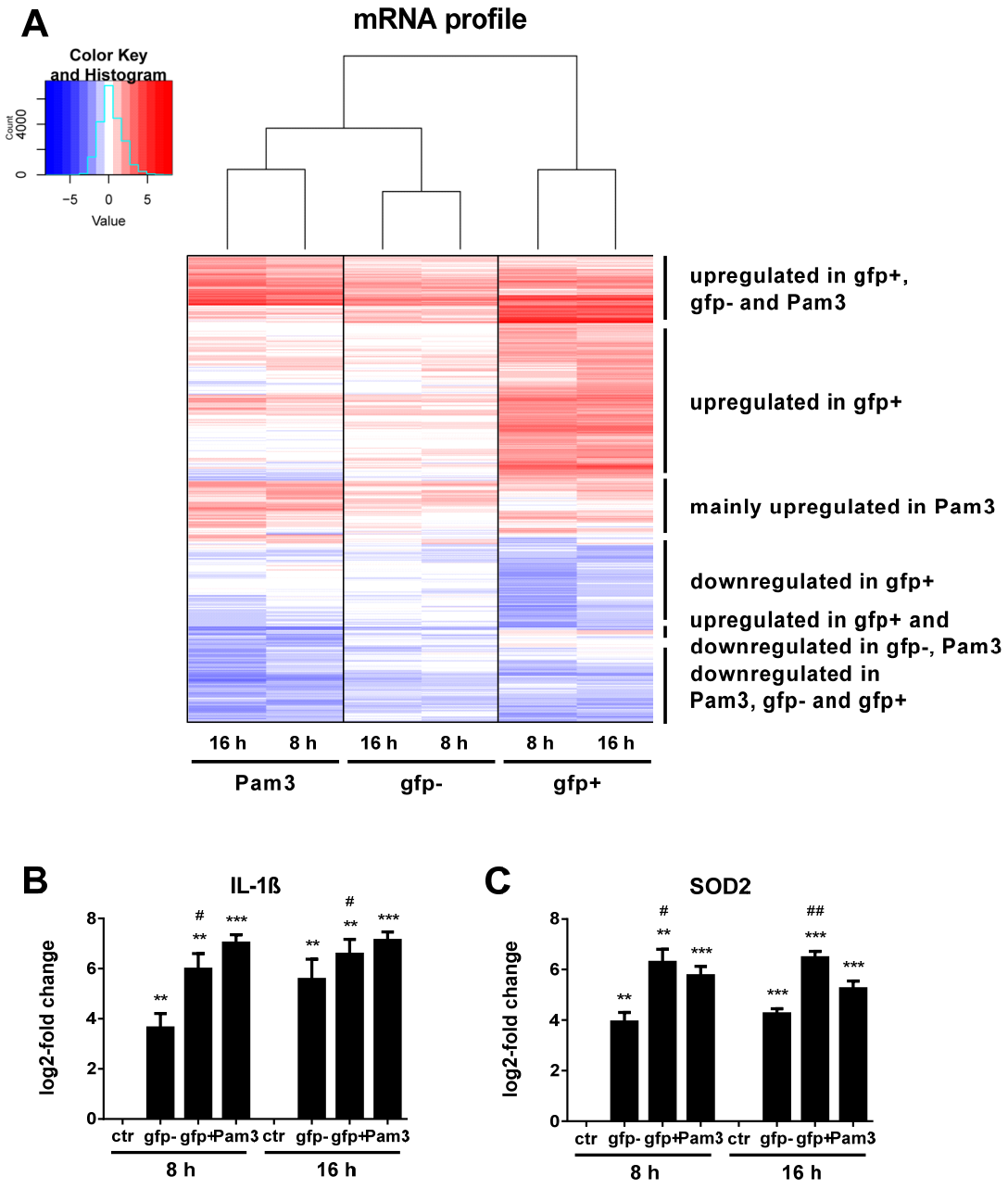


**Figure 3.19: Differentially expressed mRNAs in macrophages during *L.p.* infection.** PMA-differentiated THP-1 cells were infected with GFP-*L.p.* (MOI 10), stimulated with 100 ng/mL Pam3CSK4 (Pam3) or left untreated (ctr). At 2 h post infection, cells were washed three times with PBS and subsequently 25 µg/mL gentamycin were added to the culture medium. Sampling was performed at 8 and 16 h post infection. RNA was isolated and rRNA depletion was performed. Samples were prepared for sequencing of three independent experiments of the following samples: mock treated cells (ctr) for each time point, bystander cells (gfp-), *L.p.* invaded cells (gfp+) and Pam3CSK4 stimulated cells (Pam3) for each time point. Random-primed libraries were prepared and sequenced without cut-off above 50 bp on an Illumina NextSeq 500 system using 75 bp read length. After read trimming and alignment, significant differentially expressed genes were identified using DESeq2. Results are shown in a heatmap (A). Expression of IL-1β (B) and SOD2 (C) mRNAs in THP-1 cells after *L.p.* infection was validated by qPCR and displayed as log2-fold change. Data are shown as mean + SEM of four independent biological replicates. Paired t-tests were performed: *p ≤ 0.05, **p ≤ 0.01, ***p ≤ 0.001, ****p ≤ 0.0001 compared to the corresponding control, or $^{\#}$p ≤ 0.05, $^{\#\#}$p ≤ 0.01 compared to gfp-cells.

Overall, the mRNA expression profile depicted in a heatmap led to the identification of clusters specific for gfp+ samples and revealed a substantial difference between gfp+ and the other two conditions. Additionally, the validation experiments confirmed the results of the sequencing which was indicated by the upregulation of IL-1β and SOD2.

### 3.2.6 Differentially expressed lncRNAs in macrophages during *L.p.* infection

The DESeq2 analysis of the lncRNAs revealed 495 differentially expressed genes. The sequencing data are visualized in a heatmap with a hierarchical clustering above (Fig. 3.20A). This dendrogram shows again a clustering for each condition between the 8 and 16 h time point. Furthermore, the Pam3 cells are not clustering with the gfp- or the gfp+ cells. The gfp- cells are clustering with the gfp+ cells rather than with the Pam3 cells. This observation stands in contrast with the clustering analysis of the mRNAs where the gfp- and Pam3 samples were clustering. In total, the heatmap shows expression clusters with transcripts mainly up- or downregulated in Pam3 cells or transcripts up- or downregulated in all conditions. Additionally, two clusters of lncRNAs specifically upregulated in gfp+ cells were recorded. Two example lncRNAs were validated using qPCR. The expression of LINC00278 (Fig. 3.20B) and LINC00346 (Fig. 3.20C) was analysed and showed a significant upregulation in gfp+ cells at 16 h post treatment. The expression of LINC00278 was even significantly downregulated at 8 h post treatment in gfp+ cells, while the expression of LINC00346 was significantly increased. No significant expression changes were detected in gfp- cells at 8 and 16 h post infection indicating that those lncRNAs are specifically regulated in gfp+ cells.

In summary, the lncRNA expression profile showed a different clustering compared to the mRNA expression profile. In addition, lncRNAs specific for gfp+ cells were identified and validated via qPCR.

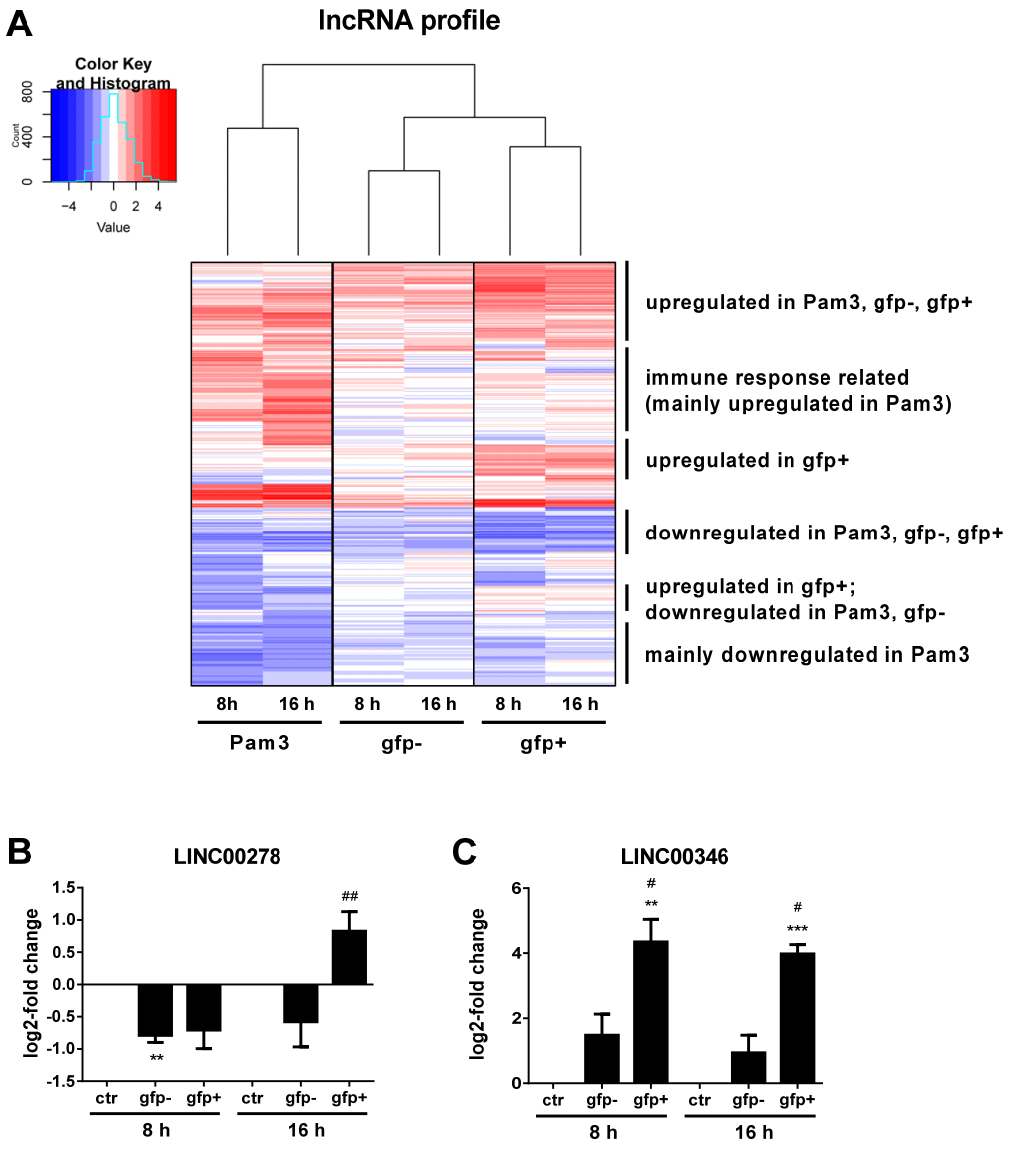


**Figure 3.20: Differentially expressed lncRNAs in macrophages during *L.p.* infection.** PMA-differentiated THP-1 cells were infected with GFP-*L.p.* (MOI 10), stimulated with 100 ng/mL Pam3CSK4 (Pam3) or left untreated (ctr). At 2 h post infection, cells were washed three times with PBS and subsequently treated with 25 µg/mL gentamycin. Sampling was performed at 8 and 16 h post infection. RNA was isolated and rRNA depletion was performed. Samples were prepared for sequencing of three independent experiments of the following samples: mock treated cells (ctr) for each time point, bystander cells (gfp-), *L.p.* invaded cells (gfp+) and Pam3CSK4 stimulated cells (Pam3) for each time point. Random-primed libraries were prepared and sequenced without cut-off above 50 bp on an Illumina NextSeq 500 system using 75 bp read length. After read trimming and alignment, significant differentially expressed genes were identified using DESeq2. Results are shown in a heatmap (A). Expression of LINC00278 (B) and LINC00346 (C) mRNAs in THP-1 cells after *L.p.* infection was validated by qPCR and displayed as log2-fold change. Data are shown as mean + SEM of four independent biological replicates. Paired t-tests were performed: *p ≤ 0.05, **p ≤ 0.01, ***p ≤ 0.001, compared to the corresponding control, or $^{\#}$p ≤ 0.05, $^{\#\#}$p ≤ 0.01 compared to gfp-cells.

### 3.2.7 Differentially expressed miRNAs in macrophages during *L.p.* infection

The DESeq2 analysis of the separated RNA fractions from host cells revealed 145 differentially expressed miRNAs. The results of the sequencing are displayed in a heatmap with a dendrogram above (Fig. 3.21A). It shows the arrangement of the clusters produced by hierarchical clustering. Based on the dendrogram, a clustering of the 8 and the 16 h time point of each condition is observable in gfp- and Pam3 cells. Additionally, the gfp+ sample at 16 h post treatment shows no clustering to the other samples. As seen for the hierarchical clustering analysis of the lncRNAs, the gfp- cells are clustering more to the gfp+ 8 h cells than to the Pam3 treated cells.

On the basis of the heatmap, no clusters specific for gfp+ at 8 and 16 h are obvious. Only genes specific for gfp+ at 16 h post treatment were detectable and showed strong regulation. Additionally, genes of Pam3 cells at 8 and 16 h post treatment are stronger regulated than genes of gfp- or gfp+ cells. In general, a gradual up or downregulation over time can be reported for all three conditions. In order to highlight the transcriptional regulation of two miRNAs investigated before, the log2-fold expression of the miR-146a-5p (Fig. 3.21B) and miR-221-3p (Fig. 3.21C) of the heatmap are depicted. The expression of miR-146a was increased in all conditions and both time points, while miR-221 showed a slightly decreased expression in gfp+ cells.

In short, the clustering analysis of the miRNAs showed no clustering of the gfp+ cells at 16 h post treatment to the other samples and only few clusters specific for cells invaded by *Legionella* as observed for the lncRNAs or the mRNAs.

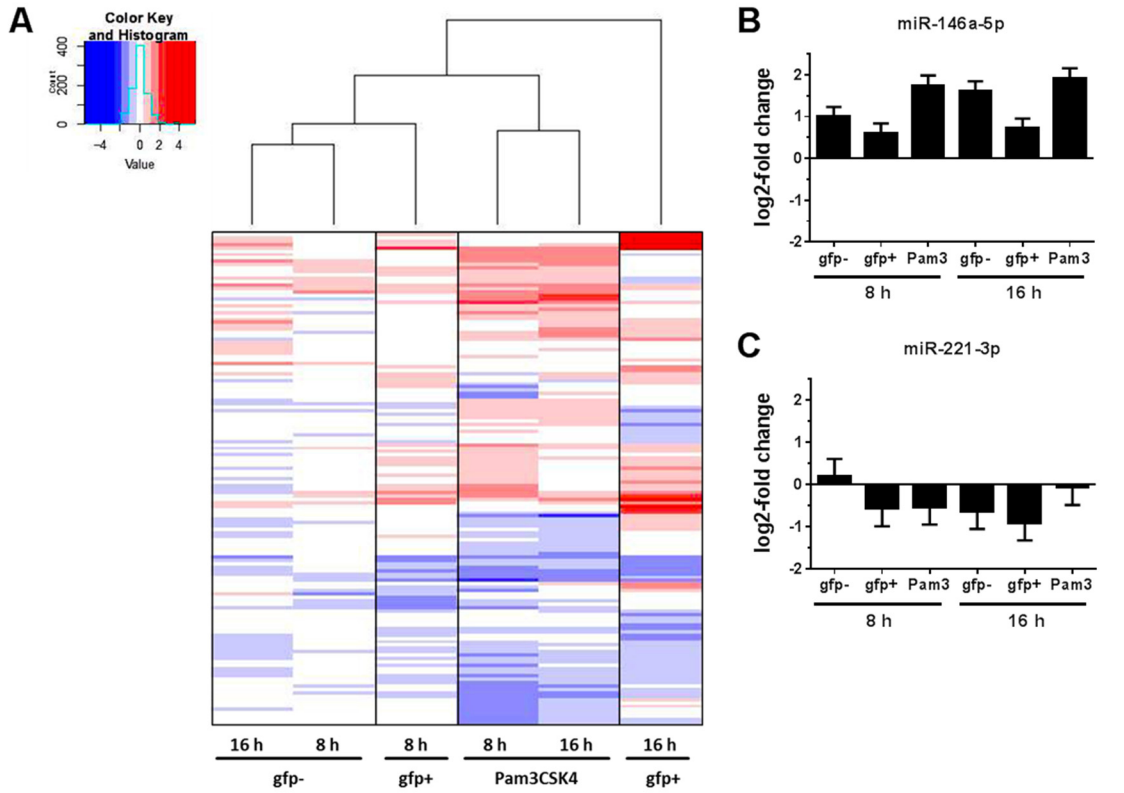


**Figure 3.21: Differentially expressed miRNAs in macrophages during *L.p.* infection.** PMA-differentiated THP-1 cells were infected with GFP-*L.p.* (MOI 10), stimulated with 100 ng/mL Pam3CSK4 (Pam3) or left untreated (ctr). At 2 h post infection, cells were washed three times with PBS and subsequently treated with 25 µg/mL. Sampling was performed at 8 and 16 h post infection. RNA was isolated and rRNA depletion was performed. Samples were prepared for sequencing of three independent experiments of the following samples: mock treated cells (ctr) for each time point, bystander cells (gfp-), *L.p.* invaded cells (gfp+) and Pam3CSK4 stimulated cells (Pam3) for each time point. Random-primed libraries were prepared and sequenced without cut-off above 50 bp on an Illumina NextSeq 500 system using 75 bp read length. After read trimming and alignment, significant differentially expressed genes were identified using DESeq2. Results are shown in a heatmap (A). Expression of miR-146a-5p (B) and miR-221-3p (C) from the heatmap are highlighted in sub-panels and displayed as log2-fold change + SEM.

### 3.2.8 Identification of genes specifically regulated in *Legionella* invaded cells

In order to identify significantly regulated genes specific for gfp+ cells, an Edwards-Venn diagram was created using the JavaScript library jvenn. It processes lists and produces Venn diagrams (Bardou, Mariette et al. 2014). A Venn diagram consists of multiple overlapping closed curves and each of them represents a different set of data. They are commonly used to display logical relations between a finite collection of different sets. Therefore, Venn diagrams allow the comparison between different experimental conditions (Edwards 2004). Six different input lists were used to present the results in the Edwards-Venn diagram: 8 h gfp- (blue), 16 h gfp- (purple), 8 h gfp+ (yellow), 16 h gfp+ (green), 8 h Pam3 (red) and 16 h Pam3 (orange) (Fig. 3.22). All differentially expressed genes with an adjusted p-value lower than 0.05 and a

log2-fold change higher than 1.5 or lower than -1.5 for each condition are listed. Different interesting sections were identified. For instance, 89 genes significantly regulated in all conditions, such as SOD2 and IL-1β, were pointed out. Furthermore, a section of *Legionella* specific genes appearing in the overlap between 8 h gfp-, 16 h gfp-, 8 h gfp+ and 16 h gfp+ could be detected. Only one gene (microtubule associated protein 1 light chain 3 gamma (MAP1LC3C)) specific for the bystander cells (gfp-) is displayed in the Venn diagram. Eleven genes showed differential gene expression in response to TLR and cytokine signaling are depicted in the section between the bystander (gfp-) and the Pam3 cells. Notably, the Venn diagram revealed 1,128 differentially expressed genes which were exclusively significantly regulated in the invaded cells (gfp+ 8 and 16 h) and not significantly regulated in Pam3 stimulated (Pam3) or bystander cells (gfp-).

Overall, many possible markers for *Legionella* infections within this setting were identified using JavaScript library jvenn.

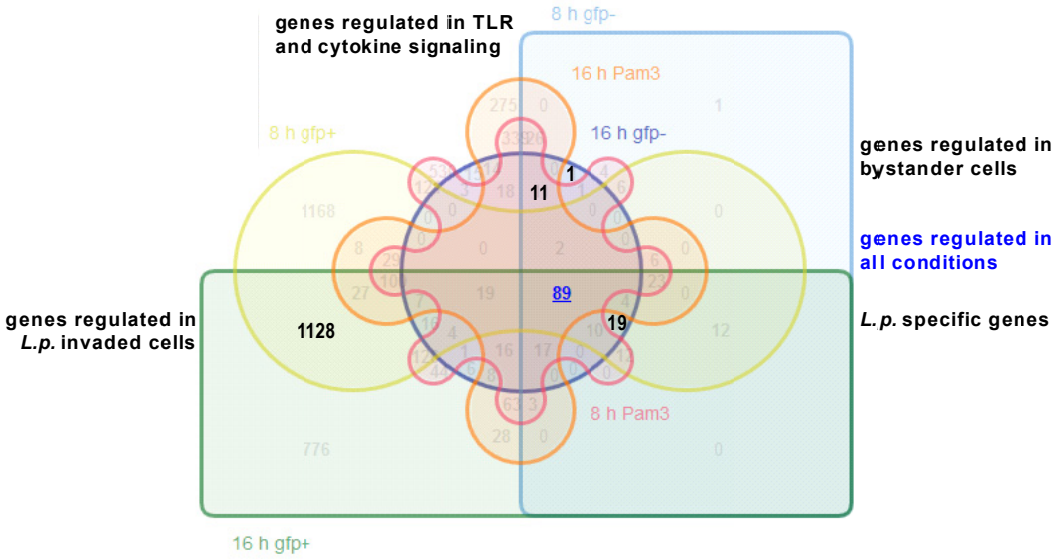


**Figure 3.22: Identification of genes specifically regulated in *Legionella* invaded cells.** The Venn diagram shows the overlap of all differentially expressed host genes of mock treated cells (ctr), bystander cells (gfp-), *L.p.* invaded cells (gfp+) and Pam3CSK4 stimulated cells (Pam3) across 8 and 16 h. Different sections are highlighted as indicated.

### 3.2.9 Validation of genes identified using jvenn

The above mentioned results indicate that 1,128 differentially expressed genes were exclusively regulated in invaded cells (gfp+ fraction), while 19 genes were only regulated in bystander cells and *Legionella* invaded cells. Validation experiments were performed to confirm the sequencing results. The expression of nine different genes was analyzed via qPCR

(Fig. 3.23): B-Cell CLL/Lymphoma 10 (BCL10), Superoxide Dismutase 1 (SOD1), Insulin Receptor Substrate 1 (IRS1), Cysteine Rich Angiogenic Inducer 61 (CYR61), Autophagy Related 5 (ATG5), Rho Family GTPase 3 (RND3), Jun Proto-Oncogene (JUN), Zinc Finger AN1-Type Containing 2A (ZFAND2A) and Heat Shock Protein Family A (Hsp70) Member 1A (HSPA1A). The genes ZFAND2A and HSPA1A were considered to be *Legionella* specific, while the other validated genes were found to be exclusively regulated in *Legionella* invaded cells.

All examined genes were significantly upregulated in invaded cells (gfp+) compared to not infected control cells (ctr) at both time points (8 and 16 h). In the bystander cells, the genes BCL10 (Fig. 3.23A), CYR61 (Fig. 3.23D), RND3 (Fig. 3.23F), JUN (Fig. 3.23G), ZFAND2A (Fig. 3.23H) and HSPA1 (Fig. 3.23I) showed significant upregulation either at 8 or 16 h post infection compared to control cells. It is worth noting that these genes were moderately upregulated (log2-fold change of 0.5 to 1.5) with the exception of ZFAND2A and HSPA1A (log2-fold change of 1.9 to 5.4). These two genes were identified using jvenn to be regulated in gfp- as well as in gfp+ cells, which can be confirmed by the qPCR results.

The genes SOD1 (Fig. 3.23B), IRS1 (Fig. 3.23C) and ATG5 (Fig. 3.23E) showed no significant regulation in gfp- cells, but a significant increased upregulation in gfp+ cells. For Pam3 cells, selected genes were either downregulated or only slightly upregulated. Nevertheless, the analysis revealed eight genes (BCL10, SOD1, IRS1, CYR61, ATG5, RND3, ZFAND2A and HSPA1) which were significantly upregulated in the infected cells and showed a significant difference to non-infected bystander cells at both time points. The gene JUN demonstrated a significant difference at 16 h, but not at 8 h post infection.

Overall, all selected mRNAs, identified by the Venn diagram, were exclusively upregulated in the infected cells, and can be used as specific markers of *Legionella* infection in this infection setting.

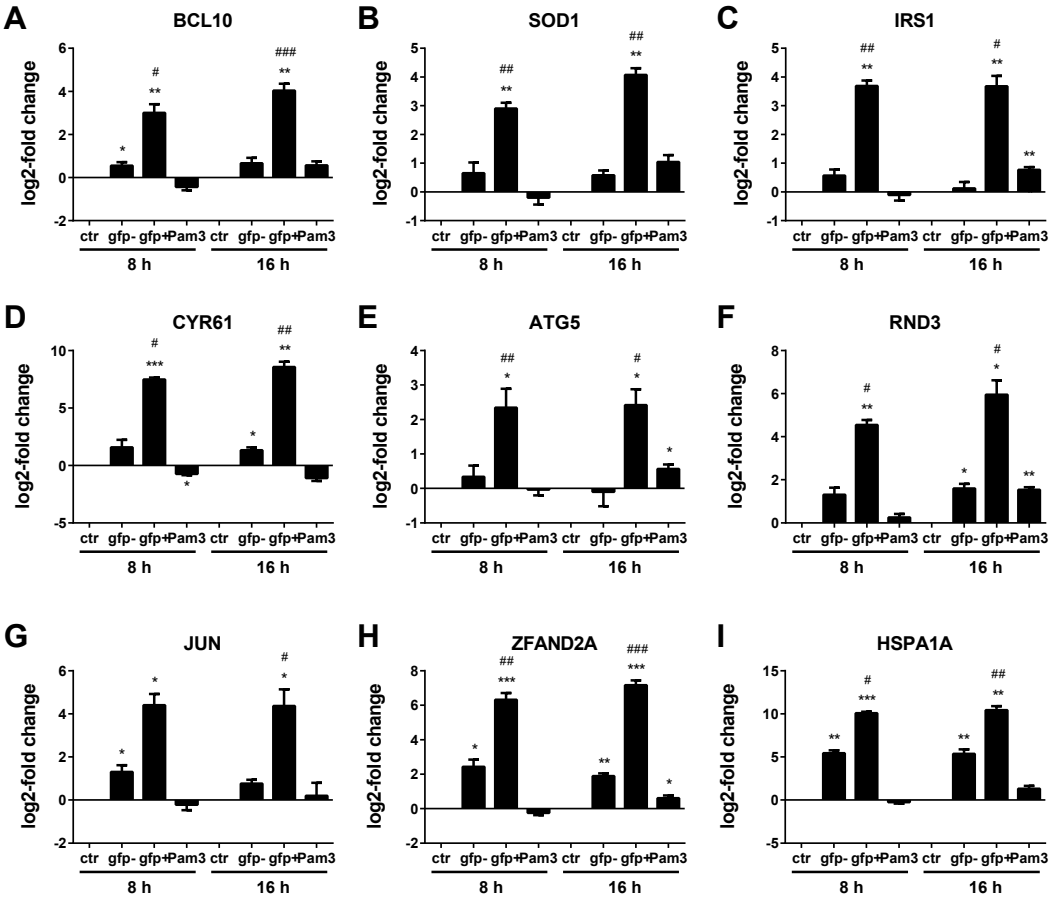


**Figure 3.23: Validation of genes using jvenn.** PMA-differentiated THP-1 cells were infected with GFP-*L.p.* (MOI 10), stimulated with 100 ng/mL Pam3CSK4 (Pam3) or left untreated (ctr). At 2 h post infection, cells were washed three times with PBS and subsequently treated with 25 µg/mL gentamycin. Sampling was performed at 8 and 16 h post infection. Expression of BCL10 (A), SOD1 (B), IRS1 (C), CYR61 (D), ATG5 (E), RND3 (F), JUN (G), ZFAND2A (H) and HSPA1 (I) was investigated via qPCR and displayed as log2-fold changes + SEM. Paired t-tests were performed: *p ≤ 0.05, **p ≤ 0.01, ***p ≤ 0.001, compared to the corresponding control, or $^{\#}$p ≤ 0.05, $^{\#\#}$p ≤ 0.01, $^{\#\#\#}$p ≤ 0.001 compared to gfp-cells.

### 3.2.10 Differentially expressed mRNAs of *Legionella* during *L.p.* infection

The analysis of the dual RNA-seq data revealed not only the regulation of different RNA species from the human side, but also the gene expression of the pathogen within the human macrophages was also analysed. The separation of host and pathogen reads was performed *in silico.* After bioinformatics analysis, differentially expressed mRNAs of *Legionella* during the course of infection at 8 and 16 h post infection were identified using DESeq2. As reference control, bacteria from inoculum solution were used and sequencing data were normalized to them. After applying cut-offs (adjusted p-value needed to be lower than 0.05 and the log2-fold change higher than 1.5 or lower than -1.5), DESeq2 analysis revealed 2,707 differentially expressed *Legionella* genes across both time points (8 and 16 h post infection). Among them,

798 genes were upregulated and 596 showed a downregulation at 8 h post infection, while at the 16 h time point 759 genes were significantly upregulated and 554 genes were detected as downregulated (Fig. 24A). Thus, more genes showed an upregulation at both time points. The sequencing data are visualized in a heatmap and all differentially expressed mRNAs of *Legionella* are displayed (Fig. 24B left). Most of the genes showed the same tendency of regulation at 8 h and at 16 h post infection. However, one interesting section was highlighted in the graph, which is located in the middle section of the heatmap. This section is displayed enlarged on the right side of Fig. 24B. This enlarged section shows a switch between the 8 h and the 16 h time point. Therefore, genes showing a regulation at 8 h post infection are either not regulated or downregulated at 16 h post infection. This observation was also seen for the 16 h time point. It includes factors involved in iron metabolism (such as feoA and feoB) and stress response (heatshock proteins (hsp) such as dnaK, htpG, clpB), which are downregulated at 8 h post infection and are upregulated at the 16 h time point. Furthermore, the genes fabFn and waaM (important for lipid biosynthesis) and korB (involved in the glycolysis pathway) were differentially regulated in intracellular vs. control bacteria. They are first upregulated at 8 h and downregulated at 16 h post infection. Furthermore, the genes flgB and flgG are both upregulated at the 16 h time point and are components of flagellum and necessary for bacterial motility.

In short, the DESeq2 analysis of the protein coding genes of *Legionella* revealed many differentially expressed genes. This includes one interesting section harbouring genes which were inversely regulated across both time points. The genes of this section were implicated in different processes such as, iron metabolism and bacterial stress responses.

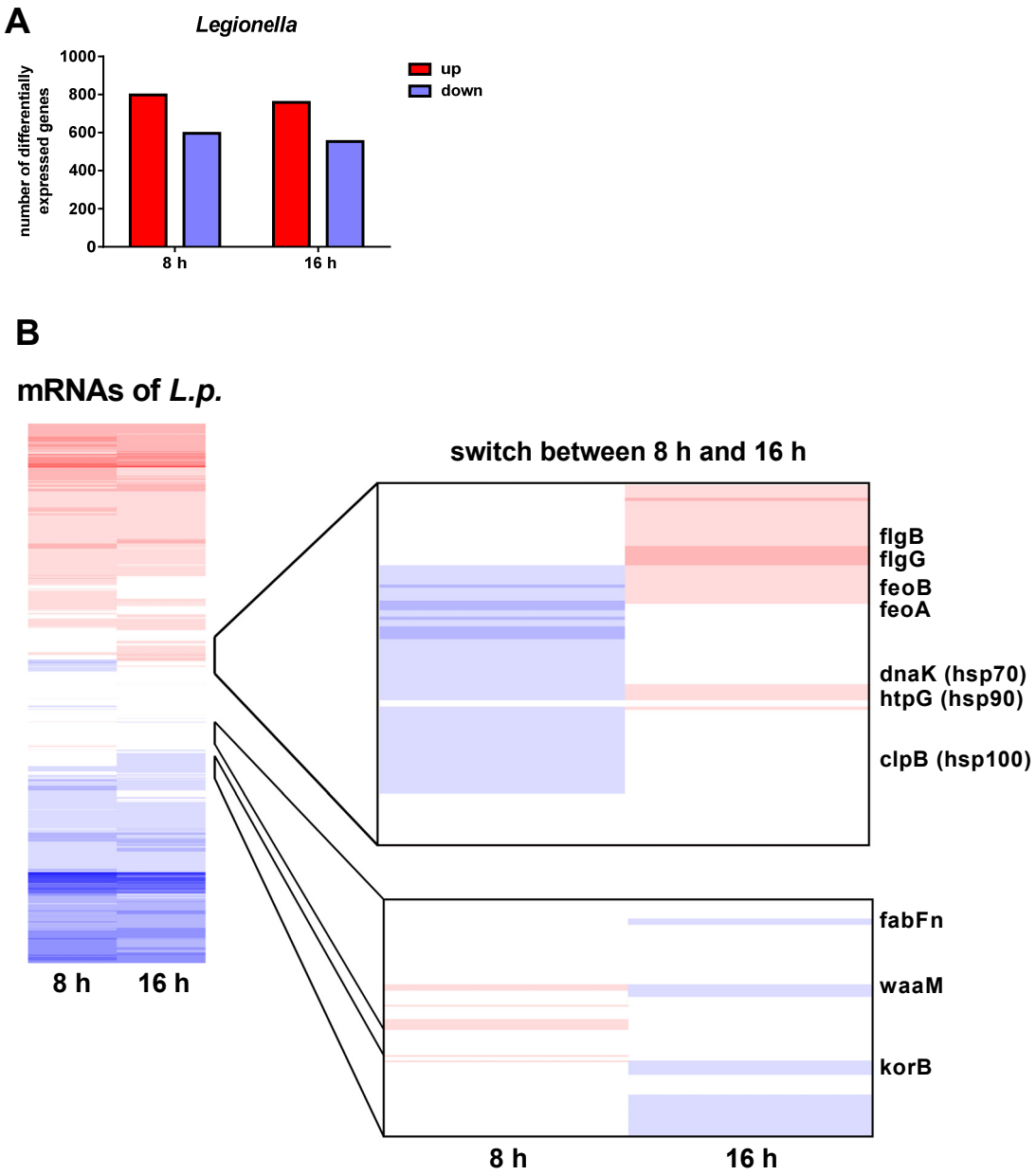


**Figure 3.24: Differentially expressed mRNAs of *Legionella* during *L.p.* infection.** PMA-differentiated THP-1 cells were infected with GFP-*L.p.* (MOI 10), stimulated with 100 ng/mL Pam3CSK4 (Pam3) or left untreated (ctr). At 2 h post infection, cells were washed three times with PBS and 25 µg/mL gentamycin was added to the culture medium. Sampling was performed at 8 and 16 h post infection. After RNA isolation, rRNA was depleted. Libraries were prepared for sequencing of three independent experiments of the following samples: Bacteria from inoculum solution (*L.p.* T0), mock treated cells (ctr), bystander cells (gfp-) and the invaded cells (gfp+) for each time point. Random-primed libraries were prepared and sequenced without cut-off above 50 bp on an Illumina NextSeq 500 system using 75 bp read length. After read trimming and alignment, significant differentially expressed genes were identified using DESeq2. Cut-offs were set $p \leq 0.05$, p adjusted $\leq 0.05$ and log2-fold change $> 1.5$. The numbers of differentially expressed genes in *Legionella* compared to T0 are indicated for 8 and 16 h post infection in macrophages. The sum of all differentially up- (red) and downregulated (blue) genes is shown (A). Differentially expressed genes in *Legionella* are displayed in a heatmap. A sub-panel indicates mRNAs contradictorily regulated between 8 and 16 h post infection.

# 4 Discussion

*Legionella pneumophila* is an intracellular pathogen accounting for 4% of ambulant pneumonia cases in Germany (Robert-Koch-Institut 2012). This gram-negative bacterium is highly adapted to intracellular replication. It manipulates vital host cell functions like vesicle trafficking and gene expression by secretion of specific virulence factors into the host cell cytosol. Thus, *Legionella* modifies host gene regulation for its own benefit. One main goal of this study was to characterize transcriptional expression changes of different RNA species in response to infection with *Legionella* in human macrophages.

An unbiased and global analysis of the molecular changes and biological processes that are associated with bacterial infections of eukaryotic cells can provide new insights into host-pathogen interactions. The increasing sensitivity of high-throughput RNA sequencing enables dual RNA-Seq which allows the parallel transcriptomic analysis of two different organisms interacting with each other. This procedure was used to quantify deregulated RNA species during the course of *Legionella* infection in macrophages and to further characterize host-pathogen interactions in a complex network of coding and non-coding RNAs. Overall, this technique enables the identification of new virulence factors from the pathogen side, or new pathways in the host cell that respond to the exposure to specific pathogens (Westermann, Gorski et al. 2012). In this study, the first steps were done to identify the interaction network between *Legionella* and human macrophages.

In the last decades, non-coding RNAs have been found to be important regulators of immune function. Especially miRNAs have been established as regulators of immune function. They are regulating immune responses of mammalian cells to a pathogenic threat at the post-transcriptional level to prevent harmful consequences of immune mechanisms. Therefore, one specific goal of this study was to identify the miRNA profile of *Legionella*-infected macrophages and to determine the functional impact of selected miRNAs.

## 4.1 *L.p.*-induced changes of miRNA expression and their importance for bacterial replication

miRNAs are critical regulators of many biological processes including cell proliferation, metabolic pathways, immune response, and development (Bartel 2004; Kloosterman and Plasterk 2006; Taganov, Boldin et al. 2007; O'Connell, Rao et al. 2010; Deiuliis 2016). Furthermore, it is known that miRNAs are also key mediators of the host response to infection, since they are involved in innate and adaptive immune pathways, such as the regulation of TLR

signaling. One known strategy adopted by intracellular bacteria to survive in host cells is the modulation of miRNAs that regulate TLR pathways. Therefore, pathogens have evolved to interfere with miRNAs and alter the inflammatory response (Das, Garnica et al. 2016).

*Legionella pneumophila* manipulates its host in a highly sophisticated way to promote its own replication. Thus, it is very likely, that miRNA regulation in *L.p.*-infected macrophages is not only due to host response, but may also be directly influenced by *Legionella*.

In humans, *L.p*. infects alveolar macrophages (Chandler, Hicklin et al. 1977). Since the availability of human alveolar macrophages for experimental purposes is limited, primary human blood-derived macrophages were used in this study to mimic the infection with *L.p.* in the lung. As described before, BDMs can been cultured either in presence of M-CSF, GM-CSF or human serum in order to differentiate to macrophages. It has been shown that M-CSF circulates at high concentrations in the blood, while GM-CSF is predominant in the lung and regulates alveolar macrophage differentiation (Shibata, Berclaz et al. 2001). Additionally, cultivation in the presence of human serum gives rise to macrophages that resemble tissue macrophages that develop in the GM-CSF rich environment of the lung (Akagawa, Kamoshita et al. 1988; Waldo, Li et al. 2008). Thus, isolated monocytes from the blood of healthy donors were cultivated in human off-the-clot AB serum to generate blood-derived macrophages *in vitro* to resemble alveolar macrophages. These cells were considered suitable *L.p.*-hosts.

### 4.1.1 Infection of macrophages with *L.p.* for miRNA expression analysis

In order to identify differentially expressed miRNAs in response to infection, human BDMs were infected with different MOIs for 24 and 48 h. MOI 0.25 and MOI 0.5 were selected for further analysis, since the cells showed a substantial inflammatory response with low cytotoxicity (Fig. 3.1A,B).

When higher amounts of cells were needed, PMA-differentiated THP-1 cells were chosen as an experimental model for primary human macrophages in this study. The availability of primary human monocytes is limited and accounts for only 3-9% of all blood leukocytes. Additionally, donor variability, accessibility, and contamination with other blood components can interfere or mask biologically significant results (Qin 2012). Some experiments were repeated in BDMs to rule out cell line specific effects. To compare the inflammatory response of *L.p.*-infected THP-1 cells and BDMs, the secretion levels of different cytokines, including CXCL-8, IL-1β, IL-6, GM-CSF, TNF-α and IL-10, were tested (Fig. 3.1C, D; 3.2A-J). According to our results, the secretion pattern of both cell types was very similar and comparable. Furthermore, a previous study showed that differentiated THP-1 cells behave more like native monocyte-derived

macrophages, compared to other human myeloid cell lines, such as HL-60, U937, KG-1, or HEL cell lines (Auwerx 1991). Thus, THP-1 cells seem to be a suitable cell line model for primary BDMs. Furthermore, both investigated cell types (THP-1 cells and BDMs) showed an increased secretion of pro-inflammatory cytokines in response to an infection with *L.p.*. This is not surprising, since the stimulation or the infection with *L.p.* triggers TLR signaling in macrophages leading to NF-κB activation and to active transcription of pro-inflammatory genes, such as CXCL8 (Massis and Zamboni 2011; Cunha and Zamboni 2014; Naujoks, Lippmann et al. 2017). Copenhaver and colleagues found that alveolar macrophages and neutrophils are the primary, intracellular reservoir for *L.p.* in mice and that these cell types are the major source of pro-inflammatory cytokines, such as TNF-α and IL-1β which contribute to the host immune response (Copenhaver, Casson et al. 2014). In this study, similar results were obtained using primary macrophages or THP-1 cells instead of alveolar macrophages. The secretion of TNF-α and IL-1β was significantly increased in *L.p.*-infected BDMs and THP-1 cells compared to non-infected control cells, which indicated the successful stimulation of the cells with *L.p.*. Thus, deep sequencing analysis of BDMs infected with *L.p.* at an MOI of 0.25 for 24 and 48 h was performed to identify differentially expressed.

### 4.1.2 Changes in the miRNA profile of human BDMs in response to infection

To date, miRNA studies have been performed for several other intracellular pathogens, such as *Mycobacteria tuberculosis*, *Salmonella typhimurium*, *Listeria monocytogenes*, and *Francisella tularensis* (Das, Garnica et al. 2016). For *Legionella*, the miRNA profile was only determined in murine macrophages via TaqMan Low Density Arrays (TLDA) where the expression of pre-selected miRNAs was determined (Jentho, Bodden et al. 2017). The present study describes for the first time the total miRNA regulation in human blood-derived macrophages (primary BDMs) in response to *L.p.*-infection. DESeq2 analysis of the sequencing data revealed 54 differentially expressed miRNAs in human BDMs infected with *L.p.* at an MOI of 0.25 for 24 and 48 h. The results showed a time dependent upregulation or downregulation of the miRNAs in response to infection with *L.p.* (Fig. 3.3A). Thus, miRNA regulation seems to be stronger after 48 h of infection. Studies investigating the miRNA response to other pathogens have also chosen longer infection time points (Schulte, Eulalio et al. 2011; Liu, Zhou et al. 2014). This was also confirmed by further experiments where the expression levels of selected miRNAs were tested via qPCR. The chosen miRNAs showed stronger or more frequently significant regulations at 48 h post infection. Exemplarily, the miRNAs miR-146a, miR-155, miR-27a and miR-125a were upregulated, while miR-221, miR-222, miR-125b, miR-26a and miR-29b were

downregulated in response to *L.p.*-infection in BDMs at 48 h post infection (Fig. 3.3B, D). miR-146a and miR-155 are well known miRNAs that are involved in inflammatory responses to pathogens (O'Connell, Taganov et al. 2007; Nahid, Satoh et al. 2011a; O'Connell, Rao et al. 2012). Other studies also described an upregulation of miR-146a and miR-155 in macrophages following infection with intracellular pathogens. For instance, miR-146a and miR-155 were upregulated in BCG-infected RAW264.7 macrophages (Li, Yue et al. 2013), in *Salmonella*-infected RAW264.7 macrophages (Schulte, Eulalio et al. 2011) and in *Listeria*-infected murine bone marrow derived macrophages (Schnitger, Machova et al. 2011b). This upregulation is not surprising, since TLR4-mediated sensing of bacterial lipopolysaccharide (LPS) and downstream NF-κB activity induces the expression of miR-146a and miR-155 and are known to accumulate following stimulation of macrophages with bacterial LPS (Taganov, Boldin et al. 2006; O'Connell, Taganov et al. 2007; Androulidaki, Iliopoulos et al. 2009; Ceppi, Pereira et al. 2009). Furthermore, upregulation of miR-125a was also observed in response to infection with *M. tuberculosis* and *L. monocytogenes* (Schnitger, Machova et al. 2011a; Kim, Yuk et al. 2015). Schnitger et al. found that miR-125a regulation was TLR2- and MyD88-dependent. Intriguingly, this MyD88-dependent upregulation of miR-125a-3p was also confirmed in murine BMMs infected with *L.p.* by another study (Jentho, Bodden et al. 2017). Thus, miR-125a regulation in this study may be due to TLR2 activation by *Legionella*-LPS and hints towards a mechanism that is conserved across species.

Furthermore, the miRNAs miR-3196 and miR-4284 were highly upregulated in *L.p.*-infected BDMs and showed only high abundances in infected BDMs. miR-3196 is a promising miRNA for further investigation, since this miRNA is implicated in the regulation of apoptosis in lung cancer cells via targeting the p53 upregulated modulator of apoptosis (PUMA) pathway (Xu, Zhang et al. 2016). Additionally, this miRNA has been found to be upregulated in different types of cancer (Sand, Skrygan et al. 2012; Pena-Chilet, Martinez et al. 2014; Gao, Zhou et al. 2016). Since it is known that *L.p.* secretes effector proteins to inhibit apoptosis, this miRNA may be upregulated by *Legionella* to prevent apoptosis of the host cell (Ge, Gong et al. 2012). Additionally, it has been demonstrated that downregulation of miR-4284 increased the phosphorylation and activity of the c-Jun N-terminal kinase (JNK)/stress-activated protein kinase (SAPK), resulting in an increased abundance of phosphorylated c-Jun and total c-Fos. Both are major components of the transcription factor AP-1 which plays an important role in regulation of apoptosis. Thus, the miR-4284 also seems to be a promising candidate for further investigations.

Highly downregulated miRNAs following infection with *L.p.* in BDMs were miR-1180 and miR-1228. It has been shown that miR-1180 is involved in the regulation of apoptosis and cell

proliferation. Thus, downregulation of miR-1180 is associated with different types of cancer, including bladder cancer (Wang, Chen et al. 2014) and pancreatic cancer (Gu, Zhang et al. 2017). Different studies claimed that overexpression of miR-1180 may exert anti-cancer effects (Ge, Wang et al. 2017). Downregulation of miR-1228 in A549 cells has been shown to be associated with cellular apoptosis through a mitochondria-dependent pathway. Another study found a reduction of miR-1228 expression in apoptotic cells. Induced miR-1228 expression attenuated the progression of cellular apoptosis via targeting MOAP1 signaling pathway. Furthermore, miR-1228 was shown to be upregulated in breast cancer cell lines and tissues and an increased expression provoked cell growth, invasion and migration. Since both described miRNA are involved in the regulation of apoptosis, they could have a role in *L.p.*-infections. Downregulation of miR-1228 could be a host response, since it is known that an infection with *L.p.* induces apoptosis (Mou and Leung 2018), whereas the reduced expression of miR-1180 could be actively achieved by *Legionella*, since *L.p.* can prevent host cell death to ensure multiplication within macrophages (Ge, Gong et al. 2012). Regulation of apoptosis by miRNAs could represent a battleground of host and pathogen during the course of infection. All four miRNAs have been described to be involved in regulating apoptosis and may be interesting candidates for further investigations, as their opposing functions might represent such a battleground of host and pathogen.

In this study, the expression of miR-146a, miR-155, miR-27a, miR-125a, miR-221, miR-221, miR-125b, miR-26a and miR-29b was investigated in *L.p.*-infected BDMs via qPCR and confirmed the sequencing results. Some of the validated miRNAs, including miR-146a, miR-155, miR-125b and miR-221, were chosen to be tested in THP-1 cells. Indeed, the selected miRNAs showed the same expression profile in BDMs as in THP-1 cells after *L.p.*-infection (Fig. 3.3C, E). Other studies also confirmed this observation, since they reported that miRNA regulation of several miRNAs, such as miR-146a/b, miR-132, miR-155, miR-214, miR-195a and miR-16, was comparable in THP-1 and primary cells (Qin 2012). Thus, the miRNA profile in THP-1 cells seems to be largely comparable to that of primary BDMs, as observed in the present study. Furthermore, the correlation in global gene expression between THP-1 cells and primary cells in response to LPS stimulation was investigated by Sharif and colleagues. They found that the LPS-induced transcriptional response in THP-1 cells is very similar to primary monocyte-derived macrophages. Compared to that, the LPS response in U937 cells was dramatically different to both, THP-1 and monocyte-derived macrophages, suggesting that THP-1 cells represent a better model system for investigating the mechanisms of LPS and NF-κB dependent gene expression in macrophages (Sharif, Bolshakov et al. 2007). Another study compared the transcriptional alterations between PMA-treated THP-1 cells and GM-CSF

treated monocytes via microarray (Kohro, Tanaka et al. 2004). They found 75 and 104 significantly changed genes in PMA-treated THP-1 cells and GM-CSF treated monocytes, respectively. The comparison between the two cell types revealed high similarity and only small differences in the transcriptome of PMA-differentiated THP-1 cells and primary macrophages. Nevertheless, Kohro et al. argued that the results of experiments done with THP-1 cells need to be carefully interpreted (Kohro, Tanaka et al. 2004). Furthermore, one study demonstrated that PMA-differentiated THP-1 cells contain elevated levels of MHC class I and class II mRNAs even in the absence of additional activating factors, which displays a critical, immunologically relevant macrophage function. This observation enhances the utility of PMA-differentiated THP-1 cells as a macrophage model for *in vitro* studies (Asseffa, Dickson et al. 1993). Taken together, under certain circumstances, the gene expression in THP-1 cells is comparable to that of primary cells, as observed in the present study for the miRNA regulation. Thus, THP-1 cells can be used as cell line model instead of BDMs when higher amounts of cells were necessary.

Overall, 54 different miRNAs were differentially expressed in BDMs upon *L.p.*-infection. Some of them were validated in BDMs as well as in THP-1 cells, representing the comparability between the cell line and the primary cells. Given that each miRNA may affect the expression of hundreds of genes (Selbach, Schwanhausser et al. 2008), further investigation of the 54 differentially expressed miRNAs can reveal interesting candidates that play an important role in *Legionella* infection in human macrophages.

### 4.1.3 miRNAs in macrophages are regulated on the transcriptional level in response to *Legionella*-infection

In order to understand the mechanism of miRNA regulation in response to *L.p.*-infection, the histone H4 acetylation of the promoter region of the four selected miRNAs (miR-146a, miR-155, miR-221 and miR-125b) was investigated (Fig. 3.4A). Acetylation of histones is one of the master regulators of gene expression in mammalian development and human disease (Egger, Liang et al. 2004) and can strongly impact inflammatory and host defence responses (Ribet and Cossart 2010). Acetylation is controlled by histone acetyltransferases (HATs) and histone deacetylases (HDACs) and often associated with active transcription by rendering chromosomal domains more accessible to the transcription machinery. Thus, it is plausible that the histone H4 acetylation grade of the miRNA-promoter regions correlated with the miRNA expression post infection (Fig. 4A-E). For instance, an open chromatin structure within the promoter region leads to transcription of the pri-miRNAs resulting in increased levels of

mature miRNAs by processing with Drosha and Dicer. Thus, the pri-miR expression of the selected miRNAs and the expression of Dicer and Drosha upon infection with *L.p.* for 24 and 48 h were investigated. The correlation of the pri-miR expression with the acetylation level of the promoter region following infection with *L.p.* in face of the unchanged expression of Dicer and Drosha, led to the conclusion that miRNAs are transcriptionally regulated in macrophages in response to a *Legionella*-infection. A transcriptional regulation of the promoter region of a miRNA has exemplarily been described for miR-127. This miRNA is also controlled by epigenetic alterations in its promoter region, including DNA methylation and active histone marks, as shown by inhibitors of HDACs and DNA methylation (Saito, Liang et al. 2006).

It has been shown that some bacteria alter the acetylation of histones and thereby change gene transcription. For instance, the infection of endothelial cells with *L. monocytogenes* led to an activation of p38 and ERK/MAPK pathways which was linked to an increased acetylation of histone H3 and H4 and led thereby to transcriptional activation of MAPK induced genes (Schmeck, Beermann et al. 2005). A study focusing on *Anaplasma phagocytophilum,* which is a tick-transmitted *Rickettsia* and an intracellular pathogen, demonstrated that an infection of macrophages led to silencing of host defence gene expression which was correlated with an increase in HDAC1 activity and a decrease in histone H3 acetylation on the promoters of defence genes (Garcia-Garcia, Barat et al. 2009).

*Legionella* can also influence the histone code of the host by secreting the effector RomA via T4SS, which localizes to the nucleus of the infected cell. There, it promotes a burst of H3K14 methylation and consequently decreases H3K14 acetylation, an activating histone mark, to repress gene expression. Thus, *L.p.* is actively modifying host histones to promote efficient intracellular replication (Rolando, Sanulli et al. 2013).

In summary, the acetylation levels of the miRNA promoters were altered in response to *L.p.* infection. Alterations of the acetylation levels can be caused by the host cell as response to the infection or histone acetylation on gene promoters can be actively manipulated by *Legionella*.

### 4.1.4 miRNAs can manipulate *Legionella* replication inside human macrophages

In the present study, miR-125b and miR-221 were significantly downregulated upon *L.p.*-infection in both, THP-1 cells and BDMs. It has been found that miR-125b, miR-221 and miR-579 are implicated in the process of endotoxin tolerance. These miRNAs were shown to be upregulated in tolerant macrophages to prevent the translation of TNF-α and therefore leading to a diminished immune response (El Gazzar and McCall 2010). This process required the disruption of protein synthesis and the TLR4-dependent induction of miR-221, miR-579,

and miR-125b. The miRNAs were coupled to RNA-binding proteins TTP, AUF1, and TIAR at the 3' untranslated region to arrest protein synthesis of TNF-α. TIAR was bound to miR-125b and miR-579, whereas miR-221 was linked to TTP and AUF1 proteins. They found that miR-221 led to TNF-α mRNA decay, while miR-125b and miR-579 mediated translational arrest. Thus, they found an implication of these miRNAs in diminishing the inflammatory response in macrophages (El Gazzar and McCall 2010). Based on these finding, the role of the three miRNAs during *L.p.* infection was investigated. In order to assess if manipulation of miR-125b, miR-221 and miR-579 provokes an influence on intracellular replication of *L.p.*, CFU-assays were performed upon overexpression or inhibition of the three miRNAs. Indeed, an overexpression of all three miRNAs caused an increased replication of *L.p.*, whereas a downregulation of all three miRNAs led to a decreased replication of *Legionella* (Fig. 3.5A-D). It is important to point out that a combination of all three miRNAs was necessary for this effect and an overexpression of each miRNA separately or pairwise did not alter *L.p.*-replication.

miR-125b is a highly conserved miRNA that has multiple targets, including proteins regulating apoptosis, innate immunity, inflammation, and differentiation (Chaudhuri, So et al. 2011; Le, Shyh-Chang et al. 2011; Surdziel, Cabanski et al. 2011). miR-125b targets 20 genes that are involved in apoptosis and proliferation including TP53, BAK1, CDC25C and CDKN2C, which are part of the p53 network, and is therefore implicated in the regulation of oncogenesis (Le, Shyh-Chang et al. 2011). Depending on the cellular context, miR-125b shows different patterns of regulation. For instance, in some tumor types, miR-125b is upregulated and displays oncogenic potential, while in other tumor entities, miR-125b is heavily downregulated and acting as tumor suppressor gene (Banzhaf-Strathmann and Edbauer 2014). Moreover, miR-125b has been found to be downregulated in macrophages upon TLR4 ligation (Tili, Michaille et al. 2007; Androulidaki, Iliopoulos et al. 2009; Murphy, Guyre et al. 2010), which is in accordance with the finding of this study. In contrast to that, one study reports that miR-125b promoted macrophage activation, IFN-γ response and immune function in macrophages (Chaudhuri, So et al. 2011): Overexpression of miR-125b led to reduced levels of IRF4, which is a negative regulator of pro-inflammatory pathways in macrophages. Thus, the study of Chaudhuri and colleagues argues against the observed replication effect in the present study, since an increased pro-inflammatory response seems not to be compatible with an increased *Legionella* replication within macrophages. Furthermore, Chaudhuri et al. claim that downregulation of miR-125b serves as natural mechanism to limit inflammatory response. However, it has been observed by El Gazzar and McCall that increased expression and not downregulation of miR-125b prevented an exaggerated inflammatory response. Furthermore, one study showed that miR-125b overexpression suppresses NO production in activated, murine macrophages via

targeting CCNA2 and eEF2K. This observation is in accordance with the present study, since NO production in macrophages is important for killing pathogens (MacMicking, Xie et al. 1997). An impact of miR-125b on bacterial replication has been described before by Liu and colleagues. They showed that an infection of macrophages with *Brucella abortus*, an intracellular pathogen, downregulated the expression of miR-125b, which is in line with the observation of the present study (Liu, Wang et al. 2016). Furthermore Liu et al. and others found that miR-125b targets A20, an inhibitor of NF-κB (Kim, Ramasamy et al. 2012; Haemmig, Baumgartner et al. 2014; Liu, Wang et al. 2016). The inhibition of A20 mediated by miR-125b led to decreased intracellular replication of *Brucella abortus* (Liu, Wang et al. 2016). This observation is in contrast to the finding of the present study where an enhanced miR-125b expression led to an increased replication of *L.p.* within macrophages. However, another study showed the reversed effect with an influence on viral replication. An inhibition of miR-125b expression resulted in decreased hepatitis B virus (HBV) replication in hepatoma cells (Deng, Zhang et al. 2017), which is in accordance with the present study, since a downregulation of all three miRNAs led to a decreased *L.p.*-replication. The variability of the results that were obtained from different research groups implicate that the role of miR-125b is highly dependent on the cell type and the pathogen used.

miR-221 und miR-222 belong to the same miRNA-family, share the same seed sequence and were both downregulated following *Legionella*-infection in the present study. They are encoded as a cluster located on chromosome X and have been reported to be overexpressed in many types of cancer (Sun, Yang et al. 2009). The oncogenic activity of miR-221 has been linked to the ability to regulate cell cycle progression by targeting CDKN1C/p57 and CDKN1B/p27 (Visone, Russo et al. 2007; Fornari, Gramantieri et al. 2008). The key cell cycle inhibitor, p27, influenced by miR-221, seems to be important during dendritic cell development and maturation of human monocytes (Lu, Huang et al. 2011). Moreover, it has been shown that miR-221 is important for the regulation of several cellular processes in human umbilical vascular endothelial cells (HUVECs). One study showed that miR-221/-222 overexpression decreased p38/NF-κB and ICAM-1 expression leading to less pro-inflammatory responses (Liu, Sung et al. 2017). Chen et al. found that miR-221 represses adiponectin receptor protein 1 (AdipoR1) expression in HUVECs and thereby inhibits NO production (Chen, Huang et al. 2015). If NO production and both p38- and NF-κB-signalling pathways are repressed by miR-221 in macrophages, the increased replication of *L.p.* within macrophages following overexpression of miR-221 could be partly explained. Furthermore, miR-221 and miR-222 inhibit endothelial cell migration, proliferation, and angiogenesis *in vitro* by targeting the stem cell factor receptor c-kit and indirectly regulating endothelial nitric oxide synthase

expression in endothelial cells (Urbich, Kuehbacher et al. 2008). Additionally, it has been shown that miR-221 expression was selectively decreased in LPS-treated macrophages as well as in the lungs of LPS-challenged mice (Zhao, Zhuang et al. 2016). Although the experiments were performed in mice, this observation is in line with the finding of the present study, where a downregulation of miR-221 in response to a *Legionella*-infection was observed. On the other hand, in the same study, Zhao et al. found that overexpression of miR-221 in macrophages significantly increases NF-κB and MAPK activation which was associated with the production of pro-inflammatory cytokines. These findings do not support the observations of the present study, since an increased pro-inflammatory response would not provoke an enhanced *Legionella*-replication in macrophages. Moreover, one study describing regulated miRNAs in porcine *Salmonella* infections showed a suppressed expression of miR-221, miR-125b and miR-27b in peripheral blood at 2 days after *Salmonella* inoculation and confirmed the miRNA-downregulation in response to an intracellular bacterium (Yao, Gao et al. 2016). The study showed that FOS is a direct target of miR-221 and miR-125b can suppress MAPK14. Thereby, the involvement of miR-125b and miR-221 in *Salmonella* infections in pigs was demonstrated and supports the replicative effect observed in the present study (Yao, Gao et al. 2016). The controversial findings about miR-221 underline again the importance of the experimental setup.

miR-579 is a poorly characterized miRNA. Besides its role during LPS tolerance in macrophages, it has been shown to act as master regulator of melanoma progression and drug resistance (Fattore, Mancini et al. 2016). However, an involvement in inflammatory responses to bacteria has not been described so far.

Taken together, the three miRNAs are involved in LPS tolerance and influence *Legionella* replication in macrophages. Many targets of miR-125b and miR-221 are described which regulate several different cellular processes, including cell cycle control and apoptosis. Despite that, the mechanism responsible for the altered replication of *Legionella* in macrophages upon miRNA manipulation observed in the present study needed to be determined.

### 4.1.5 MX1 is an indirect target of the miR-125b, miR-221, miR-579

Having shown that the manipulation of the expression of miR-125b, miR-221 and miR-579 can affect intracellular replication, the direct or indirect target responsible for this effect was to be determined next. A miRNA can regulate many of its targets at the transcriptional level without affecting mRNA abundance (Grosshans and Filipowicz 2008). For instance, Leivonen et al. found that only a minority (13%) of miR-193b targets showed a repression at mRNA level

according to microarray gene expression data (Leivonen, Rokka et al. 2011). Thus, proteomics methods are best suited for revealing the full spectrum of miRNA targets. In order to unravel the molecular mechanism responsible for the observed replication effect of *L.p.*, SILAC was performed. For this method, isotopically labeled amino acids (mostly arginine and lysine) are added to the THP-1 culture medium. Proteins of cells cultivated in medium containing either normal amino acids (light) or labeled amino acids (heavy) are quantified and analyzed by tandem MS. SILAC quantifies a great number of proteins and has the advantage of incorporating the labeled amino acids during cultivation and before preparation. This markedly reduces potential biases due to separate handling of the samples (Gruhler and Kratchmarova 2008). One limitation of this method is that it cannot be used for autotrophic organisms, tissue and body fluid samples (Elliott, Smith et al. 2009). However, it is applicable to cultured cells and can be used for THP-1 cells. Additionally, for this study, secreted proteins were not measured since supernatants were removed and cells were lysed before sample preparation. As already shown, SILAC was used for the identification of miRNA targets for several studies. For instance, Lössner et al. identified 46 putative targets of miR-155 in HEK293-T cells (Lossner, Meier et al. 2011). Chou et al. showed that ERF is a direct target of miR-27 in lung cancer cells by the successful application of SILAC for miRNA target identification (Chou, Lin et al. 2010). However, miRNA-mediated regulation of proteins with long half-lives may not be detected by measuring steady-state protein level, since proteins have different turnover times and miRNAs mostly cause slight decreases in protein translation. Thus, the proteome of different conditions and time points (not infected 24 h, infected with *L.p.* MOI 0.5 for 24 h, infected with *L.p.* MOI 0.5 for 48 h) was analyzed to identify protein expression changes mediated by the three miRNAs (miR-125b, miR-221, miR-579). MX1 protein was found to be downregulated following overexpression of all three miRNAs in all tested conditions (Fig. 3.5E). Since it was shown to be implicated in restricting viral replication, it was further investigated (Haller and Kochs 2011).

The human gene MX1 encodes a 78 kDa protein called MX1 or MxA (Aebi, Fah et al. 1989; Horisberger, McMaster et al. 1990) and belongs to and shares many properties of the dynamin superfamily of large GTPases (Haller, Gao et al. 2010). It consists of 3 domains, an N-terminal GTPase domain that binds and hydrolyses GTP, a middle domain mediating self-assembly, and a carboxy-terminal GTPase effector domain which is also involved in self-assembly, but additionally mediates viral target recognition (Haller and Kochs 2011). MX1 proteins appear to assemble into long filamentous structures at physiological salt concentration which are detectable by electron microscopy. In the presence of guanosine nucleotides the filaments rearrange into rings that tubulate negatively charged liposomes, and associate with the smooth ER (Accola, Huang et al. 2002; Kochs, Haener et al. 2002). At present, the role of

membrane binding for MX1 protein is still poorly understood. It may have some general function in intracellular protein transport and sorting (Haller, Staeheli et al. 2015).

MX1 downregulation following overexpression of all three miRNAs was validated via immunofluorescence with subsequent cytometric analysis (Fig. 3.6B, C). MX1 is induced predominantly by type I and II IFNs and its non-constitutive expression is tightly regulated by these IFNs (Holzinger, Jorns et al. 2007). Although it has been previously described that interferon-related genes, including MX1, are upregulated following transfection of 23-mer miRNA mimics - independently of their sequence - triggered by double-stranded RNA (Goldgraben, Russell et al. 2016), MX1 expression was reduced following overexpression of the miRNA pool in the present study. Compared with the nuclear rodent Mx1, human MX1 protein is located in the cytoplasm. Human MX1 protein exhibits about 70% amino acid sequence similarity to rodent Mx2 proteins, while it shares only 63% amino acid sequence similarity to human MX2 (Haller, Staeheli et al. 2015). Furthermore, human MX1 is more closely related to bovine, porcine, canine, feline, and bat Mx1 than to the human MX2 protein that in turn shares more sequence similarity to Mx2 proteins of these species (Haller, Staeheli et al. 2015). While it has been newly identified that human MX2 is a restriction factor for HIV-1 and other primate lentiviruses, human MX1 is able to inhibit a broad set of DNA and RNA viruses that replicate in the cytoplasm or in the nucleus, such as vesicular stomatitis virus (VSV) (Staeheli and Pavlovic 1991), human parainfluenza virus-3 (hPIV3) (Zhao, De et al. 1996), hepatitis B virus (HBV) (Yu, Wang et al. 2008; Li, Zhang et al. 2012), La Crosse virus (LACV) (Kochs, Janzen et al. 2002), Influenza A virus (IAV) (Xiao, Killip et al. 2013), African swine fever virus (ASFV) (Netherton, Simpson et al. 2009) and avian influenza A viruses (FLUAV) (Deeg, Mutz et al. 2013). The antiviral activities of human MX1 are mediated by the direct interaction with crucial viral components. For instance, the nucleocapisd of FLUAV and THOV consists of genomic RNA segments associated with viral nucleoprotein and RNA polymerase (vRNPs). The nuclear translocation of these vRNPs is blocked by MX1 which leads to the inhibition of transcription and replication of the virus genomes. Thus, MX1 interferes with synthesis and/or nuclear import of newly synthesized viral components (Kochs and Haller 1999). Furthermore, it is known that VSV replicates in the cytoplasm. There, MX1 inhibits primary transcription of incoming viral nucleocapsids (Staeheli and Pavlovic 1991). In the case of Bunyaviruses, such as LACV, MX1 sequesters viral N protein into perinuclear complexes. The viral N protein is crucially needed for viral genome replication by the viral polymerase and synthesized in the early viral transcription. Thus MX1 blocks the viral replication (Reichelt, Stertz et al. 2004).

Based on these findings, it was tested if knockdown of MX1 interferes with *Legionella* replication. Indeed, a knockdown of MX1 in THP-1 cells and BDMs, validated by Western Blot,

lead to an enhanced intracellular replication (Fig. 3.7A-F). It is known that *L.p.* manipulates various key host regulatory pathways in order to establish a LCV. The LCV is decorated with many bacterial and host factors to prevent bacterial degradation and enable intracellular replication. Proteomics screens identified that several small and large GTPases are associated with the LCV. It was demonstrated that these GTPases are functionally involved in the LCV formation as well as in the replication process (Hilbi, Rothmeier et al. 2014; Hilbi and Kortholt 2017). The ER membrane is associated with many large GTPases that mediate membrane fusion and remodel the shape of the entire ER (Hu and Rapoport 2016). Since MX1 belongs to the dynamin superfamily of large GTPases, it seems likely that it also influences *Legionella* replication. For instance, it has been observed that the large GTPase dynamin-related protein 1 (Drp1 or Dnm1l) is involved in *Legionella* replication (Arasaki, Mikami et al. 2017). Together with syntaxin 17, Drp1 regulates mitochondrial dynamics and autophagy. The secreted effector protein Lpg1137 binds and cleaves syntaxin 17 during intracellular replication leading to an altered activity of the large GTPase Drp1 and changed *Legionella* replication. Thus, modulation of ER by hijacking, either directly or indirectly, large GTPases can impact *Legionella* replication (Arasaki, Mikami et al. 2017).

In contrast to this hypothesis, MX1 cannot be found in the proteome of LCVs within human macrophages as shown by Bruckert and Kwaik (Bruckert and Abu Kwaik 2015). Bruckert and Kwaik infected U937 macrophages with *L.p.* strain AA100/130b which is a different cell line and bacterial strain as used in this study. As discussed before, it has been shown that the LPS response in U937 cells was dramatically different to both THP-1 and blood-derived macrophages. Therefore, their response to a *Legionella*-infection could also differ compared to THP-1 cells and BDMs. Furthermore, it is possible that MX1 mediates its effects on *Legionella* replication without being associated to the LCV. One possibility could be that MX1 binds liposomes which are important for LCV formation leading to the diminished replication. Its ability to restrict *Legionella* replication could also be mediated by trap of ER tubules which normally promote the organelle remodeling and LCV formation.

Overall, MX1 protein expression was downregulated following overexpression of all three miRNAs (miR-125b, miR-221, miR-579). SiRNA-mediated knockdown of MX1 protein led to an increased intracellular replication of *L.p.*, as observed following overexpression of the three miRNAs. Thus, MX1 protein expression is influenced by the three miRNAs. Since it possesses no binding sites for the three miRNAs in its 3'UTR, MX1 seems to be indirectly targeted. In order to determine the targets of the miRNAs that influence MX1 protein expression, Ingenuity pathway analysis (IPA) was performed and revealed possible targets (DDX58 and TP53) (Fig. 3.8), which were tested via luciferase assay.

### 4.1.6 DDX58 as target of miR-221 with impact on replication

Luciferase reporter assays revealed the binding of miR-221 to the 3'UTR of DDX58, as predicted by computational analysis (IPA) (Fig. 3.9C). An interaction and co-expression (i.e. controlled by the same transcriptional regulatory program, functionally related, or members of the same pathway or protein complex) of MX1 and DDX58 was also suggested by the String Database (Szklarczyk, Morris et al. 2017) and additionally confirmed by the DDX58 knockdown experiments with subsequent staining and cytometric analysis of intracellular MX1 protein performed in the present study (Fig. 3.9D). Furthermore, the targeting of DDX58 by miR-221 seems to be specific, as mutation of the seed region abrogated the reduction of the relative luminescence activity. For miR-579, a reduction of the relative luminescence activity was detected, but targeting does not seem to be specific as indicated by luciferase assay, where the seed region for miR-579 was mutated. Thus, this study describes for the first time the direct targeting of DDX58 by miR-221. It has been only reported that miR-545 (Song, Ji et al. 2014; Liu, Dou et al. 2016), miR-34a (Wang, Zhang et al. 2016) and miR-485 (Ingle, Kumar et al. 2015) target DDX58 and thereby influence viral replication or apoptosis in cancer cells.

The gene DDX58 encodes the cytosolic RIG-I-like receptor (RLR) RIG-I. RLRs, including MDA5 and RIG-I, recognize cytosolic double-stranded RNA or single-stranded RNA containing 5'-triphosphate (5'-ppp). An activation of RIG-I or MDA5 activates MAVS to trigger a large-scale amplification of a signaling cascade. This cascade involves the recruitment of cytosolic adaptor molecules, followed by the activation of the canonical IKKs, the MAPK and the non-canonical IKK-related kinase. Ultimately, specific transcription factors, such as IRF3 and NF-κB are activated and translocated to the nucleus. Within the nucleus, expression of type I IFN-dependent genes and pro-inflammatory cytokines are induced (Vabret and Blander 2013). It has been demonstrated by several groups that type I IFNs restrict *Legionella* replication in macrophages and epithelial-like cell lines (Schiavoni, Mauri et al. 2004; Opitz, Vinzing et al. 2006; Stetson and Medzhitov 2006). Opitz and colleagues claimed that the translocation of IRF3 and NF-κB-p65 to the nucleus to induce type I IFN genes requires the IFN-β promoter stimulator 1 (IPS-1, also known as MAVS), but not RIG-I or MDA5. However, they used epithelial cells and not macrophages, but the type I IFN response accounted for bacterial growth restriction. An addition of exogenous type I IFN to macrophages inhibited the replication of *L.p.* in non-permissive macrophages (Schiavoni, Mauri et al. 2004; Plumlee, Lee et al. 2009).

Although RIG-I and MDA5 were initially reported as sensors of viral infection, it has been shown that *Legionella* also activates the RIG-I/MDA5 pathway. Furthermore, the RIG-I pathway was required for the response to *L.p.*-RNA, but not to *L.p.*-DNA. Thus, the authors suggested

that *L.p.*-RNA is released to the cytosol of host cells and triggers the RIG-I/MDA5 pathway (Monroe, McWhirter et al. 2009). An active translocation of bacterial RNA to the cytoplasm has also been described for other bacteria, such as *L. monocytogenes and H. pylori* (Rad, Ballhorn et al. 2009). In both cases, the release of bacterial RNA led to the activation of RIG-I (Rad, Ballhorn et al. 2009; Abdullah, Schlee et al. 2012; Hagmann, Herzner et al. 2013).

On the other hand, *L.p.*-DNA secreted into the host cytosol via the T4SS also stimulated the induction of type I IFN genes. Double-stranded DNA of *L.p.* was reported to be converted to intermediary double-stranded RNA via the DNA-dependent RNA-polymerase (Pol-III) which leads to the activation of the RIG-I/MDA5 pathway (Stetson and Medzhitov 2006; Chiu, Macmillan et al. 2009). This observation was confirmed by inhibition of Pol-III which leads to abrogation of IFN-β induction by *L.p.* and promotes bacterial growth (Chiu, Macmillan et al. 2009). Additionally, *in vitro* resistance to an infection with *L.p.* in macrophages is dependent on STING- and IRF3-mediated production of type I IFNs. An upregulation of type I IFN genes suppressed replicating and non-replicating *L.p.* within their LCVs, and protected against *Legionella* lung infections *in vivo* (Lippmann, Muller et al. 2011). Furthermore, RNA Pol-III, which transcribes foreign cytosolic DNA into the RIG-I ligand 5'-triphosphate RNA, seems to be involved in the restriction of *S. flexeneri* infection. Thus, RIG-I is able to sense DNA and RNA. Furthermore, it has been shown, that *Legionella* secretes a bacterial protein, SdhA, which suppresses the RIG-I/MDA5 pathway (Monroe, McWhirter et al. 2009) suggesting the importance of this pathway to influence *Legionella* replication.

All described observations hint to a role of this pathway in *Legionella* infections. A knockdown of RIG-I mediated by siRNA (Fig. 3.10A, B) increased the replication of *Legionella* in BDMs and THP-1 cells (Fig. 3.10C, D). It is possible that both, the direct inhibition of RIG-I as well as the inhibited activation of MX1 by RIG-I, are contributing to the replication effect observed in this study.

### 4.1.7 TP53 as target of miR-125b with impact on replication

Ingenuity pathway analysis showed that TP53 is a direct target of miR-125b, which was already demonstrated by others (Le, Teh et al. 2009; Qin, Zhao et al. 2014; Ahuja, Goyal et al. 2016). In this study, the direct binding of miR-125b to the 3'UTR of TP53 was also validated by the mutation of the binding sites via luciferase assay (Fig. 3.11C).

TP53 or p53 is a master regulator of the cellular mechanisms controlling responses to cellular stress such as DNA damage, aberrant oncogene activation, loss of normal cell-cell contacts, nutrient deprivation, and abnormal reactive oxygen species (ROS) production. Cellular stress

provokes an activation of TP53. TP53 acts as a transcriptional regulator, which controls the expression of effector proteins and miRNAs, leading to the regulation of apoptosis, cellular proliferation, and autophagy (Sullivan, Galbraith et al. 2018). Thus, inactivation of TP53 is a hallmark of cancer development. The TP53 gene is the most frequently mutated gene in human cancer, highlighting the crucial role of this gene in regulating cellular proliferation and apoptosis (Kandoth, McLellan et al. 2013; Soussi and Wiman 2015). Since regulation of the cellular stress response is tightly connected with metabolic regulation, p53 is also involved in the cellular energy metabolism and the redox balance regulating glycolysis. It dampens glycolysis and promotes oxidative phosphorylation (Itahana and Itahana 2018).

Furthermore, p53 also seems to be important in viral infections. Mice deficient in p53 are more permissive to viral infection (Munoz-Fontela, Garcia et al. 2005). It is induced in response to viral infections as a downstream transcriptional target of type I IFN signaling (Takaoka, Hayakawa et al. 2003). Furthermore, p53 is also activated indirectly by type I IFN through other IFN-inducible proteins, such as promyelocytic leukemia protein (PML), STAT1, or IFIXα-1 (Townsend, Scarabelli et al. 2004; Ding, Lee et al. 2006; Pampin, Simonin et al. 2006). In addition, one study showed the association between TP53 and MX1 in IFN signaling. An increased expression of p53 was accompanied by enhanced expression of MX1, as well as RIG-I and IRF7 which strengthens its implication in the type I IFN signaling (Munoz-Fontela, Macip et al. 2008).

Many viruses, including SV40, Influenza A virus, human papillomavirus, Kaposi's sarcoma herpesvirus, adenoviruses, and even RNA viruses such as polioviruses, have evolved mechanisms to affect p53 expression and abrogate p53-dependent responses to enable viral replication. Furthermore, it was shown that the interferon-stimulated gene ISG15 is induced by p53 and that p53 is required for optimal gene induction by double-stranded RNA (dsRNA) (Hummer, Li et al. 2001). For instance, the small DNA tumor polyomavirus SV40 binds p53 and inhibits p53-dependent transcription, resulting in accumulation of inactivated p53 protein and cellular transformation (Bargonetti, Reynisdottir et al. 1992; Jiang, Srinivasan et al. 1993). Thus, p53 inhibition is beneficial for viral replication.

Since *L.p.* also activates a type I IFN response, the influence of TP53 knockdown on intracellular replication was tested. Indeed, the knockdown of TP53 (Fig. 3.12A) led to an increased replication of *Legionella*(Fig. 3.12B).

Several studies showed that TP53 has a role in controlling bacterial infection and that inhibition of p53 may confer certain selective advantages to bacteria (Zaika, Wei et al. 2015). The first described bacterium, which inhibits p53 and induces its degradation, is *H. pylori*. This gram-negative bacterium is strongly linked to gastric cancer. It is estimated that in the absence

of *H. pylori*, 75% of gastric cancers would not occur. Typically, infections with *H. pylori* induce cellular stress because the bacteria induce DNA damage and disturb normal cellular homeostasis leading to p53 activation (Baik, Youn et al. 1996; Toller, Neelsen et al. 2011). However, *H. pylori* dampens the activity of p53 protein by inducing its degradation (Wei, Nagy et al. 2010; Buti, Spooner et al. 2011). Additionally, *H. pylori* alters the expression profile of p53 isoforms to change the cellular stress response (Wei, Noto et al. 2012). An inhibition of p53 activity was also observed for infection with *Mycoplasma* bacteria (Logunov, Scheblyakov et al. 2008). Furthermore, it was shown that *Chlamydia trachomatis* (*C. trachomatis*) also induces degradation of p53. The downregulation of p53 provide the bacteria with necessary metabolites and protects against oxidative stress (Siegl, Prusty et al. 2014). As *Chlamydiae*, *Legionella* are intracellular bacteria, which strictly rely on host resources. Since metabolic control of p53 provides antibacterial protection, inhibition of p53 seems to be important for bacterial survival and growth, as seen in this study.

In the present study, the knockdown of TP53 by an siRNA-pool was not successful in THP-1 cells. Several studies argue that TP53 is not expressed or not functional in THP-1 cells (Traore, Trush et al. 2005). One study claimed that p53 mRNA from THP-1, U937, and UT-7 had partial deletions of 26, 46, and 136 bases, respectively (Sugimoto, Toyoshima et al. 1992). Furthermore, Akashi and colleagues showed that THP-1 cells and U937 do not express p53 mRNA. Also treatment of THP-1 cells with PMA showed no induction. However, they stimulated the cells only for 4 h with different concentrations of PMA (0.2, 2 or 20 nM) (Akashi, Osawa et al. 1999). In the present study, THP-1 cells were stimulated for at least 24 h with 20 nM PMA, which may induce differences in the expression profile. Furthermore, THP-1 cells used in the present study were expressing p53 mRNA, which was proven via qPCR. The sequencing data, performed in this study supporting the observation that the used THP-1 cells express p53 mRNA. Furthermore, the data of the human protein atlas also indicating an expression of p53 in THP-1 cells, with a Transcripts per Kilobase Million (TPM) of 4.9. The RNA-Sequencing data of the human protein atlas (HPA) project can give detailed information about a specific cell line and a TPM value of 1.0 is defined as a threshold for expression of the corresponding protein.(www.proteinatlas.org ; Uhlen, Fagerberg et al. 2015). Other studies also showed an expression of p53 on mRNA and even on protein level in THP-1 cells after diverse treatments (de Kreutzenberg, Ceolotto et al. 2010; Suzuki, Sasaki et al. 2010; Chen, Lin et al. 2011). Furthermore, Khatri et al showed that p53 mRNA level was also induced when PMA-differentiated THP-1 cells were treated with nanoparticles (Khatri, Bello et al. 2013), arguing again for an inducible expression of p53 in THP-1 cells.

In contrast to the progenitor cell populations, the non-proliferating, mature cell populations, identified by CD20 (B-lymphocytes), CD3 (T-lymphocytes), CD15 (granulocytes), and CD 14 (monocytes), express low, but detectable levels of p53. The expression of p53 in CD14-positive monocytes was examined via flow cytometric analysis (Kastan, Radin et al. 1991). Additionally, they showed that the expression of p53 can be induced upon cell differentiation. This was confirmed by the present study, since differentiated BDMs expressed p53 on mRNA and protein level. A study showed that ML-1 cells, a myeloid, leukemia cell line, such as THP-1 cells, were stimulated with PMA leading to increased protein levels of p53, differentiation into macrophages and cell replication stop. Thus, this study hints also towards a stable induction of p53 protein following PMA stimulation. Therefore, the p53 protein expression of the THP-1 cells, used in the present study, was analysed. Indeed, p53 is expressed in THP-1 cells as shown by the Western Blot (supplement 1B). Additionally, PMA stimulation lead to an induced expression of p53 protein and was reduced by an infection with *Legionella*. Furthermore, a partial knockdown of p53 by the siRNA pool was achieved as indicated by the western Blot (reduction to 80%) (supplement 1C). This change of p53 protein was not significant and there was no difference in mRNA level detectable. Thus, further experiments are important to make a conclusion about the influence of p53 on *L.p.*-replication in THP-1 cells.
However, the results of the present study, performed in BDMs, indicate a role of p53 in *Legionella* replication, which was also shown for other bacteria.

### 4.1.8 LGALS8 as target for miR-579 with impact on replication

Ingenuity pathway analysis revealed only two putative targets for miR-579 that might be involved in MX1 regulation: DDX58 and IFNA2. IFNA2 was expressed at low levels in THP-1 cells, thus it is not considered to be the primary target of miR-579 that leads to the regulation of bacterial replication. Binding of miR-579 to the 3'UTR of DDX58 was demonstrated, but the mutation of the seed region did not reverse the reduction. Thus, direct binding of miR-579 was unlikely. Another target of miR-579 appears to be important for the replication effect, since all three miRNAs were necessary for the effect on *Legionella* replication. LGALS8 was detected by SILAC to be downregulated following overexpression of all three miRNAs (Fig. 3.5E). Furthermore, LGALS8 expression was significantly reduced following miR-579 overexpression and its 3'UTR possesses two binding sites for miR-579 (Fig. 3.13A, B). Thus, luciferase assays were performed to confirm the binding of miR-579 to the 3'UTR. Indeed, a binding of miR-579 was validated. A mutation of the seed region led to a slight restoration of relative luciferase activity indicating a reduction of miR-579 binding to the 3'UTR (Fig. 3.13C). In order to

completely prevent the binding of miR-579, a deletion of the whole miRNA binding site may be useful. Nevertheless, binding of miR-579 was confirmed and mutation of the seed region led to a significant increase in relative luciferase activity. A miRNA regulation of LGALS8 has not been described before. Thus, this study describes for the first time a targeting of LGALS8 by miR-579.

The gene LGALS8 encodes the protein galectin-8 which belongs to the galectin family. Galectins are glycan-binding, evolutionary conserved proteins and have pleiotropic roles in innate and adaptive immune responses (Yang, Rabinovich et al. 2008; Rabinovich and Toscano 2009). For the binding to carbohydrates, galectins contain one or more carbohydrate-recognition domains (CRDs) (Yang, Rabinovich et al. 2008). Galectins are localized in the intracellular compartment and in the cell nuclei. Moreover, several galectins are secreted by cells through an unusual route that requires intact carbohydrate-binding activity of the secreted protein, where they bind glycans to modulate cellular behavior (Yang, Rabinovich et al. 2008). Within the cytosol, galectins prevent the formation of complex carbohydrates. Thus, they function as a kind of danger and pattern-recognition receptor. For instance, galectin-3 accumulates on damaged bacteria-containing vesicles (Paz, Sachse et al. 2010). Galectin-3 as marker for vacuole integrity was used for different intracellular pathogens, such as *S. enterica* serovar Typhimurium, *Shigella flexneri*, and *Trypanosoma cruzi* (Paz, Sachse et al. 2010; Machado, Cruz et al. 2014). It was shown that the cytosolic lectin, galectin-8, also localizes to damaged vesicles and restricts *Salmonella* replication in HeLa cells (Thurston, Wandel et al. 2012). In addition, the data of Thurston et al. are in line with the results of the present study, since an siRNA-mediated knockdown (Fig. 3.14A, B) of galectin-8 led to an increased replication of *Legionella* (Fig. 3.14C, D). Furthermore, Thurston and colleagues demonstrated that galectin-8 monitors endosomal and lysosomal integrity and detects bacterial invasion by binding host glycans exposed on damaged *Salmonella*-containing vacuoles. Additionally, they showed that galectin-8 activates antibacterial autophagy by recruiting the adaptor NDP52, a xenophagy-specific receptor. Since galectin-8 also detected sterile damage to endosomes or lysosomes they claimed that galectin-8 serves as a versatile receptor for vesicle-damaging pathogens. Thus, galectin-8 seems to be a danger receptor to combat infection by monitoring endosomal and lysosomal integrity and the absence of galectin-8 could explain the enhanced replication of *Legionella* (Thurston, Wandel et al. 2012). An association of galectin-8 within the LCV of infected human macrophages at 6 h post infection was already validated, hinting towards the role as danger receptor (Truchan, Christman et al. 2017).

Overall, galectin-8 was validated as a target of miR-579. Furthermore, the role of galectin-8 as danger receptor to restrict the replication of intracellular bacteria was confirmed, since a knockdown of galectin-8 enhanced intracellular replication of *Legionella*.

### 4.1.9 Proposed model

In order to summarize the major findings of this study, a schematic model is displayed in Fig. 4.1. The results indicate that changes of miRNA expression influence bacterial replication, since overexpression of the miRNA-pool (miR-125b, miR-221 and miR-579) led to an increased *Legionella* replication. Moreover, miR-125b binds to the 3'UTR of TP53 and reduces its expression, while miR-221 targets DDX58 (RIG-I). Thereby, both miRNAs downregulate their targets, which co-occurs with downregulation of MX1 and altered *Legionella* replication. In addition to its known antiviral activities, MX1 possesses an antibacterial effect on *Legionella*. Furhtermore, miR-579 affects LGALS8 by reducing its expression which also influences *Legionella* replication. Thus, both, MX1 and LGALS8, are responsible for the restriction of *L.p.*-replication within human macrophages.

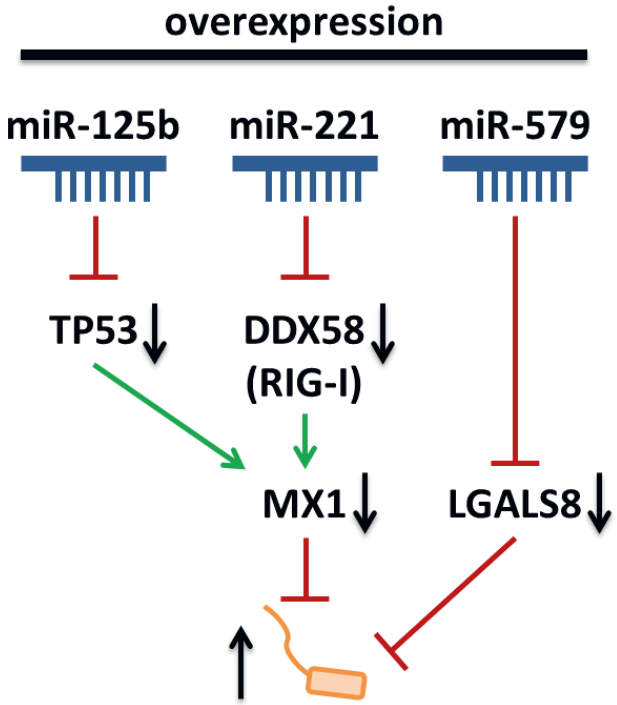


**Figure 4.1: Scheme of MX1 and LGALS8 regulation by overexpressed miRNAs to influence *L.p.* replication in macrophages.** Overexpressed miRNA-125b reduces the expression of TP53, while DDX58 (RIG-I) is targeted by miRNA-221. Both targets further regulate the protein expression of MX1, which possesses an antibacterial effect on *Legionella*. Furthermore, miRNA-579 further acts on LGALS8 to reduce its expression. Thus, reduction of MX1 and LGALS8 expression lead to an increased replication of *Legionella* in macrophages. In conclusion, these miRNAs are influencing the expression of their targets and have an impact on *Legionella*-replication.

## 4.2 Identification of the gene expression profile during the course of *Legionella* infection in human macrophages by dual RNA-Seq

In order to understand host-pathogen interactions, it is crucial to detect gene expression changes in both, the pathogen and the host. Since bacterial transcripts differ dramatically from eukaryotic transcripts in terms of quantity and composition of their RNA (Westermann, Gorski et al. 2012), it is necessary to separate the transcriptomes. Usually, probe-dependent approaches require the pathogen and host cells to be physically separated before gene expression analysis. For instance, in order to analyse bacterial gene expression during infection via microarray or sequencing, the dominating host material has to be depleted prior to analysis (Westermann, Barquist et al. 2017). Therefore, the majority of host-pathogen studies have focused on either the pathogen or the host at a given time post infection. The studies were limited in understanding the interaction between host and pathogen during the course of infection (Westermann, Gorski et al. 2012). To overcome this limitation, RNA-Seq is a helpful technique to analyze the transcriptome of both in parallel. Thus, the dual RNA-Seq method had been established in the lab of Prof. Jörg Vogel in Würzburg and applied for the first time for *Salmonella* infection of human epithelial cells (Westermann, Forstner et al. 2016).

A challenging technical issue to overcome is the minute fraction of bacterial transcripts in a mixed RNA pool. Typically, a single mammalian cell contains 20 pg of total RNA, which is approximately 100 to 200 times more than a bacterial cell with ~0.1 pg RNA (Alberts 2002). Thus, assuming an infected host cell is associated with ten bacteria, the relative difference in total RNA content is still ~10 to 20-fold (Westermann, Gorski et al. 2012). Since the bacterial RNA pool consists predominantly of rRNA and only ~5% account for mRNAs and sRNAs, the number of bacterial transcripts is further limited. Therefore, different methods are used to enrich for bacterial transcripts: by sequencing cDNA libraries to high depth (Humphrys, Creasy et al. 2013), partially enriching bacterial transcripts prior to sequencing (Humphrys, Creasy et al. 2013; Mavromatis, Bokil et al. 2015), by enriching for invaded host cells by FACS (Avraham, Haseley et al. 2015; Westermann, Forstner et al. 2016) or laser capture microdissection (Vannucci, Foster et al. 2013), by depleting rRNA of the bacterium and host either in series or in parallel (Humphrys, Creasy et al. 2013; Baddal, Muzzi et al. 2015; Mavromatis, Bokil et al. 2015; Rienksma, Suarez-Diez et al. 2015; Avraham, Haseley et al. 2016; Westermann, Forstner et al. 2016) or by combinations of different methods.

To date, dual RNA-Seq was performed for the following bacteria: *Chlamydia trachomatis* serovar E (Humphrys, Creasy et al. 2013), *Lawsonia intracellularis* (Vannucci, Foster et al. 2013), uropathogenic *Escherichia coli* (UPEC) (Mavromatis, Bokil et al. 2015), *Mycobacterium bovis* Bacillus Calmette-Guérin (Rienksma, Suarez-Diez et al. 2015), nontypeable *Haemophilus*

*influenza* (Baddal, Muzzi et al. 2015), *Salmonella Typhimurium* (Avraham, Haseley et al. 2015; Westermann, Forstner et al. 2016) and *Streptococcus pneumoniae* (Aprianto, Slager et al. 2016).

In this study, the dual RNA-Seq method was adapted and applied for the first time to *Legionella* infection of human macrophages. Invaded host cells were separated from non-infected bystander cells by FACS, and rRNA of *L.p.* and the macrophages was depleted to facilitate accurate quantification of bacterial gene expression.

The full coverage of protein-coding and non-coding RNA from human macrophages (mRNA, miRNA, lncRNA, circRNA) and *L.p.* (mRNA, sRNA) during infection by a dual RNA-Seq approach was determined.

### 4.2.1 Adaption of the dual RNA-Seq procedure to detect the transcriptional profile of *L.p.* and THP-1 cells during the course of infection

One of the most important preparative steps was the adaptation and optimization of the infection protocol for the dual RNA-Seq procedure. Therefore, inflammatory response, cytotoxicity, infection rate and sort purity were tested (Fig. 3.15 and Fig. 3.16). Based on these findings, the dual RNA-Seq procedure in this study was performed in PMA-differentiated THP-1 cells, which were first infected with GFP-*L.p*. Corby at an MOI of 10 for 2 h. Infection was performed for a total of 8 h and 16 h.

The GFP-expressing strain was used for infection of macrophages to separate invaded cells from non-invaded-bystander-cells and the responsiveness of THP-1 cells infected with the GFP-strain was compared to that of cells infected with the wildtype strain by controlling CXCL8 and miRNA-146a expression. Both strains triggered a comparable inflammatory response in THP-1 cells (Fig. 3.15E, F). Variations in log2-fold changes can be explained by different realised MOIs, since the real MOI can differ from the expected MOI.

To separate extracellular pathogen recognition from *L.p.*-specific effects, THP-1 cells were stimulated with the TLR2 agonist Pam3CSK4 (Pam3). For stimulation, a concentration of 100 ng/mL was used for the sequencing approach, since it was the lowest concentration yielding a significantly increased CXCL8 expression for both time points (8 and 16 h). Pam3CSK4 is a synthetic tripalmitoylated lipopeptide that mimics the acylated amino terminus of bacterial lipoproteins. Bacterial lipoproteins are cell wall components of both gram-negative and gram-positive bacteria. The stimulatory activity of bacterial lipoproteins resides in their acylated amino terminus. Pam3CysSerLys4 (Pam3CSK4) is recognized by TLR2 which cooperates with TLR1 through their cytoplasmic domain, leading to the activation of the pro-

inflammatory transcription factor NF-kB (Aliprantis, Yang et al. 1999; Ozinsky, Underhill et al. 2000). An infection of macrophages with *L.p.* triggers the activation of many different PRRs (Massis and Zamboni 2011; Cunha and Zamboni 2014; Naujoks, Lippmann et al. 2017). Lipopeptides and lipoproteins of *L.p.* activate TLR2. TLR2-signalling is critical for the outcome of *L.p.* infections in mice (Hawn, Smith et al. 2006). Furthermore, the LPS of *Legionella* is mainly recognized by TLR2 (Akamine, Higa et al. 2005; Shim, Kim et al. 2009). Therefore, Pam3CSK4 as TLR2 agonist can serve as a positive control for extracellular activation of macrophages, which should induce an inflammatory response due to NF-kB activation.

For synchronisation of the infection cycle, cells were centrifuged for 10 minutes at 500 x g directly after administration of bacteria. After 2 h, cells were washed 3 times with PBS to remove all extracellular, not internalized bacteria. Gentamicin was added to the medium for further cultivation to prevent reinfection. Gentamicin is a bactericidal antibiotic, which interrupts protein synthesis of the bacteria by irreversibly binding the 30S subunit of the bacterial ribosome (Hahn 1969). Reinfection was successfully prevented since no increase of the infection rate was observed in the flow cytometric analyses at 8 and 16 h post infection (Fig. 3.116B).

The 8 h time point was chosen, since infected host cells showed a peak in CXCL8 expression at that time point (Fig. 3.15C). The time points were chosen to characterize the infection process within the host cells and different growth stages of *Legionella* during the course of infection. *L.p.* exhibits a biphasic life-cycle and expresses different virulence factors during the course of infection and while it switches between an infectious, non-replicating form and an intracellular, replicative form (Rowbotham 1986; Byrne and Swanson 1998; Molofsky and Swanson 2004). In this study, *L.p.* of three different time points were sampled: (1) *L.p.* from the inoculum solution which resembles the highly virulent, transmissive form, (2) replicating *L.p.* inside the host cell from the 8 h time point, which represents the avirulent, non-motile and replicative form, and (3) *L.p.* inside the host cell from the 16 h time point, which should present the transition of the replicaitve form into the flagellated, transmissive form. *L.p.* differentiates into this form, when nutrients and living space become scarce. Since the vacuoles within the host cells at the 16 h time point are packed with a high amount of *L.p.*, it is likely that the bacteria within the macrophages are promoting the transmission to a new host cell at this stage. Thus, different growth stages of *L.p.* were expected at the chosen time points to shed light on the expression pattern of genes, relevant for the infection process within macrophages.

The replication of *L.p.* over the two time points (8 and 16 h) can be ascertained by the increased fluorescence intensity over time detected, while the infection rate (amount of gfp+

events) is not increasing (Fig. 3.16B). Furthermore, the verification of the applied sort strategy, where a part of each sorted cell fraction was lysed and plated on BCYE-agar plates to quantify bacterial growth, indicated a 10-fold increase of CFU/ml comparing the 8 h with the 16 h time point (Fig. 3.16C). This represents again the replication of *L.p.* within the host cells over time.

During the FACS process, different external factors associated with cell sorting such as flow rate, pressure, and droplet charge, can cause modulations in cellular physiology including RNA transcript levels. Sorted cells can experience physiologic stress and even a decrease in viability which can lead to altered RNA expression patterns or to potential RNA degradation (Arbibe, Kim et al. 2007). Therefore, it is important to reduce cellular activation or perturbation during the FACS procedure for accurate RNA analyses (Nishimoto, Newkirk et al. 2007). Deviating from the provided protocol of Alexander Westermann, cells were not fixed in RNAlater prior sorting. Zaiton and colleagues found that RNAlater treatment reduces GFP and YFP fluorescence, making separation of fluorescent (infected with *L.p.*) and non-fluorescent cells (non-infected bystander cells) difficult or impossible. They found that the pH of RNAlater is 5.6 (Zaitoun, Erickson et al. 2010). It has been reported that GFP and its variants is pH dependent (Saeed and Ashraf 2009). Since 80% of GFP fluorescence is lost at pH 6.5 and lower, RNAlater might have a quenching effect on GFP and YFP fluorescence of *L.p.*.

In order to minimize cellular perturbation or downstream physiologic responses, cells were sorted at 4°C into RNAprotect™ solution to recover high quality RNA from cells separated by FACS. According to manufacturer's protocol, this reagent provides immediate stabilization of RNA in sorted or cultured cells. Cells are stabilized at room temperature and can be stored or transported at ambient temperature prior to RNA purification. A comparable approach to characterize host microbe interaction was chosen by Nishimoto and colleagues. They recommended to sort cells, isolated by FACS, into RNAlater solution to minimize RNA degradation and perturbation of mRNA expression or downstream physiologic responses in the presence of a foreign pathogen or microbe, since host cells can respond very quickly to interactions with microbes (Nishimoto, Newkirk et al. 2007). The difference between both reagents is that RNAlater is recommended for tissue, while RNAprotect™ solution is specifically suggested for cultured or sorted cells by the manufacturer.

Overall, different protocols can be applied to investigate and quantify transcriptional changes in host-pathogen interactions. In this study, RNA was isolated using the mirVana™ miRNA Isolation Kit. Bacterial ribosomal RNA (rRNA), eukaryotic cytoplasmic rRNA and mitochondrial rRNA was removed. No polyA enrichment was performed to preserve circular RNAs and bacterial RNAs for sequencing. Random-primed libraries without cutoff above 50 bp were prepared from biological triplicates and sequenced commercially by Vertis Biotechnologie AG

(Freising, Germany) on an Illumina Illumina NextSeq 500 system with a 75 bp read length. Compared to that, sequencing the miRNA fraction required additional steps. First, the small RNA fraction (<200 bp) was purified from the total RNA and concentrated using RNeasy MinElute Cleanup kit (Qiagen). Secondly, the miRNAs were isolated by nuclear acid fractionation (Caliper LabChip XT) by help of an internal size marker. Afterwards, the samples were processed and sequenced. In total, an average of over 11 million reads could be mapped at 8 and 16 h post infection (Fig. 3.17A), respectively after discarding of reads mapping to both genomes. This observation is comparable with the results of other dual RNA-Seq studies varying from 1 million to a maximum of 40 million detected reads (Westermann, Barquist et al. 2017). Moreover, 2% of the mapped reads of invaded cells at 8 h post infection were from *Legionella* origin (Fig. 3.17B). The bacterial reads were increasing to 4.5% mapped reads at 16 h post infection reflecting the intracellular replication of *L.p.*. The reads from *Legionella* (T0) or THP-1 cells alone mapped to their respective genomes with high stringency. Nearly no reads were mapped to the *Legionella* genome from the bystander cells, indicating that the gates for sorting (Fig. 3.16B) were kept conservative enough to prevent cross-contaminations of the two fractions, which is also observable in the high sort purity (Fig. 3.16C). Similar mapping results were achieved by Rienksma and colleagues. They infected THP-1 cells with *M. bovis* at an MOI of 10 for 4 h, centrifuged the cells, washed and sampled at 20 h post infection (Rienksma, Suarez-Diez et al. 2015). Thus, a different bacterium, but a similar protocol was used for the infection.

Focusing on the host side, the distribution of the RNA species showed a comparable pattern to other sequencing data depleted for ribosomal RNA (Fig. 3.18A). In this study, the abundance of miRNAs (with 0.55% to 0.1%) was higher and the abundance of lncRNAs (with 4.75% compared to 15%) was lower than in the study of Westermann and colleagues (Westermann, Forstner et al. 2016). Differences can be attributed to different cell lines and bacteria used in the studies. After performing differential gene expression analysis using DESeq2, 4,144 differentially expressed genes were identified. Mostly, significantly expressed genes were detected in gfp+ cells across both time points. More genes are regulated in cells invaded by *Legionella* than in bystander cells or TLR2-activated cells (Fig. 3.18B). This observation hints towards a specific transcriptional change following *Legionella* invasion. It has been shown that the transcriptome of human monocyte-derived macrophages infected with *Legionella* was dominated by upregulation of inflammatory and anti-apoptotic pathways, as well as downregulation of protein synthesis pathways (Price and Abu Kwaik 2014). As intracellular pathogen, *L.p.* interferes with host gene transcription to manipulate the host for its own benefit, explaining the increased number of regulated genes in the *Legionella*-invaded cells (gfp+). Another

explanation for the low amount of differentially expressed genes in the bystander cells could be that the extracellular stimulation with the bacteria was only performed for 2 h, since all non-internalized bacteria were washed away and inactivated by gentamicin. Thus, after 2 h, only stimulation of the bystander cells by secreted chemokines or cytokines of infected cells could take place.

Furthermore, a PCA and a correlation analysis of all differentially expressed genes were performed to examine the quality of the data and the association between the samples. The PCA shows a clustering of samples according to their treatment, reflecting again the high sort purity and the good quality of the sequencing data. In general, the correlation plot showed a high similarity between gfp- and Pam3 cells, while the gfp+ cells are not correlated to the other two cell fractions. This observation can be explained by the high expression changes within *Legionella*-invaded host cells. Pam3 and gfp- cells are both stimulated extracellularly either by *Legionella* or by the TLR2-ligand or by cytokines from infected cells with the result of TLR-dependent NF-κB activation (Archer and Roy 2006; Archer, Alexopoulou et al. 2009), while within gfp+ cells, several intracellular PRRs could be activated such as NOD1, NOD2, NAIP5/NLRC4 inflammasome or TLR9 (Naujoks, Lippmann et al. 2017).

Overall, the dual RNA-Seq protocol performed in this study yielded high quality sequencing data and can be compared with other dual RNA-Seq protocols for diverse intracellular and extracellular bacteria. The data set is the first one for *L.p.*-infection in human macrophages.

Especially for *Legionella*, several transcriptome analyses have been performed with just a one-sided focus on the pathogen. One study compared the global transcriptional changes of *L.p.* grown in a rich medium to that of *L.p.* exposed to an artificial freshwater medium (Li, Mendis et al. 2015). Another study used RNA deep sequencing to analyse the transcriptional landscape of exponentially (replicative) and post-exponentially (virulent) grown *L.p.* in medium (Sahr, Rusniok et al. 2012). These growth phases should mimic the biphasic life cycle of *L.p.*, where the non-virulent replicative phase (RP) of the bacterium is transitioned to a highly virulent, transmissive phase (TP) (Molofsky and Swanson 2004). The bacteria are grown in BYE broth and the exponential phase culture represents the RP, while the post-exponential stationary phase models TP of the bacteria after infection (Molofsky and Swanson 2003). Within those two studies, no internalized bacteria by host cells were analysed. A third publication monitored the transcriptional response of *L.p.* during exponential and post-exponential broth growth and compared it to the *Legionella* transcriptome during the replicative and transmissive phase of infection inside *A. castellanii*. Therefore, they analysed the transcriptional response of *L.p.* during an infection of host cells (Weissenmayer, Prendergast et al. 2011). This comparison of intracellular bacteria to bacteria grown in broth during the

exponential and post-exponential phase was also performed by Faucher and colleagues. The difference between those studies was that another host was used for infection (Faucher, Mueller et al. 2011). Faucher et al. infected PMA-differentiated THP-1 cells with the *L.p.* strain JR32 at an MOI of 1 for 6 and 18 h. In principle, they used a similar protocol for the infection, but the bacterial transcripts were separated from host cDNA by SCOTS, a selective hybridization to bacterial genomic DNA (gDNA). Thus, the focus was set again on the pathogen side and the transcripts of the host were not analysed.

In contrast, two other publications concentrated their transcriptional analyses on the host side (Fortier, Faucher et al. 2011; Price and Abu Kwaik 2014). Fortier and colleagues investigated the transcriptional profile in macrophages from C57BL6J mice (B6), and from congenic mice (BcA75) carrying the partial loss-of-function A/J-derived allele (Naip5(A/J)) on a B6 background, infected or not with wild-type *L.p.* or flagellin-deficient mutant (Fortier, Faucher et al. 2011). Thus, they identified genes regulated by flagellin and by Naip5. Bone marrow derived macrophages (BMDMs) were infected with *L.p.* Philadelphia-1 strain Lp02 at an MOI of 10 for 1 h and cells were harvested at 4 h following infection. The host transcriptome was analysed using microarrays. Therefore, host cells from another species, a different infection protocol, a different bacterial strain, as well as another transcriptome analysis platform was used compared to this study (Fortier, Faucher et al. 2011). Thus, comparative analyses between the studies can hardly be done.

Much more similar to the experimental design of this study are the experiments done by Price and Kwaik. They infected human monocyte-derived macrophages with *L.p.* strain AA100/130b at an MOI of 20 for 1 h and treated the cells for 1 h with gentamycin to kill remaining extracellular bacteria. The infection was performed with either the wildtype or the ankB mutant strain of *L.p.* for a total of 8 h. Data were analysed using microarrays meaning not all existing transcripts of the host were analysed (Price and Abu Kwaik 2014). However, the gene expression profile of the macrophages infected with the wildtype strain can still be compared to the data generated in this study although another strain of *L.p.* was used for infection. This comparison is discussed in the section 4.1.5.

Taken together, these described studies have focused on either the pathogen or the host at a given time (Westermann, Gorski et al. 2012), but this study investigates for the first time both, *L.p.* and macrophages, simultaneously during the course of infection using deep sequencing.

### 4.2.2 Identification of differentially expressed host RNA species

After differential expression analysis using DESeq2, the mRNA, lncRNA and miRNA regulation was displayed in heatmaps. The mRNA heatmap enabled the identification of gene clusters specific for *Legionella*-invaded cells or genes upregulated in all fractions. The expression of SOD2 and IL-1β could be validated via qPCR, showing a significant upregulation in all fractions. Several studies have shown that *L.p.* stimulates the production of many pro-inflammatory cytokines such as IL-1α, IL-1β, IL-6, IL-8, TNF-α, IFN-γ, IL-12, IL-17 and IL-18 in mouse BMDMs, human macrophage cell lines, murine models of *L.p.* infection or in patients with Legionnaires' disease (Tateda, Matsumoto et al. 1998; McHugh, Yamamoto et al. 2000; Fernandez-Serrano, Dorca et al. 2003; Shin, Case et al. 2008; Barry, Fontana et al. 2013). For instance, IL-1β is an important mediator of the inflammatory response and member of the IL-1 family of cytokines. It is produced by activated macrophages as a pro-protein and cleaved to its active form by caspase-1. It is suggested that IL-1β is critical for neutrophil recruitment in response to *L.p.*. They showed that *L.p.* infected macrophages produce IL-β which signals through the IL-1 receptor (IL-1R) expressed by airway epithelial cells (AECs). In response to IL-1β stimulation, AECs produce chemokines including CXCL1 and CXCL2 which stimulate the rapid recruitment of neutrophils to the lung to clear infection (LeibundGut-Landmann, Weidner et al. 2011). Furthermore, Copenhaver and colleagues showed that *Legionella*-infected macrophages in mice produce IL-1α and IL-1β for host protection. They measured the expression levels of sorted populations of T4SS-infected (invaded cells) and uninfected cells (bystander cells). They used a fluorescence-based reporter system that detects the translocated effector protein RalF of *Legionella* to discriminate between the two populations. Copenhaver and colleagues showed a marked increase in transcript levels in Il1α, Il1β, Tnf and Il6 relative to uninfected cells, but more in infected cells exhibiting significantly greater increase in cytokine transcript levels than uninfected cells (Copenhaver, Casson et al. 2015). Thus, this observation is consistent with the finding of the present study and others (Asrat, Dugan et al. 2014). Furthermore, it is comparable, since a separation of invaded and bystander cells was performed as done in the present study. Copenhaver et al. also analysed the secretion of IL-1α and IL-β and found that those cytokines were robustly produced by both T4SS-injected and uninjected cells (Copenhaver, Casson et al. 2015). In the present study, the secretion of cytokine was not measured, since the analysis here focusses on the expression profile of different RNA species.

In summary, genes identified via sequencing were validated and primarily encode mediators of the immune response.

### 4.2.3 Identification of differentially expressed host lncRNA

Overall, 495 differentially expressed lncRNAs were detected in bystander cells, in *Legionella*-invaded cells and in cells stimulated with Pam3. Although the dendrogram of the lncRNA profile shows clustering of gfp- to gfp+ cells, a cluster of genes was identified where genes showed an upregulation specific for gfp+ cells, or even a downregulation in gfp- and pam3 cells. Two lncRNAs LINC00278 and LINC00346 were validated using qPCR and confirmed the sequencing data. Regarding the sequencing data, LINC00278 was downregulated in Pam3 and gfp- cells, while LINC00346 was upregulated in gfp+ cells.

LINC000346 showed a significant upregulation at 8 and 16 h post infection in *Legionella* invaded cells, arguing for an infection-relevant lncRNA. LINC00346 has been previously described to be implicated in different types of cancer including non-small cell lung cancer (NSCLC), bladder cancer, breast cancer and hepatocellular carcinoma (Zhang, Fan et al. 2015; Liu, Li et al. 2016; Wang, Chen et al. 2017; Ye, Ding et al. 2017). Liu and colleagues found LINC00346 to be upregulated in breast cancer and associated with poor overall survival (Liu, Li et al. 2016). Another study showed that LINC00346 was upregulated in bladder cancer tissues compared to normal tissues. They demonstrated that a knockdown of LINC00346 inhibited bladder cancer cell proliferation and migration, induced cell cycle arrest and cell apoptosis (Ye, Ding et al. 2017). Thus, they postulate a role of LINC00346 as potential oncogene and a therapeutic target in bladder cancer. Furthermore, Wang and colleagues showed that LINC00346 was upregulated in tissue of patients with NSCLC and promoted proliferation and inhibits apoptosis through regulating the JAK-STAT signaling pathway (Wang, Chen et al. 2017). Therefore, an involvement of LINC00346 in *Legionella* infection is very likely, since the JAK/STAT pathway is active in macrophages infected by *Legionella*, which was shown by the phosphorylation of STAT1 upon the uptake of the bacteria (Schiavano, Dominici et al. 2016). Furthermore, LINC00346 was exclusively upregulated in *Legionella* invaded cells and it has been shown to be implicated in cell survival and cell cycle control which is crucial to diminish infection.

LINC00278 was downregulated in bystander cells, while in invaded cells it was downregulated at 8 h and upregulated at 16 h post infection. Until now, no studies were focusing on this lncRNA. One study found the expression of LINC00278 to be unique in males (Bybjerg-Grauholm, Hagen et al. 2017). Implications of this lncRNA in inflammation or other biological processes are still missing. Thus, it could be an interesting target to further focus on, since 60 - 70% of the reported cases of Legionnaires' disease are male (WHO 2017).

It is known that lncRNAs can be key regulators of innate immunity. For instance, NRAV was dramatically downregulated during infection with several viruses and it was found that it

significantly promotes influenza A virus (IAV) replication and virulence by negatively regulating the initial transcription of multiple critical interferon-stimulated genes (ISGs), including IFITM3 and MxA, by affecting histone modification of these genes (Ouyang, Zhu et al. 2014). Thus, it could be shown that lncRNAs can modulate the immune response to pathogens. Further significantly regulated lncRNAs of the sequencing data in *Legionella* invaded cells should be validated and analyzed by knockdown and overexpression experiments for the characterization of their function during the immune response or the infection process.
Taken together, lncRNAs may serve as markers for *Legionella* infection and their implication in the infection process needs to be determined.

### 4.2.4 Identification of differentially expressed host miRNAs

Based on the hierarchical clustering of the miRNA profiles, no association of the *Legionella*-invaded cells at 16 h post treatment to the other samples was found. Furthermore, strong miRNA regulations were only detectable in *Legionella*-invaded cells at 16 h and not at 8 h post infection. miRNA regulation in response to *Legionella* infection seems to require more time to show stronger effects. This observation agrees with the miRNA sequencing data from section 3.1.3, where a time-dependent regulation of several miRNAs upon infection was observed. In this experiment, more miRNAs were significantly regulated at 48 h post infection, which coincides with the stronger regulation of miRNAs at 16 h post infection observed in the dual RNA-Seq data. Other studies investigating the altered host miRNA expression in response to bacterial infections have also chosen longer infection time points (at least 24 h) (Schulte, Eulalio et al. 2011; Liu, Zhou et al. 2014). Moreover, Pam3 stimulated cells showed strong miRNA regulation. Pam3 is a TLR2-agonist and many miRNAs are regulated in response to TLR signaling (Sonkoly, Stahle et al. 2008; Nahid, Satoh et al. 2011b). Thus, it is not surprising that many miRNAs are differentially expressed upon TLR2 activation, since the Pam3 stimulation was performed for 8 and 16 h.
Furthermore, an upregulation of miR-146a and downregulation of miR-221 were detected in gfp+ cells at both time points. This observation also confirms the miRNA regulation observed in section 3.1.3, where miR-146a showed an upregulation, while miR-221 was downregulated following an infection with *Legionella* at an MOI of 0.25 for 24 h and 48 h. Thus, miRNA regulation of miR-146a and miR-221 in response to *L.p.* infection was confirmed by both sequencing approaches with different MOIs and infection time points.

Taken together, miRNA regulation requires more infection/stimulation time to show stronger regulations and differentially expressed miRNAs of *L.p.*-infected BDMs from section 3.1.3 were also dysregulated in *L.p.*-infected and sorted THP-1 cells.

### 4.2.5 Identification of mRNA as markers for *Legionella* infections

The hierarchical clustering revealed that especially mRNAs are contributing to the separation of the gfp+ cells from the other two fractions (Fig. 3.19A). Compared to the heatmap of miRNAs and lncRNAs, the mRNA heatmap showed several promising cluster with genes specifically upregulated in *Legionella*-invaded cells. Therefore, different mRNAs were selected to identify markers specific for *Legionella*-invaded host cells in this setting. In order to identify significantly regulated genes specific for gfp+ cells, an Edwards-Venn diagram was created using jvenn (Fig. 3.22). Notably, 1,128 differentially expressed genes which were exclusively regulated in invaded cells were detected. Seven gfp+ specific mRNAs (BCL10, SOD1, IRS2, CYR61, ATG5, RND3 and JUN) and two mRNAs regulated in gfp- and gfp+ cells (ZFAND2A and HSPA1) were validated via qPCR (Fig. 3.23).

The protein encoded by the gene B-Cell CLL/Lymphoma 10 (BCL10) contains a caspase recruitment domain (CARD) at its amino-terminal region. The CARD domain is suggested to mediate the binding between adapter molecules and found in many proteins that regulate apoptosis (Bouchier-Hayes and Martin 2002). It was identified as a candidate gene responsible for low grade B cell lymphomas of mucosa-associated lymphoid tissue (Du, Peng et al. 2000). BCL10 knockout mouse exhibits few defects that can be attributed to dysregulation of apoptosis, but the primary defect is a profound deficiency in NF-κB activation in the context of T- and B-cell receptor stimulation (Ruland, Duncan et al. 2001). BCL10 binds several CARD proteins and forms a signaling complex, which induces NFκB activation (Bertin, Guo et al. 2000; Bertin, Wang et al. 2001; Wang, Guo et al. 2001). Additionally, it has been found that after PRR activation a complex consisting of caspase-associated recruitment domain 9 (CARD9), BCL10 and mucosa-associated lymphoid tissue lymphoma translocation protein 1 (MALT1) is formed. This CARD9/BCL10/MALT1 complex, called CBM complex, activates NF-κB and triggers an immune response against fungi, bacteria, and viruses (Gross, Gewies et al. 2006; Hsu, Zhang et al. 2007; Roth and Ruland 2013). Thus, it is likely that upregulation of BCL10 represents the host response to the infection with *L.p.*.

Superoxide dismutase 1 (SOD1) is antioxidant enzymes that protects cells from reactive oxygen species (ROS). Macrophages kill phagocytosed bacteria through oxygen-dependent and oxygen-independent bactericidal systems. ROS are the major agents that cause damage to

phagocytosed bacteria in the oxygen-dependent bactericidal system. ROS include superoxide anion (SOA) ($O_2^-$), hydrogen peroxide ($H_2O_2$), hypochlorous acid (HOCl), and the hydroxyl radical ($OH^-$). Thus, macrophages, which have phagocytosed bacteria, show an increased production of ROS. In macrophages, SOA is converted into hydrogen peroxide or the hydroxyl radical, which kills bacteria (Fang 2004). The protein SOD1 is a soluble cytoplasmic enzyme and acts as a homodimer to degrade SOAs that are generated endogenously either by oxidoreductases or as a byproduct of reactions with electron transfer to hydrogen peroxide and oxygen (Fridovich 1975; Forman and Torres 2001). One study of Harada and colleagues could show that wildtype *L.p.* could suppress ROS production in macrophages, while intracellular growth-deficient strains could not (Harada, Miyake et al. 2007). However, they could not clarify the details of the mechanism of inhibition of host ROS production by wild type strains. Moreover, another study showed that SOD1 was required for caspase-1 activation (Meissner, Molawi et al. 2008). Thus, increased SOD1 expression led to the increased release of the caspase-1-dependent cytokines IL-1β and IL-18 and therefore to pyroptosis, which argues for a host defence mechanism to reduce bacterial replication.

Another mRNA specifically upregulated in gfp+ cells was the insulin receptor substrate 1 (IRS1). It encodes a protein which plays a role in mediating signals from the insulin and insulin-like growth factor-1 (IGF-1) receptors to intracellular pathways PI3K/Akt and Erk MAP kinase pathways (Copps and White 2012). It is described that IRS-1 protein is involved in various types of cancer, including colorectal, lung and breast cancer (Gibson, Ma et al. 2007; Houghton, Rzymkiewicz et al. 2010; Esposito, Aru et al. 2012). Furthermore, it has been shown that IRS-1 plays an important biological role in both metabolic and mitogenic (growth promoting) pathways, since mice deficient of IRS1 have a pronounced growth impairment and only mild diabetes. However, IRS-1 seems to be involved in *Legionella* infection of macrophages, but its role in bacterial infection has not been described, yet.

The cysteine rich angiogenic inducer 61 (CYR61) is a secreted, extracellular matrix (ECM)-associated signaling protein of the CCN family (CCN intercellular signaling protein) (Jun and Lau 2011; Lau 2011). Several studies have shown that CYR61 cooperates with and modulates the activities of several inflammatory cytokines, including TNF-α, Fas ligand, and TRAIL, which indicates that it plays a role in the inflammatory response (Chen, Young et al. 2007; Franzen, Chen et al. 2009; Juric, Chen et al. 2009). CYR61 supports macrophage adhesion and activates NF-κB signaling in macrophages, leading to the expression of multiple pro-inflammatory cytokines and chemokines characteristic for M1 macrophages. Thus, CYR61 regulates the inflammatory response of macrophages through integrin signaling (Bai, Chen et al. 2010). Moreover, an increased expression of CYR61 in macrophages in response to *Legionella*

infection has not been described, yet. It could be shown that the expression of CYR61 in epithelial cells is induced by many different bacteria, including *Yersinia enterocolitica*, *Escherichia coli*, *Pseudomonas aeruginosa*, *Enterococcus faecalis*, or *Staphylococcus aureus*. This observation suggests a common response mediated by identical or similar components of all these bacteria (Wiedmaier, Muller et al. 2008). However, CYR61 expression was not significantly induced in Pam3CSK4 stimulated cells in the present study, suggesting a TLR2-independent activation mechanism at least in macrophages.

The protein encoded by the gene autophagy related 5 (ATG5) is an essential molecule required for autophagy and functions as an essential mediator of LC3-I to LC3-II conversion (Mizushima, Yamamoto et al. 2001; Klionsky, Cregg et al. 2003). Autophagy is the selective engulfment of cytoplasm, which also promotes antibacterial immunity (Levine, Mizushima et al. 2011; Huang and Brumell 2014). Macrophages activate autophagy as a barrier to infection (Deretic, Saitoh et al. 2013). Thus, certain intracellular pathogens, including *L.p.*, perturb autophagosome maturation to avoid or delay their delivery to toxic lysosomes (Baxt, Garza-Mayers et al. 2013). For instances, *L.p.* injects the effector RavZ to inactivate Atg8 proteins during infection, thereby dampening the autophagy processes (Choy, Dancourt et al. 2012). Furthermore, it has been shown that $Atg5^{-/-}$ cells are unable to execute autophagy as a result of a defect in autophagosome formation (Mizushima, Yamamoto et al. 2001). Moreover, it has been described that ATG5 influences *Legionella* replication in mice. An siRNA-mediated knockdown of ATG5 resulted in an enhanced replication of *L.p.* compared to the non-targeting siRNA-transfected cells (Matsuda, Fuiji et al. 2009). Therefore, upregulation of ATG5 in *Legionella*-invaded cells (gfp+) in this study might be a host response to limit *Legionella* replication.

Rho family GTPase 3 (RND3), also known as RhoE, is a member of the small GTPase protein superfamily. Members of this family are important regulators of actin organization, as well as many other cellular processes, including cell adhesion and migration, vesicle trafficking, cytokinesis, and apoptosis (Hall 1998; Etienne-Manneville and Hall 2002). The protein constitutively binds GTP and its activity does not depend on a GDP/GTP switch, but is regulated by expression, localization and phosphorylation (Chardin 2006). Treffers and colleagues showed that RND3 protein expression was downregulated in 293/ACE2 cells upon chikungunya virus infection, promoting viral replication (Treffers, Tas et al. 2015). Since small GTPases are involved in many cellular processes, they represent an attractive target for *Legionella* effectors during establishment of the LCV (Ge and Shao 2011; Steiner, Weber et al. 2017). However, *L.p.* effector proteins predominantly target Arf/Sar, Rab and Ran family GTPases, whereas the majority of effectors of other pathogens target the family of Rho GTPases (Aktories 2011). A manipulation of RhoE by *Legionella* is not known. Nevertheless,

RND3 seems to be an important factor for the host defence and could be upregulated in *Legionella*-invaded cells as kind of host response to limit bacterial replication.

The protein encoded by the gene Jun proto-oncogene (JUN) forms the transcription factor AP-1 with c-Fos. It is activated through phosphorylation on serine 63 and serine 73 in the $NH_2$-terminal activation domain by the c-Jun N-terminal kinases (JNK) pathway, but it can act also phosphorylation-independent (Adler, Polotskaya et al. 1992; Hibi, Lin et al. 1993; Wisdom, Johnson et al. 1999). It is regulated by peptide growth factors, pro-inflammatory cytokines and other forms of cellular stress. C-Jun protects cells from apoptosis and regulates cell cycle progression (Wisdom, Johnson et al. 1999). An involvement of the JNK pathway in bacterial infections has been shown, since an infection of epithelial cells with *S. pneumoniae* resulted in JNK phosphorylation and increased AP-1-DNA-binding, which led to increased CXCL8 expression (Schmeck, Moog et al. 2006). In addition, Welsh et al. demonstrated the importance of the stress-activated protein kinase/c-Jun N-terminal kinase or p38 pathway for intracellular replication and survival of *Legionella*. They showed that *Legionella* infection led to increased activity of c-Jun N-terminal kinase and an inhibition of the activity decreased the ability of *Legionella* to replicate intracellularly (Welsh, Summersgill et al. 2004). Thus, the JNK pathway is involved in bacterial infections. Whether an increased expression of JUN following *Legionella* infection leads to an increased activation of AP-1, needs to be further investigated.

Zinc Finger AN1-Type Containing 2A (ZFAND2A), also known as arsenite-inducible RNA-associated protein (AIRAP), is highly conserved among mammals (Sok, Calfon et al. 2001). It was detected to be upregulated in gfp- and gfp+ cells in this study. ZFAND2A is suggested to be regulated by NF-κB (McElwee, Song et al. 2009). One study could show that it acts as a canonical heat shock gene. Its expression is temperature-dependent and strictly controlled by central regulator of heat-induced transcriptional responses Heat shock factor-1 (HSF1) (Rossi, Trotta et al. 2010). AIRAP function, as well as its role in infection or inflammation, is still not defined, but it seems to be involved in the TLR2-independent sensing of *Legionella* as indicated by the expression results of this study (induced in gfp- and gfp+ cells, no significant regulation in Pam3 stimulated cells).

The protein encoded by the gene heat shock protein family A (Hsp70) member 1A (HSPA1A), also known as Hsp72, is a stress-inducible intracellular protein with functions in prevention of protein aggregation, facilitation of protein refolding, and chaperoning of proteins. HSP70 is one of the major HSPs and includes the constitutive Hsp73 and stress-induced Hsp72 family members (Kiang and Tsokos 1998). It has been shown that HSP70 expression is upregulated in various states of physiological and environmental stresses, including infections, inflammation, cellular injury, or heat stress (Pockley, Muthana et al. 2008). Hsp72 prevents cell death in a

variety of stressful conditions by the suppression of a stress-induced apoptotic program (Gabai, Mabuchi et al. 2002). Hsp72 can be released from both, necrotic and viable cells, and acts as danger signal for the immune system (Basu, Binder et al. 2000; Guzhova, Kislyakova et al. 2001; Broquet, Thomas et al. 2003). Some studies report that Hsp70 activates monocytes, macrophages and dendritic cells through innate immune receptors (such as TLRs) (Asea, Kraeft et al. 2000), while others report that Hsp70 is a negative regulator of the inflammatory response. One study addressed this inconsistency and found that extracellular Hsp72 negatively regulates the production of TLR-induced pro-inflammatory cytokines and contributes to dampen the inflammatory response (Ferat-Osorio, Sanchez-Anaya et al. 2014). No literature is known that hints towards a connection between Hsp70 and *Legionella* infection. Therefore, the role of Hsp72 during the course of *Legionella* infection needs to be determined, since the data of this study indicate an upregulation following stimulations with *Legionella*.

In order to compare the sequencing data of this study with the transcriptomics data of other studies, the expression of the validated genes was compared to the publication of Price and Kwaik (Price and Abu Kwaik 2014). Regarding the experimental design, this study showed the greatest similarity to the present study. Only three (RND3, JUN, HSPA1A) of the nine herein described genes were identified to be upregulated in the microarray data of Price and Kwaik. As aforementioned, they identified the transcriptome of human MDMs infected with *L.p.* strain AA100/130b wt for 8 h and no separation of bystander and *Legionella*-invaded cells was performed. Thus, the microarray data can detect only the sum expression of genes from non-infected bystander cells and *Legionella*-invaded cells. The genes BCL10, SOD1, IRS1, CYR61, ATG5 and ZFAND2A were not regulated in response to *Legionella* (wt) infection. The genes RND3 (FC of 1.99), JUN (FC of 2.28) and HSPA1A (1.85) showed an up to 2.3-fold upregulation compared to untreated cells. Differences of the expression data can be explained by the performed separation of infected and non-infected in this study and the different cell types and strains used for infection. Nevertheless, these genes showed the same tendencies of regulation, but not to the same extent as in the present study.

Overall, the differential expression data emphasized that the mRNAs can be used as markers for *Legionella* infection in this setting, since the validation experiment via qPCR showed the expected results.

### 4.2.6 Identification of differentially expressed mRNAs of *Legionella*

2,707 differentially expressed *Legionella* genes were identified across both time points. A switch of genes between the 8 and 16 h time point was detected, meaning genes were inversely regulated across both time points.

Bacterial survival and replication requires the acquisition of essential nutrients including iron and amino acids as energy and carbon sources (Tesh, Morse et al. 1983). Therefore, macrophages actively sequester essential nutrients from invading bacterial pathogens to combat infection (Becker and Skaar 2014).

Iron is crucial for the replication and virulence of *Legionella* (James, Mauchline et al. 1995; Cianciotto 2015). For instance, IFN-γ-activated macrophages are non-permissive for *L.p.* replication due to decreased levels of intracellular iron (Nash, Libby et al. 1988). Thus, the intracellular growth of *L.p.* depends on its ability to sequester iron from the host cell. *L.p.* uses different strategies to acquire iron in culture, but it was not known until recently how *L.p.* obtains iron during intracellular growth in macrophages (Cianciotto 2015). Isaac et al. found that this acquisition is mediated by more regions allowing vacuolar co-localization N (MavN), which is a protein translocated by T4SS (Isaac, Laguna et al. 2015). This factor was necessary for intracellular growth and was highly upregulated during iron starvation, while it was not required for growth in media (Isaac, Laguna et al. 2015; Portier, Zheng et al. 2015).

FeoA and feoB are ferrous iron transporters that have already been described for *E. coli*. A loss of feoA or feoB resulted in decreased ferrous iron uptake (Kammler, Schon et al. 1993). FeoAB of *L.p.* shares homology to *E. coli* feoAB, *Salmonella enterica* serovar Typhimurium feoAB and *H. pylori* feoB (Kammler, Schon et al. 1993; Tsolis, Baumler et al. 1996; Velayudhan, Hughes et al. 2000). In *Legionella*, both genes are known to be iron regulated (Robey and Cianciotto 2002). In addition, it has been shown that feoB of *L.p*. is important for both, extracellular growth in artificial media and intracellular growth in macrophages and amoeba, especially in iron-limited environments (Robey and Cianciotto 2002). For feoA, no further investigations exist for characterization of its function. Overall, the ability to acquire iron from the host cells is a critical determinant in the outcome of *L.p.* infection (Cianciotto 2015) and therefore an interesting domain for further investigations.

*L.p.* alternates between a replicating form and a transmissive/virulent form. Nutrient starvation and environmental stress induce the transition from the metabolically active, replicating bacteria to the virulent, motile and stress-resistant form (Molofsky and Swanson 2004). Bacteria express the transmissive traits such as motility (flagella) and become cytotoxic and infectious (Molofsky and Swanson 2004). Thus, at 16 h post infection when nutrients within the macrophages become scarce, genes that encode for parts of the flagellum were

detected to be upregulated (flgB and flgG). The flagellar basal-body rod protein flgB and flgG are components of the flagellum and crucial for motility. Is has been shown that flgB is induced upon iron depletion, which supports the observation of this study (Portier, Zheng et al. 2015). At 8 h post infection, when *L.p.* is in the replicative form, genes coding for flagellin are downregulated. In this study, heat shock proteins (hsp70, hsp90, hsp100) were found to be first downregulated at 8 h and upregulated at 16 h post infection. It is known that heat shock proteins participate in the induction of an immunological response to infections caused by *Legionella*. For instance, HSP60 is located in the periplasm on the surface of *Legionella*, but may localize to the bacterial cell surface when the bacteria are intracellular (Gabay and Horwitz 1985; Hoffman, Houston et al. 1990). It triggers cytokine production including TNF-α, IFN-α, IFN–β, IL-1, IL-6 and GM-CSF in a protein kinase C-dependent manner (Retzlaff, Yamamoto et al. 1994; Retzlaff, Yamamoto et al. 1996). Furthermore, T cells obtained from patients with confirmed legionellosis proliferate upon stimulation with Hsp60 of *L.p.*. This observation suggests that Hsp60 is targeted by the cellular immune system early in infection (Eisenstein, Tamada et al. 1984). Another study found that a virulent strain of *L.p.* preferentially synthesizes and secretes Hsp60 early in the course of infection which correlates with virulence and is only secreted in contact with host cells (Fernandez, Logan et al. 1996). Thus, the upregulation of genes coding for heat shock proteins could display the transition of the replicating form to the transmissive form, when the bacteria become virulent. Furthermore, there is a hint that heat shock proteins could interact with host heat shock proteins. Nasrallah et al. confirmed the binding of Hsp60 to the mammalian small Hsp10 using a yeast two-hybrid system. Since it is known that chaperonins are required to interact with co-chaperonins to function properly in protein folding, they claimed that *Legionella* Hsp60 recruits the host cell Hsp10 to appropriately interact with SAMDC, a cytoplasmic protein required for synthesis of host polyamines that are important for intracellular growth of *L.p.* (Nasrallah 2015). Nevertheless, the function of the heat shock proteins detected in this study still needs to be determined.

Overall, genes upregulated at 16 h post infection can be interesting candidates, since they could be important virulence factors for *Legionella* infection. These genes showing a switch across both time points are involved in iron metabolism, stress response and motility. Their role during the course of infection still needs to be determined.

## 4.3 Outlook

Despite the significant biological findings of this study, this work also poses a number of questions. It was shown that MX1 downregulation facilitates *Legionella*-replication within human macrophages. The role of MX1 in limiting viral replication is well studied, but this study describes for the first time an implication of MX1 in bacterial infections. In the present study, the mechanism MX1-mediated restriction of *Legionella*-replication was not clarified. The localization of the protein could shed light on its function. Immunofluorescence staining for MX1 protein could be performed to determine the localization of MX1 upon infection in macrophages. Additionally, co-immunoprecipitation (co-IP) assays could reveal MX1 interaction partners, giving further information about its function and involvement in different pathways. Furthermore, the role of galectin-8 as danger receptor, monitoring endosomal and lysosomal integrity needs, to be confirmed in *Legionella* infection, since it has been only described in infections with *Salmonella*, *Listeria* or *Shigella* (Paz, Sachse et al. 2010; Thurston, Wandel et al. 2012; Machado, Cruz et al. 2014). Also here, immunofluorescence staining could be performed to test the co-localization of galectin-8 with e.g. LC3-positive autophagosomes. Knockout studies in mice for both, galectin-8 and MX1, might be of limited scientific use. Galectin-8 is not found within the LCV of infected murine macrophages (Truchan, Christman et al. 2017) and human MX1 is not functionally related to rodent MX1 and localized in different cellular compartments. Moreover, both murine *Mx* genes are defective in classical inbred mouse strains (Staeheli and Sutcliffe 1988). They are only intact in wild mice and in some laboratory strains derived from them (Jin, Yamashita et al. 1998). Thus, to characterize the detailed role of galectin-8 and MX1, human systems, like human lung tissue explants or organoid models should be used. Looking into databases from clinical cohorts of *Legionella* induced pneumonia, one could search for patients carrying mutations in MX1 or LGALS8, including mono- and bi-allelic variations, and correlate these findings with disease severity.

Within the present study, many differentially expressed miRNAs have been identified upon *Legionella* infection. Besides the described role of miR-125b, miR-221 and miR-579, it remains to be studied whether also other miRNAs contribute to *Legionella* pathogenesis or replication. Given the fact that miRNAs are essential mediators of the host response to pathogens, miRNAs are possible targets for the development of therapeutics and biomarkers. A prominent example of a clinical application of miRNAs as therapeutic targets is miravirsen, which is an oligonucleotide inhibitor of miR-122. Since HCV depends on expression of host miR-122 (a liver specific miRNA) to survive and replicate, miravirsen restricts HCV replication (Jopling, Yi et al. 2005). It was proved to be safe and well tolerated in HCV-infected patients in a phase IIa trial (van der Ree, van der Meer et al. 2014). With regard to the identified differentially expressed

miRNAs upon *Legionella* infection, potential biomarkers or therapeutics for *Legionella* infection could be introduced.

The dual RNA-Seq protocol applied in this study yielded high quality sequencing data. Thus, it is possible to study and further validate other critical RNA species. Additionally, the impact of some interesting identified RNA species on pathogen recognition and modulation of the immune response should be investigated with respect to therapeutic applications. The overall goal is to identify a complex network of coding and non-coding RNAs to gain a deep understanding of the infection process. In order to achieve a full understanding of RNA regulation during the course of infection, the expression changes of sRNAs of *Legionella* and circular RNAs (circRNAs) of the macrophages also needs to be identified. The dual RNA-Seq data combined with advanced bioinformatics could provide the necessary information to identify such changes.

CircRNA are generated by non-sequential backsplicing of exons, introns or a combination of both (Starke, Jost et al. 2015). They form a covalently closed loop feature without 5' end caps or 3' Poly (A) tails and are highly stable due to their nuclease resistance properties (Liang and Wilusz 2014). It has been found that some circRNAs can act as miRNA sponges to absorb and sequester miRNAs and fulfill regulatory functions in gene expression (Zhao and Shen 2017). Therefore, circRNAs can influence the infection process by counteracting miRNA-mediated degradation of mRNA. The use of miR-sponges for therapeutic applications is of emerging interest. Thus, after determination of circRNA expression, sponges could be designed based on their model and tested for antibacterial activities in *Legionella*-infected macrophages.

On the other hand, bacterial small non-coding RNAs have a length of about 50 - 300 nucleotides and regulate gene expression by translational activation/inhibition or by affecting mRNA stability (Waters and Storz 2009). They play a crucial role in many biological processes including environmental sensing and stress adaptation, virulence and infectivity (Gottesman and Storz 2011). Besides the sRNAs RsmY, RsmZ and 6 S RNA, little is known about the role of sRNAs in *Legionella,* since the *Legionella* genome is not completely annotated (Rasis and Segal 2009; Sahr, Bruggemann et al. 2009; Faucher, Friedlander et al. 2010). For instance, the 6 S RNA of *Legionella* regulates expression of genes encoding T4SS effectors, stress response genes, and genes involved in acquisition of nutrients. In addition, deletion of 6 S RNA in *Legionella* affected intracellular multiplication, while growth in rich medium was not influenced (Faucher, Friedlander et al. 2010). This observation highlights the potential gene regulation by sRNAs in response to host adaptation. Thus, interesting candidates for further analysis could be revealed by the analysis of expression patterns of sRNAs during the course of

infection. Mutant strains of *L.p.* deficient for a selected sRNA could be generated to identify sRNA function in order to determine their implication in virulence and pathogenesis.

Given the fact that about 10% of the genome of *L.p.* code for effector proteins which harbour eukaryotic-like motifs for targeting host pathways, unknown effector proteins could be identified and studied (Al-Quadan, Price et al. 2012). Their importance for infection and multiplication could be investigated via knockout studies with subsequent infection assays.

Since RNA expression does not always correlate with protein abundance, dual proteomics could be performed to complement the dual RNA-Seq data and the deep understanding of the infection process. One advantage of dual proteomics is the detection of post translational protein modifications, giving information about activation or inhibition of specific pathways. Thus, the comparison of the data could expand the knowledge how *Legionella* regulate its adaptation to the invaded host, allowing intracellular replication and how the host regulates its immune response to cope with the invading bacteria. Proteomic studies are technically more demanding than transcriptional profiling because of the small number of bacteria present in the invaded host cells. No *in silico* separation of bacterial and host proteins within invaded host cells, as performed for the dual RNA-Seq approach, is possible because the huge excess of host-derived proteins masks the expression of bacterial proteins. In order to bypass this problem, enrichment of bacterial proteins needs to be performed. Bacteria can be separated via sorting from lysed host cells to enable isolated quantification of bacterial proteins. Further experiments are necessary to establish this method for *Legionella*-infected macrophages.

Overall, the data and tools from this study can be used as a repository to identify RNA species regulated upon *L.p.* infection. The high quality dual RNA-Seq data could be a useful tool for further characterization of promising RNA molecules. Furthermore, the three miRNAs identified to play significant role in *L.p.*-replication can potentially be used as therapeutic targets. Taken miravirsen as a pioneer in miRNA therapeutics, further novel drugs will follow. A miRNA sponge with binding sites for all three miRNA (miR-125b, miR-221 and miR-579) could be the first step of a drug development to treat *Legionella* pneumonia in humans.

# 5 Bibliography

(2018). https://ecdc.europa.eu/en/legionnaires-disease/surveillance/atlas

Abdel-Nour M, Duncan C, et al. (2013). Biofilms: the stronghold of Legionella pneumophila. International journal of molecular sciences 14(11): 21660-21675. doi 10.3390/ijms141121660

Abdelhady H and Garduno RA (2013). The progeny of Legionella pneumophila in human macrophages shows unique developmental traits. FEMS microbiology letters 349(2): 99-107. doi 10.1111/1574-6968.12300

Abdullah Z, Schlee M, et al. (2012). RIG-I detects infection with live Listeria by sensing secreted bacterial nucleic acids. The EMBO journal 31(21): 4153-4164. doi 10.1038/emboj.2012.274

Accola MA, Huang B, et al. (2002). The antiviral dynamin family member, MxA, tubulates lipids and localizes to the smooth endoplasmic reticulum. Journal of Biological Chemistry 277(24): 21829-21835. doi 10.1074/jbc.M201641200

Adler V, Polotskaya A, et al. (1992). Affinity-purified c-Jun amino-terminal protein kinase requires serine/threonine phosphorylation for activity. The Journal of biological chemistry 267(24): 17001-17005

Aebi M, Fah J, et al. (1989). cDNA structures and regulation of two interferon-induced human Mx proteins. Molecular and cellular biology 9(11): 5062-5072

Ahuja D, Goyal A, et al. (2016). Interplay between RNA-binding protein HuR and microRNA-125b regulates p53 mRNA translation in response to genotoxic stress. RNA biology 13(11): 1152-1165. doi 10.1080/15476286.2016.1229734

Akagawa KS, Kamoshita K, et al. (1988). Effects of granulocyte-macrophage colony-stimulating factor and colony-stimulating factor-1 on the proliferation and differentiation of murine alveolar macrophages. J Immunol 141(10): 3383-3390

Akamine M, Higa F, et al. (2005). Differential roles of Toll-like receptors 2 and 4 in in vitro responses of macrophages to Legionella pneumophila. Infection and immunity 73(1): 352-361. doi 10.1128/IAI.73.1.352-361.2005

Akashi M, Osawa Y, et al. (1999). p21WAF1 expression by an activator of protein kinase C is regulated mainly at the post-transcriptional level in cells lacking p53: important role of RNA stabilization. The Biochemical journal 337 ( Pt 3): 607-616

Aktories K (2011). Bacterial protein toxins that modify host regulatory GTPases. Nature reviews Microbiology 9(7): 487-498. doi 10.1038/nrmicro2592

Al-Quadan T, Price CT, et al. (2012). Exploitation of evolutionarily conserved amoeba and mammalian processes by Legionella. Trends in microbiology 20(6): 299-306. doi 10.1016/j.tim.2012.03.005

Alberts B (2002) Molecular biology of the cell. Garland Science, New York.

Aliprantis AO, Yang RB, et al. (1999). Cell activation and apoptosis by bacterial lipoproteins through toll-like receptor-2. Science 285(5428): 736-739

Alli OA, Gao LY, et al. (2000). Temporal pore formation-mediated egress from macrophages and alveolar epithelial cells by Legionella pneumophila. Infection and immunity 68(11): 6431-6440

Alvarez-Dominguez JR, Hu W, et al. (2014). Global discovery of erythroid long noncoding RNAs reveals novel regulators of red cell maturation. Blood 123(4): 570-581. doi 10.1182/blood-2013-10-530683

(2017) American Lung Association, http://www.lung.org/lung-health-and-diseases/lung-disease-lookup/pneumonia/

Androulidaki A, Iliopoulos D, et al. (2009). The kinase Akt1 controls macrophage response to lipopolysaccharide by regulating microRNAs. Immunity 31(2): 220-231. doi 10.1016/j.immuni.2009.06.024

Aprianto R, Slager J, et al. (2016). Time-resolved dual RNA-seq reveals extensive rewiring of lung epithelial and pneumococcal transcriptomes during early infection. Genome biology 17(1): 198. doi 10.1186/s13059-016-1054-5

Arasaki K, Mikami Y, et al. (2017). Legionella effector Lpg1137 shuts down ER-mitochondria communication through cleavage of syntaxin 17. Nature communications 8: 15406. doi 10.1038/ncomms15406

Arbibe L, Kim DW, et al. (2007). An injected bacterial effector targets chromatin access for transcription factor NF-kappaB to alter transcription of host genes involved in immune responses. Nature immunology 8(1): 47-56. doi 10.1038/ni1423

Archer KA, Alexopoulou L, et al. (2009). Multiple MyD88-dependent responses contribute to pulmonary clearance of Legionella pneumophila. Cellular microbiology 11(1): 21-36. doi 10.1111/j.1462-5822.2008.01234.x

Archer KA and Roy CR (2006). MyD88-dependent responses involving toll-like receptor 2 are important for protection and clearance of Legionella pneumophila in a mouse model of Legionnaires' disease. Infection and immunity 74(6): 3325-3333. doi 10.1128/IAI.02049-05

Arnow PM, Chou T, et al. (1982). Nosocomial Legionnaires' disease caused by aerosolized tap water from respiratory devices. The Journal of infectious diseases 146(4): 460-467

Arora S, Dev K, et al. (2017). Macrophages: Their role, activation and polarization in pulmonary diseases. Immunobiology. doi 10.1016/j.imbio.2017.11.001

Asea A, Kraeft SK, et al. (2000). HSP70 stimulates cytokine production through a CD14-dependant pathway, demonstrating its dual role as a chaperone and cytokine. Nature medicine 6(4): 435-442. doi 10.1038/74697

Asrat S, Dugan AS, et al. (2014). The frustrated host response to Legionella pneumophila is bypassed by MyD88-dependent translation of pro-inflammatory cytokines. Plos Pathog 10(7): e1004229. doi 10.1371/journal.ppat.1004229

Asseffa A, Dickson LA, et al. (1993). Phorbol myristate acetate-differentiated THP-1 cells display increased levels of MHC class I and class II mRNA and interferon-gamma-inducible tumoricidal activity. Oncology research 5(1): 11-18

Atianand MK, Caffrey DR, et al. (2017). Immunobiology of Long Noncoding RNAs. Annual review of immunology 35: 177-198. doi 10.1146/annurev-immunol-041015-055459

Auwerx J (1991). The human leukemia cell line, THP-1: a multifacetted model for the study of monocyte-macrophage differentiation. Experientia 47(1): 22-31

Avraham R, Haseley N, et al. (2015). Pathogen Cell-to-Cell Variability Drives Heterogeneity in Host Immune Responses. Cell 162(6): 1309-1321. doi 10.1016/j.cell.2015.08.027

Avraham R, Haseley N, et al. (2016). A highly multiplexed and sensitive RNA-seq protocol for simultaneous analysis of host and pathogen transcriptomes. Nature protocols 11(8): 1477-1491. doi 10.1038/nprot.2016.090

Baddal B, Muzzi A, et al. (2015). Dual RNA-seq of Nontypeable Haemophilus influenzae and Host Cell Transcriptomes Reveals Novel Insights into Host-Pathogen Cross Talk. Mbio 6(6): e01765-01715. doi 10.1128/mBio.01765-15

Bai T, Chen CC, et al. (2010). Matricellular protein CCN1 activates a proinflammatory genetic program in murine macrophages. J Immunol 184(6): 3223-3232. doi 10.4049/jimmunol.0902792

Baik SC, Youn HS, et al. (1996). Increased oxidative DNA damage in Helicobacter pylori-infected human gastric mucosa. Cancer research 56(6): 1279-1282

Banzhaf-Strathmann J and Edbauer D (2014). Good guy or bad guy: the opposing roles of microRNA 125b in cancer. Cell communication and signaling : CCS 12: 30. doi 10.1186/1478-811X-12-30

Bardou P, Mariette J, et al. (2014). jvenn: an interactive Venn diagram viewer. BMC bioinformatics 15: 293. doi 10.1186/1471-2105-15-293

Bargonetti J, Reynisdottir I, et al. (1992). Site-specific binding of wild-type p53 to cellular DNA is inhibited by SV40 T antigen and mutant p53. Genes & development 6(10): 1886-1898

Barry KC, Fontana MF, et al. (2013). IL-1 alpha Signaling Initiates the Inflammatory Response to Virulent Legionella pneumophila In Vivo. Journal of Immunology 190(12): 6329-6339. doi 10.4049/jimmunol.1300100

Bartel DP (2004). MicroRNAs: genomics, biogenesis, mechanism, and function. Cell 116(2): 281-297

Bartlett JM and Stirling D (2003). A short history of the polymerase chain reaction. Methods Mol Biol 226: 3-6. doi 10.1385/1-59259-384-4:3

Basu S, Binder RJ, et al. (2000). Necrotic but not apoptotic cell death releases heat shock proteins, which deliver a partial maturation signal to dendritic cells and activate the NF-kappa B pathway. International immunology 12(11): 1539-1546

Baxt LA, Garza-Mayers AC, et al. (2013). Bacterial subversion of host innate immune pathways. Science 340(6133): 697-701. doi 10.1126/science.1235771

Becker KW and Skaar EP (2014). Metal limitation and toxicity at the interface between host and pathogen. FEMS microbiology reviews 38(6): 1235-1249. doi 10.1111/1574-6976.12087

Beltran M, Puig I, et al. (2008). A natural antisense transcript regulates Zeb2/Sip1 gene expression during Snail1-induced epithelial-mesenchymal transition. Genes & development 22(6): 756-769. doi 10.1101/gad.455708

Berger KH and Isberg RR (1993). Two distinct defects in intracellular growth complemented by a single genetic locus in Legionella pneumophila. Molecular microbiology 7(1): 7-19

Berger KH, Merriam JJ, et al. (1994). Altered intracellular targeting properties associated with mutations in the Legionella pneumophila dotA gene. Molecular microbiology 14(4): 809-822

Bertin J, Guo Y, et al. (2000). CARD9 is a novel caspase recruitment domain-containing protein that interacts with BCL10/CLAP and activates NF-kappa B. Journal of Biological Chemistry 275(52): 41082-41086. doi DOI 10.1074/jbc.C000726200

Bertin J, Wang L, et al. (2001). CARD11 and CARD14 are novel caspase recruitment domain (CARD)/membrane-associated guanylate kinase (MAGUK) family members that interact with BCL10 and activate NF-kappa B. The Journal of biological chemistry 276(15): 11877-11882. doi 10.1074/jbc.M010512200

Bertrams W (2014) MicroRNAs in alternative and classic activation of macrophages. Doctoral, Humboldt University Berlin

Beveridge TJ (1999). Structures of gram-negative cell walls and their derived membrane vesicles. Journal of bacteriology 181(16): 4725-4733

Bierhoff H, Schmitz K, et al. (2010). Noncoding transcripts in sense and antisense orientation regulate the epigenetic state of ribosomal RNA genes. Cold Spring Harbor symposia on quantitative biology 75: 357-364. doi 10.1101/sqb.2010.75.060

Birney E, Stamatoyannopoulos JA, et al. (2007). Identification and analysis of functional elements in 1% of the human genome by the ENCODE pilot project. Nature 447(7146): 799-816. doi 10.1038/nature05874

Bjornsti MA and Megonigal MD (1999). Resolution of DNA molecules by one-dimensional agarose-gel electrophoresis. Methods Mol Biol 94: 9-17. doi 10.1385/1-59259-259-7:9

Boldin MP, Taganov KD, et al. (2011). miR-146a is a significant brake on autoimmunity, myeloproliferation, and cancer in mice. The Journal of experimental medicine 208(6): 1189-1201. doi 10.1084/jem.20101823

Borchert GM, Lanier W, et al. (2006). RNA polymerase III transcribes human microRNAs. Nature structural & molecular biology 13(12): 1097-1101. doi 10.1038/nsmb1167

Borges V, Nunes A, et al. (2016). Legionella pneumophila strain associated with the first evidence of person-to-person transmission of Legionnaires' disease: a unique mosaic genetic backbone. Scientific reports 6: 26261. doi 10.1038/srep26261

Bouchier-Hayes L and Martin SJ (2002). CARD games in apoptosis and immunity. EMBO reports 3(7): 616-621. doi 10.1093/embo-reports/kvf139

Bourdon JC, Fernandes K, et al. (2005). p53 isoforms can regulate p53 transcriptional activity. Genes & development 19(18): 2122-2137. doi 10.1101/gad.1339905

Bozue JA and Johnson W (1996). Interaction of Legionella pneumophila with Acanthamoeba castellanii: uptake by coiling phagocytosis and inhibition of phagosome-lysosome fusion. Infection and immunity 64(2): 668-673

Brand BC, Sadosky AB, et al. (1994). The Legionella pneumophila icm locus: a set of genes required for intracellular multiplication in human macrophages. Molecular microbiology 14(4): 797-808

Brenner DJ, Steigerwalt AG, et al. (1979). Classification of the Legionnaires' disease bacterium: Legionella pneumophila, genus novum, species nova, of the family Legionellaceae, familia nova. Ann Intern Med 90(4): 656-658

Brockdorff N (2011). Chromosome silencing mechanisms in X-chromosome inactivation: unknown unknowns. Development 138(23): 5057-5065. doi 10.1242/dev.065276

Broquet AH, Thomas G, et al. (2003). Expression of the molecular chaperone Hsp70 in detergent-resistant microdomains correlates with its membrane delivery and release. The Journal of biological chemistry 278(24): 21601-21606. doi 10.1074/jbc.M302326200

Bruckert WM and Abu Kwaik Y (2015). Complete and ubiquitinated proteome of the Legionella-containing vacuole within human macrophages. Journal of proteome research 14(1): 236-248. doi 10.1021/pr500765x

Burckstummer T, Baumann C, et al. (2009). An orthogonal proteomic-genomic screen identifies AIM2 as a cytoplasmic DNA sensor for the inflammasome. Nature immunology 10(3): 266-272. doi 10.1038/ni.1702

Buti L, Spooner E, et al. (2011). Helicobacter pylori cytotoxin-associated gene A (CagA) subverts the apoptosis-stimulating protein of p53 (ASPP2) tumor suppressor pathway of the host. Proceedings of the National Academy of Sciences of the United States of America 108(22): 9238-9243. doi 10.1073/pnas.1106200108

Bybjerg-Grauholm J, Hagen CM, et al. (2017). RNA sequencing of archived neonatal dried blood spots. Molecular genetics and metabolism reports 10: 33-37. doi 10.1016/j.ymgmr.2016.12.004

Byrne B and Swanson MS (1998). Expression of Legionella pneumophila virulence traits in response to growth conditions. Infection and immunity 66(7): 3029-3034

Cabili MN, Trapnell C, et al. (2011). Integrative annotation of human large intergenic noncoding RNAs reveals global properties and specific subclasses. Genes & development 25(18): 1915-1927. doi 10.1101/gad.17446611

Cai X, Hagedorn CH, et al. (2004). Human microRNAs are processed from capped, polyadenylated transcripts that can also function as mRNAs. RNA 10(12): 1957-1966. doi 10.1261/rna.7135204

Cameron JE, Yin Q, et al. (2008). Epstein-Barr virus latent membrane protein 1 induces cellular MicroRNA miR-146a, a modulator of lymphocyte signaling pathways. Journal of virology 82(4): 1946-1958. doi 10.1128/JVI.02136-07

Carninci P, Kasukawa T, et al. (2005). The transcriptional landscape of the mammalian genome. Science 309(5740): 1559-1563. doi 10.1126/science.1112014

Carthew RW and Sontheimer EJ (2009). Origins and Mechanisms of miRNAs and siRNAs. Cell 136(4): 642-655. doi 10.1016/j.cell.2009.01.035

Cazalet C, Rusniok C, et al. (2004). Evidence in the Legionella pneumophila genome for exploitation of host cell functions and high genome plasticity. Nature genetics 36(11): 1165-1173. doi 10.1038/ng1447

Ceppi M, Pereira PM, et al. (2009). MicroRNA-155 modulates the interleukin-1 signaling pathway in activated human monocyte-derived dendritic cells. Proceedings of the National Academy of Sciences of the United States of America 106(8): 2735-2740. doi 10.1073/pnas.0811073106

Chandler FW, Hicklin MD, et al. (1977). Demonstration of the agent of Legionnaires' disease in tissue. The New England journal of medicine 297(22): 1218-1220. doi 10.1056/NEJM197712012972206

Chardin P (2006). Function and regulation of Rnd proteins. Nature reviews Molecular cell biology 7(1): 54-62. doi 10.1038/nrm1788

Chaudhuri AA, So AY, et al. (2011). MicroRNA-125b potentiates macrophage activation. J Immunol 187(10): 5062-5068. doi 10.4049/jimmunol.1102001

Chen CC, Young JL, et al. (2007). Cytotoxicity of TNFalpha is regulated by integrin-mediated matrix signaling. The EMBO journal 26(5): 1257-1267. doi 10.1038/sj.emboj.7601596

Chen CF, Huang J, et al. (2015). MicroRNA-221 regulates endothelial nitric oxide production and inflammatory response by targeting adiponectin receptor 1. Gene 565(2): 246-251. doi 10.1016/j.gene.2015.04.014

Chen CH, Lin WC, et al. (2011). Role of redox signaling regulation in propyl gallate-induced apoptosis of human leukemia cells. Food and chemical toxicology : an international journal published for the British Industrial Biological Research Association 49(2): 494-501. doi 10.1016/j.fct.2010.11.031

Chen YG, Satpathy AT, et al. (2017). Gene regulation in the immune system by long noncoding RNAs. Nature immunology 18(9): 962-972. doi 10.1038/ni.3771

Chien A, Edgar DB, et al. (1976). Deoxyribonucleic acid polymerase from the extreme thermophile Thermus aquaticus. Journal of bacteriology 127(3): 1550-1557

Chiu YH, Macmillan JB, et al. (2009). RNA polymerase III detects cytosolic DNA and induces type I interferons through the RIG-I pathway. Cell 138(3): 576-591. doi 10.1016/j.cell.2009.06.015

Chou YT, Lin HH, et al. (2010). EGFR promotes lung tumorigenesis by activating miR-7 through a Ras/ERK/Myc pathway that targets the Ets2 transcriptional repressor ERF. Cancer research 70(21): 8822-8831. doi 10.1158/0008-5472.CAN-10-0638

Choy A, Dancourt J, et al. (2012). The Legionella effector RavZ inhibits host autophagy through irreversible Atg8 deconjugation. Science 338(6110): 1072-1076. doi 10.1126/science.1227026

Cianciotto NP (2013). Type II secretion and Legionella virulence. Current topics in microbiology and immunology 376: 81-102. doi 10.1007/82_2013_339

Cianciotto NP (2015). An update on iron acquisition by Legionella pneumophila: new pathways for siderophore uptake and ferric iron reduction. Future microbiology 10(5): 841-851. doi 10.2217/fmb.15.21

Cianciotto NP and Fields BS (1992). Legionella pneumophila mip gene potentiates intracellular infection of protozoa and human macrophages. Proceedings of the National Academy of Sciences of the United States of America 89(11): 5188-5191

Clemens DL, Lee BY, et al. (2000). Deviant expression of Rab5 on phagosomes containing the intracellular pathogens Mycobacterium tuberculosis and Legionella pneumophila is associated with altered phagosomal fate. Infection and immunity 68(5): 2671-2684

Cobos Jimenez V, Bradley EJ, et al. (2014). Next-generation sequencing of microRNAs uncovers expression signatures in polarized macrophages. Physiological genomics 46(3): 91-103. doi 10.1152/physiolgenomics.00140.2013

Copenhaver AM, Casson CN, et al. (2015). IL-1R signaling enables bystander cells to overcome bacterial blockade of host protein synthesis. Proceedings of the National Academy of Sciences of the United States of America 112(24): 7557-7562. doi 10.1073/pnas.1501289112

Copenhaver AM, Casson CN, et al. (2014). Alveolar macrophages and neutrophils are the primary reservoirs for Legionella pneumophila and mediate cytosolic surveillance of type IV secretion. Infection and immunity 82(10): 4325-4336. doi 10.1128/IAI.01891-14

Copps KD and White MF (2012). Regulation of insulin sensitivity by serine/threonine phosphorylation of insulin receptor substrate proteins IRS1 and IRS2. Diabetologia 55(10): 2565-2582. doi 10.1007/s00125-012-2644-8

Correia AM, Ferreira JS, et al. (2016). Probable Person-to-Person Transmission of Legionnaires' Disease. The New England journal of medicine 374(5): 497-498. doi 10.1056/NEJMc1505356

Cox J and Mann M (2008). MaxQuant enables high peptide identification rates, individualized p.p.b.-range mass accuracies and proteome-wide protein quantification. Nature biotechnology 26(12): 1367-1372. doi 10.1038/nbt.1511

Crossland RE, Norden J, et al. (2016). Evaluation of optimal extracellular vesicle small RNA isolation and qRT-PCR normalisation for serum and urine. Journal of immunological methods 429: 39-49. doi 10.1016/j.jim.2015.12.011

Cullen BR (2011). Viruses and microRNAs: RISCy interactions with serious consequences. Genes & development 25(18): 1881-1894. doi 10.1101/gad.17352611

Cunha BA, Burillo A, et al. (2016). Legionnaires' disease. Lancet 387(10016): 376-385. doi 10.1016/S0140-6736(15)60078-2

Cunha BA, Connolly J, et al. (2015). Increase in pre-seasonal community-acquired Legionnaire's disease due to increased precipitation. Clinical microbiology and infection : the official publication of the European Society of Clinical Microbiology and Infectious Diseases 21(6): e45-46. doi 10.1016/j.cmi.2015.02.015

Cunha LD and Zamboni DS (2014). Recognition of Legionella pneumophila nucleic acids by innate immune receptors. Microbes and infection 16(12): 985-990. doi 10.1016/j.micinf.2014.08.008

Das K, Garnica O, et al. (2016). Modulation of Host miRNAs by Intracellular Bacterial Pathogens. Frontiers in cellular and infection microbiology 6: 79. doi 10.3389/fcimb.2016.00079

de Felipe KS, Glover RT, et al. (2008). Legionella eukaryotic-like type IV substrates interfere with organelle trafficking. Plos Pathog 4(8): e1000117. doi 10.1371/journal.ppat.1000117

de Kreutzenberg SV, Ceolotto G, et al. (2010). Downregulation of the longevity-associated protein sirtuin 1 in insulin resistance and metabolic syndrome: potential biochemical mechanisms. Diabetes 59(4): 1006-1015. doi 10.2337/db09-1187

DebRoy S, Dao J, et al. (2006). Legionella pneumophila type II secretome reveals unique exoproteins and a chitinase that promotes bacterial persistence in the lung. Proceedings of the National Academy of Sciences of the United States of America 103(50): 19146-19151. doi 10.1073/pnas.0608279103

Deeg C, Mutz P, et al. (2013). Transgenic mice carrying interferon-regulated human MxA locus are highly resistant to avian but not human influenza A viruses. Cytokine 63(3): 258-258. doi 10.1016/j.cyto.2013.06.067

Deiuliis JA (2016). MicroRNAs as regulators of metabolic disease: pathophysiologic significance and emerging role as biomarkers and therapeutics. Int J Obes (Lond) 40(1): 88-101. doi 10.1038/ijo.2015.170

Delneste Y, Beauvillain C, et al. (2007). [Innate immunity: structure and function of TLRs]. Medecine sciences : M/S 23(1): 67-73. doi 10.1051/medsci/200723167

Deng W, Zhang X, et al. (2017). MicroRNA-125b-5p mediates post-transcriptional regulation of hepatitis B virus replication via the LIN28B/let-7 axis. RNA biology 14(10): 1389-1398. doi 10.1080/15476286.2017.1293770

Deretic V, Saitoh T, et al. (2013). Autophagy in infection, inflammation and immunity. Nature reviews Immunology 13(10): 722-737. doi 10.1038/nri3532

Derrien T, Johnson R, et al. (2012). The GENCODE v7 catalog of human long noncoding RNAs: analysis of their gene structure, evolution, and expression. Genome research 22(9): 1775-1789. doi 10.1101/gr.132159.111

Ding Y, Lee JF, et al. (2006). Interferon-inducible protein IFIXalpha1 functions as a negative regulator of HDM2. Molecular and cellular biology 26(5): 1979-1996. doi 10.1128/MCB.26.5.1979-1996.2006

Dreyfus LA (1987). Virulence associated ingestion of Legionella pneumophila by HeLa cells. Microb Pathog 3(1): 45-52

Drury RE, O'Connor D, et al. (2017). The Clinical Application of MicroRNAs in Infectious Disease. Frontiers in immunology 8: 1182. doi 10.3389/fimmu.2017.01182

Du Bois I, Marsico A, et al. (2016). Genome-wide Chromatin Profiling of Legionella pneumophila-Infected Human Macrophages Reveals Activation of the Probacterial Host Factor TNFAIP2. The Journal of infectious diseases 214(3): 454-463. doi 10.1093/infdis/jiw171

Du MQ, Peng H, et al. (2000). BCL10 gene mutation in lymphoma. Blood 95(12): 3885-3890

Edwards AWF (2004) Cogwheels of the mind : the story of Venn diagrams. Johns Hopkins University Press, Baltimore.

Egger G, Liang G, et al. (2004). Epigenetics in human disease and prospects for epigenetic therapy. Nature 429(6990): 457-463. doi 10.1038/nature02625

Eisenreich W and Heuner K (2016). The life stage-specific pathometabolism of Legionella pneumophila. FEBS letters 590(21): 3868-3886. doi 10.1002/1873-3468.12326

Eisenstein TK, Tamada R, et al. (1984). Vaccination against Legionella pneumophila: serum antibody correlates with protection induced by heat-killed or acetone-killed cells against intraperitoneal but not aerosol infection in guinea pigs. Infection and immunity 45(3): 685-691

El Gazzar M and McCall CE (2010). MicroRNAs distinguish translational from transcriptional silencing during endotoxin tolerance. The Journal of biological chemistry 285(27): 20940-20951. doi 10.1074/jbc.M110.115063

Elliott MH, Smith DS, et al. (2009). Current trends in quantitative proteomics. Journal of mass spectrometry : JMS 44(12): 1637-1660. doi 10.1002/jms.1692

Engleberg NC, Carter C, et al. (1989). DNA sequence of mip, a Legionella pneumophila gene associated with macrophage infectivity. Infection and immunity 57(4): 1263-1270

Engvall E and Perlmann P (1971). Enzyme-linked immunosorbent assay (ELISA). Quantitative assay of immunoglobulin G. Immunochemistry 8(9): 871-874

Ensminger AW (2016). Legionella pneumophila, armed to the hilt: justifying the largest arsenal of effectors in the bacterial world. Current opinion in microbiology 29: 74-80. doi 10.1016/j.mib.2015.11.002

Escoll P, Rolando M, et al. (2013). From amoeba to macrophages: exploring the molecular mechanisms of Legionella pneumophila infection in both hosts. Current topics in microbiology and immunology 376: 1-34. doi 10.1007/82_2013_351

Espinoza CA, Allen TA, et al. (2004). B2 RNA binds directly to RNA polymerase II to repress transcript synthesis. Nature structural & molecular biology 11(9): 822-829. doi 10.1038/nsmb812

Esposito DL, Aru F, et al. (2012). The insulin receptor substrate 1 (IRS1) in intestinal epithelial differentiation and in colorectal cancer. PloS one 7(4): e36190. doi 10.1371/journal.pone.0036190

Essandoh K, Li Y, et al. (2016). MiRNA-Mediated Macrophage Polarization and its Potential Role in the Regulation of Inflammatory Response. Shock 46(2): 122-131. doi 10.1097/SHK.0000000000000604

Etienne-Manneville S and Hall A (2002). Rho GTPases in cell biology. Nature 420(6916): 629-635. doi 10.1038/nature01148

Eulalio A, Schulte L, et al. (2012). The mammalian microRNA response to bacterial infections. RNA biology 9(6): 742-750. doi 10.4161/rna.20018

Everitt B (1998) The Cambridge dictionary of statistics. Cambridge University Press, Cambridge, UK ; New York.

Fang FC (2004). Antimicrobial reactive oxygen and nitrogen species: concepts and controversies. Nature reviews Microbiology 2(10): 820-832. doi 10.1038/nrmicro1004

Fang Z and Rajewsky N (2011). The impact of miRNA target sites in coding sequences and in 3'UTRs. PloS one 6(3): e18067. doi 10.1371/journal.pone.0018067

Fattore L, Mancini R, et al. (2016). miR-579-3p controls melanoma progression and resistance to target therapy. Proceedings of the National Academy of Sciences of the United States of America 113(34): E5005-5013. doi 10.1073/pnas.1607753113

Faucher SP, Friedlander G, et al. (2010). Legionella pneumophila 6S RNA optimizes intracellular multiplication. Proceedings of the National Academy of Sciences of the United States of America 107(16): 7533-7538. doi 10.1073/pnas.0911764107

Faucher SP, Mueller CA, et al. (2011). Legionella Pneumophila Transcriptome during Intracellular Multiplication in Human Macrophages. Frontiers in microbiology 2: 60. doi 10.3389/fmicb.2011.00060

Feng J, Bi C, et al. (2006). The Evf-2 noncoding RNA is transcribed from the Dlx-5/6 ultraconserved region and functions as a Dlx-2 transcriptional coactivator. Genes & development 20(11): 1470-1484. doi 10.1101/gad.1416106

Ferat-Osorio E, Sanchez-Anaya A, et al. (2014). Heat shock protein 70 down-regulates the production of toll-like receptor-induced pro-inflammatory cytokines by a heat shock factor-1/constitutive heat shock element-binding factor-dependent mechanism. J Inflamm (Lond) 11: 19. doi 10.1186/1476-9255-11-19

Ferkol T and Schraufnagel D (2014). The global burden of respiratory disease. Annals of the American Thoracic Society 11(3): 404-406. doi 10.1513/AnnalsATS.201311-405PS

Fernandes-Alnemri T, Yu JW, et al. (2009). AIM2 activates the inflammasome and cell death in response to cytoplasmic DNA. Nature 458(7237): 509-513. doi 10.1038/nature07710

Fernandez-Serrano S, Dorca J, et al. (2003). Molecular inflammatory responses measured in blood of patients with severe community-acquired pneumonia. Clin Diagn Lab Immun 10(5): 813-820. doi 10.1128/Cdli.10.5.813-820.2003

Fernandez RC, Logan SM, et al. (1996). Elevated levels of Legionella pneumophila stress protein Hsp60 early in infection of human monocytes and L929 cells correlate with virulence. Infection and immunity 64(6): 1968-1976

Fields BS (1996). The molecular ecology of legionellae. Trends in microbiology 4(7): 286-290

Fields BS, Benson RF, et al. (2002). Legionella and Legionnaires' disease: 25 years of investigation. Clinical microbiology reviews 15(3): 506-526

Finch ML, Marquardt JU, et al. (2014). Regulation of microRNAs and their role in liver development, regeneration and disease. The international journal of biochemistry & cell biology 54: 288-303. doi 10.1016/j.biocel.2014.04.002

Forman HJ and Torres M (2001). Redox signaling in macrophages. Molecular aspects of medicine 22(4-5): 189-216

Fornari F, Gramantieri L, et al. (2008). MiR-221 controls CDKN1C/p57 and CDKN1B/p27 expression in human hepatocellular carcinoma. Oncogene 27(43): 5651-5661. doi 10.1038/onc.2008.178

Fortier A, Faucher SP, et al. (2011). Global cellular changes induced by Legionella pneumophila infection of bone marrow-derived macrophages. Immunobiology 216(12): 1274-1285. doi 10.1016/j.imbio.2011.06.008

Franco IS, Shuman HA, et al. (2009). The perplexing functions and surprising origins of Legionella pneumophila type IV secretion effectors. Cellular microbiology 11(10): 1435-1443. doi 10.1111/j.1462-5822.2009.01351.x

Franzen CA, Chen CC, et al. (2009). Matrix protein CCN1 is critical for prostate carcinoma cell proliferation and TRAIL-induced apoptosis. Molecular cancer research : MCR 7(7): 1045-1055. doi 10.1158/1541-7786.MCR-09-0017

Fraser DW, Deubner DC, et al. (1979). Nonpneumonic, short-incubation-period Legionellosis (Pontiac fever) in men who cleaned a steam turbine condenser. Science 205(4407): 690-691

Fraser DW, Tsai TR, et al. (1977). Legionnaires' disease: description of an epidemic of pneumonia. The New England journal of medicine 297(22): 1189-1197. doi 10.1056/NEJM197712012972201

Fridovich I (1975). Superoxide dismutases. Annual review of biochemistry 44: 147-159. doi 10.1146/annurev.bi.44.070175.001051

Friedman RC, Farh KK, et al. (2009). Most mammalian mRNAs are conserved targets of microRNAs. Genome research 19(1): 92-105. doi 10.1101/gr.082701.108

Frutuoso MS, Hori JI, et al. (2010). The pattern recognition receptors Nod1 and Nod2 account for neutrophil recruitment to the lungs of mice infected with Legionella pneumophila. Microbes and infection 12(11): 819-827. doi 10.1016/j.micinf.2010.05.006

Gabai VL, Mabuchi K, et al. (2002). Hsp72 and stress kinase c-jun N-terminal kinase regulate the bid-dependent pathway in tumor necrosis factor-induced apoptosis. Molecular and cellular biology 22(10): 3415-3424

Gabay JE and Horwitz MA (1985). Isolation and characterization of the cytoplasmic and outer membranes of the Legionnaires' disease bacterium (Legionella pneumophila). The Journal of experimental medicine 161(2): 409-422

Gao S, Zhou F, et al. (2016). Gastric cardia adenocarcinoma microRNA profiling in Chinese patients. Tumour biology : the journal of the International Society for Oncodevelopmental Biology and Medicine 37(7): 9411-9422. doi 10.1007/s13277-016-4824-5

Garcia-Garcia JC, Barat NC, et al. (2009). Epigenetic silencing of host cell defense genes enhances intracellular survival of the rickettsial pathogen Anaplasma phagocytophilum. Plos Pathog 5(6): e1000488. doi 10.1371/journal.ppat.1000488

Garcia-Vidal C, Labori M, et al. (2013). Rainfall is a risk factor for sporadic cases of Legionella pneumophila pneumonia. PloS one 8(4): e61036. doi 10.1371/journal.pone.0061036

Garduno RA, Garduno E, et al. (2002). Intracellular growth of Legionella pneumophila gives rise to a differentiated form dissimilar to stationary-phase forms. Infection and immunity 70(11): 6273-6283

Gay NJ, Gangloff M, et al. (2006). Toll-like receptors as molecular switches. Nature reviews Immunology 6(9): 693-698. doi 10.1038/nri1916

Ge J, Gong YN, et al. (2012). Preventing bacterial DNA release and absent in melanoma 2 inflammasome activation by a Legionella effector functioning in membrane trafficking. Proceedings of the National Academy of Sciences of the United States of America 109(16): 6193-6198. doi 10.1073/pnas.1117490109

Ge J and Shao F (2011). Manipulation of host vesicular trafficking and innate immune defence by Legionella Dot/Icm effectors. Cellular microbiology 13(12): 1870-1880. doi 10.1111/j.1462-5822.2011.01710.x

Ge Q, Wang C, et al. (2017). The suppressive effects of miR-1180-5p on the proliferation and tumorigenicity of bladder cancer cells. Histol Histopathol 32(1): 77-86. doi 10.14670/HH-11-772

Geissmann F, Manz MG, et al. (2010). Development of monocytes, macrophages, and dendritic cells. Science 327(5966): 656-661. doi 10.1126/science.1178331

Gibson SL, Ma Z, et al. (2007). Divergent roles for IRS-1 and IRS-2 in breast cancer metastasis. Cell Cycle 6(6): 631-637. doi 10.4161/cc.6.6.3987

Goldgraben MA, Russell R, et al. (2016). Double-stranded microRNA mimics can induce length- and passenger strand-dependent effects in a cell type-specific manner. RNA 22(2): 193-203. doi 10.1261/rna.054072.115

Gordanpour A, Nam RK, et al. (2012). MicroRNA detection in prostate tumors by quantitative real-time PCR (qPCR). Journal of visualized experiments : JoVE(63): e3874. doi 10.3791/3874

Gordon S (2003). Alternative activation of macrophages. Nature reviews Immunology 3(1): 23-35. doi 10.1038/nri978

Gottesman S and Storz G (2011). Bacterial small RNA regulators: versatile roles and rapidly evolving variations. Cold Spring Harbor perspectives in biology 3(12). doi 10.1101/cshperspect.a003798

Gottwein E, Mukherjee N, et al. (2007). A viral microRNA functions as an orthologue of cellular miR-155. Nature 450(7172): 1096-1099. doi 10.1038/nature05992

Greisman SE, Young EJ, et al. (1969). Mechanisms of endotoxin tolerance. V. Specificity of the early and late phases of pyrogenic tolerance. J Immunol 103(6): 1223-1236

Greub G and Raoult D (2003). Morphology of Legionella pneumophila according to their location within Hartmanella vermiformis. Res Microbiol 154(9): 619-621. doi 10.1016/j.resmic.2003.08.003

Gross O, Gewies A, et al. (2006). Card9 controls a non-TLR signalling pathway for innate anti-fungal immunity. Nature 442(7103): 651-656. doi 10.1038/nature04926

Grosshans H and Filipowicz W (2008). Proteomics joins the search for microRNA targets. Cell 134(4): 560-562. doi 10.1016/j.cell.2008.08.008

Grote P, Wittler L, et al. (2013). The tissue-specific lncRNA Fendrr is an essential regulator of heart and body wall development in the mouse. Developmental cell 24(2): 206-214. doi 10.1016/j.devcel.2012.12.012

Gruhler S and Kratchmarova I (2008). Stable isotope labeling by amino acids in cell culture (SILAC). Methods Mol Biol 424: 101-111. doi 10.1007/978-1-60327-064-9_9

Gu L, Zhang J, et al. (2017). The effects of miRNA-1180 on suppression of pancreatic cancer. American journal of translational research 9(6): 2798-2806

Guay C and Regazzi R (2013). Circulating microRNAs as novel biomarkers for diabetes mellitus. Nature reviews Endocrinology 9(9): 513-521. doi 10.1038/nrendo.2013.86

Guttman M, Donaghey J, et al. (2011). lincRNAs act in the circuitry controlling pluripotency and differentiation. Nature 477(7364): 295-300. doi 10.1038/nature10398

Guzhova I, Kislyakova K, et al. (2001). In vitro studies show that Hsp70 can be released by glia and that exogenous Hsp70 can enhance neuronal stress tolerance. Brain research 914(1-2): 66-73

Haemmig S, Baumgartner U, et al. (2014). miR-125b controls apoptosis and temozolomide resistance by targeting TNFAIP3 and NKIRAS2 in glioblastomas. Cell death & disease 5: e1279. doi 10.1038/cddis.2014.245

Hagmann CA, Herzner AM, et al. (2013). RIG-I detects triphosphorylated RNA of Listeria monocytogenes during infection in non-immune cells. PloS one 8(4): e62872. doi 10.1371/journal.pone.0062872

Hahn FE (1969). The time course of killing of bacteria and the kinetics of bactericidal effect of gentamicin: comments. The Journal of infectious diseases 119(4): 395

Hall A (1998). Rho GTPases and the actin cytoskeleton. Science 279(5350): 509-514

Haller O, Gao S, et al. (2010). Dynamin-like MxA GTPase: Structural Insights into Oligomerization and Implications for Antiviral Activity. Journal of Biological Chemistry 285(37): 28419-28424. doi 10.1074/jbc.R110.145839

Haller O and Kochs G (2011). Human MxA protein: an interferon-induced dynamin-like GTPase with broad antiviral activity. Journal of interferon & cytokine research : the official journal of the International Society for Interferon and Cytokine Research 31(1): 79-87. doi 10.1089/jir.2010.0076

Haller O, Staeheli P, et al. (2015). Mx GTPases: dynamin-like antiviral machines of innate immunity. Trends in microbiology 23(3): 154-163. doi 10.1016/j.tim.2014.12.003

Hammer BK, Tateda ES, et al. (2002). A two-component regulator induces the transmission phenotype of stationary-phase Legionella pneumophila. Molecular microbiology 44(1): 107-118

Hansson GK and Edfeldt K (2005). Toll to be paid at the gateway to the vessel wall. Arteriosclerosis, thrombosis, and vascular biology 25(6): 1085-1087. doi 10.1161/01.ATV.0000168894.43759.47

Harada T, Miyake M, et al. (2007). Evasion of Legionella pneumophila from the bactericidal system by reactive oxygen species (ROS) in macrophages. Microbiology and immunology 51(12): 1161-1170

Harapan H, Fitra F, et al. (2013). The roles of microRNAs on tuberculosis infection: meaning or myth? Tuberculosis (Edinb) 93(6): 596-605. doi 10.1016/j.tube.2013.08.004

Hawn TR, Berrington WR, et al. (2007). Altered inflammatory responses in TLR5-deficient mice infected with Legionella pneumophila. J Immunol 179(10): 6981-6987

Hawn TR, Smith KD, et al. (2006). Myeloid differentiation primary response gene (88)- and toll-like receptor 2-deficient mice are susceptible to infection with aerosolized Legionella pneumophila. The Journal of infectious diseases 193(12): 1693-1702. doi 10.1086/504525

Hawn TR, Verbon A, et al. (2003). A common dominant TLR5 stop codon polymorphism abolishes flagellin signaling and is associated with susceptibility to legionnaires' disease. The Journal of experimental medicine 198(10): 1563-1572. doi 10.1084/jem.20031220

Hayes CN and Chayama K (2016). MicroRNAs as Biomarkers for Liver Disease and Hepatocellular Carcinoma. International journal of molecular sciences 17(3): 280. doi 10.3390/ijms17030280

He L and Hannon GJ (2004). MicroRNAs: small RNAs with a big role in gene regulation. Nature reviews Genetics 5(7): 522-531. doi 10.1038/nrg1379

Helbig JH, Uldum SA, et al. (2003). Clinical utility of urinary antigen detection for diagnosis of community-acquired, travel-associated, and nosocomial legionnaires' disease. Journal of clinical microbiology 41(2): 838-840

Heuner K, Brand BC, et al. (1999). The expression of the flagellum of Legionella pneumophila is modulated by different environmental factors. FEMS microbiology letters 175(1): 69-77

Hibi M, Lin A, et al. (1993). Identification of an oncoprotein- and UV-responsive protein kinase that binds and potentiates the c-Jun activation domain. Genes & development 7(11): 2135-2148

Hilbi H and Kortholt A (2017). Role of the small GTPase Rap1 in signal transduction, cell dynamics and bacterial infection. Small GTPases: 1-7. doi 10.1080/21541248.2017.1331721

Hilbi H, Rothmeier E, et al. (2014). Beyond Rab GTPases Legionella activates the small GTPase Ran to promote microtubule polymerization, pathogen vacuole motility, and infection. Small GTPases 5(3): 1-6. doi 10.4161/21541248.2014.972859

Hoffman PS, Houston L, et al. (1990). Legionella pneumophila htpAB heat shock operon: nucleotide sequence and expression of the 60-kilodalton antigen in L. pneumophila-infected HeLa cells. Infection and immunity 58(10): 3380-3387

Holzinger D, Jorns C, et al. (2007). Induction of MxA gene expression by influenza A virus requires type I or type III interferon signaling. Journal of virology 81(14): 7776-7785. doi 10.1128/JVI.00546-06

Horisberger MA, McMaster GK, et al. (1990). Cloning and sequence analyses of cDNAs for interferon- and virus-induced human Mx proteins reveal that they contain putative guanine nucleotide-binding sites: functional study of the corresponding gene promoter. Journal of virology 64(3): 1171-1181

Hornung V, Ablasser A, et al. (2009). AIM2 recognizes cytosolic dsDNA and forms a caspase-1-activating inflammasome with ASC. Nature 458(7237): 514-518. doi 10.1038/nature07725

Horwitz MA (1983a). Formation of a novel phagosome by the Legionnaires' disease bacterium (Legionella pneumophila) in human monocytes. The Journal of experimental medicine 158(4): 1319-1331

Horwitz MA (1983b). The Legionnaires' disease bacterium (Legionella pneumophila) inhibits phagosome-lysosome fusion in human monocytes. The Journal of experimental medicine 158(6): 2108-2126

Horwitz MA (1984). Phagocytosis of the Legionnaires' disease bacterium (Legionella pneumophila) occurs by a novel mechanism: engulfment within a pseudopod coil. Cell 36(1): 27-33

Horwitz MA (1987). Characterization of avirulent mutant Legionella pneumophila that survive but do not multiply within human monocytes. The Journal of experimental medicine 166(5): 1310-1328

Horwitz MA and Maxfield FR (1984). Legionella pneumophila inhibits acidification of its phagosome in human monocytes. The Journal of cell biology 99(6): 1936-1943

Hou F, Sun L, et al. (2011). MAVS forms functional prion-like aggregates to activate and propagate antiviral innate immune response. Cell 146(3): 448-461. doi 10.1016/j.cell.2011.06.041

Houghton AM, Rzymkiewicz DM, et al. (2010). Neutrophil elastase-mediated degradation of IRS-1 accelerates lung tumor growth. Nature medicine 16(2): 219-223. doi 10.1038/nm.2084

Hsu YM, Zhang Y, et al. (2007). The adaptor protein CARD9 is required for innate immune responses to intracellular pathogens. Nature immunology 8(2): 198-205. doi 10.1038/ni1426

Hu J and Rapoport TA (2016). Fusion of the endoplasmic reticulum by membrane-bound GTPases. Seminars in cell & developmental biology 60: 105-111. doi 10.1016/j.semcdb.2016.06.001

Hu W, Alvarez-Dominguez JR, et al. (2012). Regulation of mammalian cell differentiation by long non-coding RNAs. EMBO reports 13(11): 971-983. doi 10.1038/embor.2012.145

Hu W, Yuan B, et al. (2011). Long noncoding RNA-mediated anti-apoptotic activity in murine erythroid terminal differentiation. Genes & development 25(24): 2573-2578. doi 10.1101/gad.178780.111

Huang J and Brumell JH (2014). Bacteria-autophagy interplay: a battle for survival. Nature reviews Microbiology 12(2): 101-114. doi 10.1038/nrmicro3160

Hubber A and Roy CR (2010). Modulation of host cell function by Legionella pneumophila type IV effectors. Annual review of cell and developmental biology 26: 261-283. doi 10.1146/annurev-cellbio-100109-104034

Hummer BT, Li XL, et al. (2001). Role for p53 in gene induction by double-stranded RNA. Journal of virology 75(16): 7774-7777. doi 10.1128/JVI.75.16.7774-7777.2001

Humphrys MS, Creasy T, et al. (2013). Simultaneous transcriptional profiling of bacteria and their host cells. PloS one 8(12): e80597. doi 10.1371/journal.pone.0080597

Hutvagner G, McLachlan J, et al. (2001). A cellular function for the RNA-interference enzyme Dicer in the maturation of the let-7 small temporal RNA. Science 293(5531): 834-838. doi 10.1126/science.1062961

Ingle H, Kumar S, et al. (2015). The microRNA miR-485 targets host and influenza virus transcripts to regulate antiviral immunity and restrict viral replication. Science signaling 8(406): ra126. doi 10.1126/scisignal.aab3183

Isaac DT, Laguna RK, et al. (2015). MavN is a Legionella pneumophila vacuole-associated protein required for efficient iron acquisition during intracellular growth. Proceedings of the National Academy of Sciences of the United States of America 112(37): E5208-5217. doi 10.1073/pnas.1511389112

Isberg RR, O'Connor TJ, et al. (2009). The Legionella pneumophila replication vacuole: making a cosy niche inside host cells. Nature reviews Microbiology 7(1): 13-24. doi 10.1038/nrmicro1967

Itahana Y and Itahana K (2018). Emerging Roles of p53 Family Members in Glucose Metabolism. International journal of molecular sciences 19(3). doi 10.3390/ijms19030776

Iyer MK, Niknafs YS, et al. (2015). The landscape of long noncoding RNAs in the human transcriptome. Nature genetics 47(3): 199-208. doi 10.1038/ng.3192

James BW, Mauchline WS, et al. (1995). Influence of iron-limited continuous culture on physiology and virulence of Legionella pneumophila. Infection and immunity 63(11): 4224-4230

Jarraud S, Descours G, et al. (2013). Identification of legionella in clinical samples. Methods Mol Biol 954: 27-56. doi 10.1007/978-1-62703-161-5_2

Jentho E, Bodden M, et al. (2017). microRNA-125a-3p is regulated by MyD88 in Legionella pneumophila infection and targets NTAN1. PloS one 12(4). doi ARTN e0176204

10.1371/journal.pone.0176204

Jiang D, Srinivasan A, et al. (1993). SV40 T antigen abrogates p53-mediated transcriptional activity. Oncogene 8(10): 2805-2812

Jin HK, Yamashita T, et al. (1998). Characterization and expression of the Mx1 gene in wild mouse species. Biochemical genetics 36(9-10): 311-322

Johnson JT, Yu VL, et al. (1985). Nosocomial legionellosis in surgical patients with head-and-neck cancer: implications for epidemiological reservoir and mode of transmission. Lancet 2(8450): 298-300

Jopling CL, Yi M, et al. (2005). Modulation of hepatitis C virus RNA abundance by a liver-specific MicroRNA. Science 309(5740): 1577-1581. doi 10.1126/science.1113329

Jun JI and Lau LF (2011). Taking aim at the extracellular matrix: CCN proteins as emerging therapeutic targets. Nature reviews Drug discovery 10(12): 945-963. doi 10.1038/nrd3599

Juric V, Chen CC, et al. (2009). Fas-mediated apoptosis is regulated by the extracellular matrix protein CCN1 (CYR61) in vitro and in vivo. Molecular and cellular biology 29(12): 3266-3279. doi 10.1128/MCB.00064-09

Kammler M, Schon C, et al. (1993). Characterization of the ferrous iron uptake system of Escherichia coli. Journal of bacteriology 175(19): 6212-6219

Kandoth C, McLellan MD, et al. (2013). Mutational landscape and significance across 12 major cancer types. Nature 502(7471): 333-339. doi 10.1038/nature12634

Kapranov P, Cheng J, et al. (2007). RNA maps reveal new RNA classes and a possible function for pervasive transcription. Science 316(5830): 1484-1488. doi 10.1126/science.1138341

Kastan MB, Radin AI, et al. (1991). Levels of p53 protein increase with maturation in human hematopoietic cells. Cancer research 51(16): 4279-4286

Khatri M, Bello D, et al. (2013). Evaluation of cytotoxic, genotoxic and inflammatory responses of nanoparticles from photocopiers in three human cell lines. Particle and fibre toxicology 10: 42. doi 10.1186/1743-8977-10-42

Kiang JG and Tsokos GC (1998). Heat shock protein 70 kDa: molecular biology, biochemistry, and physiology. Pharmacology & therapeutics 80(2): 183-201

Kim JK, Yuk JM, et al. (2015). MicroRNA-125a Inhibits Autophagy Activation and Antimicrobial Responses during Mycobacterial Infection. Journal of Immunology 194(11): 5355-5365. doi 10.4049/jimmunol.1402557

Kim SW, Ramasamy K, et al. (2012). MicroRNAs miR-125a and miR-125b constitutively activate the NF-kappaB pathway by targeting the tumor necrosis factor alpha-induced protein 3 (TNFAIP3, A20). Proceedings of the National Academy of Sciences of the United States of America 109(20): 7865-7870. doi 10.1073/pnas.1200081109

Kirby JE, Vogel JP, et al. (1998). Evidence for pore-forming ability by Legionella pneumophila. Molecular microbiology 27(2): 323-336

Klionsky DJ, Cregg JM, et al. (2003). A unified nomenclature for yeast autophagy-related genes. Developmental cell 5(4): 539-545

Kloosterman WP and Plasterk RH (2006). The diverse functions of microRNAs in animal development and disease. Developmental cell 11(4): 441-450. doi 10.1016/j.devcel.2006.09.009

Koch M, Mollenkopf HJ, et al. (2012). Induction of microRNA-155 is TLR- and type IV secretion system-dependent in macrophages and inhibits DNA-damage induced apoptosis. Proceedings of the National Academy of Sciences of the United States of America 109(19): E1153-1162. doi 10.1073/pnas.1116125109

Kochs G, Haener M, et al. (2002). Self-assembly of human MxA GTPase into highly ordered dynamin-like oligomers. Journal of Biological Chemistry 277(16): 14172-14176. doi 10.1074/jbc.M200244200

Kochs G and Haller O (1999). Interferon-induced human MxA GTPase blocks nuclear import of Thogoto virus nucleocapsids. Proceedings of the National Academy of Sciences of the United States of America 96(5): 2082-2086

Kochs G, Janzen C, et al. (2002). Antivirally active MxA protein sequesters La Crosse virus nucleocapsid protein into perinuclear complexes. Proceedings of the National Academy of Sciences of the United States of America 99(5): 3153-3158. doi 10.1073/pnas.052430399

Kohro T, Tanaka T, et al. (2004). A comparison of differences in the gene expression profiles of phorbol 12-myristate 13-acetate differentiated THP-1 cells and human monocyte-derived macrophage. Journal of atherosclerosis and thrombosis 11(2): 88-97

Kornienko AE, Guenzl PM, et al. (2013). Gene regulation by the act of long non-coding RNA transcription. BMC biology 11: 59. doi 10.1186/1741-7007-11-59

Kortmann J, Brubaker SW, et al. (2015). Cutting Edge: Inflammasome Activation in Primary Human Macrophages Is Dependent on Flagellin. J Immunol 195(3): 815-819. doi 10.4049/jimmunol.1403100

Krek A, Grun D, et al. (2005). Combinatorial microRNA target predictions. Nature genetics 37(5): 495-500. doi 10.1038/ng1536

Kretz M, Siprashvili Z, et al. (2013). Control of somatic tissue differentiation by the long non-coding RNA TINCR. Nature 493(7431): 231-235. doi 10.1038/nature11661

Krol J, Loedige I, et al. (2010). The widespread regulation of microRNA biogenesis, function and decay. Nature reviews Genetics 11(9): 597-610. doi 10.1038/nrg2843

Kubori T and Nagai H (2016). The Type IVB secretion system: an enigmatic chimera. Current opinion in microbiology 29: 22-29. doi 10.1016/j.mib.2015.10.001

Lander ES (2011). Initial impact of the sequencing of the human genome. Nature 470(7333): 187-197. doi 10.1038/nature09792

Lange T, Stracke S, et al. (2017). Identification of miR-16 as an endogenous reference gene for the normalization of urinary exosomal miRNA expression data from CKD patients. PloS one 12(8): e0183435. doi 10.1371/journal.pone.0183435

Lau LF (2011). CCN1/CYR61: the very model of a modern matricellular protein. Cellular and molecular life sciences : CMLS 68(19): 3149-3163. doi 10.1007/s00018-011-0778-3

Le MT, Shyh-Chang N, et al. (2011). Conserved regulation of p53 network dosage by microRNA-125b occurs through evolving miRNA-target gene pairs. PLoS genetics 7(9): e1002242. doi 10.1371/journal.pgen.1002242

Le MT, Teh C, et al. (2009). MicroRNA-125b is a novel negative regulator of p53. Genes & development 23(7): 862-876. doi 10.1101/gad.1767609

Lederberg J (2000) Encyclopedia of microbiology. Academic Press, San Diego.

Lee RC, Feinbaum RL, et al. (1993). The C. elegans heterochronic gene lin-4 encodes small RNAs with antisense complementarity to lin-14. Cell 75(5): 843-854

Lee Y, Ahn C, et al. (2003). The nuclear RNase III Drosha initiates microRNA processing. Nature 425(6956): 415-419. doi 10.1038/nature01957

Lee Y, Kim M, et al. (2004). MicroRNA genes are transcribed by RNA polymerase II. The EMBO journal 23(20): 4051-4060. doi 10.1038/sj.emboj.7600385

LeibundGut-Landmann S, Weidner K, et al. (2011). Nonhematopoietic cells are key players in innate control of bacterial airway infection. J Immunol 186(5): 3130-3137. doi 10.4049/jimmunol.1003565

Leivonen SK, Rokka A, et al. (2011). Identification of miR-193b targets in breast cancer cells and systems biological analysis of their functional impact. Molecular & cellular proteomics : MCP 10(7): M110 005322. doi 10.1074/mcp.M110.005322

Levine B, Mizushima N, et al. (2011). Autophagy in immunity and inflammation. Nature 469(7330): 323-335. doi 10.1038/nature09782

Lewis BP, Shih IH, et al. (2003). Prediction of mammalian microRNA targets. Cell 115(7): 787-798

Li L, Mendis N, et al. (2015). Transcriptomic changes of Legionella pneumophila in water. BMC genomics 16: 637. doi 10.1186/s12864-015-1869-6

Li M, Wang J, et al. (2016). microRNA-146a promotes mycobacterial survival in macrophages through suppressing nitric oxide production. Scientific reports 6: 23351. doi 10.1038/srep23351

Li N, Zhang L, et al. (2012). MxA inhibits hepatitis B virus replication by interaction with hepatitis B core antigen. Hepatology 56(3): 803-811. doi 10.1002/hep.25608

Li S, Yue Y, et al. (2013). MicroRNA-146a represses mycobacteria-induced inflammatory response and facilitates bacterial replication via targeting IRAK-1 and TRAF-6. PloS one 8(12): e81438. doi 10.1371/journal.pone.0081438

Liang D and Wilusz JE (2014). Short intronic repeat sequences facilitate circular RNA production. Genes & development 28(20): 2233-2247. doi 10.1101/gad.251926.114

Lightfield KL, Persson J, et al. (2008). Critical function for Naip5 in inflammasome activation by a conserved carboxy-terminal domain of flagellin. Nature immunology 9(10): 1171-1178. doi 10.1038/ni.1646

Lightfield KL, Persson J, et al. (2011). Differential requirements for NAIP5 in activation of the NLRC4 inflammasome. Infection and immunity 79(4): 1606-1614. doi 10.1128/IAI.01187-10

Lin CC, Liu LZ, et al. (2011). A KLF4-miRNA-206 autoregulatory feedback loop can promote or inhibit protein translation depending upon cell context. Molecular and cellular biology 31(12): 2513-2527. doi 10.1128/MCB.01189-10

Lin YS, Stout JE, et al. (1998). Disinfection of water distribution systems for Legionella. Seminars in respiratory infections 13(2): 147-159

Lingner J, Hughes TR, et al. (1997). Reverse transcriptase motifs in the catalytic subunit of telomerase. Science 276(5312): 561-567

Lippmann J, Muller HC, et al. (2011). Dissection of a type I interferon pathway in controlling bacterial intracellular infection in mice. Cellular microbiology 13(11): 1668-1682. doi 10.1111/j.1462-5822.2011.01646.x

Liu CW, Sung HC, et al. (2017). Resveratrol attenuates ICAM-1 expression and monocyte adhesiveness to TNF-alpha-treated endothelial cells: evidence for an anti-inflammatory cascade mediated by the miR-221/222/AMPK/p38/NF-kappaB pathway. Scientific reports 7: 44689. doi 10.1038/srep44689

Liu HR, Li J, et al. (2016). Long non-coding RNAs as prognostic markers in human breast cancer. Oncotarget 7(15): 20584-20596. doi DOI 10.18632/oncotarget.7828

Liu N, Wang L, et al. (2016). MicroRNA-125b-5p suppresses Brucella abortus intracellular survival via control of A20 expression. BMC microbiology 16(1): 171. doi 10.1186/s12866-016-0788-2

Liu Y, Chen Q, et al. (2011). MicroRNA-98 negatively regulates IL-10 production and endotoxin tolerance in macrophages after LPS stimulation. FEBS letters 585(12): 1963-1968. doi 10.1016/j.febslet.2011.05.029

Liu Z, Dou C, et al. (2016). Ftx non coding RNA-derived miR-545 promotes cell proliferation by targeting RIG-I in hepatocellular carcinoma. Oncotarget 7(18): 25350-25365. doi 10.18632/oncotarget.8129

Liu Z, Zhou G, et al. (2014). Analysis of miRNA expression profiling in human macrophages responding to Mycobacterium infection: induction of the immune regulator miR-146a. The Journal of infection 68(6): 553-561. doi 10.1016/j.jinf.2013.12.017

Livak KJ and Schmittgen TD (2001). Analysis of relative gene expression data using real-time quantitative PCR and the 2(-Delta Delta C(T)) Method. Methods 25(4): 402-408. doi 10.1006/meth.2001.1262

Logunov DY, Scheblyakov DV, et al. (2008). Mycoplasma infection suppresses p53, activates NF-kappaB and cooperates with oncogenic Ras in rodent fibroblast transformation. Oncogene 27(33): 4521-4531. doi 10.1038/onc.2008.103

Longo D.L. FAS, Kasper D.L., Hauser S.L., Jameson J.L., Loscalzo J. (2012) Harrisons Innere Medizin. ABW Wissenschaftsverlag.

Lossner C, Meier J, et al. (2011). Quantitative proteomics identify novel miR-155 target proteins. PloS one 6(7): e22146. doi 10.1371/journal.pone.0022146

Lu C, Huang X, et al. (2011). miR-221 and miR-155 regulate human dendritic cell development, apoptosis, and IL-12 production through targeting of p27kip1, KPC1, and SOCS-1. Blood 117(16): 4293-4303. doi 10.1182/blood-2010-12-322503

Lu F, Weidmer A, et al. (2008). Epstein-Barr virus-induced miR-155 attenuates NF-kappaB signaling and stabilizes latent virus persistence. Journal of virology 82(21): 10436-10443. doi 10.1128/JVI.00752-08

Lu LF and Liston A (2009). MicroRNA in the immune system, microRNA as an immune system. Immunology 127(3): 291-298. doi 10.1111/j.1365-2567.2009.03092.x

Lu LF, Thai TH, et al. (2009). Foxp3-dependent microRNA155 confers competitive fitness to regulatory T cells by targeting SOCS1 protein. Immunity 30(1): 80-91. doi 10.1016/j.immuni.2008.11.010

Lund E, Guttinger S, et al. (2004). Nuclear export of microRNA precursors. Science 303(5654): 95-98. doi 10.1126/science.1090599

Lytle JR, Yario TA, et al. (2007). Target mRNAs are repressed as efficiently by microRNA-binding sites in the 5' UTR as in the 3' UTR. Proceedings of the National Academy of Sciences of the United States of America 104(23): 9667-9672. doi 10.1073/pnas.0703820104

Machado FC, Cruz L, et al. (2014). Recruitment of galectin-3 during cell invasion and intracellular trafficking of Trypanosoma cruzi extracellular amastigotes. Glycobiology 24(2): 179-184. doi 10.1093/glycob/cwt097

MacMicking J, Xie QW, et al. (1997). Nitric oxide and macrophage function. Annual review of immunology 15: 323-350. doi 10.1146/annurev.immunol.15.1.323

Mahla RS, Reddy MC, et al. (2013). Sweeten PAMPs: Role of Sugar Complexed PAMPs in Innate Immunity and Vaccine Biology. Frontiers in immunology 4: 248. doi 10.3389/fimmu.2013.00248

Maisa A, Brockmann A, et al. (2015). Epidemiological investigation and case-control study: a Legionnaires' disease outbreak associated with cooling towers in Warstein, Germany, August-September 2013. Euro surveillance : bulletin Europeen sur les maladies transmissibles = European communicable disease bulletin 20(46). doi 10.2807/1560-7917.ES.2015.20.46.30064

Mallama CA, McCoy-Simandle K, et al. (2017). The Type II Secretion System of Legionella pneumophila Dampens the MyD88 and Toll-Like Receptor 2 Signaling Pathway in Infected Human Macrophages. Infection and immunity 85(4). doi 10.1128/IAI.00897-16

Mandell GL, Bennett JE, et al. (2010) Mandell, Douglas, and Bennett's principles and practice of infectious diseases. Churchill Livingstone/Elsevier, Philadelphia, PA.

Manikandan M, Deva Magendhra Rao AK, et al. (2015). Down Regulation of miR-34a and miR-143 May Indirectly Inhibit p53 in Oral Squamous Cell Carcinoma: a Pilot Study. Asian Pacific journal of cancer prevention : APJCP 16(17): 7619-7625

Mantovani B, Rabinovitch M, et al. (1972). Phagocytosis of immune complexes by macrophages. Different roles of the macrophage receptor sites for complement (C3) and for immunoglobulin (IgG). The Journal of experimental medicine 135(4): 780-792

Marrie TJ, Haldane D, et al. (1991). Control of endemic nosocomial legionnaires' disease by using sterile potable water for high risk patients. Epidemiol Infect 107(3): 591-605

Martinez FO and Gordon S (2014). The M1 and M2 paradigm of macrophage activation: time for reassessment. F1000prime reports 6: 13. doi 10.12703/P6-13

Massis LM and Zamboni DS (2011). Innate immunity to legionella pneumophila. Frontiers in microbiology 2: 109. doi 10.3389/fmicb.2011.00109

Matsuda F, Fuiji J, et al. (2009). Autophagy induced by 2-deoxy-D-glucose suppresses intracellular multiplication of Legionella pneumophila in A/J mouse macrophages. Autophagy 5(4): 484-493. doi DOI 10.4161/auto.5.4.7760

Maudet C, Mano M, et al. (2014a). MicroRNAs in the interaction between host and bacterial pathogens. FEBS letters 588(22): 4140-4147. doi 10.1016/j.febslet.2014.08.002

Maudet C, Mano M, et al. (2014b). Functional high-throughput screening identifies the miR-15 microRNA family as cellular restriction factors for Salmonella infection. Nature communications 5: 4718. doi 10.1038/ncomms5718

Mavromatis CH, Bokil NJ, et al. (2015). The co-transcriptome of uropathogenic Escherichia coli-infected mouse macrophages reveals new insights into host-pathogen interactions. Cellular microbiology 17(5): 730-746. doi 10.1111/cmi.12397

McCoy CE, Sheedy FJ, et al. (2010). IL-10 inhibits miR-155 induction by toll-like receptors. The Journal of biological chemistry 285(27): 20492-20498. doi 10.1074/jbc.M110.102111

McCusker KT, Braaten BA, et al. (1991). Legionella pneumophila inhibits protein synthesis in Chinese hamster ovary cells. Infection and immunity 59(1): 240-246

McElwee MK, Song MO, et al. (2009). Copper activation of NF-kappaB signaling in HepG2 cells. Journal of molecular biology 393(5): 1013-1021. doi 10.1016/j.jmb.2009.08.077

McHugh SL, Yamamoto Y, et al. (2000). Murine macrophages differentially produce proinflammatory cytokines after infection with virulent vs. avirulent Legionella pneumophila. Journal of leukocyte biology 67(6): 863-868

Medzhitov R (2007). Recognition of microorganisms and activation of the immune response. Nature 449(7164): 819-826. doi 10.1038/nature06246

Meissner F, Molawi K, et al. (2008). Superoxide dismutase 1 regulates caspase-1 and endotoxic shock. Nature immunology 9(8): 866-872. doi 10.1038/ni.1633

Mercer TR, Dinger ME, et al. (2009). Long non-coding RNAs: insights into functions. Nature reviews Genetics 10(3): 155-159. doi 10.1038/nrg2521

Mercer TR and Mattick JS (2013). Structure and function of long noncoding RNAs in epigenetic regulation. Nature structural & molecular biology 20(3): 300-307. doi 10.1038/nsmb.2480

Mizushima N, Yamamoto A, et al. (2001). Dissection of autophagosome formation using Apg5-deficient mouse embryonic stem cells. The Journal of cell biology 152(4): 657-668

MMWR (2011). Legionellosis --- United States, 2000-2009. MMWR Morbidity and mortality weekly report 60(32): 1083-1086

Molmeret M, Horn M, et al. (2005). Amoebae as training grounds for intracellular bacterial pathogens. Applied and environmental microbiology 71(1): 20-28. doi 10.1128/AEM.71.1.20-28.2005

Molofsky AB, Byrne BG, et al. (2006). Cytosolic recognition of flagellin by mouse macrophages restricts Legionella pneumophila infection. The Journal of experimental medicine 203(4): 1093-1104. doi 10.1084/jem.20051659

Molofsky AB and Swanson MS (2003). Legionella pneumophila CsrA is a pivotal repressor of transmission traits and activator of replication. Molecular microbiology 50(2): 445-461

Molofsky AB and Swanson MS (2004). Differentiate to thrive: lessons from the Legionella pneumophila life cycle. Molecular microbiology 53(1): 29-40. doi 10.1111/j.1365-2958.2004.04129.x

Monroe KM, McWhirter SM, et al. (2009). Identification of host cytosolic sensors and bacterial factors regulating the type I interferon response to Legionella pneumophila. Plos Pathog 5(11): e1000665. doi 10.1371/journal.ppat.1000665

Montagner S, Orlandi EM, et al. (2013). The role of miRNAs in mast cells and other innate immune cells. Immunological reviews 253(1): 12-24. doi 10.1111/imr.12042

Morris KV (2012) Non-coding RNAs and epigenetic regulation of gene expression : drivers of natural selection. Caister Academic Press, Norfolk, UK.

Mou Q and Leung PHM (2018). Differential expression of virulence genes in Legionella pneumophila growing in Acanthamoeba and human monocytes. Virulence 9(1): 185-196. doi 10.1080/21505594.2017.1373925

Mulrane L, Klinger R, et al. (2014). microRNAs: a new class of breast cancer biomarkers. Expert review of molecular diagnostics 14(3): 347-363. doi 10.1586/14737159.2014.901153

Munoz-Fontela C, Garcia MA, et al. (2005). Resistance to viral infection of super p53 mice. Oncogene 24(18): 3059-3062

Munoz-Fontela C, Macip S, et al. (2008). Transcriptional role of p53 in interferon-mediated antiviral immunity. The Journal of experimental medicine 205(8): 1929-1938. doi 10.1084/jem.20080383

Murdoch DR, Podmore RG, et al. (2013). Impact of routine systematic polymerase chain reaction testing on case finding for Legionnaires' disease: a pre-post comparison study. Clinical infectious diseases : an official publication of the Infectious Diseases Society of America 57(9): 1275-1281. doi 10.1093/cid/cit504

Murphy AJ, Guyre PM, et al. (2010). Estradiol suppresses NF-kappa B activation through coordinated regulation of let-7a and miR-125b in primary human macrophages. J Immunol 184(9): 5029-5037. doi 10.4049/jimmunol.0903463

Murphy K, Travers P, et al. (2012) Janeway's immunobiology. Garland Science, New York.

Murray PJ, Allen JE, et al. (2014). Macrophage activation and polarization: nomenclature and experimental guidelines. Immunity 41(1): 14-20. doi 10.1016/j.immuni.2014.06.008

Nahid MA, Satoh M, et al. (2011a). Mechanistic role of microRNA-146a in endotoxin-induced differential cross-regulation of TLR signaling. J Immunol 186(3): 1723-1734. doi 10.4049/jimmunol.1002311

Nahid MA, Satoh M, et al. (2011b). MicroRNA in TLR signaling and endotoxin tolerance. Cellular & molecular immunology 8(5): 388-403. doi 10.1038/cmi.2011.26

Nash TW, Libby DM, et al. (1988). IFN-gamma-activated human alveolar macrophages inhibit the intracellular multiplication of Legionella pneumophila. J Immunol 140(11): 3978-3981

Nasrallah GK (2015). A yeast two-hybrid screen reveals a strong interaction between the Legionella chaperonin Hsp60 and the host cell small heat shock protein Hsp10. Acta microbiologica et immunologica Hungarica 62(2): 121-135. doi 10.1556/030.62.2015.2.3

Naujoks J, Lippmann J, et al. (2017). Innate sensing and cell-autonomous resistance pathways in Legionella pneumophila infection. International journal of medical microbiology : IJMM. doi 10.1016/j.ijmm.2017.10.004

Naujoks J, Tabeling C, et al. (2016). IFNs Modify the Proteome of Legionella-Containing Vacuoles and Restrict Infection Via IRG1-Derived Itaconic Acid. Plos Pathog 12(2): e1005408. doi 10.1371/journal.ppat.1005408

Netherton CL, Simpson J, et al. (2009). Inhibition of a large double-stranded DNA virus by MxA protein. Journal of virology 83(5): 2310-2320. doi 10.1128/JVI.00781-08

Newsome AL, Baker RL, et al. (1985). Interactions between Naegleria fowleri and Legionella pneumophila. Infection and immunity 50(2): 449-452

Newton CA, Perkins I, et al. (2007). Role of Toll-like receptor 9 in Legionella pneumophila-induced interleukin-12 p40 production in bone marrow-derived dendritic cells and macrophages from permissive and nonpermissive mice. Infection and immunity 75(1): 146-151. doi 10.1128/IAI.01011-06

Newton HJ, Ang DK, et al. (2010). Molecular pathogenesis of infections caused by Legionella pneumophila. Clinical microbiology reviews 23(2): 274-298. doi 10.1128/CMR.00052-09

(2011), https://www.nhlbi.nih.gov/health/health-topics/topics/pnu. Cited 7. November 2017

Nishimoto KP, Newkirk D, et al. (2007). Fluorescence activated cell sorting (FACS) using RNAlater to minimize RNA degradation and perturbation of mRNA expression from cells involved in initial host microbe interactions. Journal of microbiological methods 70(1): 205-208. doi 10.1016/j.mimet.2007.03.022

Nivaskumar M and Francetic O (2014). Type II secretion system: a magic beanstalk or a protein escalator. Biochimica et biophysica acta 1843(8): 1568-1577. doi 10.1016/j.bbamcr.2013.12.020

Nora T, Lomma M, et al. (2009). Molecular mimicry: an important virulence strategy employed by Legionella pneumophila to subvert host functions. Future microbiology 4(6): 691-701. doi 10.2217/fmb.09.47

O'Connell RM, Chaudhuri AA, et al. (2009). Inositol phosphatase SHIP1 is a primary target of miR-155. Proceedings of the National Academy of Sciences of the United States of America 106(17): 7113-7118. doi 10.1073/pnas.0902636106

O'Connell RM, Rao DS, et al. (2012). microRNA regulation of inflammatory responses. Annual review of immunology 30: 295-312. doi 10.1146/annurev-immunol-020711-075013

O'Connell RM, Rao DS, et al. (2010). Physiological and pathological roles for microRNAs in the immune system. Nature reviews Immunology 10(2): 111-122. doi 10.1038/nri2708

O'Connell RM, Taganov KD, et al. (2007). MicroRNA-155 is induced during the macrophage inflammatory response. Proceedings of the National Academy of Sciences of the United States of America 104(5): 1604-1609. doi 10.1073/pnas.0610731104

O'Neill LA, Sheedy FJ, et al. (2011). MicroRNAs: the fine-tuners of Toll-like receptor signalling. Nature reviews Immunology 11(3): 163-175. doi 10.1038/nri2957

Okazaki Y, Furuno M, et al. (2002). Analysis of the mouse transcriptome based on functional annotation of 60,770 full-length cDNAs. Nature 420(6915): 563-573. doi 10.1038/nature01266

Opitz B, Vinzing M, et al. (2006). Legionella pneumophila induces IFNbeta in lung epithelial cells via IPS-1 and IRF3, which also control bacterial replication. The Journal of biological chemistry 281(47): 36173-36179. doi 10.1074/jbc.M604638200

Ouyang J, Zhu X, et al. (2014). NRAV, a long noncoding RNA, modulates antiviral responses through suppression of interferon-stimulated gene transcription. Cell Host Microbe 16(5): 616-626. doi 10.1016/j.chom.2014.10.001

Ozinsky A, Underhill DM, et al. (2000). The repertoire for pattern recognition of pathogens by the innate immune system is defined by cooperation between toll-like receptors. Proceedings of the National Academy of Sciences of the United States of America 97(25): 13766-13771. doi 10.1073/pnas.250476497

Pal MK, Jaiswar SP, et al. (2015). MicroRNA: a new and promising potential biomarker for diagnosis and prognosis of ovarian cancer. Cancer biology & medicine 12(4): 328-341. doi 10.7497/j.issn.2095-3941.2015.0024

Palazzo AF and Lee ES (2015). Non-coding RNA: what is functional and what is junk? Frontiers in genetics 6: 2. doi 10.3389/fgene.2015.00002

Pampin M, Simonin Y, et al. (2006). Cross talk between PML and p53 during poliovirus infection: implications for antiviral defense. Journal of virology 80(17): 8582-8592. doi 10.1128/JVI.00031-06

Paz I, Sachse M, et al. (2010). Galectin-3, a marker for vacuole lysis by invasive pathogens. Cellular microbiology 12(4): 530-544. doi 10.1111/j.1462-5822.2009.01415.x

Pena-Chilet M, Martinez MT, et al. (2014). MicroRNA profile in very young women with breast cancer. BMC cancer 14: 529. doi 10.1186/1471-2407-14-529

Pereira MS, Marques GG, et al. (2011). The Nlrc4 Inflammasome Contributes to Restriction of Pulmonary Infection by Flagellated Legionella spp. that Trigger Pyroptosis. Frontiers in microbiology 2: 33. doi 10.3389/fmicb.2011.00033

Pereira MS, Morgantetti GF, et al. (2011). Activation of NLRC4 by flagellated bacteria triggers caspase-1-dependent and -independent responses to restrict Legionella pneumophila replication in macrophages and in vivo. J Immunol 187(12): 6447-6455. doi 10.4049/jimmunol.1003784

Petzold M, Ehricht R, et al. (2017). Rapid genotyping of Legionella pneumophila serogroup 1 strains by a novel DNA microarray-based assay during the outbreak investigation in Warstein, Germany 2013. International journal of hygiene and environmental health 220(4): 673-678. doi 10.1016/j.ijheh.2016.02.004

Pichlmair A, Schulz O, et al. (2006). RIG-I-mediated antiviral responses to single-stranded RNA bearing 5'-phosphates. Science 314(5801): 997-1001. doi 10.1126/science.1132998

Pierre DM, Baron J, et al. (2017). Diagnostic testing for Legionnaires' disease. Annals of clinical microbiology and antimicrobials 16(1): 59. doi 10.1186/s12941-017-0229-6

Place RF, Li LC, et al. (2008). MicroRNA-373 induces expression of genes with complementary promoter sequences. Proceedings of the National Academy of Sciences of the United States of America 105(5): 1608-1613. doi 10.1073/pnas.0707594105

Plumlee CR, Lee C, et al. (2009). Interferons direct an effective innate response to Legionella pneumophila infection. The Journal of biological chemistry 284(44): 30058-30066. doi 10.1074/jbc.M109.018283

Pockley AG, Muthana M, et al. (2008). The dual immunoregulatory roles of stress proteins. Trends in biochemical sciences 33(2): 71-79. doi 10.1016/j.tibs.2007.10.005

Pontier DB and Gribnau J (2011). Xist regulation and function explored. Human genetics 130(2): 223-236. doi 10.1007/s00439-011-1008-7

Portier E, Zheng H, et al. (2015). IroT/mavN, a new iron-regulated gene involved in Legionella pneumophila virulence against amoebae and macrophages. Environmental microbiology 17(4): 1338-1350. doi 10.1111/1462-2920.12604

Price CT and Abu Kwaik Y (2014). The transcriptome of Legionella pneumophila-infected human monocyte-derived macrophages. PloS one 9(12): e114914. doi 10.1371/journal.pone.0114914

Qin Y, Zhao J, et al. (2014). MicroRNA-125b inhibits lens epithelial cell apoptosis by targeting p53 in age-related cataract. Biochimica et biophysica acta 1842(12 Pt A): 2439-2447. doi 10.1016/j.bbadis.2014.10.002

Qin Z (2012). The use of THP-1 cells as a model for mimicking the function and regulation of monocytes and macrophages in the vasculature. Atherosclerosis 221(1): 2-11. doi 10.1016/j.atherosclerosis.2011.09.003

Quinn EM, Wang J, et al. (2012). The emerging role of microRNA in regulation of endotoxin tolerance. Journal of leukocyte biology 91(5): 721-727. doi 10.1189/jlb.1111571

Rabinovich GA and Toscano MA (2009). Turning 'sweet' on immunity: galectin-glycan interactions in immune tolerance and inflammation. Nature reviews Immunology 9(5): 338-352. doi 10.1038/nri2536

Rad R, Ballhorn W, et al. (2009). Extracellular and intracellular pattern recognition receptors cooperate in the recognition of Helicobacter pylori. Gastroenterology 136(7): 2247-2257. doi 10.1053/j.gastro.2009.02.066

Rasis M and Segal G (2009). The LetA-RsmYZ-CsrA regulatory cascade, together with RpoS and PmrA, post-transcriptionally regulates stationary phase activation of Legionella pneumophila Icm/Dot effectors. Molecular microbiology 72(4): 995-1010. doi 10.1111/j.1365-2958.2009.06705.x

Ratcliff RM (2013). Sequence-based identification of legionella. Methods Mol Biol 954: 57-72. doi 10.1007/978-1-62703-161-5_3

Rechnitzer C and Blom J (1989). Engulfment of the Philadelphia strain of Legionella pneumophila within pseudopod coils in human phagocytes. Comparison with other Legionella strains and species. APMIS : acta pathologica, microbiologica, et immunologica Scandinavica 97(2): 105-114

Reichelt M, Stertz S, et al. (2004). Missorting of LaCrosse virus nucleocapsid protein by the interferon-induced MxA GTPase involves smooth ER membranes. Traffic 5(10): 772-784. doi 10.1111/j.1600-0854.2004.00219.x

Ren T, Zamboni DS, et al. (2006). Flagellin-deficient Legionella mutants evade caspase-1- and Naip5-mediated macrophage immunity. Plos Pathog 2(3): e18. doi 10.1371/journal.ppat.0020018

Retzlaff C, Yamamoto Y, et al. (1994). Bacterial heat shock proteins directly induce cytokine mRNA and interleukin-1 secretion in macrophage cultures. Infection and immunity 62(12): 5689-5693

Retzlaff C, Yamamoto Y, et al. (1996). Legionella pneumophila heat-shock protein-induced increase of interleukin-1 beta mRNA involves protein kinase C signalling in macrophages. Immunology 89(2): 281-288

Reynolds HY and Newball HH (1974). Analysis of proteins and respiratory cells obtained from human lungs by bronchial lavage. The Journal of laboratory and clinical medicine 84(4): 559-573

Ribet D and Cossart P (2010). Post-translational modifications in host cells during bacterial infection. FEBS letters 584(13): 2748-2758. doi 10.1016/j.febslet.2010.05.012

Richards AM, Von Dwingelo JE, et al. (2013). Cellular microbiology and molecular ecology of Legionella-amoeba interaction. Virulence 4(4): 307-314. doi 10.4161/viru.24290

Rienksma RA, Suarez-Diez M, et al. (2015). Comprehensive insights into transcriptional adaptation of intracellular mycobacteria by microbe-enriched dual RNA sequencing. BMC genomics 16: 34. doi 10.1186/s12864-014-1197-2

Rinn JL and Chang HY (2012). Genome regulation by long noncoding RNAs. Annual review of biochemistry 81: 145-166. doi 10.1146/annurev-biochem-051410-092902

Rinn JL, Kertesz M, et al. (2007). Functional demarcation of active and silent chromatin domains in human HOX loci by noncoding RNAs. Cell 129(7): 1311-1323. doi 10.1016/j.cell.2007.05.022

Rizzardi K, Winiecka-Krusnell J, et al. (2015). Legionella norrlandica sp. nov., isolated from the biopurification systems of wood processing plants. International journal of systematic and evolutionary microbiology 65(Pt 2): 598-603. doi 10.1099/ijs.0.068940-0

Robert-Koch-Institut (2012) Legionärskrankheit im Jahr 2011, Epidemiologisches Bulletin, pp. 501.

Robertson P, Abdelhady H, et al. (2014). The many forms of a pleomorphic bacterial pathogen-the developmental network of Legionella pneumophila. Frontiers in microbiology 5: 670. doi 10.3389/fmicb.2014.00670

Robey M and Cianciotto NP (2002). Legionella pneumophila feoAB promotes ferrous iron uptake and intracellular infection. Infection and immunity 70(10): 5659-5669

Rolando M and Buchrieser C (2012). Post-translational modifications of host proteins by Legionella pneumophila: a sophisticated survival strategy. Future microbiology 7(3): 369-381. doi 10.2217/fmb.12.9

Rolando M, Sanulli S, et al. (2013). Legionella pneumophila effector RomA uniquely modifies host chromatin to repress gene expression and promote intracellular bacterial replication. Cell Host Microbe 13(4): 395-405. doi 10.1016/j.chom.2013.03.004

Rome S (2013). Are extracellular microRNAs involved in type 2 diabetes and related pathologies? Clinical biochemistry 46(10-11): 937-945. doi 10.1016/j.clinbiochem.2013.02.018

Rossi A, Trotta E, et al. (2010). AIRAP, a new human heat shock gene regulated by heat shock factor 1. The Journal of biological chemistry 285(18): 13607-13615. doi 10.1074/jbc.M109.082693

Roth S and Ruland J (2013). Caspase recruitment domain-containing protein 9 signaling in innate immunity and inflammation. Trends in immunology 34(6): 243-250. doi 10.1016/j.it.2013.02.006

Rowbotham TJ (1983). Isolation of Legionella pneumophila from clinical specimens via amoebae, and the interaction of those and other isolates with amoebae. Journal of clinical pathology 36(9): 978-986

Rowbotham TJ (1986). Current views on the relationships between amoebae, legionellae and man. Isr J Med Sci 22(9): 678-689

Roy CR, Berger KH, et al. (1998). Legionella pneumophila DotA protein is required for early phagosome trafficking decisions that occur within minutes of bacterial uptake. Molecular microbiology 28(3): 663-674

Ruland J, Duncan GS, et al. (2001). Bcl10 is a positive regulator of antigen receptor-induced activation of NF-kappaB and neural tube closure. Cell 104(1): 33-42

Rusca N, Deho L, et al. (2012). MiR-146a and NF-kappaB1 regulate mast cell survival and T lymphocyte differentiation. Molecular and cellular biology 32(21): 4432-4444. doi 10.1128/MCB.00824-12

Sadler AJ and Williams BR (2008). Interferon-inducible antiviral effectors. Nature reviews Immunology 8(7): 559-568. doi 10.1038/nri2314

Saeed IA and Ashraf SS (2009). Denaturation studies reveal significant differences between GFP and blue fluorescent protein. International journal of biological macromolecules 45(3): 236-241. doi 10.1016/j.ijbiomac.2009.05.010

Sahr T, Bruggemann H, et al. (2009). Two small ncRNAs jointly govern virulence and transmission in Legionella pneumophila. Molecular microbiology 72(3): 741-762. doi 10.1111/j.1365-2958.2009.06677.x

Sahr T, Rusniok C, et al. (2012). Deep sequencing defines the transcriptional map of L. pneumophila and identifies growth phase-dependent regulated ncRNAs implicated in virulence. RNA biology 9(4): 503-519. doi 10.4161/rna.20270

Sahu SK, Kumar M, et al. (2017). MicroRNA 26a (miR-26a)/KLF4 and CREB-C/EBPbeta regulate innate immune signaling, the polarization of macrophages and the trafficking of Mycobacterium tuberculosis to lysosomes during infection. Plos Pathog 13(5): e1006410. doi 10.1371/journal.ppat.1006410

Saiki RK, Gelfand DH, et al. (1988). Primer-directed enzymatic amplification of DNA with a thermostable DNA polymerase. Science 239(4839): 487-491

Saito Y, Liang G, et al. (2006). Specific activation of microRNA-127 with downregulation of the proto-oncogene BCL6 by chromatin-modifying drugs in human cancer cells. Cancer cell 9(6): 435-443. doi 10.1016/j.ccr.2006.04.020

Sand M, Skrygan M, et al. (2012). Expression of microRNAs in basal cell carcinoma. The British journal of dermatology 167(4): 847-855. doi 10.1111/j.1365-2133.2012.11022.x

Santovito D, Egea V, et al. (2016). Small but smart: MicroRNAs orchestrate atherosclerosis development and progression. Biochimica et biophysica acta 1861(12 Pt B): 2075-2086. doi 10.1016/j.bbalip.2015.12.013

Schamberger A, Sarkadi B, et al. (2012). Human mirtrons can express functional microRNAs simultaneously from both arms in a flanking exon-independent manner. RNA biology 9(9): 1177-1185. doi 10.4161/rna.21359

Schiavano GF, Dominici S, et al. (2016). Modulation of Stat-1 in Human Macrophages Infected with Different Species of Intracellular Pathogenic Bacteria. Journal of immunology research 2016: 5086928. doi 10.1155/2016/5086928

Schiavoni G, Mauri C, et al. (2004). Type I IFN protects permissive macrophages from Legionella pneumophila infection through an IFN-gamma-independent pathway. J Immunol 173(2): 1266-1275

Schmeck B, Beermann W, et al. (2005). Intracellular bacteria differentially regulated endothelial cytokine release by MAPK-dependent histone modification. J Immunol 175(5): 2843-2850

Schmeck B, Moog K, et al. (2006). Streptococcus pneumoniae induced c-Jun-N-terminal kinase- and AP-1 -dependent IL-8 release by lung epithelial BEAS-2B cells. Respir Res 7: 98. doi 10.1186/1465-9921-7-98

Schnitger AK, Machova A, et al. (2011a). Listeria monocytogenes infection in macrophages induces vacuolar-dependent host miRNA response. PloS one 6(11): e27435. doi 10.1371/journal.pone.0027435

Schnitger AKD, Machova A, et al. (2011b). Listeria monocytogenes Infection in Macrophages Induces Vacuolar-Dependent Host miRNA Response. PloS one 6(11). doi ARTN e27435

10.1371/journal.pone.0027435

Schulte LN, Eulalio A, et al. (2011). Analysis of the host microRNA response to Salmonella uncovers the control of major cytokines by the let-7 family. The EMBO journal 30(10): 1977-1989. doi 10.1038/emboj.2011.94

Schulte LN, Westermann AJ, et al. (2013). Differential activation and functional specialization of miR-146 and miR-155 in innate immune sensing. Nucleic acids research 41(1): 542-553. doi 10.1093/nar/gks1030

Schwarz DS, Hutvagner G, et al. (2003). Asymmetry in the assembly of the RNAi enzyme complex. Cell 115(2): 199-208

Schwarzenbach H, da Silva AM, et al. (2015). Data Normalization Strategies for MicroRNA Quantification. Clinical chemistry 61(11): 1333-1342. doi 10.1373/clinchem.2015.239459

Selbach M, Schwanhausser B, et al. (2008). Widespread changes in protein synthesis induced by microRNAs. Nature 455(7209): 58-63. doi 10.1038/nature07228

Sethi KK and Brandis H (1983). Direct demonstration and isolation of Legionella pneumophila (serogroup 1) from bathroom water specimens in a hotel. Zentralblatt fur Bakteriologie, Mikrobiologie und Hygiene 1 Abt Originale B, Hygiene 177(5): 402-405

Sharif O, Bolshakov VN, et al. (2007). Transcriptional profiling of the LPS induced NF-kappaB response in macrophages. BMC immunology 8: 1. doi 10.1186/1471-2172-8-1

Sharma S, Findlay GM, et al. (2011). Dephosphorylation of the nuclear factor of activated T cells (NFAT) transcription factor is regulated by an RNA-protein scaffold complex. Proceedings of the National Academy of Sciences of the United States of America 108(28): 11381-11386. doi 10.1073/pnas.1019711108

Shi J, Zhao Y, et al. (2015). Cleavage of GSDMD by inflammatory caspases determines pyroptotic cell death. Nature 526(7575): 660-665. doi 10.1038/nature15514

Shibata Y, Berclaz PY, et al. (2001). GM-CSF regulates alveolar macrophage differentiation and innate immunity in the lung through PU.1. Immunity 15(4): 557-567

Shim HK, Kim JY, et al. (2009). Legionella lipoprotein activates toll-like receptor 2 and induces cytokine production and expression of costimulatory molecules in peritoneal macrophages. Experimental & molecular medicine 41(10): 687-694. doi 10.3858/emm.2009.41.10.075

Shimada T, Noguchi Y, et al. (2009). Systematic review and metaanalysis: urinary antigen tests for Legionellosis. Chest 136(6): 1576-1585. doi 10.1378/chest.08-2602

Shin S, Case CL, et al. (2008). Type IV Secretion-Dependent Activation of Host MAP Kinases Induces an Increased Proinflammatory Cytokine Response to Legionella pneumophila. Plos Pathog 4(11). doi ARTN e1000220

10.1371/journal.ppat.1000220

Siegl C, Prusty BK, et al. (2014). Tumor suppressor p53 alters host cell metabolism to limit Chlamydia trachomatis infection. Cell Rep 9(3): 918-929. doi 10.1016/j.celrep.2014.10.004

Smyth LA, Boardman DA, et al. (2015). MicroRNAs affect dendritic cell function and phenotype. Immunology 144(2): 197-205. doi 10.1111/imm.12390

Sok J, Calfon M, et al. (2001). Arsenite-inducible RNA-associated protein (AIRAP) protects cells from arsenite toxicity. Cell stress & chaperones 6(1): 6-15

Song B, Ji W, et al. (2014). miR-545 inhibited pancreatic ductal adenocarcinoma growth by targeting RIG-I. FEBS letters 588(23): 4375-4381. doi 10.1016/j.febslet.2014.10.004

Sonkoly E, Stahle M, et al. (2008). MicroRNAs and immunity: novel players in the regulation of normal immune function and inflammation. Seminars in cancer biology 18(2): 131-140. doi 10.1016/j.semcancer.2008.01.005

Soussi T and Wiman KG (2015). TP53: an oncogene in disguise. Cell death and differentiation 22(8): 1239-1249. doi 10.1038/cdd.2015.53

Spitalny KC, Vogt RL, et al. (1984). Pontiac fever associated with a whirlpool spa. American journal of epidemiology 120(6): 809-817

Staedel C and Darfeuille F (2013). MicroRNAs and bacterial infection. Cellular microbiology 15(9): 1496-1507. doi 10.1111/cmi.12159

Staeheli P and Pavlovic J (1991). Inhibition of vesicular stomatitis virus mRNA synthesis by human MxA protein. Journal of virology 65(8): 4498-4501

Staeheli P and Sutcliffe JG (1988). Identification of a second interferon-regulated murine Mx gene. Molecular and cellular biology 8(10): 4524-4528

Starke S, Jost I, et al. (2015). Exon circularization requires canonical splice signals. Cell Rep 10(1): 103-111. doi 10.1016/j.celrep.2014.12.002

Steiner B, Weber S, et al. (2017). Formation of the Legionella-containing vacuole: phosphoinositide conversion, GTPase modulation and ER dynamics. International journal of medical microbiology : IJMM. doi 10.1016/j.ijmm.2017.08.004

Stetson DB and Medzhitov R (2006). Recognition of cytosolic DNA activates an IRF3-dependent innate immune response. Immunity 24(1): 93-103. doi 10.1016/j.immuni.2005.12.003

Stout J, Yu VL, et al. (1982). Ubiquitousness of Legionella pneumophila in the water supply of a hospital with endemic Legionnaires' disease. The New England journal of medicine 306(8): 466-468. doi 10.1056/NEJM198202253060807

Stout JE and Yu VL (1997). Legionellosis. The New England journal of medicine 337(10): 682-687. doi 10.1056/NEJM199709043371006

Struhl K (2007). Transcriptional noise and the fidelity of initiation by RNA polymerase II. Nature structural & molecular biology 14(2): 103-105. doi 10.1038/nsmb0207-103

Sugimoto K, Toyoshima H, et al. (1992). Frequent mutations in the p53 gene in human myeloid leukemia cell lines. Blood 79(9): 2378-2383

Sullivan KD, Galbraith MD, et al. (2018). Mechanisms of transcriptional regulation by p53. Cell death and differentiation 25(1): 133-143. doi 10.1038/cdd.2017.174

Sun L, Goff LA, et al. (2013). Long noncoding RNAs regulate adipogenesis. Proceedings of the National Academy of Sciences of the United States of America 110(9): 3387-3392. doi 10.1073/pnas.1222643110

Sun L, Wu J, et al. (2013). Cyclic GMP-AMP synthase is a cytosolic DNA sensor that activates the type I interferon pathway. Science 339(6121): 786-791. doi 10.1126/science.1232458

Sun T, Yang M, et al. (2009). Role of microRNA-221/-222 in cancer development and progression. Cell Cycle 8(15): 2315-2316. doi 10.4161/cc.8.15.9221

Surdziel E, Cabanski M, et al. (2011). Enforced expression of miR-125b affects myelopoiesis by targeting multiple signaling pathways. Blood 117(16): 4338-4348. doi 10.1182/blood-2010-06-289058

Surget S, Khoury MP, et al. (2013). Uncovering the role of p53 splice variants in human malignancy: a clinical perspective. OncoTargets and therapy 7: 57-68. doi 10.2147/OTT.S53876

Suzuki H, Sasaki T, et al. (2010). Malondialdehyde-modified low density lipoprotein (MDA-LDL)-induced cell growth was suppressed by polycyclic aromatic hydrocarbons (PAHs). The Journal of toxicological sciences 35(2): 137-147

Swaminathan S, Murray DD, et al. (2013). miRNAs and HIV: unforeseen determinants of host-pathogen interaction. Immunological reviews 254(1): 265-280. doi 10.1111/imr.12077

Szklarczyk D, Morris JH, et al. (2017). The STRING database in 2017: quality-controlled protein-protein association networks, made broadly accessible. Nucleic acids research 45(D1): D362-D368. doi 10.1093/nar/gkw937

Taganov KD, Boldin MP, et al. (2007). MicroRNAs and immunity: tiny players in a big field. Immunity 26(2): 133-137. doi 10.1016/j.immuni.2007.02.005

Taganov KD, Boldin MP, et al. (2006). NF-kappaB-dependent induction of microRNA miR-146, an inhibitor targeted to signaling proteins of innate immune responses. Proceedings of the National Academy of Sciences of the United States of America 103(33): 12481-12486. doi 10.1073/pnas.0605298103

Takaoka A, Hayakawa S, et al. (2003). Integration of interferon-alpha/beta signalling to p53 responses in tumour suppression and antiviral defence. Nature 424(6948): 516-523. doi 10.1038/nature01850

Tateda K, Matsumoto T, et al. (1998). Serum cytokines in patients with Legionella pneumonia: Relative predominance of Th1-type cytokines. Clin Diagn Lab Immun 5(3): 401-403

Tesh MJ, Morse SA, et al. (1983). Intermediary metabolism in Legionella pneumophila: utilization of amino acids and other compounds as energy sources. Journal of bacteriology 154(3): 1104-1109

Thounaojam MC, Kundu K, et al. (2014). MicroRNA 155 regulates Japanese encephalitis virus-induced inflammatory response by targeting Src homology 2-containing inositol phosphatase 1. Journal of virology 88(9): 4798-4810. doi 10.1128/JVI.02979-13

Thurston TL, Wandel MP, et al. (2012). Galectin 8 targets damaged vesicles for autophagy to defend cells against bacterial invasion. Nature 482(7385): 414-418. doi 10.1038/nature10744

Tili E, Michaille JJ, et al. (2007). Modulation of miR-155 and miR-125b levels following lipopolysaccharide/TNF-alpha stimulation and their possible roles in regulating the response to endotoxin shock. J Immunol 179(8): 5082-5089

Tilney LG, Harb OS, et al. (2001). How the parasitic bacterium Legionella pneumophila modifies its phagosome and transforms it into rough ER: implications for conversion of plasma membrane to the ER membrane. Journal of cell science 114(Pt 24): 4637-4650

Toller IM, Neelsen KJ, et al. (2011). Carcinogenic bacterial pathogen Helicobacter pylori triggers DNA double-strand breaks and a DNA damage response in its host cells. Proceedings of the National Academy of Sciences of the United States of America 108(36): 14944-14949. doi 10.1073/pnas.1100959108

Townsend PA, Scarabelli TM, et al. (2004). STAT-1 interacts with p53 to enhance DNA damage-induced apoptosis. The Journal of biological chemistry 279(7): 5811-5820. doi 10.1074/jbc.M302637200

Traore K, Trush MA, et al. (2005). Signal transduction of phorbol 12-myristate 13-acetate (PMA)-induced growth inhibition of human monocytic leukemia THP-1 cells is reactive oxygen dependent. Leukemia research 29(8): 863-879. doi 10.1016/j.leukres.2004.12.011

Treffers EE, Tas A, et al. (2015). Temporal SILAC-based quantitative proteomics identifies host factors involved in chikungunya virus replication. Proteomics 15(13): 2267-2280. doi 10.1002/pmic.201400581

Trionfini P, Benigni A, et al. (2015). MicroRNAs in kidney physiology and disease. Nature reviews Nephrology 11(1): 23-33. doi 10.1038/nrneph.2014.202

Truchan HK, Christman HD, et al. (2017). Type II Secretion Substrates of Legionella pneumophila Translocate Out of the Pathogen-Occupied Vacuole via a Semipermeable Membrane. Mbio 8(3). doi 10.1128/mBio.00870-17

Tsolis RM, Baumler AJ, et al. (1996). Contribution of TonB- and Feo-mediated iron uptake to growth of Salmonella typhimurium in the mouse. Infection and immunity 64(11): 4549-4556

Tsuchiya S, Yamabe M, et al. (1980). Establishment and characterization of a human acute monocytic leukemia cell line (THP-1). International journal of cancer 26(2): 171-176

Turkington C and Ashby B (2007) The encyclopedia of infectious diseases. Facts On File, New York.

Tyson JY, Pearce MM, et al. (2013). Multiple Legionella pneumophila Type II secretion substrates, including a novel protein, contribute to differential infection of the amoebae Acanthamoeba castellanii, Hartmannella vermiformis, and Naegleria lovaniensis. Infection and immunity 81(5): 1399-1410. doi 10.1128/IAI.00045-13

Uhlen M, Fagerberg L, et al. (2015). Proteomics. Tissue-based map of the human proteome. Science 347(6220): 1260419. doi 10.1126/science.1260419

Ulitsky I and Bartel DP (2013). lincRNAs: genomics, evolution, and mechanisms. Cell 154(1): 26-46. doi 10.1016/j.cell.2013.06.020

Urbich C, Kuehbacher A, et al. (2008). Role of microRNAs in vascular diseases, inflammation, and angiogenesis. Cardiovascular research 79(4): 581-588. doi 10.1093/cvr/cvn156

Vabret N and Blander JM (2013). Sensing microbial RNA in the cytosol. Frontiers in immunology 4: 468. doi 10.3389/fimmu.2013.00468

van Bergenhenegouwen J, Plantinga TS, et al. (2013). TLR2 & Co: a critical analysis of the complex interactions between TLR2 and coreceptors. Journal of leukocyte biology 94(5): 885-902. doi 10.1189/jlb.0113003

van der Ree MH, van der Meer AJ, et al. (2014). Long-term safety and efficacy of microRNA-targeted therapy in chronic hepatitis C patients. Antiviral research 111: 53-59. doi 10.1016/j.antiviral.2014.08.015

Vannucci FA, Foster DN, et al. (2013). Laser microdissection coupled with RNA-seq analysis of porcine enterocytes infected with an obligate intracellular pathogen (Lawsonia intracellularis). BMC genomics 14: 421. doi 10.1186/1471-2164-14-421

Vasudevan S, Tong Y, et al. (2007). Switching from repression to activation: microRNAs can up-regulate translation. Science 318(5858): 1931-1934. doi 10.1126/science.1149460

Velayudhan J, Hughes NJ, et al. (2000). Iron acquisition and virulence in Helicobacter pylori: a major role for FeoB, a high-affinity ferrous iron transporter. Molecular microbiology 37(2): 274-286

Verma S, Mohapatra G, et al. (2015). Salmonella Engages Host MicroRNAs To Modulate SUMOylation: a New Arsenal for Intracellular Survival. Molecular and cellular biology 35(17): 2932-2946. doi 10.1128/MCB.00397-15

Visone R, Russo L, et al. (2007). MicroRNAs (miR)-221 and miR-222, both overexpressed in human thyroid papillary carcinomas, regulate p27Kip1 protein levels and cell cycle. Endocrine-related cancer 14(3): 791-798. doi 10.1677/ERC-07-0129

Waldo SW, Li Y, et al. (2008). Heterogeneity of human macrophages in culture and in atherosclerotic plaques. Am J Pathol 172(4): 1112-1126. doi 10.2353/ajpath.2008.070513

Wang C, Chen Z, et al. (2014). Up-regulation of p21(WAF1/CIP1) by miRNAs and its implications in bladder cancer cells. FEBS letters 588(24): 4654-4664. doi 10.1016/j.febslet.2014.10.037

Wang F, Chen JG, et al. (2017). Up-regulation of LINC00346 inhibits proliferation of non-small cell lung cancer cells through mediating JAK-STAT3 signaling pathway. European review for medical and pharmacological sciences 21(22): 5135-5142

Wang JH, Zhang L, et al. (2016). microRNA-34a-Upregulated Retinoic Acid-Inducible Gene-I Promotes Apoptosis and Delays Cell Cycle Transition in Cervical Cancer Cells. DNA and cell biology 35(6): 267-279. doi 10.1089/dna.2015.3130

Wang L, Guo Y, et al. (2001). Card10 is a novel caspase recruitment domain/membrane-associated guanylate kinase family member that interacts with BCL10 and activates NF-kappa B. The Journal of biological chemistry 276(24): 21405-21409. doi 10.1074/jbc.M102488200

Wang N, Liang H, et al. (2014). Molecular mechanisms that influence the macrophage m1-m2 polarization balance. Frontiers in immunology 5: 614. doi 10.3389/fimmu.2014.00614

Wang P, Hou J, et al. (2010). Inducible microRNA-155 feedback promotes type I IFN signaling in antiviral innate immunity by targeting suppressor of cytokine signaling 1. J Immunol 185(10): 6226-6233. doi 10.4049/jimmunol.1000491

Wardlaw TMJ, Emily White; Hodge, Matthew; World Health Organization; UNICEF (2006) Pneumonia: the forgotten killer of children.

Washietl S, Pedersen JS, et al. (2007). Structured RNAs in the ENCODE selected regions of the human genome. Genome research 17(6): 852-864. doi 10.1101/gr.5650707

Watarai M, Derre I, et al. (2001). Legionella pneumophila is internalized by a macropinocytotic uptake pathway controlled by the Dot/Icm system and the mouse Lgn1 locus. The Journal of experimental medicine 194(8): 1081-1096

Waters LS and Storz G (2009). Regulatory RNAs in bacteria. Cell 136(4): 615-628. doi 10.1016/j.cell.2009.01.043

Watson RO, Bell SL, et al. (2015). The Cytosolic Sensor cGAS Detects Mycobacterium tuberculosis DNA to Induce Type I Interferons and Activate Autophagy. Cell Host Microbe 17(6): 811-819. doi 10.1016/j.chom.2015.05.004

Weber JA, Baxter DH, et al. (2010). The microRNA spectrum in 12 body fluids. Clinical chemistry 56(11): 1733-1741. doi 10.1373/clinchem.2010.147405

Wei J, Nagy TA, et al. (2010). Regulation of p53 tumor suppressor by Helicobacter pylori in gastric epithelial cells. Gastroenterology 139(4): 1333-1343. doi 10.1053/j.gastro.2010.06.018

Wei J, Noto J, et al. (2012). Pathogenic bacterium Helicobacter pylori alters the expression profile of p53 protein isoforms and p53 response to cellular stresses. Proceedings of the National Academy of Sciences of the United States of America 109(38): E2543-2550. doi 10.1073/pnas.1205664109

Weis JH, Tan SS, et al. (1992). Detection of rare mRNAs via quantitative RT-PCR. Trends in genetics : TIG 8(8): 263-264

Weissenmayer BA, Prendergast JG, et al. (2011). Sequencing illustrates the transcriptional response of Legionella pneumophila during infection and identifies seventy novel small non-coding RNAs. PloS one 6(3): e17570. doi 10.1371/journal.pone.0017570

Welsh CT, Summersgill JT, et al. (2004). Increases in c-jun n-terminal Kinase/Stress-Activated protein kinase and p38 activity in monocyte-derived macrophages following the uptake of Legionella pneumophila. Infection and immunity 72(3): 1512-1518. doi 10.1128/Iai.72.3.1512-1518.2004

Werner A, Carlile M, et al. (2009). What do natural antisense transcripts regulate? RNA biology 6(1): 43-48

Westermann AJ, Barquist L, et al. (2017). Resolving host-pathogen interactions by dual RNA-seq. Plos Pathog 13(2): e1006033. doi 10.1371/journal.ppat.1006033

Westermann AJ, Forstner KU, et al. (2016). Dual RNA-seq unveils noncoding RNA functions in host-pathogen interactions. Nature 529(7587): 496-501. doi 10.1038/nature16547

Westermann AJ, Gorski SA, et al. (2012). Dual RNA-seq of pathogen and host. Nature reviews Microbiology 10(9): 618-630. doi 10.1038/nrmicro2852

(2017) World Health Organization, http://www.who.int/mediacentre/factsheets/fs331/en/. Cited 7 November 2017

Wiedmaier N, Muller S, et al. (2008). Bacteria induce CTGF and CYR61 expression in epithelial cells in a lysophosphatidic acid receptor-dependent manner. International journal of medical microbiology : IJMM 298(3-4): 231-243. doi 10.1016/j.ijmm.2007.06.001

Winter J, Jung S, et al. (2009). Many roads to maturity: microRNA biogenesis pathways and their regulation. Nature cell biology 11(3): 228-234. doi 10.1038/ncb0309-228

Wisdom R, Johnson RS, et al. (1999). c-Jun regulates cell cycle progression and apoptosis by distinct mechanisms. The EMBO journal 18(1): 188-197. doi 10.1093/emboj/18.1.188

Wu R, Su Y, et al. (2016). Characters, functions and clinical perspectives of long non-coding RNAs. Molecular genetics and genomics : MGG 291(3): 1013-1033. doi 10.1007/s00438-016-1179-y

. www.proteinatlas.org

Xiao C and Rajewsky K (2009). MicroRNA control in the immune system: basic principles. Cell 136(1): 26-36. doi 10.1016/j.cell.2008.12.027

Xiao H, Killip MJ, et al. (2013). The human interferon-induced MxA protein inhibits early stages of influenza A virus infection by retaining the incoming viral genome in the cytoplasm. Journal of virology 87(23): 13053-13058. doi 10.1128/JVI.02220-13

Xu C, Zhang L, et al. (2016). MicroRNA-3196 is inhibited by H2AX phosphorylation and attenuates lung cancer cell apoptosis by downregulating PUMA. Oncotarget 7(47): 77764-77776. doi 10.18632/oncotarget.12794

Yang RY, Rabinovich GA, et al. (2008). Galectins: structure, function and therapeutic potential. Expert reviews in molecular medicine 10: e17. doi 10.1017/S1462399408000719

Yao M, Gao W, et al. (2016). The regulation roles of miR-125b, miR-221 and miR-27b in porcine Salmonella infection signalling pathway. Bioscience reports 36(4). doi 10.1042/BSR20160243

Ye TY, Ding W, et al. (2017). Long noncoding RNA linc00346 promotes the malignant phenotypes of bladder cancer. Biochemical and biophysical research communications 491(1): 79-84. doi 10.1016/j.bbrc.2017.07.045

Yi R, Qin Y, et al. (2003). Exportin-5 mediates the nuclear export of pre-microRNAs and short hairpin RNAs. Genes & development 17(24): 3011-3016. doi 10.1101/gad.1158803

Yoneyama M, Kikuchi M, et al. (2004). The RNA helicase RIG-I has an essential function in double-stranded RNA-induced innate antiviral responses. Nature immunology 5(7): 730-737. doi 10.1038/ni1087

Yu VL, Plouffe JF, et al. (2002). Distribution of Legionella species and serogroups isolated by culture in patients with sporadic community-acquired legionellosis: an international collaborative survey. The Journal of infectious diseases 186(1): 127-128. doi 10.1086/341087

Yu Z, Wang Z, et al. (2008). GTPase activity is not essential for the interferon-inducible MxA protein to inhibit the replication of hepatitis B virus. Archives of virology 153(9): 1677-1684. doi 10.1007/s00705-008-0168-9

Zahringer U, Knirel YA, et al. (1995). The lipopolysaccharide of Legionella pneumophila serogroup 1 (strain Philadelphia 1): chemical structure and biological significance. Progress in clinical and biological research 392: 113-139

Zaika AI, Wei J, et al. (2015). Microbial Regulation of p53 Tumor Suppressor. Plos Pathog 11(9): e1005099. doi 10.1371/journal.ppat.1005099

Zaitoun I, Erickson CS, et al. (2010). Use of RNAlater in fluorescence-activated cell sorting (FACS) reduces the fluorescence from GFP but not from DsRed. BMC research notes 3: 328. doi 10.1186/1756-0500-3-328

Zeng Y and Cullen BR (2004). Structural requirements for pre-microRNA binding and nuclear export by Exportin 5. Nucleic acids research 32(16): 4776-4785. doi 10.1093/nar/gkh824

Zhang J, Fan DH, et al. (2015). Cancer Specific Long Noncoding RNAs Show Differential Expression Patterns and Competing Endogenous RNA Potential in Hepatocellular Carcinoma. PloS one 10(10). doi ARTN e0141042

10.1371/journal.pone.0141042

Zhang Y, Zhang M, et al. (2013). Expression profiles of miRNAs in polarized macrophages. Int J Mol Med 31(4): 797-802. doi 10.3892/ijmm.2013.1260

Zhao D, Zhuang N, et al. (2016). MiR-221 activates the NF-kappaB pathway by targeting A20. Biochemical and biophysical research communications 472(1): 11-18. doi 10.1016/j.bbrc.2015.11.009

Zhao H, De BP, et al. (1996). Inhibition of human parainfluenza virus-3 replication by interferon and human MxA. Virology 220(2): 330-338. doi 10.1006/viro.1996.0321

Zhao ZJ and Shen J (2017). Circular RNA participates in the carcinogenesis and the malignant behavior of cancer. RNA biology 14(5): 514-521. doi 10.1080/15476286.2015.1122162

Ziegler-Heitbrock L, Ancuta P, et al. (2010). Nomenclature of monocytes and dendritic cells in blood. Blood 116(16): e74-80. doi 10.1182/blood-2010-02-258558

# Supplements

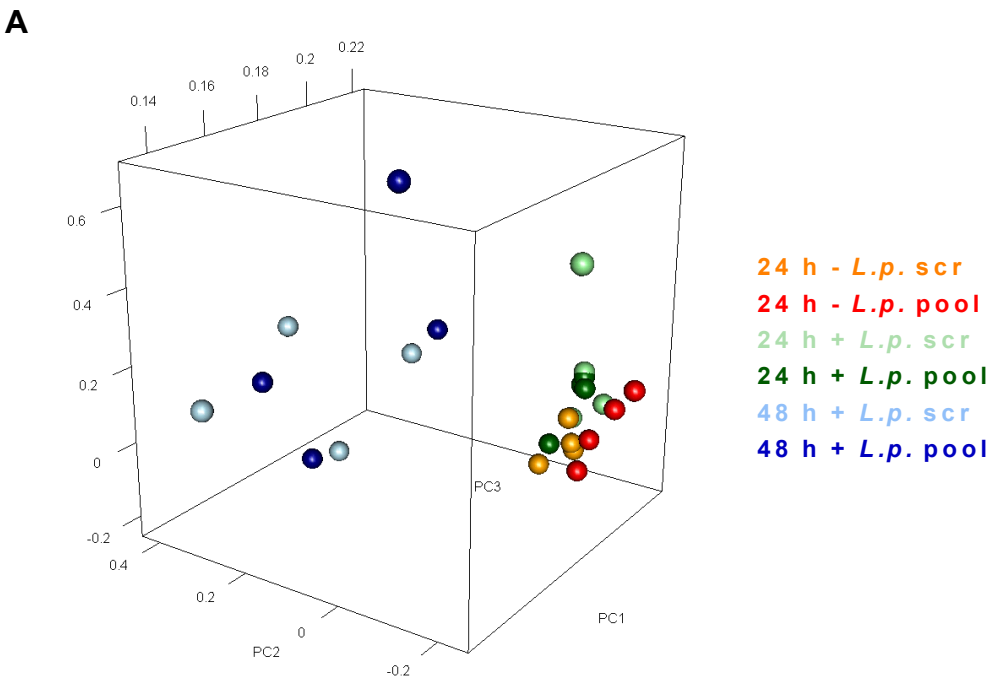


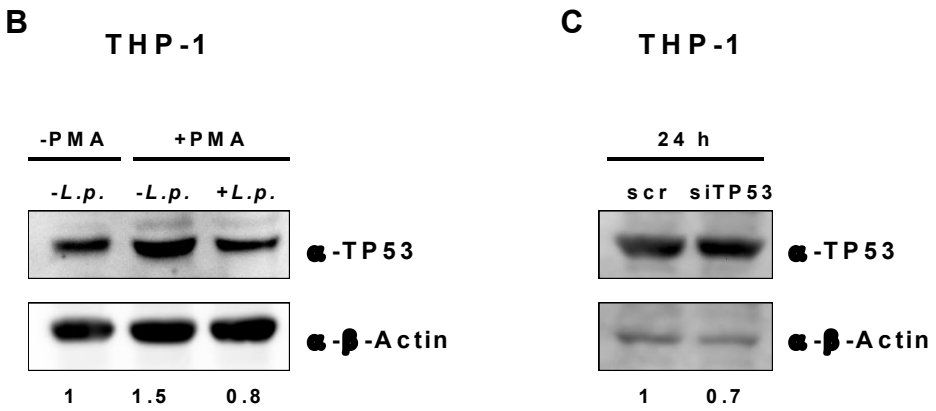


**Supplements 1:**
**A: PCA of the SILAC data.** Principal component analysis (PCA) of all detected proteins (normalized ratios (heavy vs. light)) was performed.
**B: Detection of TP53 protein in THP-1 cells.** THP-1 cells were stimulated with 20 nM PMA (+PMA) for 24 h or left untreated (-PMA). Differentiated THP-1 cells were not infected (*-L.p.*) or infected with *L.p.* at an MOI of 0.5 for 24 h (*+L.p.*).
**C: Knockdown test of TP53 in THP-1 cells.** THP-1 cells were transfected with a small interfering RNA targeting TP53 (siTP53) or with a scrambled siRNA as control (scr). 24 h post transfection, THP-1 cells were stimulated with PMA (20 nM) for 24 h. Knockdown of TP53 protein was verified and quantified by Western Blot at 24 h post PMA-treatment.

## Data directory

Differentially expressed genes of the RNA sequencing data or fold changes of detected proteins of the SILAC approach are listed in an excel file.

**Excel file (1)**

Data of Figure 3.3A: Differentially expressed miRNAs in BDMs following infection with *L.p.* at an MOI of 0.25 for 24 or 48 h.

**Excel file (2)**

Data of Figure 3.5E: Fold change of proteins detected in scramble or miRNA pool transfected and PMA-treated THP-1 cells. Cells were either infected with *L.p.* at an MOI of 0.5 for 24 or 48 h or left untreated as control.

**Excel file (3)**

Data of figure 3.19A, 3.20A, 3.21A and 3.24B: List of all differentially expressed genes of the host (in sheet 1) or the pathogen (in sheet 2 for 8 h and sheet 3 for 16 h post infection) of the dual RNA-Seq approach in THP-1 cells.

**Excel file (4)**

Gene names of 3.22: Six different input lists were used to present the results in the Edwards-Venn diagram. All differentially expressed genes with an adjusted p-value lower than 0.05 and a log2-fold change higher than 1.5 or lower than -1.5 for each condition are listed.

## Verzeichnis der akademischen Lehrer

Meine akademischen Lehrer waren die Damen und Herren in Gießen:

Clauß, Dammann, Dorresteijn, Ehlers, Ekschmitt, Evguenieva-Hackenberg, Forchhammer, Forreiter, Fox, Friedhoff, Fronius, Gläser, Göttlich, Gottschalk, Grünhage, Hafke, Holz, Hughes, Kauschke, Klar, Klug, Lakes-Harlan, Martin, Marxsen, Meiss, Pingoud, Renkawitz, Richter, Schindler, Schmidt, Selzer, Stenzel, Trenczek, Treuner-Lange, VanBel, Wende, Wilhelm, Wissemann, Wolters, Zeidler

## Danksagung

An dieser Stelle möchte ich all jenen danken, die durch ihre fachliche und persönliche Unterstützung zum Gelingen dieser Arbeit beigetragen haben.

Mein besonderer Dank gilt Prof. Dr. Bernd Schmeck für die Aufnahme in seine Arbeitsgruppe und die Überlassung des interessanten Promotionsthemas, sowie für die konstruktiven Anregungen und Diskussionen. Des Weiteren möchte ich mich für das von Ihnen entgegengebrachte Vertrauen und Ihre Unterstützung bei der Fertigstellung dieser Arbeit bedanken.

Außerdem möchte ich all meinen Kooperationspartnern danken, die mich bei dieser Arbeit unterstützt haben. Sascha Blankenburg, Dr. Kristin Surmann und Prof. Dr. Uwe Völker aus Greifswald danke ich für die Bearbeitung, Analyse und Auswertung der zugeschickten SILAC Proben. Mein spezieller Dank gilt allerdings Dr. Brian Caffrey und Prof Dr. Annalisa Marsico, die mit ihren bioinformatischen Auswertungen der erhobenen Hochdurchsatzdaten wesentlich zur Entstehung dieser Arbeit beigetragen haben. Brian Caffrey danke ich außerdem für die Korrekturen der in Englisch verfassten Arbeit.

Außerdem möchte ich allen aktuellen und ehemaligen Mitgliedern des Instituts für Lungenforschung meinen Dank für die schöne Zusammenarbeit, die tolle Arbeitsatmosphäre und die wunderschöne Zeit während meiner Promotionszeit aussprechen. Ich freue mich sehr, dass ich viele zu meinen wirklich guten Freunden zählen kann. Dabei möchte ich einigen Personen meinen besonderen Dank aussprechen: Dr. Alexandra Sittka-Stark für ihren wissenschaftlichen Rat, die Betreuung und ihre Unterstützung während der Anfangszeit meiner Promotion; Dr. Wilhelm Bertrams für die wissenschaftlichen Diskussionen, die große Unterstützung und wertvollen Hinweise während meiner Promotionszeit und zur Vollendung dieser Arbeit; Dr. Anna Lena Jung für die gemeinsame Promotionszeit, die moralische Unterstützung in manchen denkbar schlimmen Situationen, ihre Freundschaft und die zahlreichen wissenschaftlichen Diskussionen und Tipps zur Durchführung von Versuchen; André Wesener für die gemeinsame Promotionszeit, die fachliche und moralische Unterstützung während des Verfassens dieser Arbeit und die ausgiebigen Diskussionen über GoT Folgen, Star Wars und Marvel Filme, die immer wieder für eine kleine Ablenkung gut waren; Katrin Bedenbender (endlich noch ein „richtiges“ Mädchen, die so schnell reden kann!) für das Korrekturlesen dieser Arbeit, den gemeinsamen Sporteinheiten und den kreativen Hilfestellung bei Designfragen; Marina Aznaourova für ihren guten wissenschaftlichen Rat und Hilfe und den gemeinsamen Abenden außerhalb des Labors; Nadine Siebert für den guten Start in Marburg, ihre moralische Unterstützung und ihre Hilfe bei meinen ersten Versuchen im Labor; Dr. Evelyn Vollmeister für den interessanten wissenschaftlichen und nicht-

wissenschaftlichen Austausch und das Ablenken während schwieriger Phasen durch das ein oder andere Tischfußballspiel mit obligatorischem Feierabendbier; Marlene von Schenck zu Schweinsberg für die Sicherheit ihrer immerwährenden Hilfestellung und Beratung bei organisatorischen und administrativen Problemen; den ehemaligen und aktuellen, Bachelor-, Master- und Promotionsstudenten Diana Böhm, Nora Lindhauer, Philipp Burkhard, Sebastian Müller, Harsha Janga, Johanna Harke und Stephan Ringshandl für die wunderbare, gemeinsame Zeit im aber auch außerhalb des Labors. Es war ein toller Sommer 2017! Vor allem die langen Abende mit Diana Böhm und Nora Lindhauer werden mir immer im Gedächtnis bleiben. Außerdem danke ich Patrick Schuhmachers für seine engagierte Laborarbeit und tollen Ergebnissen, die bestimmt noch zu einer Publikation führen.

Ein besonders großes Dankeschön widme ich allerdings Kerstin Hoffmann für ihre Hilfe und Unterstützung bei den Experimenten. Gerade nach einer Nachtschicht oder den 10.000 CFU-Assays war deine Hilfe Goldwert. Des Weiteren möchte ich mich bei dir für den Spaß während der gemeinsamen Laborarbeit und deinen unermüdlichen Einsatz für meine Versuche bedanken. Wir sind ein eingespieltes Team und ohne dich wäre die Promotionszeit bei Weitem nicht so schön und erfolgreich gewesen!

Des Weiteren möchte ich mich bei meiner WG für den Rückhalt während der Promotionszeit bedanken! Vielen Dank für die Ablenkung durch gemeinsame Feiern und Kochabende. Ein großes Dankeschön an Carolin Woermann, die mich oft aus meiner Hungersnot nach langen Arbeitstagen gerettet hat.

Julia Obert danke ich vor allem für die spaßige und tolle Studienzeit, für die Hilfe bei der Formatierung und kreative Unterstützung bei Abbildungen, die nachmittäglichen Kaffeepausen und natürlich für die aufbauenden Worte nach großer Frustration und Schreibblockaden (wie „Stückchen für Stückchen“).

Außerdem möchte ich selbstverständlich meinen Eltern und meinen Brüdern danken, die mich während meines Studiums und meiner Promotionszeit immer unterstützt haben und ohne die das Alles nicht möglich gewesen wäre. Besonders möchte ich meiner Zwillingsschwester danken. Du hast mich immer wortlos verstanden. Wir haben alles gemeinsam durchgezogen: Kindergarten, Schule und Studium. Erst zur Promotionszeit haben wir uns getrennt, aber dennoch immer gegenseitig unterstützt! Danke, dass du auf mich gewartet hast!

Zu guter Letzt, danke ich meinem Freund André Frania. Danke, dass Du an mich geglaubt und mich in meinem Werdegang unterstützt hast. Du hast mich in schwierigen Phasen immer aufgemuntert, mir zugehört und mich wieder motiviert. Ohne deine Liebe, deinen Witz und deine moralische Unterstützung wäre die Erstellung dieser Arbeit nicht möglich gewesen! Ich danke Dir für die letzten Jahre und freue mich auf unsere gemeinsame Zukunft!